

ENGINEERING PROPERTIES OF A WHEAT

Thesis submitted to the University of Ottawa
in partial fulfilment of the requirements for the
Degree of M.A.Sc. in Civil Engineering.

by

Manoher S. S. Chawla, B.Sc.Eng. (Punjabi University, India)

Department of Civil Engineering

April, 1970.

SUMMARY

Storing of wheat is a common practice and for satisfactory and economical design of bins and handling devices, a knowledge of the engineering properties of wheats, namely their bulk densities, shear strengths and their sliding resistances on structural surfaces, is required.

Because of the limited availability of sufficient data on the engineering properties of wheat, it was decided to make a comprehensive study of the bulk density, shear strength and sliding resistance on structural surfaces of a winter wheat from Alberta.

The minimum and maximum bulk densities of a mass of wheat grains were obtained. Numerous techniques of loosely placing the wheat were used to obtain minimum bulk density; and methods such as static compaction and vibratory compaction were used to obtain maximum bulk density. These densities were measured on wheat samples at different moisture contents.

It was observed that the bulk density of the wheat decreased as the moisture content in the wheat kernels was increased. The vibratory stresses were most effective in

increasing the bulk density of the wheat at all moisture contents. With an increase in moisture content, this effect was observed to become slightly more marked. The magnitude of the static pressure had practically no effect on the bulk density of the wheat at low moisture contents. At high moisture contents, however, static pressure was fairly effective although not as much as vibratory stresses.

The shear strength of the wheat was found by performing direct shear and triaxial compression tests. The effects of the moisture content and porosity on the shear strength parameters of the wheat were studied. The magnitude of the cohesion between the grains, not having been previously reported in the literature, was determined for the first time.

The relationship between coefficient of friction and moisture content depicted an optimum moisture content at which the wheat had a minimum value of the coefficient of friction. The cohesion of the wheat increased as the moisture content was increased. Both the coefficient of friction and cohesion intercept increased as the porosity of the sample was decreased.

The sliding resistance of the wheat on wood, steel and concrete was found by performing direct shear tests. These tests were carried out on samples having different moisture contents, at minimum and maximum possible porosities.

The coefficient of friction of wheat on wood and concrete increased as the moisture content of the wheat was increased. The adhesion of the wheat on wood and steel increased with the increase in the moisture content of the wheat grains.

The coefficient of friction and adhesion were not appreciably affected by the porosity of the wheat mass, when the structural surfaces were wood and steel. However, in case of concrete as the structural surface, both of these sliding resistance parameters increased with decreasing porosity.

The standard engineering tests were used in the present research with the expectation that they may become a basis for future work to be compared with the results obtained in this study.

TABLE OF CONTENTS

	Page
ACKNOWLEDGEMENTS	x
LIST OF TABLES	xi
LIST OF FIGURES	xiii
PRINCIPAL SYMBOLS	xvi
CHAPTER 1 - INTRODUCTION	1
1.1 General	1
1.2 Statement of Problem	1
1.3 Objectives of the Study	2
1.4 Outline of Thesis	4
CHAPTER 2 - LITERATURE REVIEW	5
2.1 General	5
2.2 Bulk Density	5
2.3 Shearing Strength	9
CHAPTER 3 - THEORETICAL CONCEPTS FOR PACKING, BULK DENSITY AND SHEAR STRENGTH OF GRANULAR MATERIALS	15
3.1 General	15
3.2 Packing of Ellipsoids	15
3.2.1 Cubical Packing	16
3.2.2 Single Staggered Packing	18
3.2.3 Double Staggered Packing	18

	Page
3.2.4 Pyramidal Packing	19
3.2.5 Tetrahedral Packing	20
3.3 Bulk Density	20
3.3.1 Theory	22
3.4 Shear Strength	25
3.4.1 Strength Theory	26
CHAPTER 4 - TESTING PROGRAM	27
4.1 General	27
4.2 Material Used	27
4.3 Procedure of Obtaining Sample of Required Moisture Content	29
4.4 Moisture Content Determination	31
4.5 Apparatus and Experimental Procedure	32
4.5.1 Specific Gravity Test	32
4.5.1.1 Apparatus	33
4.5.1.2 Procedure	33
4.5.1.3 Calculation	35
4.5.2 Crushing Load Test	36
4.5.2.1 Apparatus	
4.5.2.2 Procedure	37
4.5.3 Minimum Bulk Density Test	39
4.5.3.1 Apparatus	39
4.5.3.2 Procedure	39
4.5.3.3 Calculations	41

	Page
4.5.4 Maximum Bulk Density Test	42
4.5.4.1 Vibratory Test	42
4.5.4.1.1 Apparatus	42
4.5.4.1.2 Procedure	43
4.5.4.1.3 Calculations	46
4.5.4.2 Static Compression Test	47
4.5.4.2.1 Apparatus	47
4.5.4.2.2 Procedure	49
4.5.4.2.3 Calculation.	50
4.5.5 Direct Shear Test	51
4.5.5.1 Apparatus	51
4.5.5.2 Procedure	51
4.5.5.3 Calculation	53
4.5.6 Triaxial Compression Test	56
4.5.6.1 Apparatus	56
4.5.6.2 Procedure	58
4.5.6.3 Calculations	59
4.5.7 Shear Resistance of Wheat on Structural Surfaces	60
4.5.7.1 Apparatus	60
4.5.7.2 Procedure	60
4.5.7.3 Calculations	60

	Page
CHAPTER 5 - DISCUSSION OF TEST RESULTS	61
5.1 General	61
5.2 Specific Gravity	61
5.3 Crushing Load of Wheat Kernels	64
5.4 Bulk Density	68
5.4.1 General	68
5.4.2 Minimum Bulk Density	69
5.4.3 Maximum Bulk Density	73
5.4.3.1 Magnitude of Surcharge Weights	73
5.4.3.2 Time of Vibration	79
5.4.3.3 Amplitude of Vibration	79
5.4.4 Comparison of Experimental and Theoretical Packing	80
5.4.5 Comparison of Bulk Densities of Different Wheats	83
5.4.6 Static Compression	84
5.4.7 Discussion	93
5.5 Shear Strength of Wheat	96
5.5.1 General	96
5.5.2 Direct Shear Tests	97
5.5.2.1 Stress-Deformation and Volume Change Curves	97
5.5.2.2 Failure Envelope Plots	102

	Page
5.5.3 Triaxial Compression Tests	102
5.5.3.1 Stress-Strain Curves	104
5.5.3.2 Mohr Coulomb Envelopes	107
5.5.4 Shear Strength Parameters	107
5.5.4.1 Coefficient of Friction	107
5.5.4.2 Cohesion	116
5.5.5 Comparison with Other Work	122
5.6 Sliding Resistance of Wheat on Structural Surfaces	123
5.6.1 Direct Shear Tests	124
5.6.1.1 Stress-Horizontal Deformation and Volume Change Curves	124
5.6.1.1.1 Wheat on Wood	126
5.6.1.1.2 Wheat on Steel	127
5.6.1.1.3 Wheat on Concrete	128
5.6.1.1.4 Discussion	130
5.6.1.2 Failure Envelope Plots	131
5.6.2 Sliding Resistance Parameters	133
5.6.2.1 Wheat on Wood	136
5.6.2.2 Wheat on Steel	137
5.6.2.3 Wheat on Concrete	141
5.6.3 Comparison with Other Work	142
CHAPTER 6 - CONCLUSIONS AND RECOMMENDATIONS	146
6.1 Conclusions	146
6.2 Recommendations	149

	Page
BIBLIOGRAPHY	151
APPENDIX A	155
A.1 Shear Strength Theory	155
A.1.1 Direct Shear Tests on Granular Material	155
A.1.2 Triaxial Compression Test on Granular Material	158

ACKNOWLEDGEMENTS

This research was carried out under the guidance of Dr. J.D. Scott, Professor and Chairman, Department of Civil Engineering, to whom the author expresses his sincerest gratitude for his advice, encouragement and keen interest during the course of this investigation.

The author is grateful to Dr. D.H. Shields, Professor of Civil Engineering for reviewing the manuscript and for his valuable comments.

It is a pleasure for the writer to express his thanks to his colleagues in the Department of Civil Engineering and especially to Mr. Narendra S. Verma for their kind cooperation.

Finally, the author acknowledges his indebtedness to the National Research Council of Canada for the financial assistance which made this study possible.

LIST OF TABLES

TABLE NO.	Page
2.1 Bulk density as affected by moisture content	7
4.1 Size of wheat grain	28
5.4.1 Bulk density of wheat	94
5.1 Relationship between shear strength parameters of wheat (ϕ and C) and sliding resistance parameters of wheat on wood (δ_w and A_w)	138
5.2 Relationship between shear strength parameters of wheat (ϕ and C) and sliding resistance parameters of wheat on steel (δ_s and A_s)	140
5.3 Relationship between shear strength parameters of wheat (ϕ and C) and sliding resistance parameters of wheat on concrete (δ_c and A_c)	143
A.1 Specific gravity of wheat	199
A.2 Crushing load of individual wheat grain	199
A.3 Minimum bulk density of wheat	201
A.3.1 Pouring with a funnel 1 inch above the surface of wheat	201
A.3.2 Pouring with a scoop as close to the surface as possible	201
A.3.3 Pouring from 2 gallon pail (half filled) resting on the lip of the mould	201
A.3.4 Pouring with a half filled 2 gallon pail 5 inches above the mould	201

A.4	Maximum bulk density of wheat by vibratory method	202
A.5	Deformation under static loading	209
A.5.1	Container size: 2.5 inches diameter and 1.1 inches height	209
A.5.1.1	Vertical deformation dial readings of samples under compression	209
A.5.1.2	Values of vertical deformation ($\frac{\Delta L}{L}$ %) computed from A.5.1.1	210
A.5.1.3	Variation of bulk density or porosity under static pressure	211
A.5.2	Container size: 6 inches diameter and 1½ inches height	212
A.5.2.1	Vertical deformation dial readings of samples under compression	212
A.5.2.2	Values of vertical deformation ($\frac{\Delta L}{L}$ %) computed from A.5.2.1	213
A.5.2.3	Variation of bulk density or porosity under static pressure	214
A.6	Direct shear tests on wheat	215
A.7	Triaxial compression tests on wheat	216
A.8	Direct shear tests of wheat on three structural surfaces	217
A.8.1	Wheat on wood	217
A.8.2	Wheat on steel	217
A.8.3	Wheat on concrete	217

LIST OF FIGURES

FIGURE	Page
2.1 Bulk density as effected by moisture content	6
2.2 Bulk density as affected by moisture content	8
2.3 Variation of coefficient of friction with confining pressure	11
2.4 Coefficient of friction of winter wheat on structural surfaces	13
3.1 Different types of packing of ellipsoids	17
3.2 Theoretical packing of ellipsoids	21
4.3.1 Mixing unit	30
4.5.1 Specific gravity apparatus	34
4.5.2 Triaxial compression machine	38
4.5.3 Minimum density apparatus	40
4.5.4 Relationship between amplitude of vibration and rheostat setting at zero load	44
4.5.5 Relationship between amplitude of vibration and load	45
4.5.6 Consolidation unit	48
4.5.7 Direct shear apparatus	52
4.5.8 Shear force-horizontal deformation curve for direct shear test	54
4.5.9 Failure envelope for direct shear test	55
4.5.10 Triaxial compression apparatus	57
5.1 Specific gravity of wheats at different moisture contents	62

5.2	Load-deformation characteristics of individual wheat grains	66
5.3	Crushing load of individual wheat grains	67
5.4	Bulk density of different wheats	70
5.5	Porosity of different wheats	71
5.6 - 5.10	Bulk density and porosity from vibratory tests	74 - 78
5.11	Packing of ellipsoids and wheat grains	81
5.12	Relationship between static pressure and deformation for static compression tests (small container)	86
5.13	Relationship between static pressure and porosity for static compression tests (small container)	87
5.14	Relationship between static pressure and deformation for static compression tests (large container)	90
5.15	Relationship between static pressure and porosity for static compression tests (large container)	91
5.16	Stress deformation curves for direct shear box	98 - 99
5.17	Failure envelope plots for direct shear box tests	103
5.18	Stress strain curves for triaxial tests	105
5.18a	Typical photograph of sample failure	108
5.19	Mohr Coulomb failure envelopes for triaxial compression tests	109
5.20	Coefficient of friction from direct shear tests	110
5.21	Coefficient of friction from triaxial tests	111
5.22	Coefficient of friction from direct shear and triaxial tests	113

5.23	Cohesion intercept from direct shear tests	117
5.24	Cohesion intercept from triaxial tests	118
5.25	Cohesion intercept from direct shear and triaxial tests	119
5.26	Stress deformation of wheat on structural surfaces	125
5.27	Failure envelop plots of wheat on structural surfaces	132
5.28	Coefficient of friction of wheat on structural surfaces	134
5.29	Adhesion intercept of wheat on structural surfaces	135
5.30	Coefficient of friction of wheats on structural surfaces	144
A.1	Friction between blocks	155
A.2	Friction in soil	156
A.3	Shearing of soil in shear box	157
A.4	Relation of stresses at a point and development of Mohr's diagram	159
A.5	Mohr's graphical determination of ϕ and C	163
A.6 - A.10	Stress-deformation curves for direct shear box	164 - 170
A.11 - A.15	Failure envelope plots for direct shear box	171 - 175
A.16 - A.19	Stress strain curves for triaxial tests	176 - 179
A.20 - A.23	Mohr Coulomb failure envelope for triaxial compres- sion tests	180 - 183
A.24	Stress deformation of wheat on wood	184 - 185
A.25	Stress-deformation curves of wheat on steel	186 - 187
A.26	Stress-deformation curves of wheat on concrete	188 - 191
A.27	Failure envelope plots of wheat on wood	192 - 193
A.28	Failure envelope plots of wheat on steel	194 - 195
A.29	Failure envelope plots of wheat on concrete	196 - 198

PRINCIPAL SYMBOLS

a	Major axis of an ellipsoid
b	Minor axis of an ellipsoid
C	Cohesion intercept
\bar{A}	Adhesion intercept
A_w	Adhesion intercept of wheat on wood
A_s	Adhesion intercept of wheat on steel
A_c	Adhesion intercept of wheat on concrete
e	Void ratio
G	Specific gravity
L	Length of sample
n	Porosity
S	Shear strength
V	Total volume of sample
V_a	Volume of air
V_s	Volume of solid matter
V_v	Volume of voids
V_w	Volume of water
w	Water content
W_s	Weight of sample

γ	Bulk density
Δ	Increment
δ	Angle of friction of wheat on structural surface
δ_w	Angle of friction of wheat on wood
δ_s	Angle of friction of wheat on steel
δ_c	Angle of friction of wheat on concrete
ϵ	Strain
π	3.14159
σ	Normal stress
σ_1	Major principal stress
σ_3	Minor principal stress
τ	Shearing stress
ϕ	Angle of internal friction
μ	Coefficient of friction
μ_s	Coefficient of surface friction
ϕ_w	True angle of friction between material and surface
r	Interlocking angle due to wall roughness
m.c.	Moisture content

CHAPTER 1

INTRODUCTION

1.1 General

Study of the engineering properties of agricultural granular materials is of significant importance to Agricultural and Civil Engineers. For satisfactory and economical design of storage structures and handling devices, a knowledge of the fundamental physical properties of granular materials, viz bulk density, shearing strength and shearing resistance of the granular materials on structural surfaces is necessary.

At present, a limited literature is available on the engineering properties of agricultural granular materials. This research was carried out for a better understanding of these properties.

1.2 Statement of Problem

The storage and handling of agricultural granular materials leads to three main questions which are of concern

to storage and transportation agencies.

1. What is the bulk density of a mass of wheat grain?
2. What is the shearing strength of a mass of wheat grain?
3. What is the shearing resistance of wheat on different structural surfaces?

It was proposed to provide answers to these questions by carrying out experimental investigations on a western Canadian hard wheat. Engineering tests developed for granular materials were to be performed and physical properties of wheat were to be examined by considering the mechanics of granular media.

1.3 Objectives of the Study

It was realized that very little was known about the engineering properties of wheat. The purpose of this investigation was to understand better the effect of the moisture content in the kernels of wheat on the engineering properties of wheat.

The first objective was to find the minimum bulk density and maximum bulk density which could be obtained in a mass of wheat. The latter was to be found by vibratory compaction methods. The variables influencing the bulk densities

were also to be studied. These variables are moisture content of the kernels, method of placing wheat in the density containers, size of the density containers, magnitude of the surcharge load, amplitude of vibration and time of vibration of the wheat mass. In order to study the bulk density and porosity of a mass of wheat grain it was first necessary to carry out two other series of tests. These were the specific gravity of wheat at different moisture contents and the crushing load of individual wheat grains at different moisture contents. It was also the objective of this research to compare the minimum and maximum bulk densities obtained by the above experimental methods with those obtained from the study of the theoretical packing of uniform ellipsoids. The ellipsoid seems to approximate best the geometric shape of wheat grains. The change in bulk density from a static load as occurs in storage bins was also studied.

The second objective was to find the shearing strength of wheat by carrying out direct shear tests and tri-axial compression tests. The tests were to be carried out at different confining pressures and with different porosities on wheat samples having different moisture contents. The porosity, moisture content and shearing strength were then to be related to each other.

The third objective was to perform direct shear tests with selected structural surfaces such as hard oak wood, hot rolled plate steel and plain concrete. These tests were to be performed at different confining pressures and with different porosities on wheat samples of different moisture contents. Here also, the structural surfaces, moisture content and shearing resistance parameters were to be related.

1.4 Outline of Thesis

In the chapter that follows, a general survey is given of the existing literature on the engineering properties of agricultural granular materials.

Chapter 3 deals with theoretical packing of uniform ellipsoids, the theoretical concepts of bulk density and the shear strength of granular materials.

Chapter 4 describes the material used, the procedure used to obtain grain of the required moisture content, the procedure used for moisture content determinations, and the experimental methods.

The experimental results are discussed and analysed in chapter 5.

Chapter 6 concludes the thesis with the conclusions and the recommendations for future research.

CHAPTER 2

LITERATURE REVIEW

2.1 General

As stated previously, the literature about the engineering properties of a mass of wheat grain is limited. The work that has been done is discussed under the headings of Bulk Density and Shearing Strength.

2.2 Bulk Density

Schmidi (1955) obtained wheat samples at different moisture contents and studied the effect of moisture content on the bulk density of wheat. His results are given in Table 2.1. Schmidl however did not mention how he determined the bulk density.

Lorenzen in 1957 determined the bulk density of cereal grains by the Standard Bushel Weight Apparatus used in the United States. He found that the bulk density of the cereal grains decreased as the moisture content constituted a greater percentage of the weight. Bulk density

vs moisture curves obtained by Lorenzen for cereal grains are given in Fig. 2.1.

Table 2.1. Bulk Density as Affected by Moisture Content

Pounds per Cubic Foot

(after Schmid, 1955)

Moisture Content %	9	10	11	11	12	12	13	13	14
Bulk Density Winter Wheat 1940		48.30	46.80	46.90	46.90	--	--	--	--
Bulk Density Winter Wheat 1943	50.50	48.90	48.0	--	48.3	--	--	--	--
Bulk Density Spring Wheat 1940	--	--	46.2	46.0	45.8	46.0	45.3	46.6	44.2

Hlynka and Bushuk (1959) found that packing of the grains, shape of the kernels, and moisture content affect the bulk density of agricultural granular materials.

Curves obtained by Browne (1962) for the bulk density and moisture content of four different wheats from London are shown in Fig. 2.2. The bulk density decreases

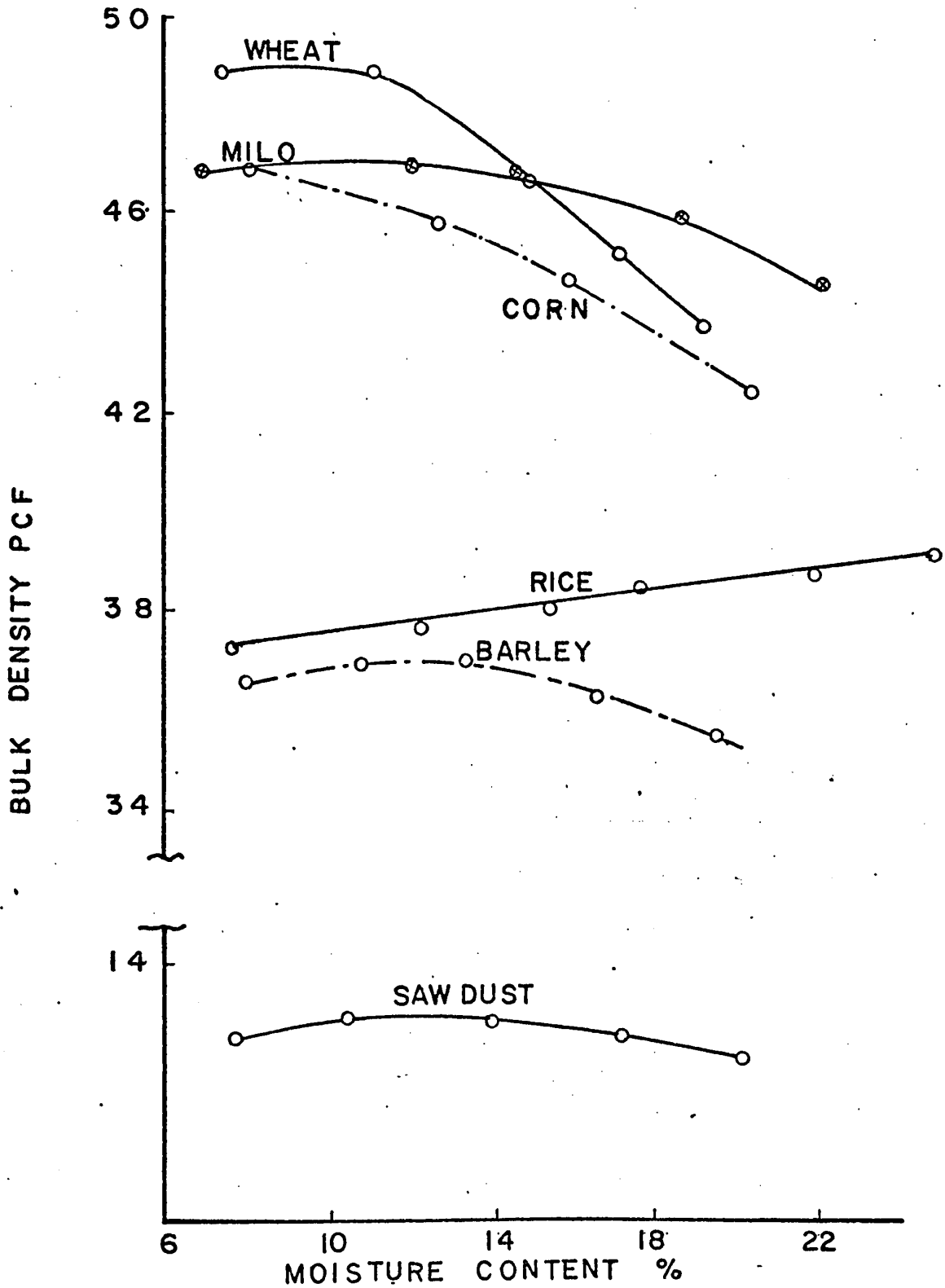


FIG 2-1 BULK DENSITY AS AFFECTED BY MOISTURE CONTENT

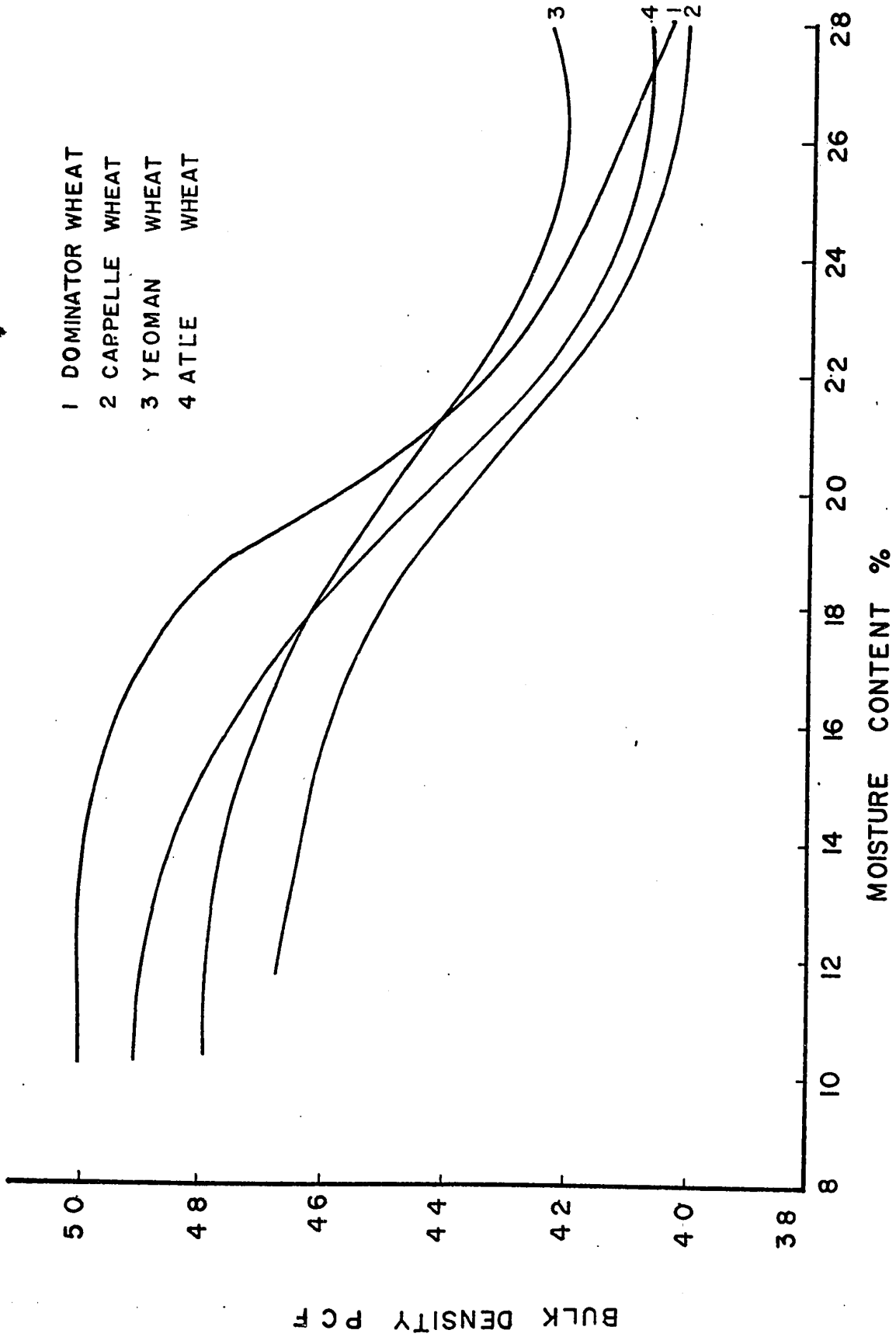


FIG 2.2 BULK DENSITY AS AFFECTED BY MOISTURE CONTENT

for all the four wheats as the moisture content increases. He measured bulk density by using two different density containers and found that the size of the density container also affects the bulk density of wheat.

Hall and Kazanian (1965) found the bulk density of white wheat to be fairly constant at 48.6 lbs. per cu. ft. in the moisture range from 0 to 10 per cent and after this, the bulk density decreased by 0.23 lb. per cu. ft. for each per cent increase in moisture content up to the maximum measured value of 20 per cent.

2.3 Shearing Strength

Considerable work has been done in studying bulk density (γ), coefficient of friction (μ) and coefficient of wall friction ($\hat{\mu}$) of non-agricultural materials. This work has been summarized in many references: Taylor (1948), Lambe (1951), Spangler (1966) and Terzaghi and Peck (1967). Very few references are available however regarding these physical properties for agricultural materials. The early workers generally assumed that the angle of repose was equal to the angle of internal friction (ϕ).

The early investigators placed no emphasis on the effect of change of moisture content on the values of μ and $\hat{\mu}$. Kramer, in 1944, however noticed that the angle of repose of rice was greatly influenced by a change of moisture content in the rice grains. Lorenzen (1957) found little change in the value of coefficient of friction when the moisture content was below 13.0 per cent, but found that μ changed considerably for cereal grains when the moisture content varied between 14.0 to 24.0 per cent. Lorenzen also found that the confining pressure on grains had a significant influence on the values of μ and $\hat{\mu}$. He reasoned that in a deep bin, variation of confining pressure would result in different values of μ and $\hat{\mu}$ which would influence the design criteria for bins.

Zakrzewski (1959) measured the angle of internal friction and the angle of wall friction by means of an apparatus similar in principle to a Shear Box. He found that ϕ and δ increased rapidly to a maximum value at a small horizontal deformation, after which these values decreased. Zakrzewski also found that the coefficient of friction changed with confining pressure as shown in Fig. 2.3. Zakrzewski determined the coefficient of friction at only one moisture content.

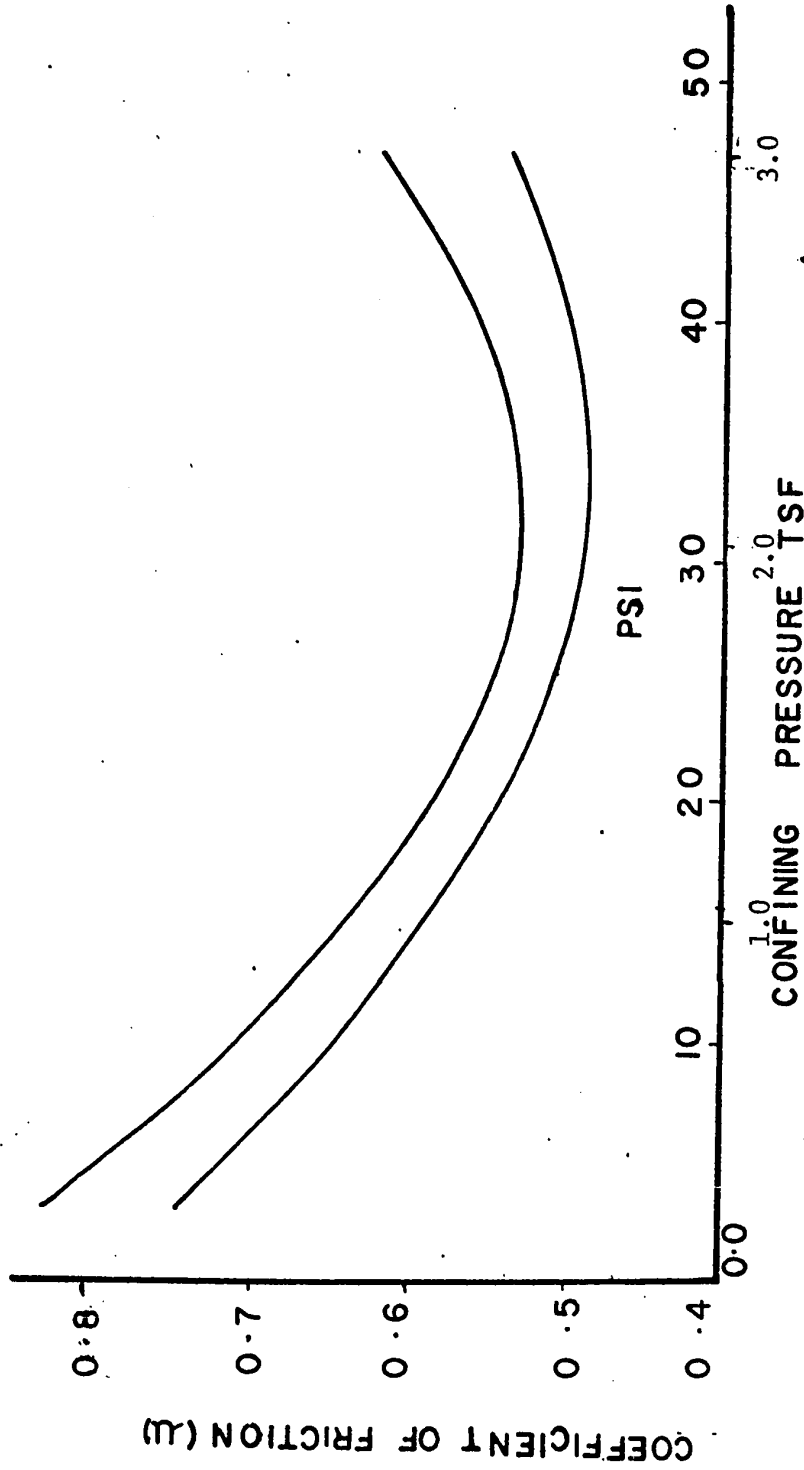


FIG 2.3 VARIATION OF μ WITH CONFINING PRESSURE

He assumed zero cohesion in the sample, which can be shown to be a wrong assumption. It has been found here and indicated by other research workers that cohesion between the grains increases as their moisture content is increased.

Brubaker and Pos (1965) determined the coefficient of wall friction of wheat, soybeans, and glass spheres on five different structural surfaces (Fig. 2.4). The μ of wheat was constant on steel and plywood in the moisture range from 9.7 to 13.2 per cent, and then rose rapidly with increase in moisture content. In their research work, they made no mention of adhesion between wheat and structural surfaces.

Bickart and Buelow (1965) studied the kinetic coefficient of friction of shelled corn and barley on plywood and sheet steel. They observed that materials deposited by grain on a solvent washed surface caused the coefficient of friction to increase. So they concluded that it was necessary to condition a surface with a particular grain before determining the coefficient of friction. They found that moisture content began to affect the coefficient of friction of shelled corn on steel at about 19 per cent (w.b.) and the coefficient of friction of barley on steel at 17.5 per cent (w.b.). They also found that the coefficient of friction of shelled corn on steel increased more than the coefficient of friction of shelled

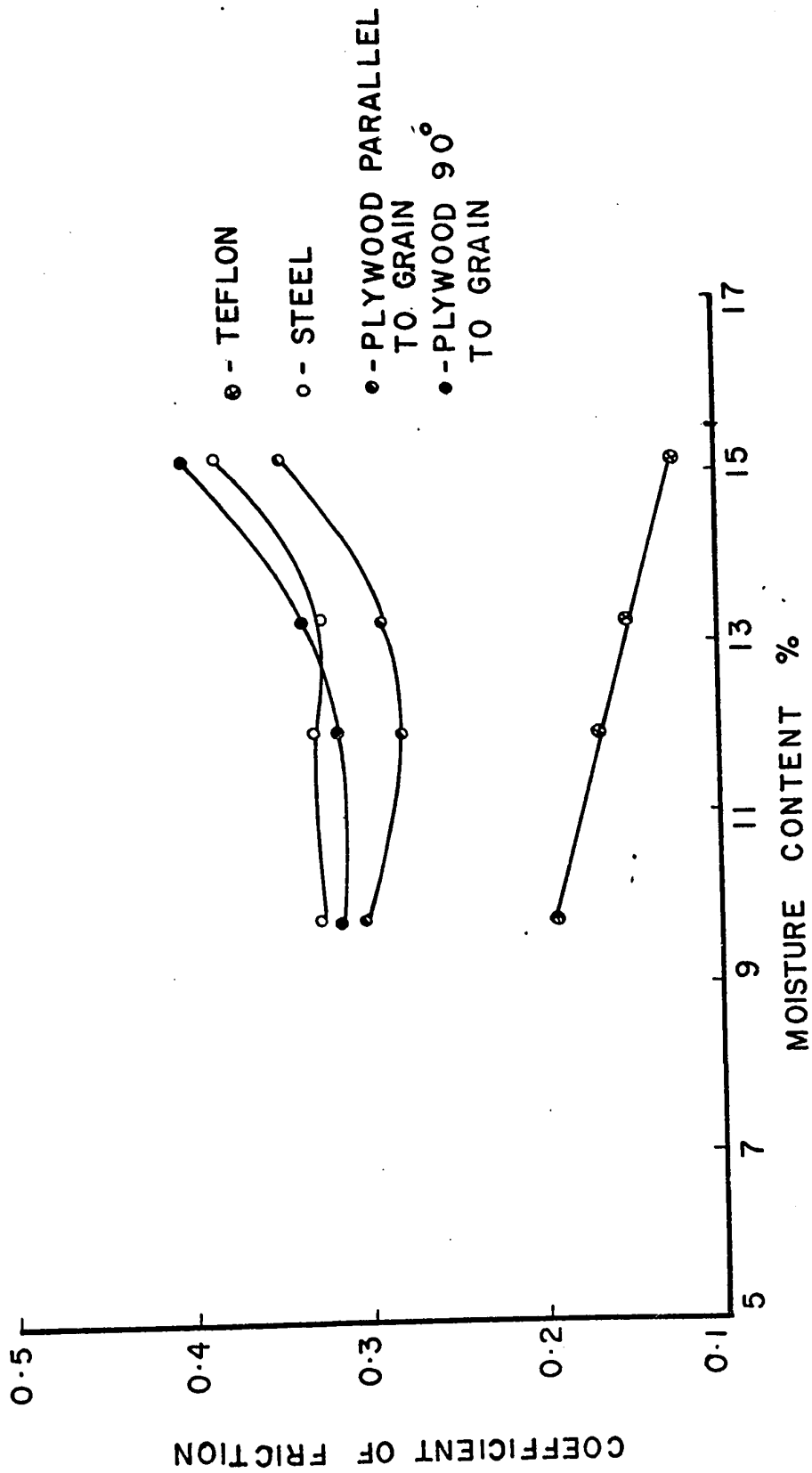


FIG 2.4 COEFFICIENT OF FRICTION OF WHEAT ON STRUCTURAL SURFACES

corn on plywood when the moisture content was increased.

Stewart (1968) used triaxial compression tests to study the effect of moisture content and bulk density on the internal friction properties of sorghum grain. His results showed that bulk density had a considerable effect on the value of the angle of internal friction of sorghum grain and ϕ increased with an increase in bulk density. He found that the angle of internal friction increased with increase in moisture content of sorghum grain. He recommended the use of triaxial compression tests for the study of the physical properties of agricultural granular materials.

CHAPTER 3

THEORETICAL CONCEPTS FOR PACKING, BULK DENSITY, AND SHEAR STRENGTH OF GRANULAR MATERIALS

3.1 General

A mass of cereal grain consists of solid kernels of grain, which contain water in their cells, and void spaces filled with air. The moisture in the kernel influences the size of the kernel and its surface texture. This changes the packing pattern, which further affects the bulk density and shear strength of the mass. To fully investigate the above phenomena, an understanding of the theoretical concepts for packing, bulk density and shear strength of granular materials is necessary.

3.2 Packing of Ellipsoids

Consideration of the theoretical packing of uniform ellipsoids, which appear to approximate best with the geometric shape of wheat grains, would indicate the upper and

lower limits of porosity of a mass of wheat grain, neglecting bridging or arching of particles and the deformation of particles under static pressures.

The packing of ellipsoids has been studied along similar lines to the packing of uniform spheres by Deresiewicz (1957) and White and Walton (1936). Uniform ellipsoids can be packed in five different ways: cubical, single staggered, double staggered, pyramidal, and tetrahedral as shown in Fig. 3.1. Equations are developed for calculating the porosity for the different configurations of packing.

3.2.1 Cubical Packing

In cubical packing, each ellipsoid touches four other ellipsoids in the same layer and every layer is the same.

V = Volume of solid figure bounding ellipsoids

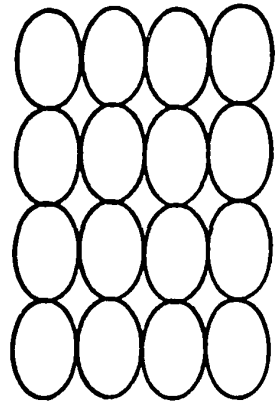
V_s = Volume of ellipsoids

n = Porosity = $\frac{V - V_s}{V} \times 100$

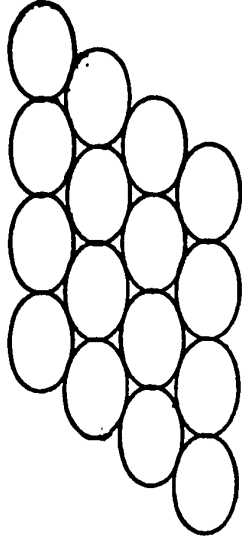
$V = a \cdot N_x \cdot b \cdot N_y \cdot b \cdot N_z$

$= ab^2 N_x \cdot N_y \cdot N_z$

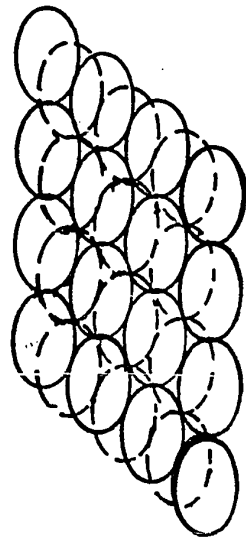
$V_s = \frac{\pi}{6} ab^2 N_x N_y \cdot N_z$



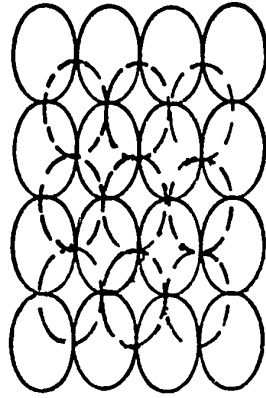
CUBICAL



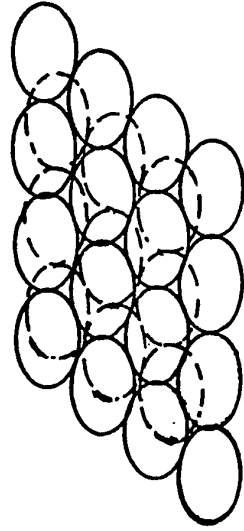
SINGLE STAGGERED



DOUBLE STAGGERED



PYRAMIDAL



TETRAHEDRAL

FIG.3.1 DIFFERENT TYPES OF PACKING OF ELLIPSOIDS

$$n = \frac{ab^2 - \frac{\pi}{6} ab^2}{ab^2} = 1 - \frac{\pi}{6}$$

a = major axis of ellipsoid

b = minor axis of ellipsoid

Nx, Ny and Nz are number of ellipsoids along each of the axes, x, y, and z.

3.2.2 Single Staggered Packing

Each ellipsoid touches six of its neighbours in the same layer.

$$V = aN_x \cdot \frac{\sqrt{3}}{2} N_y \cdot \frac{2ab}{\sqrt{3a^2 + b^2}} \cdot b \cdot N_z$$

$$= a^2 b^2 \frac{\sqrt{3}}{\sqrt{3a^2 + b^2}}$$

$$V_s = \frac{\pi}{6} ab^2 N_x \cdot N_y \cdot N_z$$

$$n = 1 - \frac{V_s}{V} = 1 - \frac{\pi}{6} \frac{ab^2}{a^2 b^2} \sqrt{\frac{3a^2 + b^2}{3}}$$

$$n = 1 - \frac{\pi}{\sqrt{3}, 6} \frac{\sqrt{3a^2 + b^2}}{a}$$

3.2.3 Double Staggered Packing

The same as single staggered except that the ellipsoids in the upper layer rest in the depression between two adjacent ellipsoids in the lower layer.

$$V = aN_x \cdot \frac{\sqrt{3}}{2} \frac{2ab}{\sqrt{3a^2 + b^2}} N_y \cdot \frac{\sqrt{3}}{2} bN_z$$

$$= \frac{3}{2} \frac{a^2 b^2}{\sqrt{3a^2 + b^2}} N_x \cdot N_y \cdot N_z$$

$$V_s = \frac{\pi}{6} ab^2 N_x \cdot N_y \cdot N_z$$

$$n = 1 - \frac{V_s}{V} = 1 - \frac{\pi}{6} ab^2 \frac{2\sqrt{3a^2 + b^2}}{3a^2 b^2}$$

$$n = 1 - \frac{\pi}{9} \frac{\sqrt{3a^2 + b^2}}{a}$$

3.2.4 Pyramidal Packing

Ellipsoids are arranged so that each ellipsoid in one layer, as in cubical packing, but ellipsoid of the upper layer rests in the depression between four adjacent ellipsoids in the lower layer.

$$V = aN_x \cdot b \cdot N_y \cdot \frac{b}{\sqrt{2}} \cdot N_z$$

$$= \frac{ab^2}{\sqrt{2}} N_x \cdot N_y \cdot N_z$$

$$V_s = \frac{\pi}{6} ab^2 N_x \cdot N_y \cdot N_z$$

$$n = 1 - \frac{V_s}{V} = 1 - \frac{ab^2}{ab^2} \sqrt{2}$$

$$n = 1 - \frac{\pi}{6} \sqrt{2}$$

3.2.5 Tetrahedral Packing

In this packing, ellipsoids are arranged as in single stagger, but the upper layer has each ellipsoid resting in the depression between three adjacent ellipsoids in the layer below.

$$V = aN_x \cdot \frac{\sqrt{3}}{2} bN_y \sqrt{\frac{2}{3}} \cdot \frac{2ab}{\sqrt{3a^2 + b^2}}$$

$$= a^2 b^2 \sqrt{\frac{2}{3a^2 + b^2}} N_x \cdot N_y \cdot N_z$$

$$V_s = \frac{\pi}{6} ab^2 N_x N_y N_z$$

$$n = 1 - \frac{V_s}{V} = 1 - \frac{\pi}{6} \frac{ab^2 \sqrt{3a^2 + b^2}}{\sqrt{2} a^2 b^2}$$

$$n = 1 - \frac{\pi}{\sqrt{2} \cdot 6} \frac{\sqrt{3a^2 + b^2}}{a}$$

Plots of theoretical packing characteristics of ellipsoids in different modes of packing for different ratios of a/b are given in Fig. 3.2.

3.3 Bulk Density

Since the Grain Standard Act of 1916 was passed, wheat has been graded according to the standards established

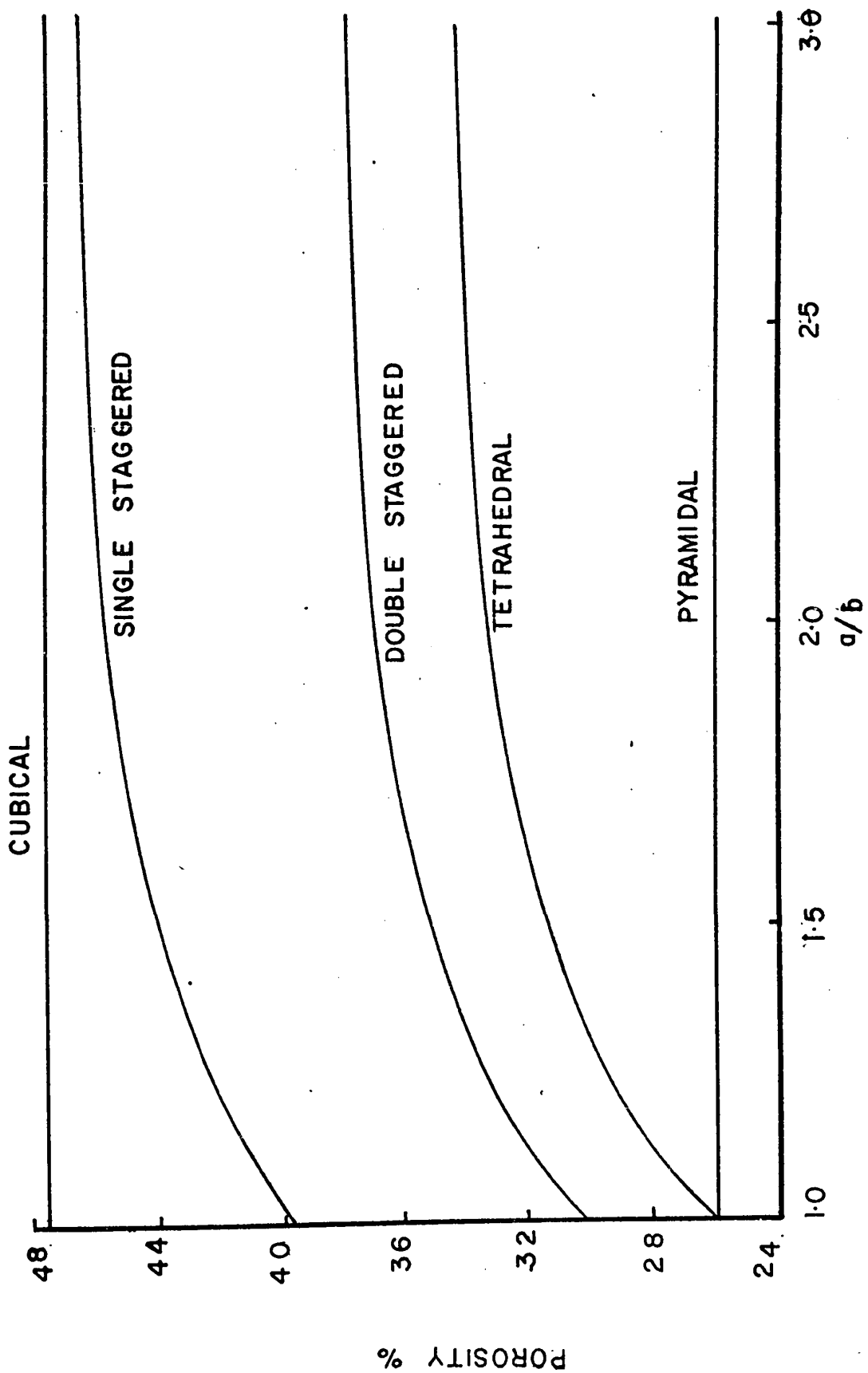


FIG 3.2 THEORITICAL PACKING OF ELLIPSOIDS

by the Federal Government. Bulk density or pounds per bushel is an important factor in the grading system. Moisture content is another important factor because it affects the wheat grade and indirectly affects the market value of wheat grain.

Volume of grain is commonly measured by the bushel for marketing purposes, and by cubic feet for engineering purposes. The standard bushel, as defined by the Canada Bureau of Standards, is a unit volume which will hold 77.6274 pounds of distilled water at a temperature of 39.2°F. A cubic foot holds 62.424 pounds of water at 39.2°F. Thus,

$$\begin{aligned} 1 \text{ bushel} &= \frac{77.6274}{62.424} \\ &= 1.2435 \text{ cubic feet.} \end{aligned}$$

3.3.1 Theory

The theoretical concept of the effect of moisture on the bulk density of wheat grain is studied by considering weight-volume relationships of the granular mass. The granular mass is commonly considered to consist of a network of solid particles, enclosing voids of varying sizes. We can designate the total volume of a given soil sample by V, which consists of two parts, the volume of solid matter

V_s and the volume of voids V_v . In the study of soils, two common relationships of these three elements of volume are in use. One is void ratio (e) and the other is porosity (n).

$$e = \frac{V_v}{V_s} \quad 3.3.1.1$$

$$n = \frac{V_v}{V} \times 100 \quad 3.3.1.2$$

Void ratio is expressed as a ratio and porosity in percentage. Porosity is used in many branches of engineering and is more familiar to engineers in general. The relation between void ratio and porosity is expressed by the equations:

$$e = \frac{n}{1 - n} \quad 3.3.1.3$$

$$n = \frac{e}{1 + e} \quad 3.3.1.4$$

The volume of voids (V_v) is subdivided into two parts: volume of water (V_w) and volume of air (V_a). In the study of the properties of wheat grain, the condition of free water or volume of water (V_w) is never encountered in the pore spaces as in the study of soils. Examination during this research showed the occurrence of no free water even under high confining pressure.

To calculate porosity from bulk density or

unit weight the specific gravity (G) is required. The specific gravity is defined as the ratio between unit weight of the given material and the unit weight of some reference substance. In most instances the reference substance is pure water at 4°C.

$$G = \frac{\gamma}{\gamma_w} \qquad 3.3.1.5$$

γ = unit weight of the solid kernels

γ_w = unit weight of water at 4°C.

For studying the engineering properties of wheat grain, the effect of moisture change in the kernel must be investigated. The weight and size of the individual particles may change. The porosity of the mass may change. The shape of the pore spaces may change. The total effect of the moisture change on the grain may be the accumulated individual effects of any or all of the above listed items.

A kernel of grain is not an inert material like most particles of soil. A kernel of grain is composed of a large number of different types of cells which respond to the process of osmosis when exposed to moisture. The water can flow into the cells and cause the cells to swell, thus changing the kernel weight and volume and affecting its specific gravity. In the lower moisture content range (below 16.0 per cent), the grains are hard, brittle and have a smooth

surface. In the higher moisture content range (over 16.0 per cent), the grains become soft, deformable and have more surface roughness.

Moisture content affects the bulk density of a granular mass, when compaction energy is applied. The amount of compaction attainable depends upon the friction between the particles and energy of compaction used to overcome this friction. In the study of the minimum bulk density of wheat grain (see section 4.5.3), no energy of compaction is applied. The change in bulk density is caused only by the effect of moisture on the kernels of wheat. From a study of maximum bulk density of wheat by the vibratory method, it can be assumed that energy of compaction obtained from the vibration of the sample also accounts for part of the change in the bulk density.

3.4 Shear Strength

Shear strength of cohesionless granular materials can be expressed by shear strength (s), coefficient of friction ($\tan \phi$) or angle of internal friction (ϕ). The frictional coefficient of granular materials is derived from sliding friction between the grains and interlocking which

depends upon the size, shape and structural packing of the grains. The coefficient of friction of a material on supporting structure is the tangent of the angle of wall friction (δ). The lateral pressure on storage structures depends on both ϕ and δ . So the analysis of these factors is required for accurate storage structure design.

3.4.1 Strength Theory

The coefficient of friction (μ) and coefficient of wall friction ($\hat{\mu}$) were studied by direct shear and triaxial compression tests. The theory of both testing techniques is based on the theory of failure and is discussed in section A.1, Appendix A.

CHAPTER 4

TESTING PROGRAM

4.1 General

This chapter includes a description of the material used and outlines the method of obtaining wheat samples at required moisture contents. The apparatus and experimental procedures used in the investigation of the minimum bulk density and maximum bulk density (the latter being found by vibratory methods), in obtaining the shear strength parameters of wheat by direct shear tests and tri-axial tests, and in obtaining the shearing resistance parameters of wheat on selected structural surfaces, wood, steel, and concrete, are discussed.

4.2 Material Used

The wheat used for the investigations was a winter wheat, grown in Alberta. It was obtained from Toronto Elevators Limited, Toronto, Ontario in 1965. The average

size of the wheat grain at different moisture contents is given in Table 4.1. The major and minor axes of the grain vary from 0.229 and 0.107 inches to 0.240 and 0.123 respectively in the moisture content range from 9.3 to 28.4 per cent. The a/b ratio varies from 2.17 to 1.91 in this moisture content range. The equilibrium moisture content of the wheat in the laboratory was 12.5 per cent.

Table 4.1

Size of wheat grain



Moisture content	a	b	a/b
	inches	$\frac{(b_1 + b_2)}{2}$ inches	
	(average of ten measurements)		
9.3%	0.226	0.104	2.17
12.2%	0.229	0.107	2.14
16.8%	0.231	0.113	2.04
22.0%	0.240	0.121	1.98
28.4%	0.235	0.123	1.91

4.3 Procedure of Obtaining Wheat Sample of Required Moisture Content

Samples of different moisture contents were used for testing. It was necessary therefore to condition the grain to the proper moisture content.

The following is an example of the calculations used: the equilibrium moisture content of the wheat was 12.51 per cent on a wet basis (w.b.). To raise the moisture content of the grain from 12.51 to 16.71 per cent w.b. required the addition of $16.71 - 12.51 = 4.20$ per cent of water. For 5.0 kilograms of weighed sample at 12.51 per cent w.b., the weight of water required was $5 \times 0.042 = 210$ grams. Now a 5.0 kilograms weighed sample of grain, along with 210 grams of free water were sealed together inside a 3 gallon plastic container.

In order to keep the water from settling to the bottom of the grain mass and over-saturating some of the kernels but not wetting the other kernels, a machine was used which contained four parallel revolving rollers, spaced $4\frac{1}{2}$ " c/c. The plastic container was placed on these rollers and rotated for 24 hours. At the end of this period, the water had been thoroughly mixed with the grain and had been absorbed into the grain. Figure 4.3.1 displays the drive unit and rollers of the mixing machine used to keep the bottle moving during

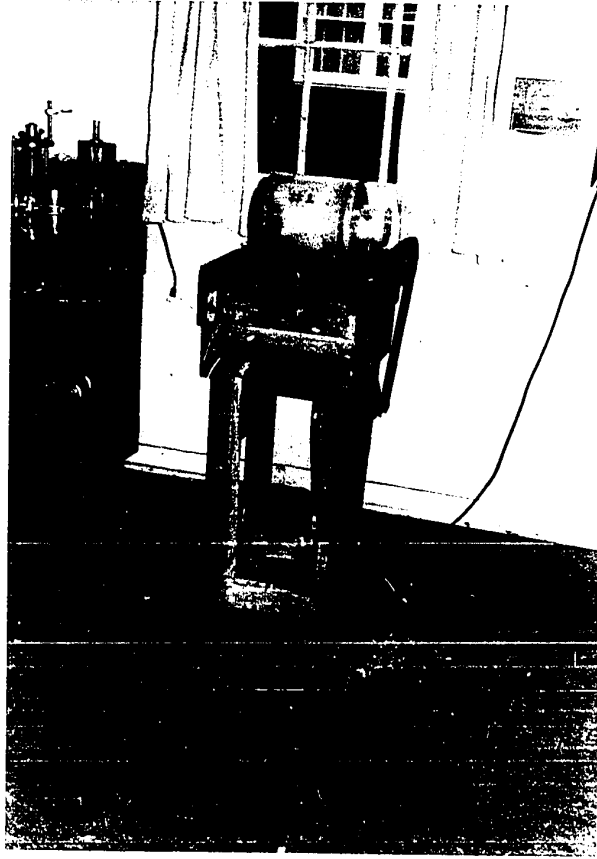


Fig. 4.3.1 Mixing Unit

the conditioning of the grain.

The sample was then stored in a vapour tight polythene bag until it was used.

Similar procedures were adopted for obtaining samples of other required moisture content percentages. It was found that samples with a high moisture content should be stored in a cool room to prevent spoilage.

In preparing samples of lower moisture content than the equilibrium moisture content, the grain was dried in the oven for 3 to 4 hours at 100°C. and then rotated in a plastic container for 24 hours on the drive unit. Then the sample was stored in a polythene bag until used.

The samples were prepared on a wet basis, but all calculations for determining the moisture contents of the samples were made on a dry basis. The conversion of moisture content of the samples from a dry basis to wet basis and vice versa was based on the equation

$$\%m.c.(dry\ basis) = \frac{100(\%m.c.(wet\ basis))}{100 - (\%m.c.(wet\ basis))}$$

4.4 Moisture Content Determination

About 10 grams of wheat were placed in a dish (oven dried at 130°C. for roughly 30 minutes and then cooled)

from the large sample in the polythene bag and then weighed. The weighed sample was inserted into the oven set at 130°C. The time of heating was measured from the moment when the oven regained a temperature of 130°C. (Browne 1962). The sample was heated in the oven for 16 hours overnight. After this time, the dishes were removed from the oven and put in a desiccator to cool. The cooled dishes plus wheat grain were weighed to the accuracy of two decimal places of a grain. The moisture content (m.c.%) was calculated:

$$\text{m.c.\%} = \frac{\text{weight of water}}{\text{weight of dry sample}} \times 100$$

4.5 Apparatus and Experimental Procedure

To obtain the data for determining the effect of moisture on bulk density, shear strength, shear resistance of wheat on structural surfaces and other related properties of grain it was necessary to perform the following tests.

4.5.1 Specific Gravity Test

To determine the porosity from the bulk density, it is necessary to know the specific gravity (G) of the wheat. The transition equations involving specific gravity, porosity

and bulk density are given:

$$G = \frac{W_s \cdot 1}{V \gamma_w} \left[\frac{1}{1 - \frac{n}{100}} \right] \quad 4.5.1.1$$

$$n = 1 - \frac{\gamma}{G \gamma_w} \quad 4.5.1.2$$

W_s = weight of wheat

V = volume of container

$\gamma = \frac{W_s}{V}$ = bulk density

γ_w = unit weight of water at 4°C.

4.5.1.1 Apparatus

A pyrex glass pycnometer of 500 ml at 20°C. with a tolerance of 0.30 ml was used. The other accessories used were toluene, a vacuum pump, a balance (0.01 gram sensitivity), a thermometer graduated to 0.1°C. and a pipette. The apparatus is shown in Fig. 4.5.1.

4.5.1.2 Procedure

The pycnometer was cleaned and weighed. One hundred and fifty grams of wheat at the desired moisture content was put into the pycnometer which was half filled with de-aired toluene. The air trapped in the grains was removed

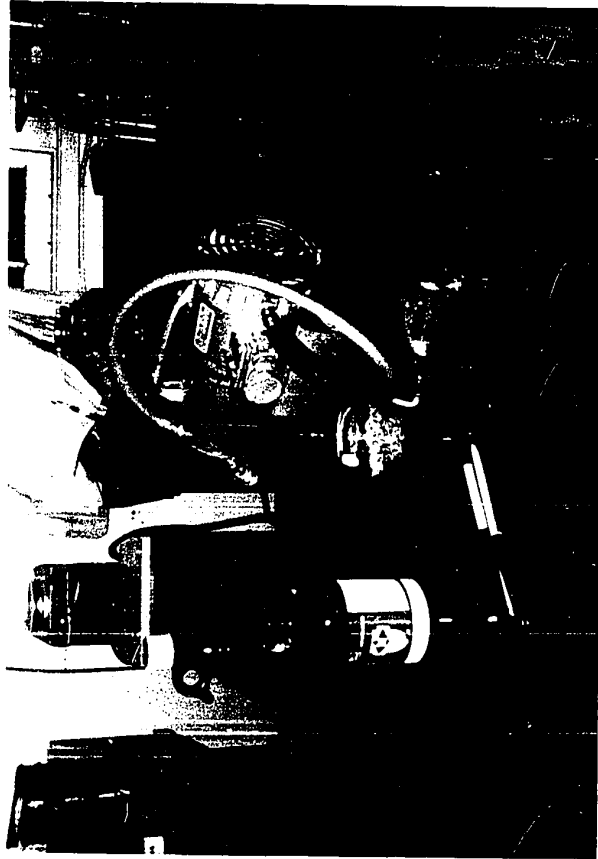


Fig. 4.5.1 Specific gravity apparatus

by the application of vacuum to the suspension of grains in toluene with a vacuum pump. This process was continued until all the entrapped air in the creases of the grains was removed. Then more toluene was added to bring the bottom of the meniscus to the calibration mark of the pycnometer. The pycnometer with wheat plus toluene was weighed and the temperature of the toluene was recorded.

4.5.1.3 Calculation

$$G = \frac{W_s G_t}{W_s - W_1 + W_2} \quad 4.5.1.3$$

G_t = specific gravity of toluene at $T^{\circ}\text{C}$.
temperature

W_s = weight of wheat

W_1 = weight of pycnometer, wheat and toluene

W_2 = weight of pycnometer and toluene

W_2 is calculated from the given equation

$$W_2 = W_B + V_B (1 + T \cdot \Delta T \cdot \epsilon) (DT - \gamma_a) \quad 4.5.1.4$$

W_B = weight of clean dry bottle

V_B = calibrated volume of pycnometer at 20°C .

T = temperature in $^{\circ}\text{C}$.. at which W_2 is desired

ΔT = $T - 20$ in $^{\circ}\text{C}$.

ϵ = thermal coefficient in cubical expansion

for pyrex glass = 0.100×10^{-4} per $^{\circ}\text{C}$.

DT = unit weight of toluene at T^oC.

γ_a = unit weight of air at temperature T and atmospheric pressure (an average value of accurate enough for tests in 0.0012 gram per cc)

DT required in equation 4.5.1.4 is calculated from the equation

$$DT = [D_s + 10^{-3}.A(T - T_s) + 10^{-6}.B(T - T_s)^2 + 10^{-9}.C(T - T_s)^3] \quad 4.5.1.5$$

The International Critical Tables of Numerical Data (1928) gives values of D_s, A, B and C of toluene at T_s^oC. DT from 4.5.1.5 is substituted in equation 4.5.1.4 to find W₂. W₂ is then substituted in equations 4.5.1.3 to obtain the value of G.

The values of specific gravities at different moisture content are discussed in chapter 5.

4.5.2 Crushing Load Test

This test was done to determine what static compaction load would cause the kernel to crush. These tests were necessary to allow a study to be made of the effect of static pressure on the one dimensional compression (therefore

porosity) of wheat grain.

4.5.2.1 Apparatus

A compression machine was used to apply a static load on individual wheat grains. The load on the grain was measured by a 100 lbs. calibrated proving ring. The deformation of the grain was measured by a dial indicator. The detail of the apparatus is shown in Fig. 4.5.2.

4.5.2.2 Procedure

A grain was positioned on the base of the compression machine. The base was then raised to make contact between the loading ram and the grain. The compressive load on the grain was applied at the rate of 0.005 inches per minute. The readings on the proving ring were recorded at definite intervals of the vertical deformation of the grain until the grain kernel crushed or had 20 per cent deformation.

For each moisture content, grains were positioned between the loading ram and the compression machine base in two different orientations, crease plane vertical, and crease

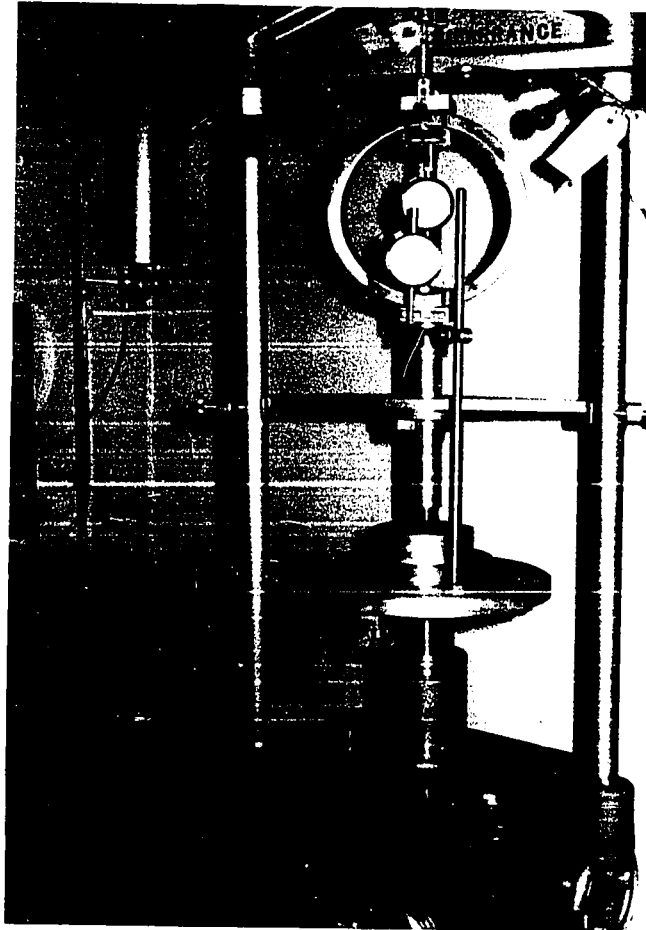


Fig. 4.5.2 Triaxial Compression Machine

plane horizontal. At least five grains were tested for each orientation.

The results of the crushing load of grains at varying moisture content are discussed in section 5.3 of chapter 5.

4.5.3 Minimum Bulk Density Test

4.5.3.1 Apparatus

The apparatus used is shown in Fig. 4.5.3. This apparatus consists of a C.B.R. mould measuring 7 inches high and 6 inches in diameter and holding 0.1145 cubic feet. The mould has a base and a 2 inch collar extension (not used in the test). The other accessories used were a funnel, a scoop, a 2-gallon pail, a steel straight edge, and a balance.

4.5.3.2 Procedure

The mould was filled from four different pouring devices:

- i) a funnel 1 inch above the surface of the wheat

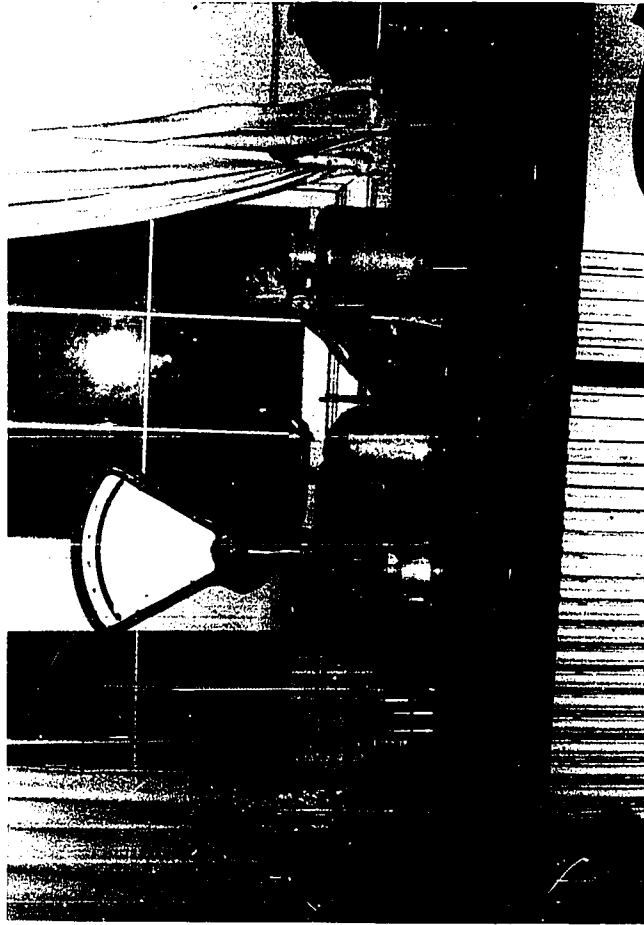


Fig. 4.5.3 Minimum Density Apparatus

- ii) a scoop as close to the surface as possible
- iii) a half filled 3-gallon pail resting on the tip of the mould
- iv) a half filled 3-gallon pail 6 inches above the mould.

The grain in the mould was leveled by striking the surface with the steel straight edge. The mould and its contents were then weighed on a balance.

4.5.3.3 Calculations

The minimum bulk density or maximum porosity was calculated from the equations:

$$\gamma_{\min} = \frac{W_s}{V} \text{ lbs. per cu. ft.} \quad 4.5.3.1$$

$$n_{\max} = 1 - \frac{\gamma_{\min}}{G \gamma_w} \quad 4.5.3.2$$

γ_{\min} = minimum bulk density

W_s = weight of wheat in the mould in lbs.

V = volume of the mould = 0.1145 cu. ft.

n_{\max} = maximum porosity

G = specific gravity of wheat grain

γ_w = unit weight of water at 4°C.

Bulk density and porosity results are discussed in chapter 5.

4.5.4 Maximum Bulk Density Test

The maximum bulk density was investigated by vibratory and static tests.

4.5.4.1 Vibratory Test

4.5.4.1.1 Apparatus

A standard ASTM vibrating table 20 x 20 inches, actuated by an electromagnetic vibrator, with a C.B.R. mould (for detail see section 4.5.3.1) fastened on its top, was used. The vibrator is a seminoiseless type with a net weight of 175 lbs. The vibrator has a frequency of 3600 vibrations per minute and its amplitude of vibration could be regulated by a rheostat control.

A surcharge plate 5 7/8 inches diameter and 1/2 inch in thickness and surcharge weights were used. The other accessories needed were a funnel, a timing device, a steel straight edge and a balance.

4.5.4.1.2 Procedure

The mould was filled from a funnel in a steady stream. The bottom of the funnel was adjusted so that the free fall of the grain was 1 inch above the centre of the mould top. The surcharge plate was placed on the wheat surface and the surcharge weights were then lowered onto the surcharge plate.

The amplitude of vibration was set with a rheostat, reading from 0 to 100. The vibrating table was calibrated under no load conditions and the relationship between the amplitude of vibration and the rheostat reading is shown in Fig. 4.5.4. It was not possible, however, to calibrate the vibrating table for any load on the table. Therefore a calibration curve was calculated based on the work by Pettibone and Hardin (1965) and the relationship obtained in the laboratory under no load conditions. The calibration curve is shown in Fig. 4.5.5.

The required amplitude of vibration was set on the rheostat and the loaded specimen vibrated for a desired period of time.

The surcharge weight, surcharge plate and collar extension of the C.B.R. mould were removed. The grain

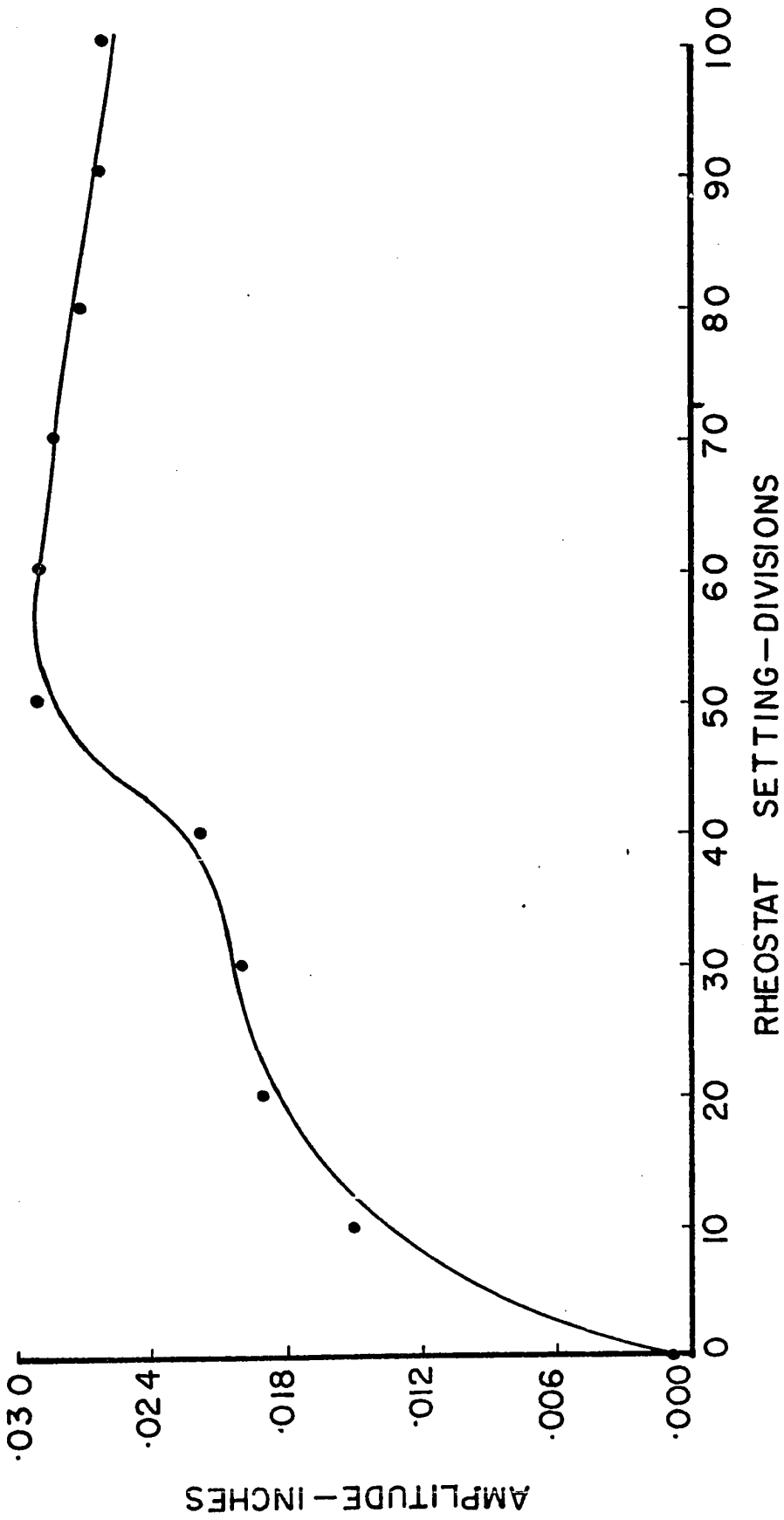


FIG 4-5-4 RELATIONSHIP BETWEEN AMPLITUDE OF VIBRATION AND RHEOSTAT SETTING AT ZERO LOAD

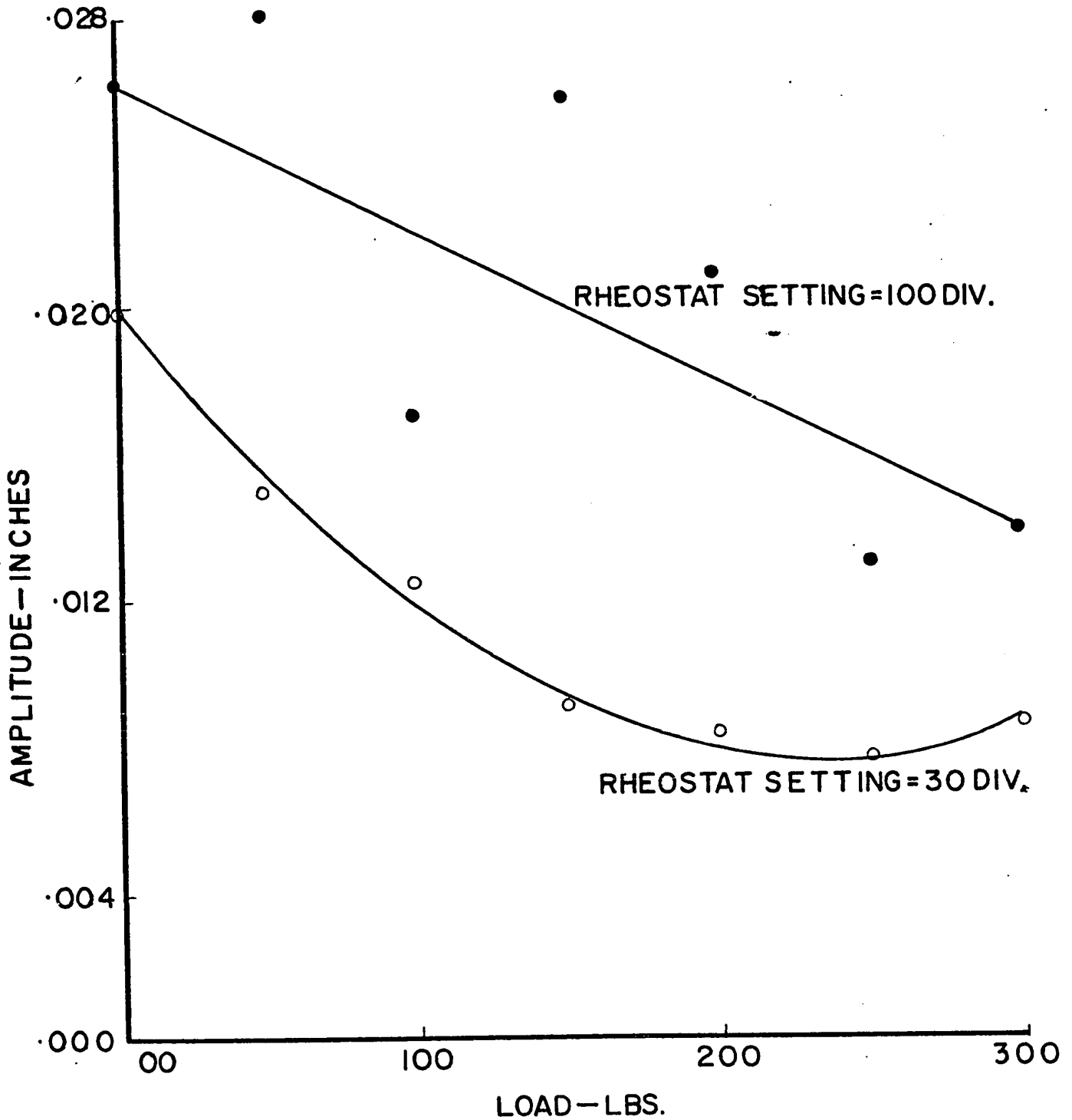


FIG.4.5.5 RELATIONSHIP BETWEEN AMPLITUDE OF VIBRATION AND LOAD

in the mould was leveled by striking the surface with a steel straight edge and then the mould and its contents were weighed.

Tests were performed to study the effects of the magnitude of surcharge, the amplitude of vibration and the time of vibration on the maximum bulk density of wheat at different moisture contents. The effect of frequency of the table was not studied because previous research (Forssblad 1965) has shown that frequencies of vibration greater than 1500-2000 rpm have no effect on the unit weight and that maximum density is attained.

4.5.4.1.3 Calculations

The maximum bulk density or minimum porosity was calculated from the equations:

$$\gamma_{\max} = \frac{W_s}{V} \text{ lbs. per cu. ft.} \quad 4.5.4.1$$

$$n_{\min} = 1 - \frac{\gamma_{\max}}{G \gamma_w} \quad 4.5.4.2$$

γ_{\max} = maximum bulk density

n_{\min} = minimum porosity

W_s , G , V and w are defined in section 4.5.3.3.

The results are given and discussed in section 5.4.3.

4.5.4.2 Static Compression Test

These tests were made to predict the bulk density or porosity of wheat at different depths in filled bins. The change in bulk density affects the shear strength parameters of the wheat which further affects the design of the bins.

4.5.4.2.1 Apparatus

Standard soil consolidation apparatus was used to determine the maximum bulk density or minimum porosity of wheat under static loads. This apparatus works on the lever arm principle and has a lever ratio of 11:1. Two containers which laterally confined the sample were used: 6 inches diameter and 1¼ inches high and 2.5 inches diameter and 1.012 inches high, respectively. The vertical compression of the sample was read on a dial indicator. The apparatus is shown in Fig. 4.5.6.

The other accessories used were: a vernier caliper, a timing device and a balance.



Fig. 4.5.6 Consolidation Unit

4.5.4.2.2 Procedure

A weighed mass of wheat grain was placed in the container by pouring the wheat through a funnel (6 inches diameter and $1\frac{1}{4}$ inches high). A loading disc was placed on the wheat sample and the sample was then compressed by applying a vertical load to achieve the required initial porosity. The assembled container was placed on the consolidation unit and the sample was subjected to static pressure. The vertical compression of the sample resulted in a decrease of sample thickness while the diameter remained constant. When the compression of the sample ceased, it attained an equilibrium porosity at a given applied static pressure. The load was increased to a higher constant value. The compression of the sample was restarted and after some time it attained equilibrium at a lower porosity.

The test was started with 0.00 psi initial static pressure, and the pressure was increased to the maximum of 14.50 psi in increments of 0.00, 0.46, 0.92, 1.65, 3.08, 5.95, 8.80 and 14.50 psi. After reaching equilibrium at 14.50 psi, the static pressure was reduced to 0.00 psi in the same increments. The reading on the dial indicator was recorded for every increment of loading and unloading of the sample.

Wheat samples of different moisture contents were tested at the same initial porosity.

In a small container (2.5 inches diameter and 1.012 inches high) the wheat samples of different moisture contents were tested at different initial porosities with no preload applied. Each sample was loaded to a maximum pressure of 21.00 psi in increments of: 0.00, 0.52, 1.05, 2.02, 3.74, 7.25, 14.1 and 21.00 psi. After attaining equilibrium at 21.00 psi, the sample was unloaded using the same increments back to 0.00 psi.

4.5.4.2.3 Calculation

If A is the area of container, L is the initial height of the sample, and W_s is the weight of wheat sample used, then

$$\text{Initial bulk density } \gamma_i = \frac{W_s}{A \times L}$$

$$\text{Initial porosity } n_i = 1 - \frac{\gamma_i}{\gamma_w}$$

Now if the sample is subjected to an increment of load and ΔL is the amount of compression of the sample, then

$$\text{Final bulk density } \gamma_f = \frac{W_s}{A \times (L - \Delta L)}$$

$$\text{Final porosity } n_f = 1 - \frac{\gamma_f}{\gamma_w}$$

$$\text{Strain } \epsilon = \frac{\Delta L}{L}$$

The results are given and discussed in section 5.4.6.

4.5.5 Direct Shear Test

4.5.5.1 Apparatus

A strain controlled direct shear machine was used to apply shear stress to the sample in a 5 inch square shear box. The applied shear force on the sample was measured by a calibrated proving ring. The vertical and horizontal deformations were recorded by means of two dial indicators. The confining pressure on the sample was applied by a counter balance assembly. The apparatus is shown in Fig. 4.5.7.

The other accessories used were a steel foot rule, a tamper, a vernier caliper and a balance.

4.5.5.2 Procedure

A weighed quantity of wheat was poured into the shear box. The wheat was compacted until the required density was achieved by bringing the pressure pad



Fig. 4.5.7 Direct Shear Apparatus

to the necessary precalculated height. The shear box assembly and its contents were placed on the direct shear machine, and a confining pressure of 1 psi was applied on the sample. The shear test on the sample was run at a shearing rate of 0.05 inch per minute. The readings on the proving ring and the vertical deformation dial were recorded after fixed intervals of shearing deformation of the sample as indicated on the horizontal deformation indicator. The test was continued until the peak load on the proving ring was recorded and the readings started to decrease. The tests were repeated on identical samples under confining pressures of 2.0 and 3.0 psi.

4.5.5.3 Calculation

A graph was plotted with shear deformation as abscissa and shear force as ordinate for each test (refer to Fig. 4.5.8). From this graph, values of shear stress at failure were determined for each test. Another graph was plotted with normal load as abscissa and shear stress at failure as ordinate from which shear strength parameters ϕ and c were determined. (Refer to Fig. 4.5.9).

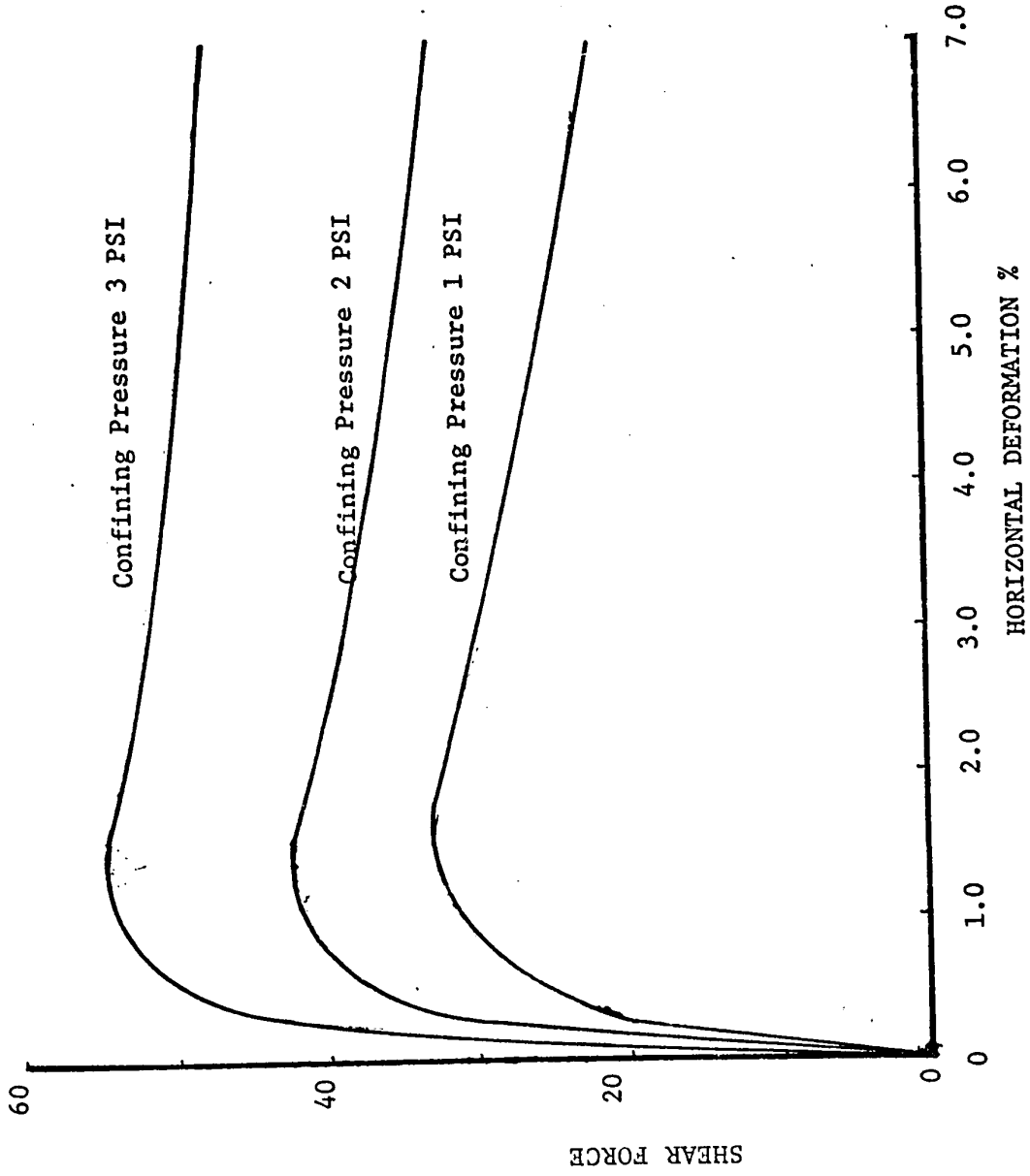


FIG. 4.5.8 SHEAR FORCE - HORIZONTAL DEFORMATION CURVE DIRECT SHEAR TEST

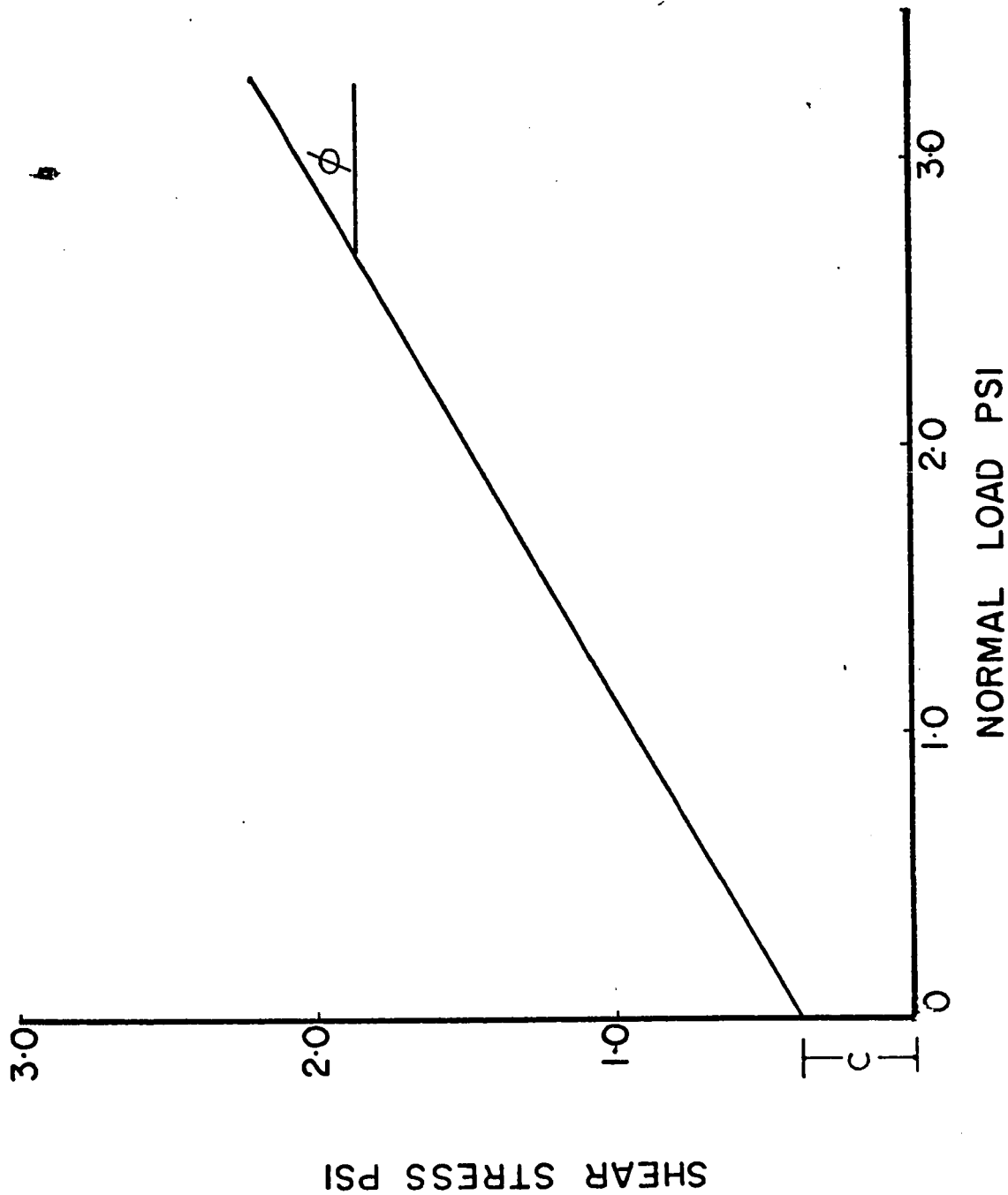


FIG. 4.5.9 FAILURE ENVELOPE FOR DIRECT SHEAR TEST

Direct shear tests were done on samples of different moisture contents at different bulk densities.

Complete results of the direct shear tests studies are discussed in section 5.5.2.

4.5.6 Triaxial Compression Test

4.5.6.1 Apparatus

A triaxial compression machine fitted with a calibrated proving ring and a dial gauge to measure axial deformation, was used for this test. The triaxial cell used was designed to handle 2 inch diameter by 4 inches high test specimens. The confining pressure on the sample was applied by means of mercury columns from a standard self compensating mercury control system. The apparatus is shown in Fig.

4.5.10.

The other accessories used were porous stones, rubber membranes, a split mould, a tamper, rubber o-rings, a steel foot rule, a vernier caliper, and a balance.

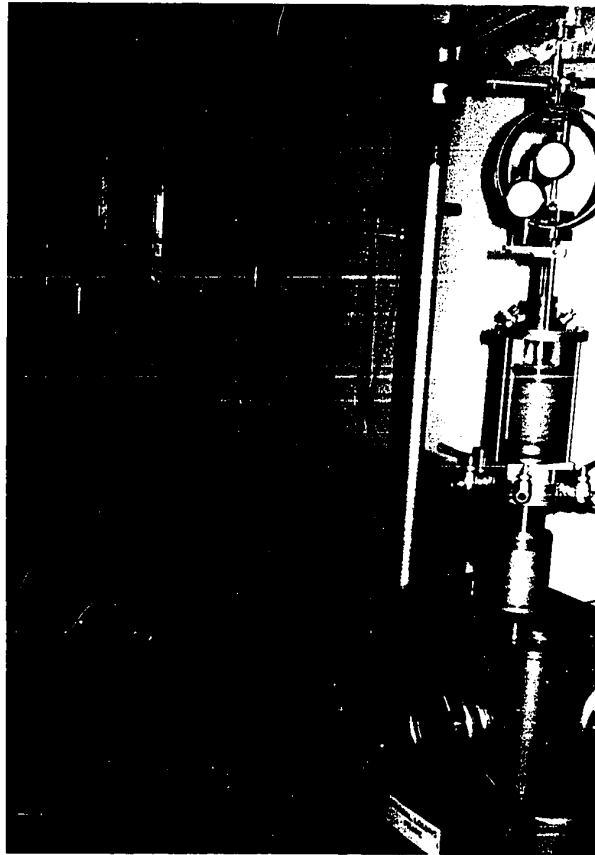


Fig. 4.5.10 Triaxial Apparatus

4.5.6.2 Procedure

Grain samples were formed inside a split mould lined with a rubber membrane. The lower end of the membrane was clamped to the base of the triaxial cell with rubber o-rings. A 2 inch diameter porous circular disc was placed on the base. The weighed quantity of wheat grain was poured into the membrane. The wheat was compacted in layers by a hand tamper to achieve the required bulk density. A porous disc and a loading cap were placed on top of the grain surface and the membrane was sealed to the cap with o-rings. A small suction was applied to the grain sample, after which the split mould was removed, and diameter and height measurements made. The formed sample was then placed within the triaxial cell.

The triaxial cell assembly was placed in the compression machine, and the confining pressure was then applied to the sample with the mercury control system. The loading ram was brought into contact with the loading cap and the initial readings of the proving ring and dial gauge were recorded. The compressive load was applied at a constant axial-deformation rate of 0.006 inch per minute. The readings of the proving ring and the dial gauge were recorded for every

0.25 per cent strain of the sample continuously throughout the loading period.

The tests were run in multi-stages. The sample was tested under three different confining pressures of 10, 20 and 30 psi. The test was started every time with a confining pressure of 10 psi and the deviator stress was applied until imminent failure occurred at this confining pressure. The deviator stress was then released and the new confining pressure of 20 psi was applied. The deviator stress was increased until the maximum value of the deviator stress was again reached. The sequence was repeated for a confining pressure of 30 psi and readings for this stage were continued after the maximum deviator stress was obtained.

The rebound of the specimen was recorded for every stage on the release of the deviator stress. An area correction was made when the deviator stress for the 20.0 psi and 30.0 psi confining pressures were calculated.

4.5.6.3 Calculations

See section A.1, Appendix A. The complete results of the triaxial tests are given in section 5.5.3.

4.5.7 Shear Resistance of Wheat on Structural Surfaces

4.5.7.1 Apparatus

A strain controlled direct shear machine was used. The lower part of the shear box was replaced by a structural surface with the shear stress being applied between the wheat grains and this structural surface. The shear force between the grain and the structural surface was measured by a calibrated proving ring and the vertical and horizontal deformation were recorded by two dial indicators. The confining pressure on the sample was applied by a counter balance assembly.

The accessories used were a steel foot rule, a tamper, a vernier caliper and a balance.

4.5.7.2 Procedure

The same procedure as discussed in section 4.5.5.2 was used.

4.5.7.3 Calculations

See section 4.5.5.3. The data for shearing resistance, porosity, moisture content, and structural surface are given in section 5.6.1.

CHAPTER 5

DISCUSSION OF TEST RESULTS

5.1 General

The test results are discussed and analysed in this chapter. These include specific gravity, crushing load, minimum bulk density, maximum bulk density, direct shear, triaxial shear, and direct shear with selected structural surfaces.

The minimum and maximum bulk densities obtained experimentally are compared with those obtained in the study of the theoretical packing of uniform ellipsoids presented in chapter 3. All test results are compared with the test results obtained by other researchers.

5.2 Specific Gravity

The effect of moisture content on the specific gravity of wheat is shown in Fig. 5.1 and listed in Table A.1, Appendix A. It can be seen that specific gravity decreases

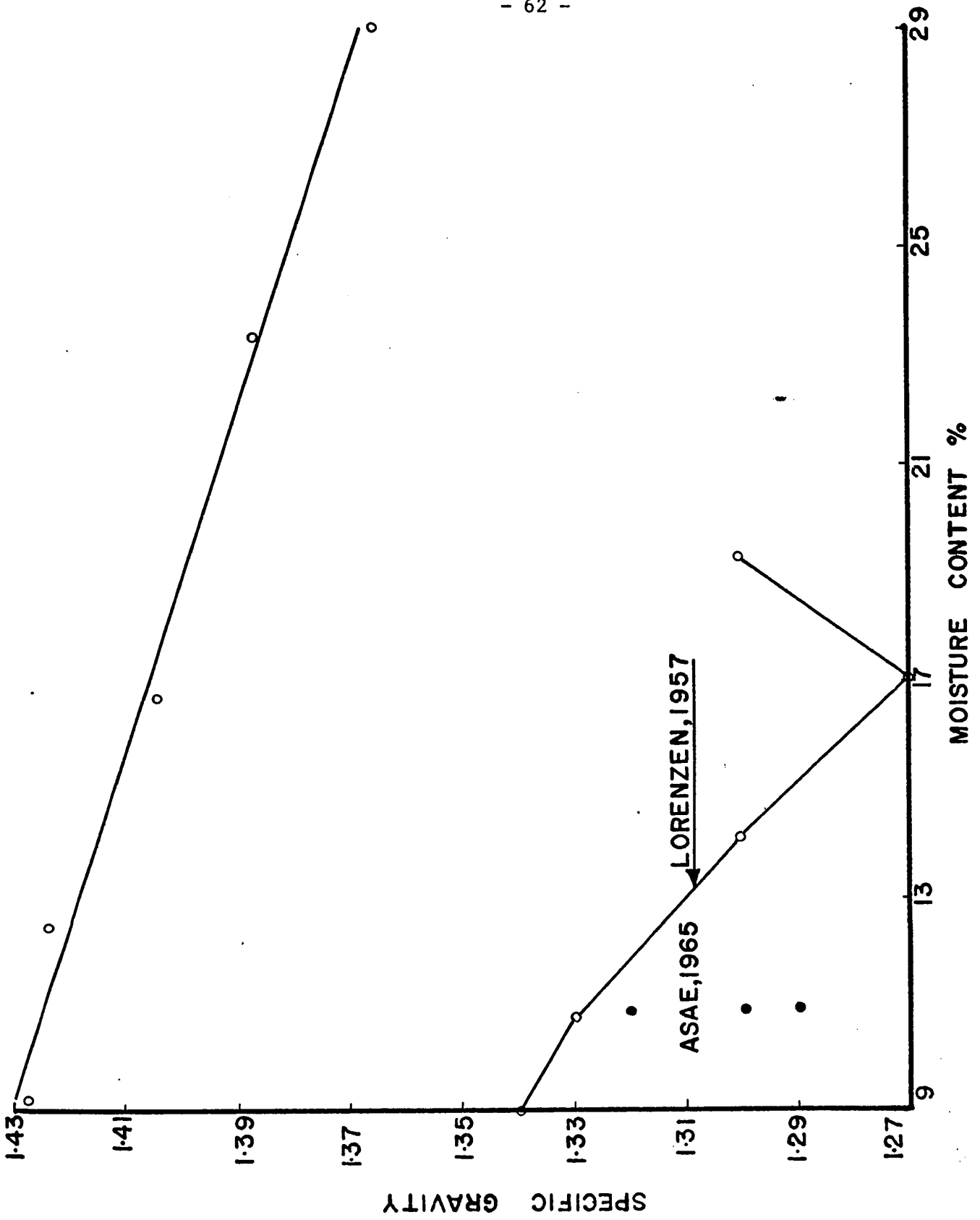


FIG.5.1 SPECIFIC GRAVITY OF WHEATS

as the moisture content of the wheat grains increases. The change in specific gravity is equivalent to a decrease of 0.0032 for one percentage increase in moisture content. The values of specific gravity are higher than the values given in the Agricultural Engineers Year Book (1965). These values were found for different types of wheat.

Lorenzen (1957) measured the porosity of wheat by pouring a measured volume of grain into a 1000 cc. graduated cylinder containing a measured amount of toluene. He calculated the specific gravity from transition equations involving specific gravity, bulk density and porosity. The specific gravity obtained by Lorenzen is lower than those found in this work. This is because Lorenzen made specific gravity tests on different wheat varieties having different biological composition. He also did not remove the air in the voids between the wheat kernels, which might have resulted in lower values of specific gravity. In the work being discussed, care was taken to remove any air entrapped in the creases of the grains by saturating the voids with toluene under negative pressure.

The decrease in specific gravity with increase in moisture content is caused by the wheat kernels absorbing water into their cells, resulting in the swelling of the kernels. An effective decrease in specific gravity of the

wheat grains therefore takes place.

5.3 Crushing Load of Wheat Kernels

These experiments were performed on wheat kernels to find a relation between the compression load taken by the kernel and corresponding strain it has undergone. In order to study the effect of surcharge load on porosity, it was important to know the permissible load to which grains at a particular moisture content could be subjected before crushing changed them into an entirely different material.

The crushing load of grain is affected by its environmental history, i.e., stage of maturity at which the grain was cut and threshed or time after maturity at which the grain was cut and threshed, changes in and method of changing moisture content, method of handling and storage conditions. These factors were kept constant for conducting these tests.

Load-deformation characteristics of wheat kernels at five different moisture contents of 9.0, 12.3, 15.8, 22.5, and 29.7 per cent were studied. For each moisture content, the grains were tested for two different orientations namely crease plane vertical and crease plane horizontal. The

load deformation curves are plotted at moisture contents of 15.8, 22.5 and 29.7 per cent for both orientations (Fig. 5.2). Load deformation curves for the 9.0 and 12.3 per cent moisture content could not be plotted because of very small deformations (1 to 2 per cent) at failure.

At low moisture contents such as 15.8 per cent or lower, the tests for both positions of the grain show that the grains are brittle, are more resistant to deformation, have a higher crushing load and have a linear load-deformation relationship. At higher moisture contents, the grains are easily strained, are permanently deformed at low loads and have smaller crushing loads.

The maximum compression load taken by the grain at any strain is regarded as the criterion for the crushing load. In cases, where maximum compression load was not reached even at high deformation, the compression load corresponding to 20 per cent deformation was considered the plausible crushing load of the grain.

It can be seen from Fig. 5.3 that the crushing load for the crease plane horizontal position is usually higher than for the crease plane vertical position. The maximum percentage difference in the crushing loads at the

MOISTURE CONTENT

CRUSHING LOAD, LBS

%	CREASE PLANE VERTICAL	CREASE PLANE HORI.
9.0	16.5	16.8
12.3	18.5	19.8

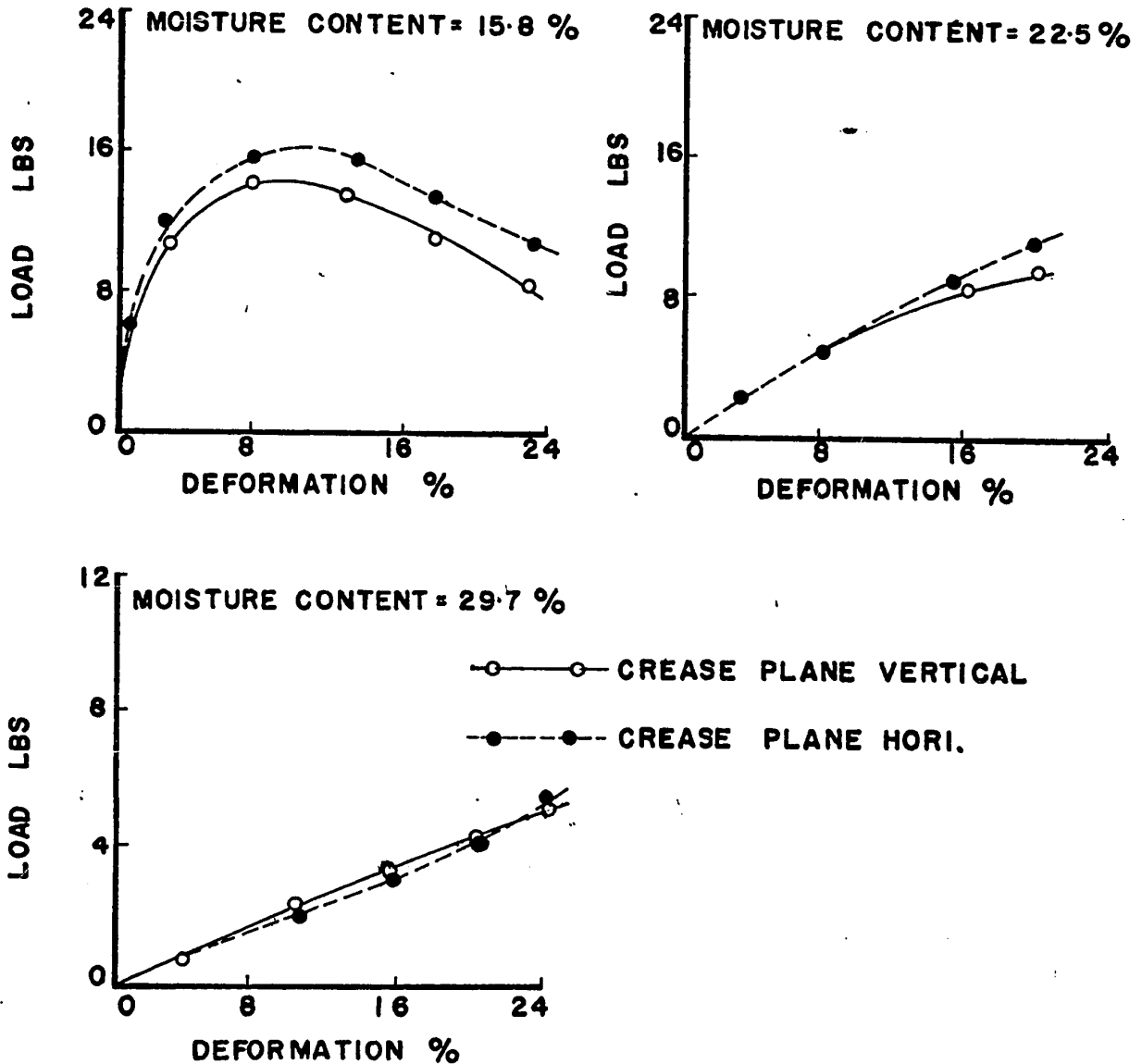


FIG.5.2 LOAD DEFORMATION CHARACTERISTICS OF INDIVIDUAL WHEAT GRAINS AT THREE MOISTURE CONTENTS

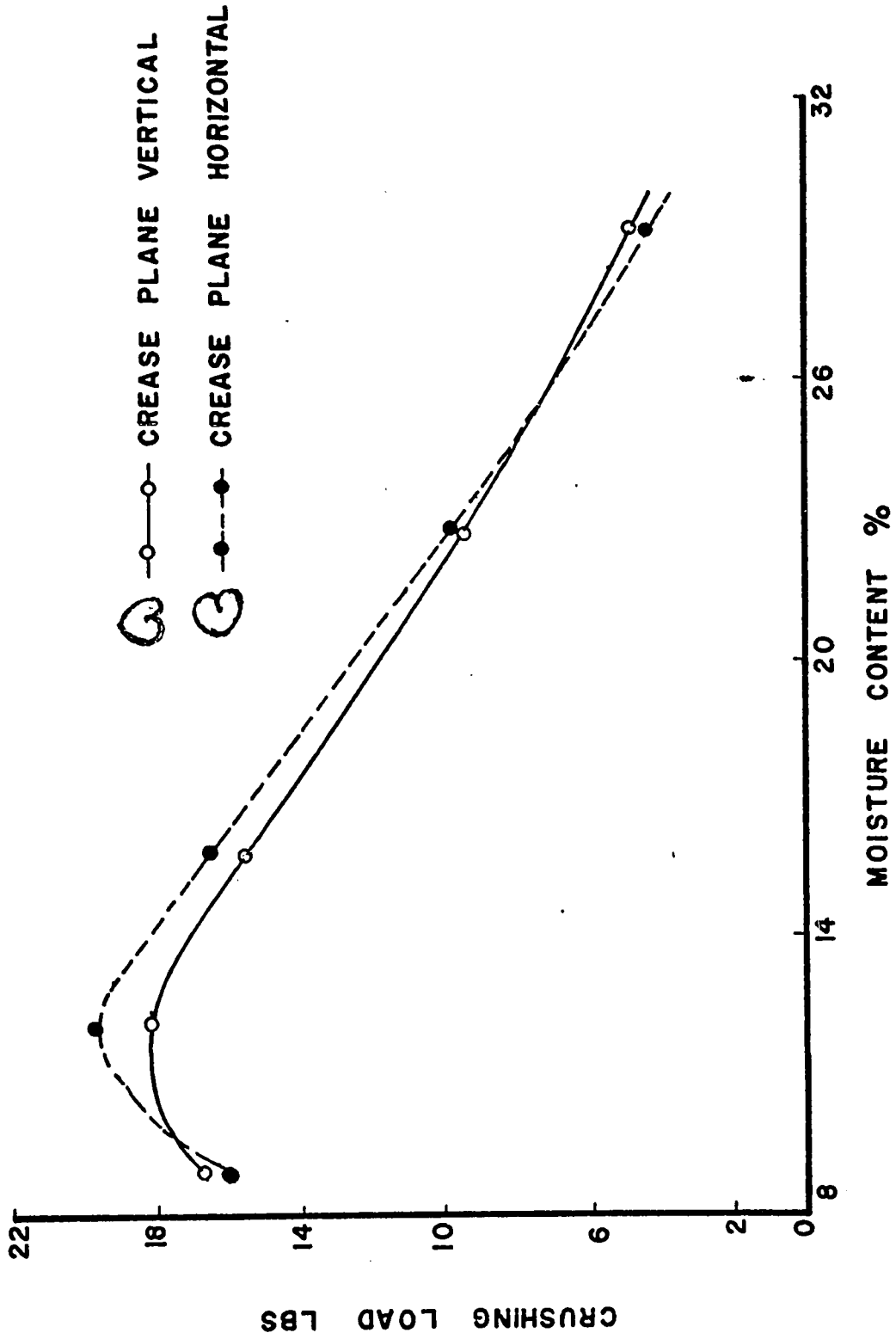


FIG.5.3 CRUSHING LOAD OF INDIVIDUAL WHEAT GRAINS

two positions is however not more than 10 per cent at any moisture content.

The crushing load increases for both grain positions up to a moisture content of approximately 12.5 per cent where it has the maximum value. For any further increase in moisture content, there is a decrease in the value of crushing load.

5.4 Bulk Density

5.4.1 General

Bulk density of granular materials can be studied by not only looking at the absolute bulk density of the material but also comparing it to the minimum and maximum bulk densities which can be obtained in the laboratory. These bulk densities are the lower and upper bounds of the density which the wheat could possess in a storage structure. The density is controlled by the method of placing wheat in the storage structure and the moisture content of the wheat.

The bulk density will increase as the wheat compresses under the weight of the overlying material. The minimum and maximum bulk densities and the change in the

bulk density under static loading have been studied.

The porosity of the material appears to be a better identification of the material structure than bulk density and therefore the value has generally been considered in terms of this parameter. The reasons for this view are (1) that the specific gravity of a wheat sample changes with moisture content and therefore it is difficult to compare the densities at different moisture contents and (2) that the porosity is a dimensionless parameter.

5.4.2 Minimum Bulk Density

Figure 5.4 and Table A.3 Appendix A show that the effect of a change of moisture content on bulk density is small for moisture contents in the range of 8.9 to 15.4 per cent but becomes important for high moisture contents. For moisture contents in the range from 8.9 to 15.4 per cent, the bulk density of wheat changes by 0.7 from 50.5 to 49.8 lbs. per cu. ft. From 15.4 to 29.7 per cent moisture content, the bulk density decreases by 6.4 from 49.8 to 43.4 lbs. per cu. ft. Figure 5.5 shows that for moisture contents in the range from 8.9 to 15.4 per cent, the porosity changes by 0.1 from 43.2 to 43.3. From 15.4 to 29.7 per cent the porosity

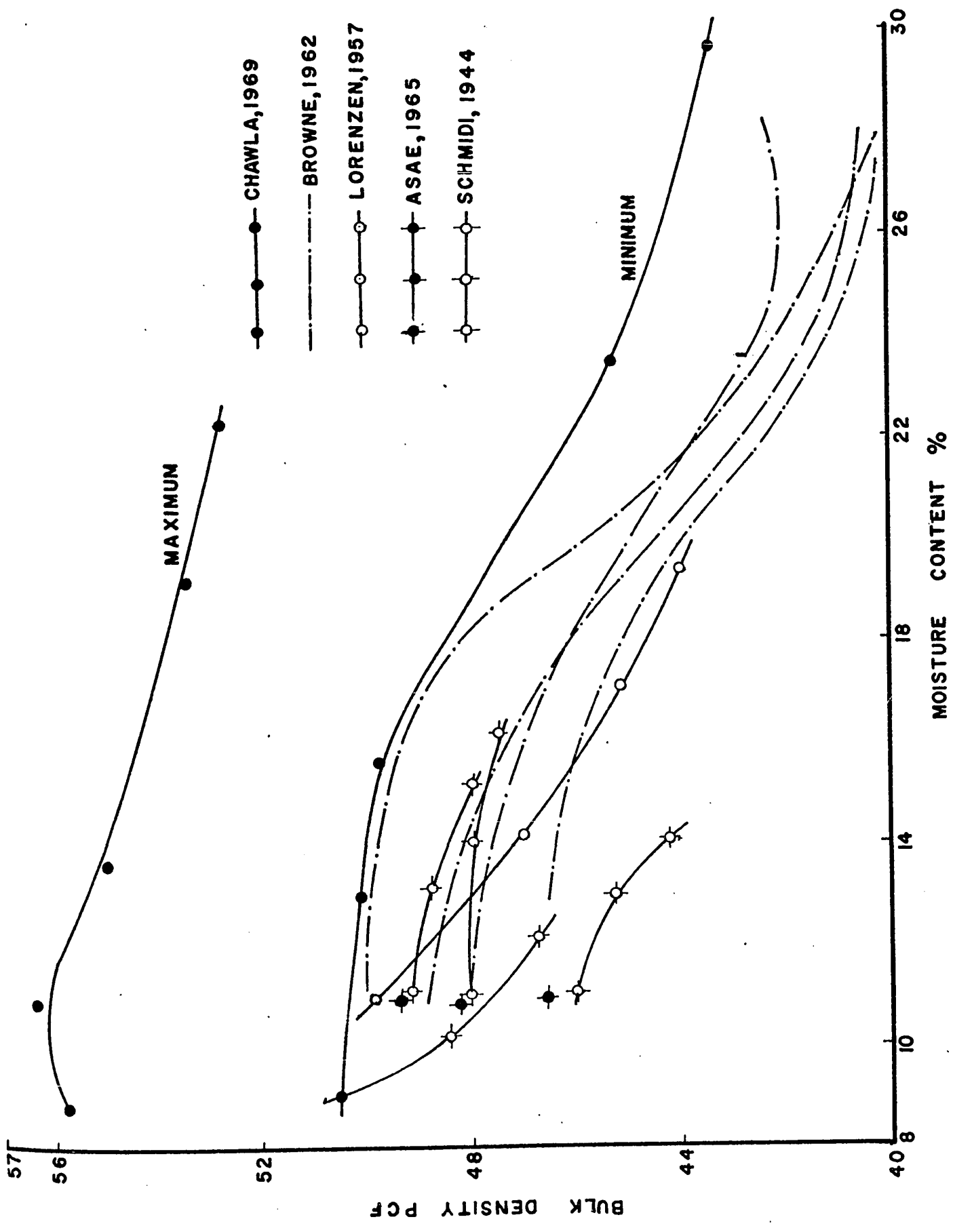


FIG.5-4 BULK DENSITIES OF DIFFERENT WHEATS

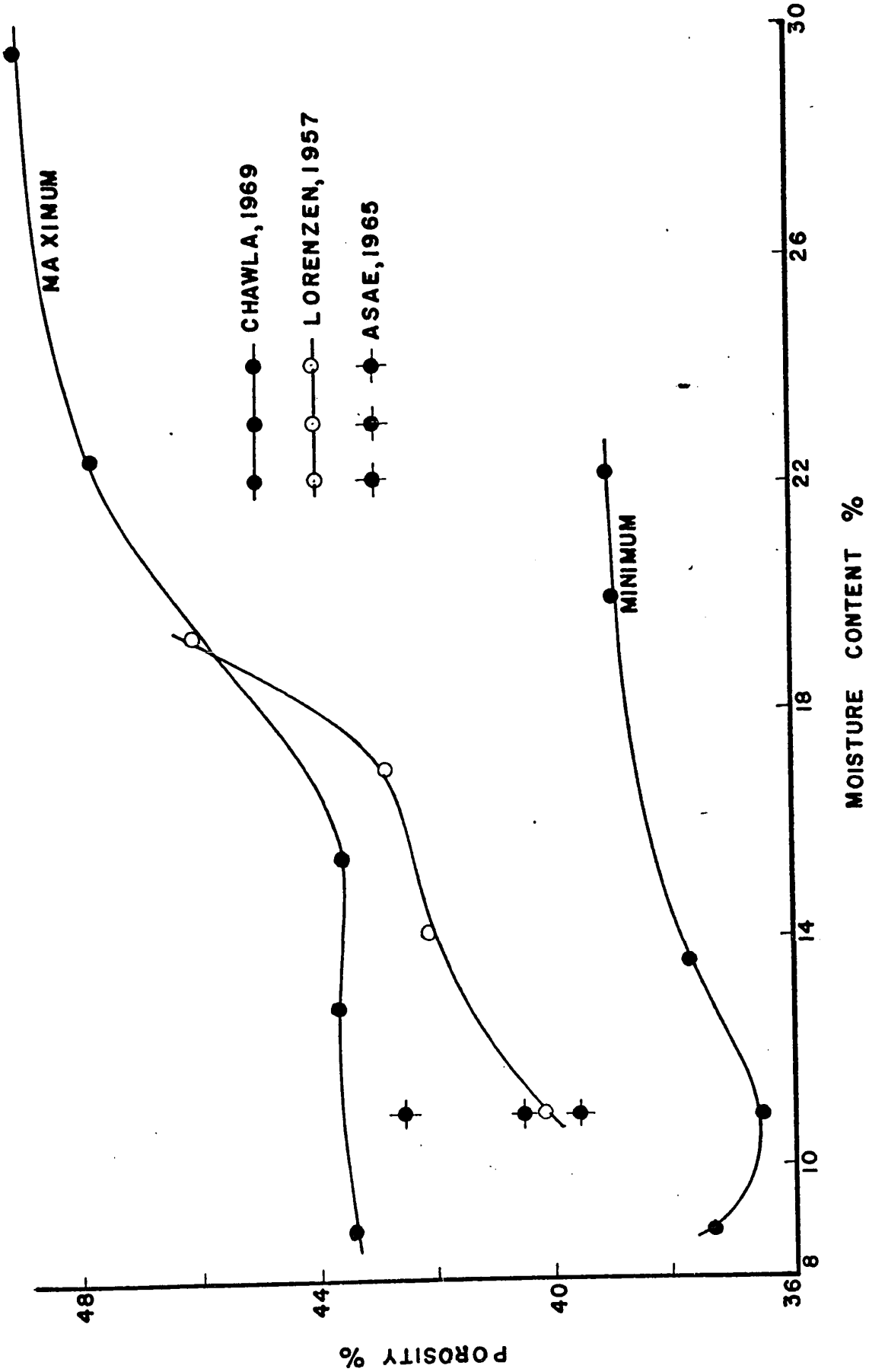


FIG. 5.5 POROSITY OF DIFFERENT WHEATS

increases by 5.8 from 43.3 to 49.1 per cent. The reasons why the bulk density decreases and the porosity increases with increase in moisture content are:

1. The specific gravity of wheat becomes less as the moisture content goes up. The bulk density of wheat is a direct function of specific gravity as can be seen from the equation

$$\gamma = G\gamma_w (1 - n) \quad 5.3.1$$

The decrease in the specific gravity of the wheat causes a decrease in the bulk density of the wheat.

2. As will be seen in section 5.5, both the cohesion intercept as well as the coefficient of friction of the wheat increase as the moisture content is increased. Due to the high cohesion and friction of wheat at higher moisture contents, the wheat does not pack as easily. Thus the porosity of wheat increases as the moisture content increases.

5.4.3 Maximum Bulk Density

At higher moisture contents the particles were exhibiting so much cohesion that they did not compact readily and the vibratory tests had little effect on the maximum density of the wheat. Therefore, the vibratory tests to determine the maximum bulk density were carried out only in the moisture range from 8.8 to 22.1 per cent.

Figures 5.6 to 5.10 and Table A.4 Appendix A show the effect on the bulk density and porosity at different moisture contents of the magnitude of surcharge, time of vibration and amplitude of vibration in the vibratory tests. The effect of each variable on the bulk density and porosity is discussed below separately.

5.4.3.1 Magnitude of Surcharge Weight

As shown in Figs. 5.6 to 5.10 the porosity increased as the surcharge load was increased. Minimum porosity was usually achieved at no surcharge. The variation of bulk density with surcharge weight was between 1 to 2 lbs. per cu. ft. The variation of porosity had been between 1 to 2 per cent.

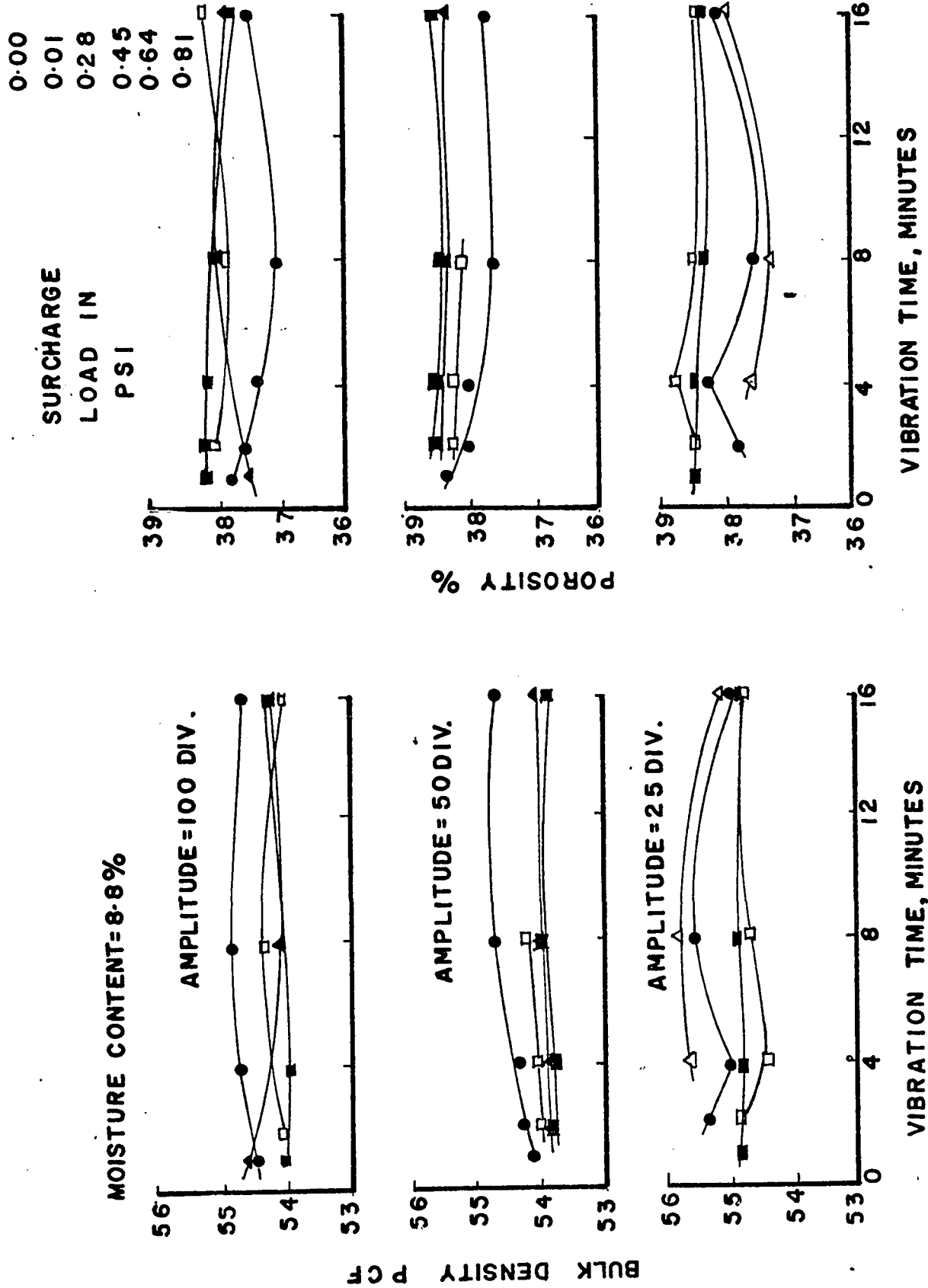


FIG. 5.6 BULK DENSITY AND POROSITY FROM VIBRATORY TESTS

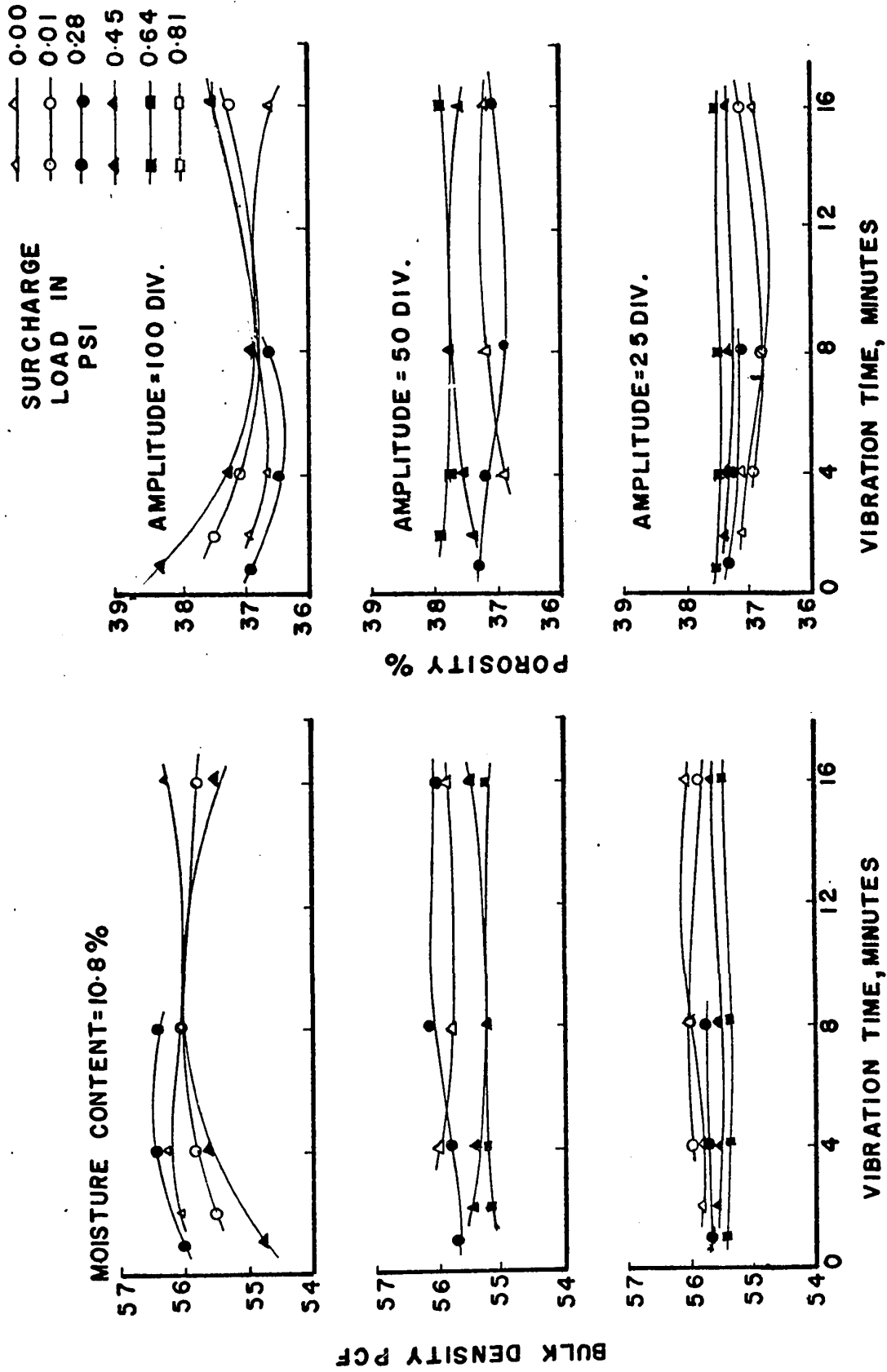


FIG.5.7 BULK DENSITY AND POROSITY FROM VIBRATORY TESTS

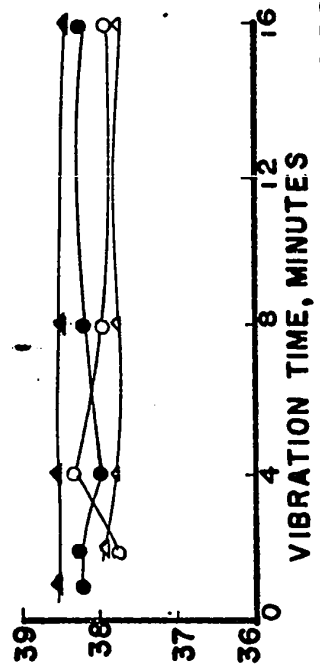
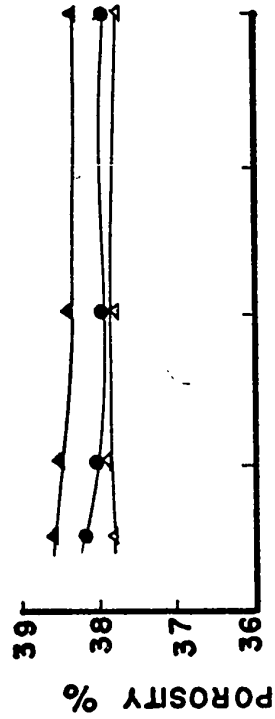
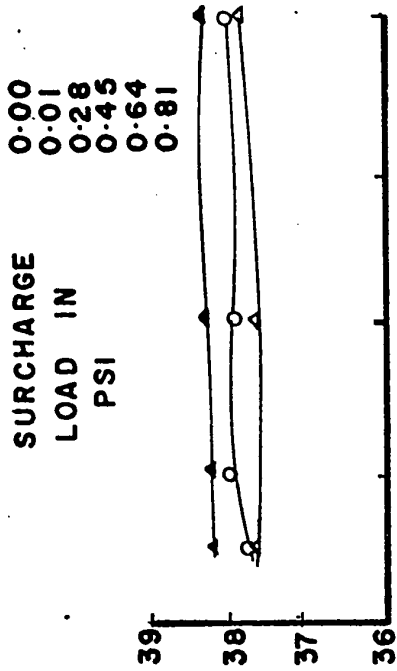


FIG. 5-8 BULK DENSITY AND POROSITY FROM VIBRATORY TESTS

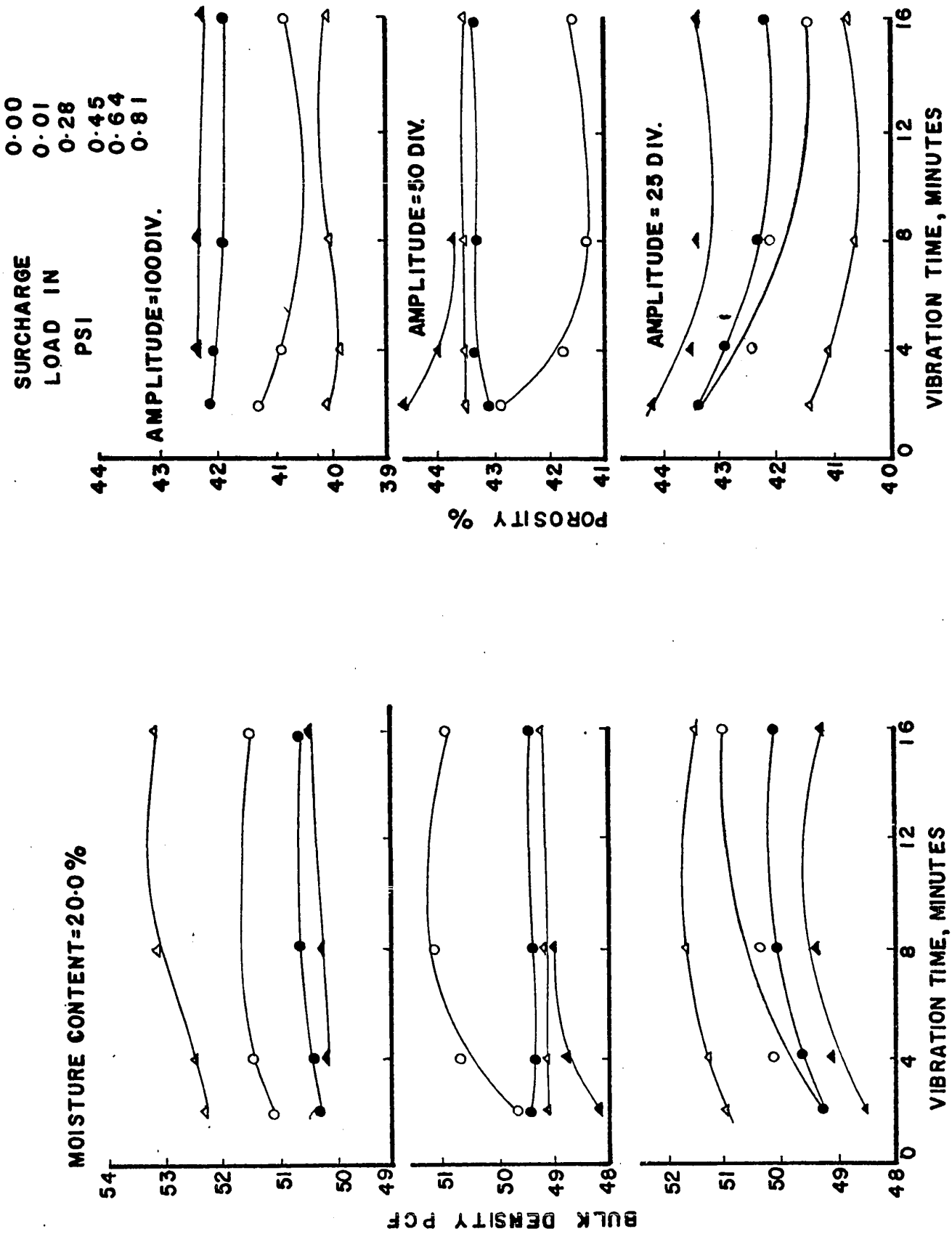


FIG.5-9 BULK DENSITY AND POROSITY FROM VIBRATORY TESTS

0.00
0.01
0.28
0.45
0.64
0.81

SURCHARGE
LOAD IN
PSI

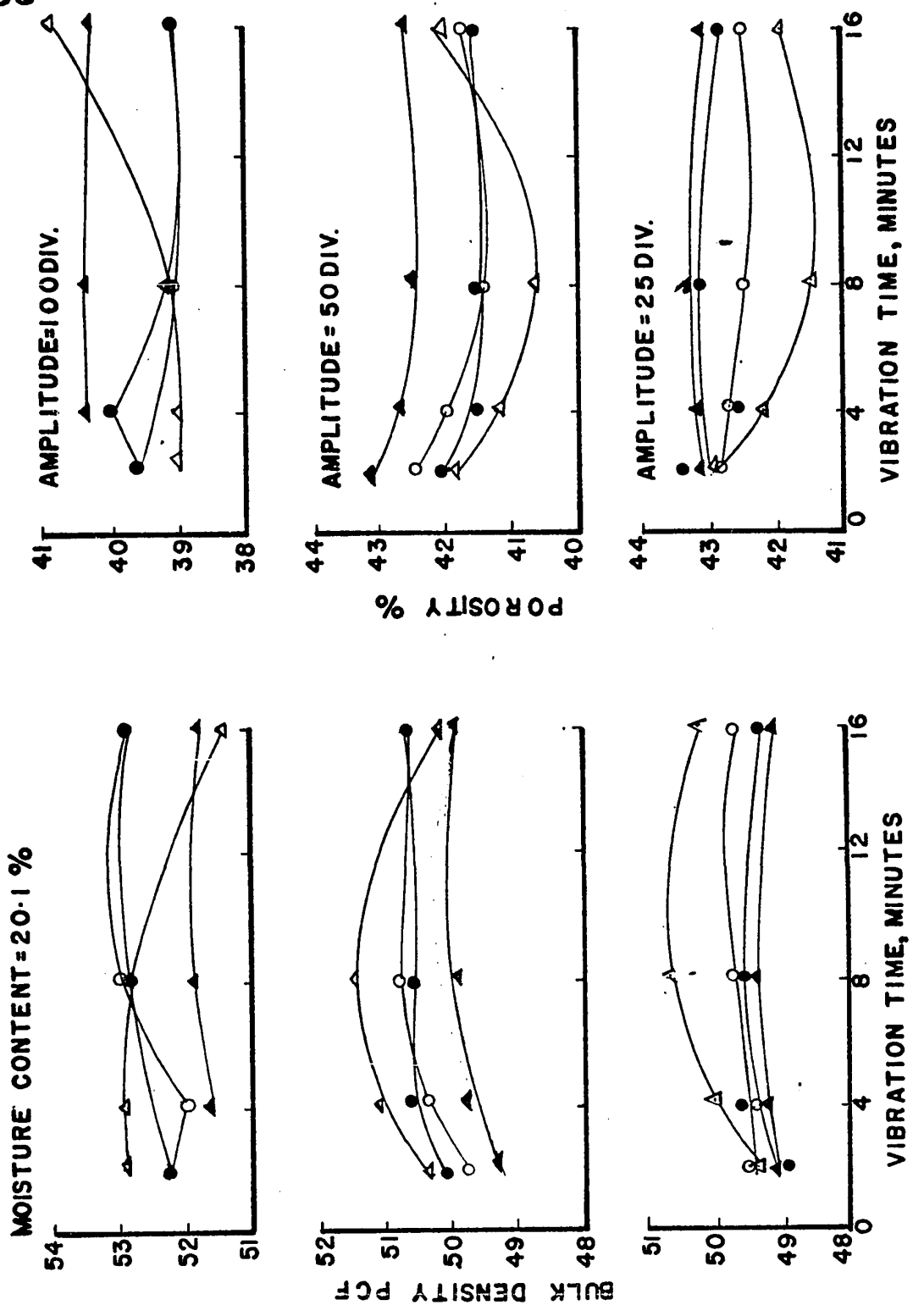


FIG.5:10 BULK DENSITY AND POROSITY FROM VIBRATORY TESTS

The investigations (Forssblad 1965) have shown that the maximum bulk density (minimum porosity) can be achieved when a surcharge weight of approximately 2 psi is used. Observations by the author indicate that the maximum density is achieved at zero surcharge weight only. The mechanism governing such a behaviour seems to be quite complex and is not well understood. Further research, particularly the study of the effect of frequency of vibration on bulk density of wheat for different amplitudes may throw some light on this aspect.

5.4.3.2 Time of Vibration

The time of vibration at which the maximum density could be achieved was studied by running tests of up to 16 minutes duration. The bulk density was measured at different time intervals. It can be seen in Figs. 5.6 to 5.10 that maximum density (minimum porosity) was usually achieved at a time interval of 6 to 8 minutes.

5.4.3.3 Amplitude of Vibration

Figures 5.6 to 5.10 show that porosity decreases

as the amplitude of vibration increases. The minimum porosity is obtained at the higher amplitudes. The increased amplitude of vibration of grains implies more shearing strains which results in sliding of grains and closer packing. The effect of amplitude of vibration is more marked at higher water contents. The reason is that at low moisture contents the shear strength parameters are smaller and particles will compact readily. To achieve minimum porosity at higher moisture contents, higher amplitude is required to overcome the higher shearing resistance of the wheat kernels.

5.4.4 Comparison of Experimental and Theoretical Packing

Figure 5.11 shows that the maximum porosities found in the laboratory are approximately equal to the maximum values obtained from the study of the theoretical packing of uniform ellipsoids. The explanation for the small discrepancy between the two values is given below.

1. The movement of wheat grains against each other is restricted due to both shear strength parameters, namely the cohesion and the internal angle of friction between the grains. This resistance increases as the moisture

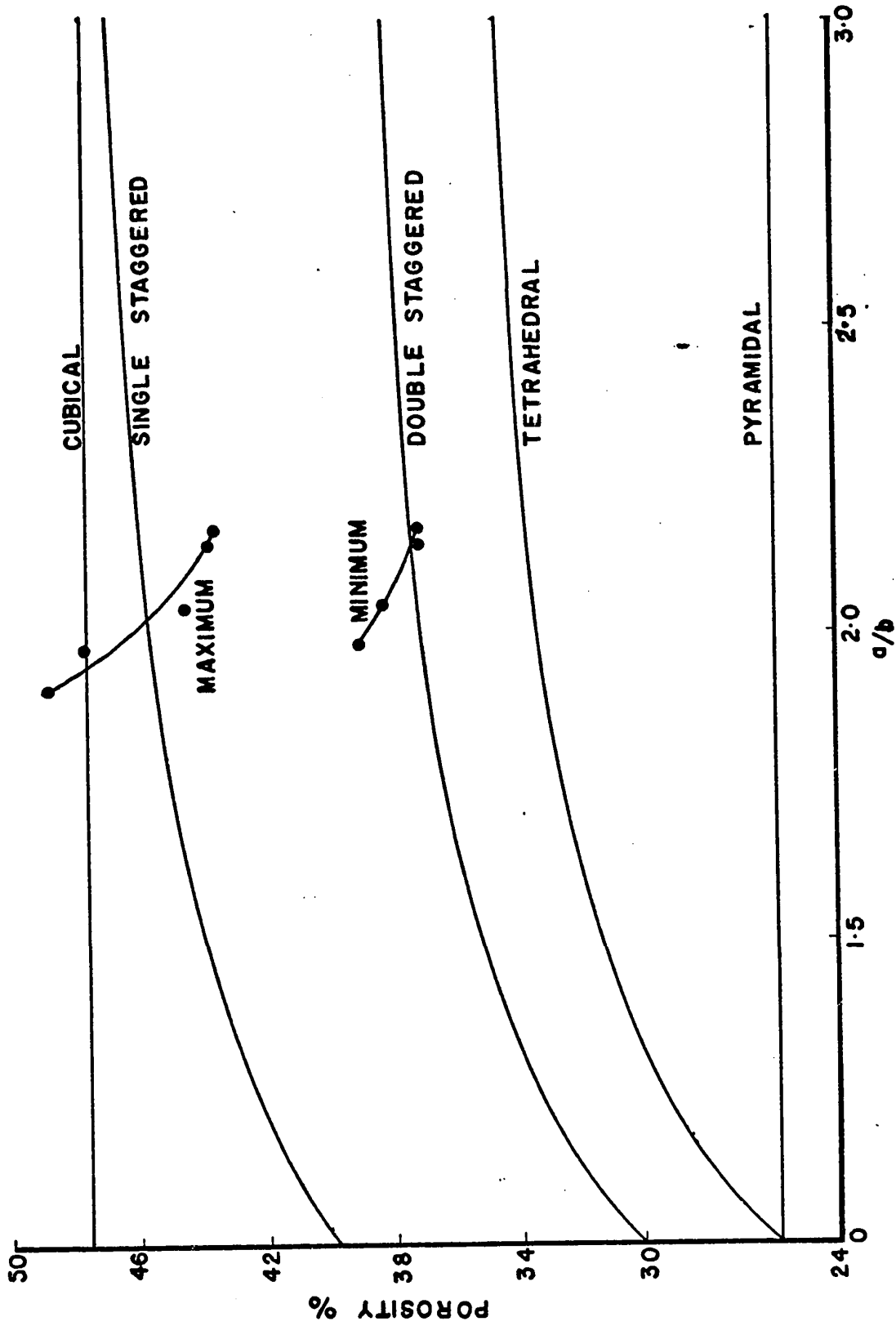


FIG.5-II PACKINGS OF ELLIPSOIDS AND WHEAT GRAINS

content of the grain is increased. If the wheat grains are poured into the mould from a height above the top surface of the grains the pouring may result in the "arching and bridging" of groups of grains, thus forming voids higher than the normal voids if there had been no arching and bridging.

2. The wheat grains are of different sizes and shapes. A grain has pointed edges as compared to a circular one for an ellipsoid. If the grains and ellipsoids are packed in the same manner, the voids for wheat grains packing would be greater than voids for ellipsoids packing. Experimental study also shows (Fig. 5.5) that there is no possibility of approaching the theoretically densest packing.

As seen from Fig. 5.11 the value of minimum porosity obtained from the vibratory tests lies between the theoretical double staggered and single staggered packings.

It was, however noted from the minimum and maximum densities tests that generally the wheat grains did not

group themselves in a specific packing because of the varying shapes and sizes. The grains were seen to lie in the mould at random positions.

The experimental curves show an increase in porosity with a decrease in the a/b ratio. This result is obtained because the increase in the moisture content decreases the a/b ratio and increases the shearing strength of the wheat. The increase in the shearing strength has a much greater effect on the porosity than the decrease in the a/b ratio.

5.4.5 Comparison of Bulk Densities of Different Wheats

The experimental bulk densities of wheat at different moisture contents were studied and are compared in Fig. 5.4 with the results of the work of other researchers (Schmidi 1944, Lorenzen 1957, Browne 1962 and A.S.A.E. 1965). The bulk densities obtained by other researchers are lower than the minimum bulk densities found herein experimentally. This is because the specific gravities of the wheat used by the various researchers are lower than the specific gravities obtained herein (Fig. 5.1). A lower value of specific gravity results in a lower bulk density. Therefore

the bulk densities obtained by others are lower.

The porosities of wheats at different moisture contents obtained in this study, obtained by Lorenzen (1957), and available in A.S.A.E. (1965) are shown in Fig. 5.5. This plot removes the variable of the differing specific gravities. The porosities obtained by Lorenzen and given by A.S.A.E. lie inbetween the minimum and maximum porosities obtained in this work and are in good agreement. Agricultural researchers determine bulk densities by using standard methods which result in a loose packing of the grains. The author performed minimum and maximum bulk densities tests to obtain the loosest and densest packings of the grains.

5.4.6 Static Compression

A mass of wheat grain in bins or other storage structures undergoes compression because of the weight of the overlying grains. The volume change of the mass of wheat grain is caused by two factors.

1. Volume change due to relative movement and displacement of the grains.
2. Volume change due to deformation of grains.

When the static compression of a wheat mass occurs, the grains

expand laterally, thus decreasing the void spaces in the wheat mass.

Two series of experiments were carried out to study the effect of static pressure on volume change (change of porosity per unit pressure). To achieve the same conditions in the laboratory as those existing in the storage bins, the lateral yield of the wheat sample was confined in both series.

In the first series, a container of 2.5 inch diameter and 1.012 inch in height was used. To study how much a wheat mass compresses under static loading it was decided that samples at different moisture contents from 8.6 per cent to 22.8 per cent should be placed and tested at their maximum porosities. The porosity of each sample was measured by using toluene. No special attempt was made to remove the air which might be entrapped in the creases of the grains, so the initial maximum porosity obtained for each sample was measured with this limitation. Each sample was loaded in steps to 0, 0.52, 1.05, 2.02, 3.74, 7.25, 14.1 and 21.0 psi and then unloaded in steps to 0 psi. The results are listed in Table A.5, Appendix A and shown in Figs. 5.12 and 5.13.

Figure 5.12 shows that the rate of vertical

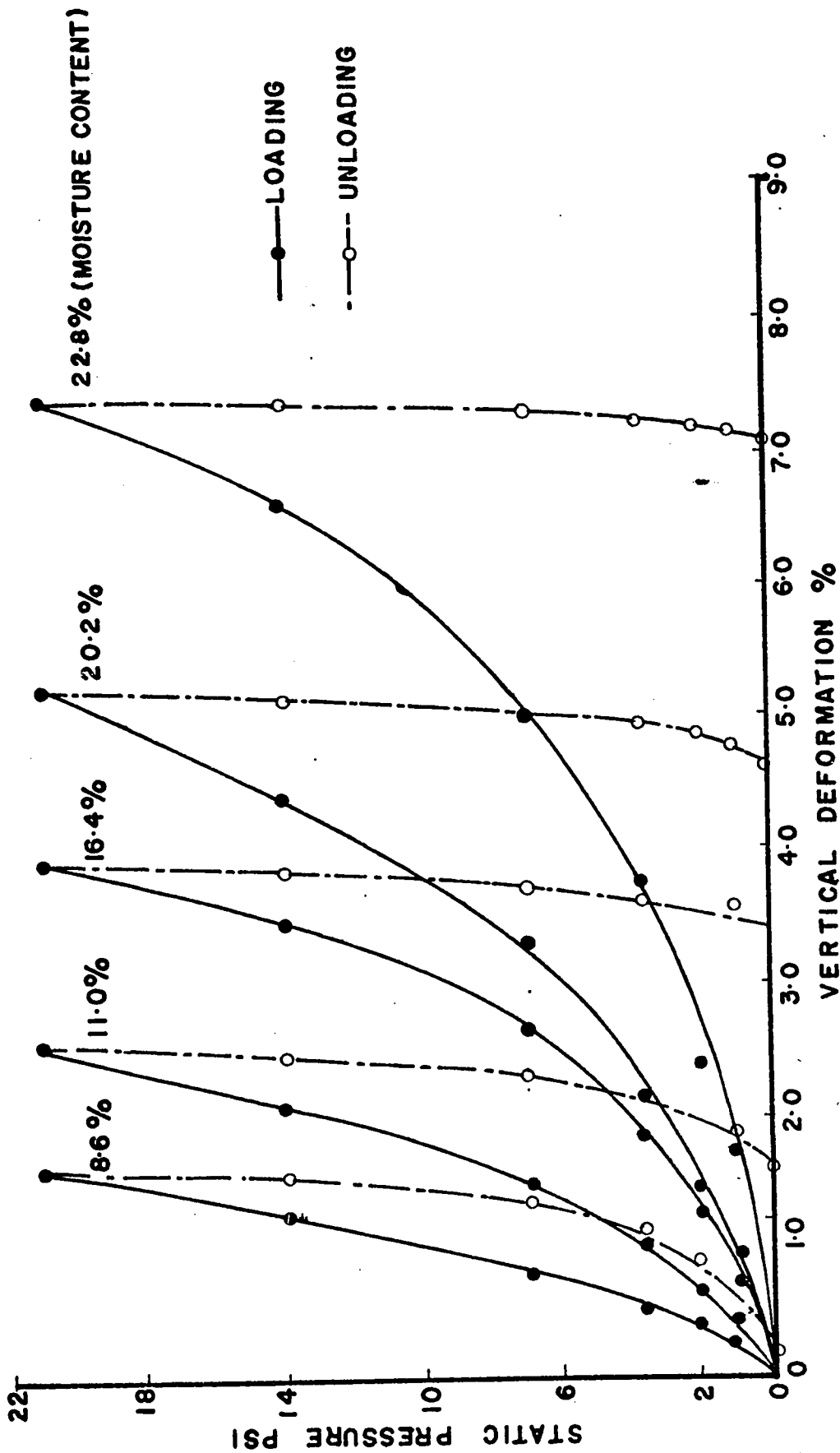


FIG.5.12 RELATIONSHIP BETWEEN STATIC PRESSURE AND DEFORMATION FOR STATIC COMPRESSION TESTS

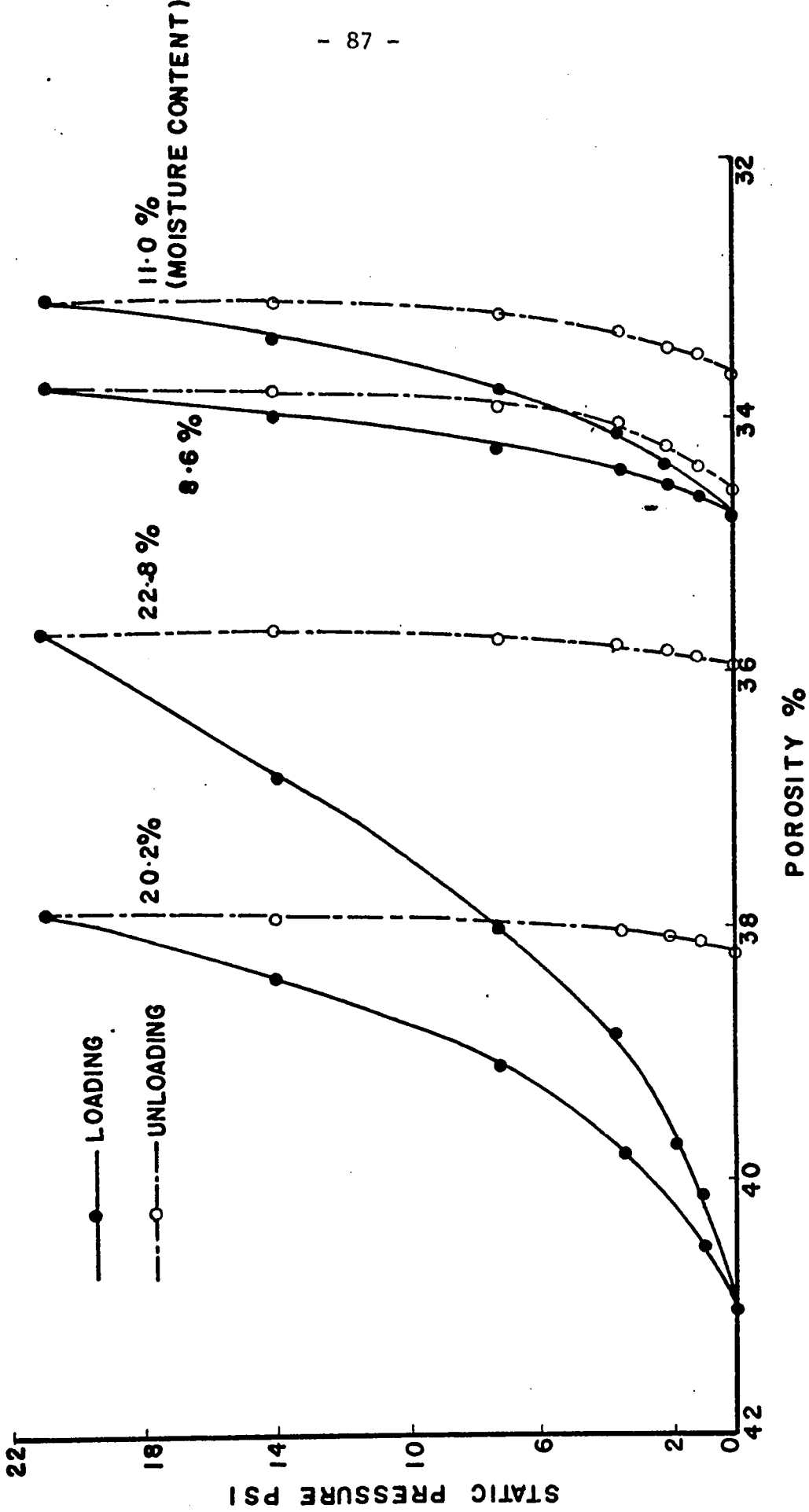


FIG.5.13 RELATIONSHIP BETWEEN STATIC PRESSURE AND POROSITY FOR STATIC COMPRESSION TESTS

deformation of wheat samples decreases with the increase of static pressure on the wheat samples for all moisture contents. The amount of vertical deformation increases with the increase in the moisture content of wheat under a particular static pressure. The maximum deformation under a static pressure of 21.0 psi varied from 1 per cent from the wheat sample at lowest moisture content to 7 per cent for wheat sample at the highest moisture content.

The maximum porosities of wheat increase with the moisture contents of the wheat grains and therefore Fig. 5.13 is plotted to show change of porosity under static loading. It can be seen that the high moisture samples, even under full static pressure, have higher porosities than the low moisture content samples at their initial porosities. As discussed above under minimum bulk density, the wheat samples at high moisture contents have much greater shearing resistance between the grains and thus higher initial porosities were obtained. The effect of the shearing resistance between the grains at higher moisture contents was so great that the final porosities of wheat samples under maximum static pressure were still higher than the initial porosities of wheat samples at low moisture contents.

It is observed from Fig. 5.13 that the change of porosity is 0.9 per cent at a moisture content of 8.6 per cent as compared to 5.0 per cent at 22.8 per cent moisture content under a static pressure of 21.0 psi.

To evaluate the effect of the differing initial porosities, a second series of tests was performed on samples of different moisture contents but with the same initial porosity. It was also decided to use a larger container because the container used in the first series was rather small compared to the wheat kernel size.

A specially designed container of 6 inches diameter and $1\frac{1}{4}$ inch height was used. Each sample was loaded in steps to 0, 0.46, 0.92, 1.65, 3.08, 5.95, 8.80 and 14.50 psi. After the samples were loaded to their maximum pressure, they were unloaded in steps. The results are listed in Table A.5, Appendix A and shown in Figs. 5.14 and 5.15.

In the second series of tests (5.14) the change in the compression of the sample at 9.4 per cent moisture content is 2.1 per cent as compared to 4.0 per cent for the sample at 23.4 per cent moisture content and 9.4 per cent for the sample at 29.7 per cent moisture content. In the second series of tests all of the samples at different moisture contents were brought to the same initial porosity, which was the porosity of the

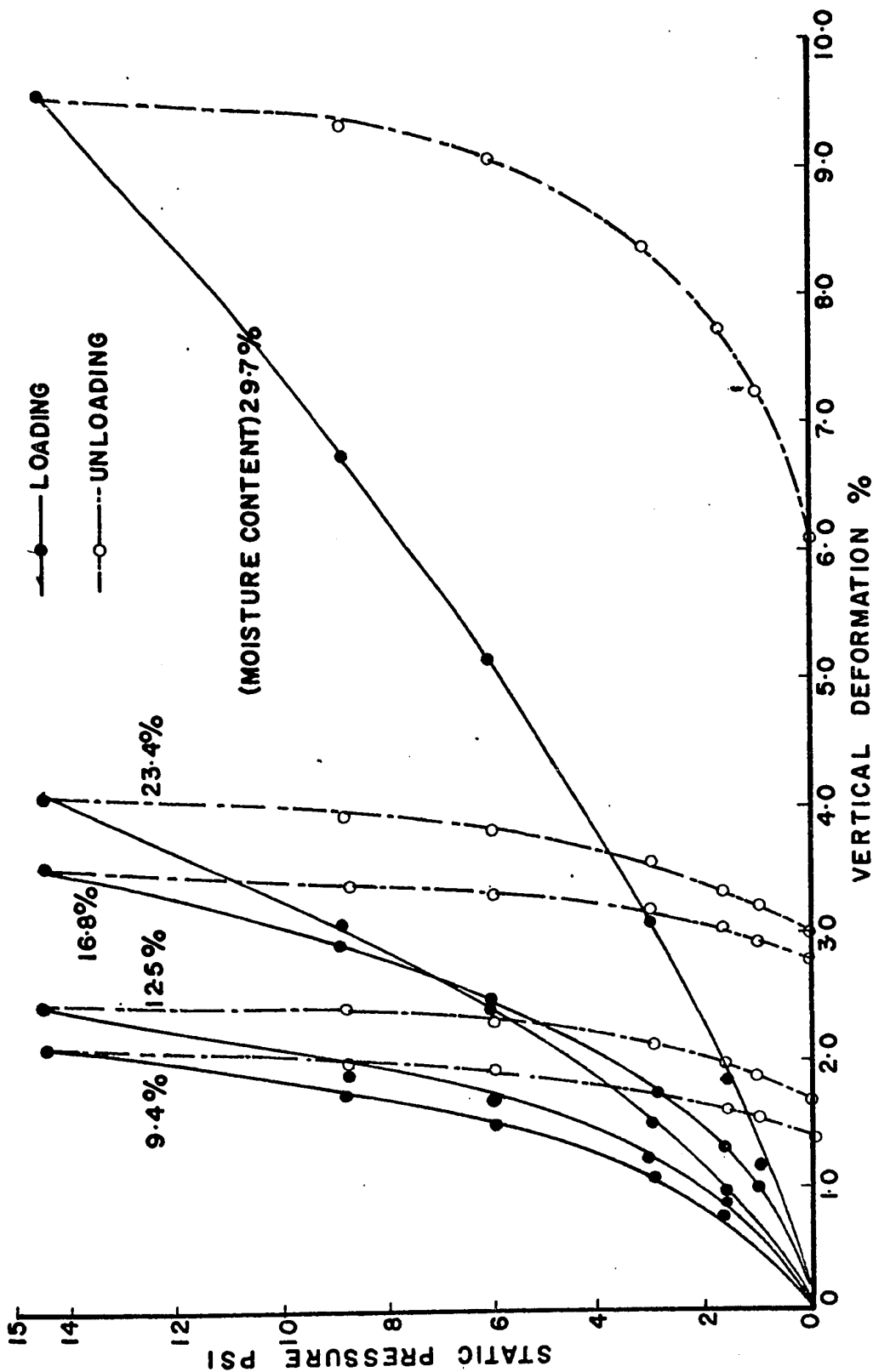


FIG.5:14 RELATIONSHIP BETWEEN STATIC PRESSURE AND DEFORMATION FOR STATIC COMPRESSION TESTS

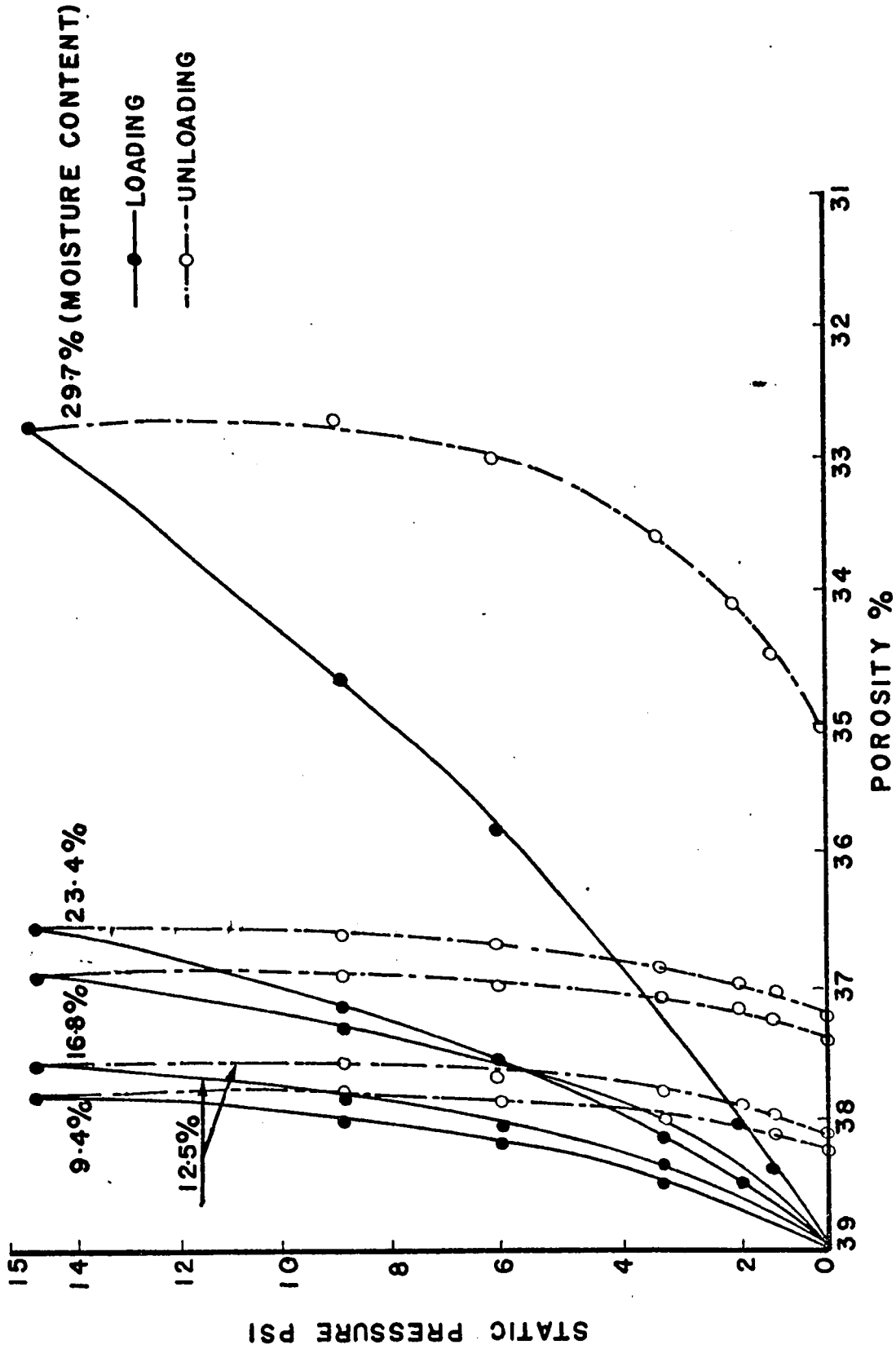


FIG. 5-15 RELATIONSHIP BETWEEN STATIC PRESSURE AND POROSITY FOR STATIC COMPRESSION TESTS

sample at the smallest moisture content. The other four samples at higher moisture contents were precompressed by a cycle of loading to reach the desired porosity. It is obvious therefore, that whereas the first sample has undergone only one cycle of loading, the other four samples have undergone one preloading cycle and the test is a reloaded cycle.

The loads to which the samples were subjected to achieve the same initial porosity were not recorded. The magnitude of the precompression in these samples was approximately proportional to their moisture content. Despite this fact, it is interesting to observe that the one dimensional compression recorded is a direct function of moisture content, and in agreement with the first series of experiments. The compression recorded in the second series of tests for the four precompressed samples was lower than obtained from the first series under a particular load. This is so because the samples were subjected to non-recoverable compression by the first cycle of loading.

As shown in Fig. 5.15 the change in porosity at 9.4 per cent moisture content is 1.3 per cent as compared to 2.5 per cent at 23.4 per cent moisture content and 6.3 per cent at a 29.7 per cent moisture content under a static pressure of 14.5 psi. Even with the precompression the change in porosity

increases with increasing moisture content.

As indicated before, the effect of the change of the moisture content on the plastic nature of the material was significant. The compressed samples at the higher moisture contents when taken out of the mould appeared as a single mass of deformed and highly bonded particles, whereas the grains at low moisture contents came apart into individual kernels when taken out of the mould.

5.4.7 Discussion

The bulk density of wheat is affected by the method of placing, the moisture content of the grain, and additional stresses acting on the grain mass after placing, such as, inertia forces from vibrations and weight of overlying grains. In bins or other storage structures, the weight of the overlying grains compresses the underlying grains thus increasing the bulk density of wheat. The bulk density of stored wheat in bins would increase with depth because of the increasing overburden pressure with depth.

Table 5.4.1 Bulk Density of Wheat

Bulk Density	Effect of					
	Method of Placing	Static Stresses		Vibratory Stresses		
lbs. per cu. ft.	8.9	Moisture Content per cent		8.8	22.1	
		29.7	8.6	22.8		
Minimum	50.6	43.4	54.6 [*]	51.4 [*]	50.6	45.3
Maximum	52.2	44.2	55.4 ^{**}	55.9 ^{**}	56.3	52.9
% increase in density	3.1	1.8	1.4	9.0	11.0	14.3

* Bulk density at zero overburden pressure

** Bulk density at 21.0 psi overburden pressure

As can be seen from the above table, the method of placing does not have a significant effect on the bulk density. It is also shown that the bulk density of wheat decreases as the moisture content in the wheat kernel is increased. The cause for such a behaviour may be contributed by two possible factors.

1. The lowering of specific gravity of the wheat grains because of the swelling of the wheat grains with increasing moisture content.

2. The increase in both cohesion and coefficient of friction of wheat at high moisture contents. Due to high shearing resistance between grains at higher moisture contents, the wheat grains do not pack as easily and thus give smaller bulk density.

It is observed that below 13.0 per cent moisture content, the bulk density of wheat remains constant with a change in moisture content. Beyond 13.0 per cent moisture content the bulk density decreases with approximately 24 per cent of the decrease due to the decrease in specific gravity of wheat and the remaining 76 per cent due to the increase in shear strength parameters with the increase in moisture content.

When subjected to static stresses by an overburden pressure of 21.0 psi, the bulk density of wheat increased respectively by 0.8 and 4.8 lbs. per cu. ft. at moisture contents of 8.6 and 22.8 per cent.

When vibrated the bulk density of wheat samples increased respectively by 5.7 and 7.6 lbs. per cu. ft. at moisture contents of 8.8 and 22.1 per cent.

It can be inferred that vibratory stresses are most effective in increasing density of the wheat grains at all moisture contents. There is an increase in the effect of vibratory

stresses with an increase in moisture content but the effect is small. The magnitude of the static overburden pressure has practically no effect at low moisture contents. At high moisture contents, however, this is fairly effective, although not as much as vibratory stresses. This influence of static stresses is possibly due to the deformability of wheat grains at high moisture contents. Placement of wheat by different methods of pouring results in practically the same density at a particular moisture content.

The calculated bulk density of wheat based on weight and measures used in the Canadian Department of Agriculture is 48.0 lbs. per cu. ft. or 60.0 lbs. per bushel. The effects of variables such as moisture content, static overburden pressure, and vibratory stresses which govern the placement bulk density are not considered. But as can be seen from the observations, these variables have a considerable effect on the bulk density of wheat. Therefore it may be either uneconomical or unsafe in structural design to use one value of bulk density for all purposes.

5.5 Shear Strength of Wheat

5.5.1 General

As discussed in chapter 2, for the design of storage bins and other such structures, knowledge of the shear strength properties of the stored materials is very important. The usual soil mechanics techniques of studying shear strength characteristics of granular materials, namely, direct shear tests and triaxial compression tests, were employed to study the shear strength behaviour of wheat.

5.5.2 Direct Shear Tests

The direct shear tests were performed on wheat samples at different moisture contents and having different porosities. Tests at normal vertical pressures of 1, 2 and 3 psi were made for each porosity and for each moisture content. The samples were not tested at high confining pressures because the large size of the shear box would have required a force larger than the frame of the machine could withstand.

5.5.2.1 Stress-Deformation and Volume Changes Curves

The stress-deformation and their corresponding volume changes curves are given in Appendix A (Figs. A.6 to A.10). Typical curves for one porosity are shown in Fig. 5.16.

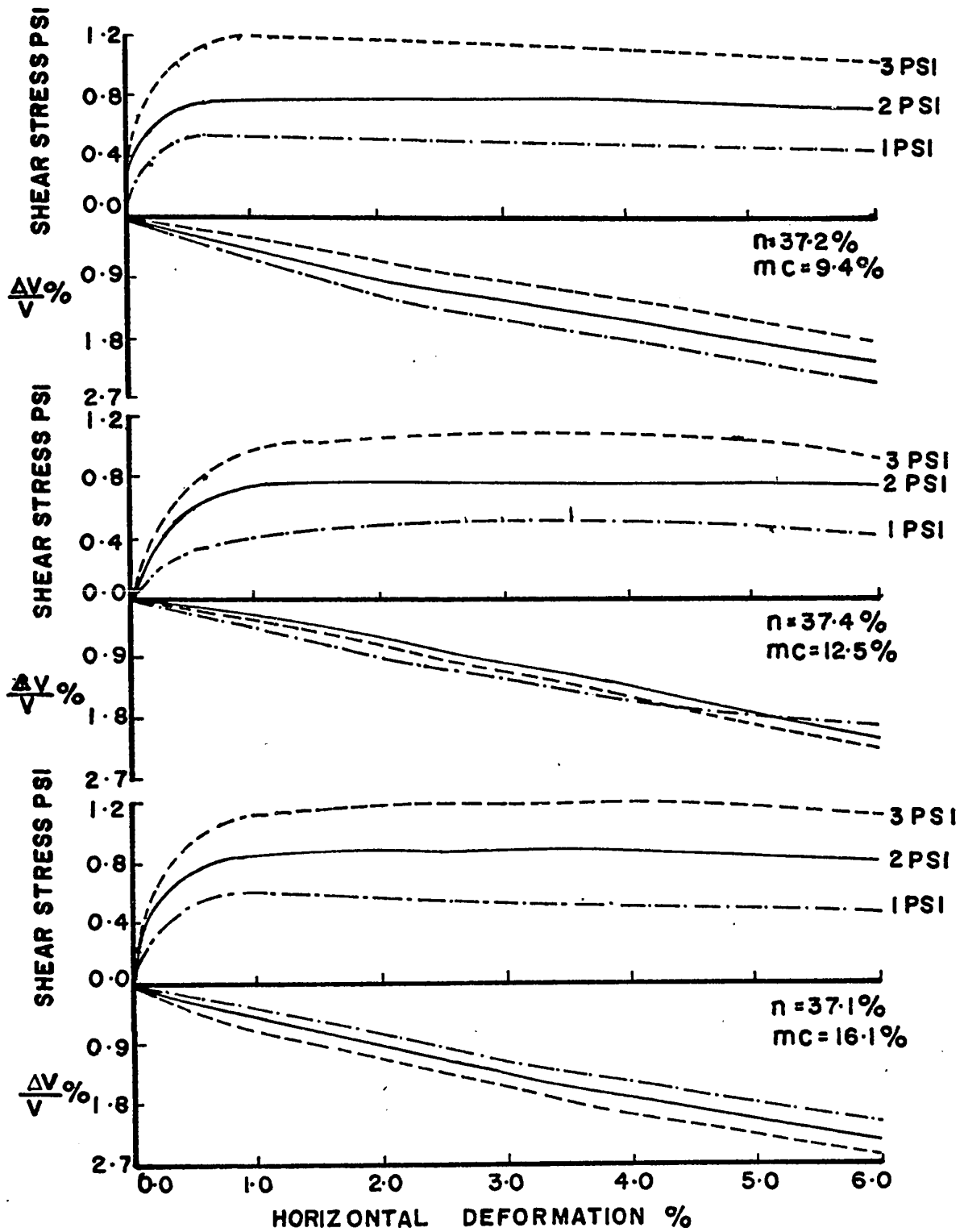


FIG.5.16 STRESS DEFORMATION CURVES FOR DIRECT SHEAR BOX

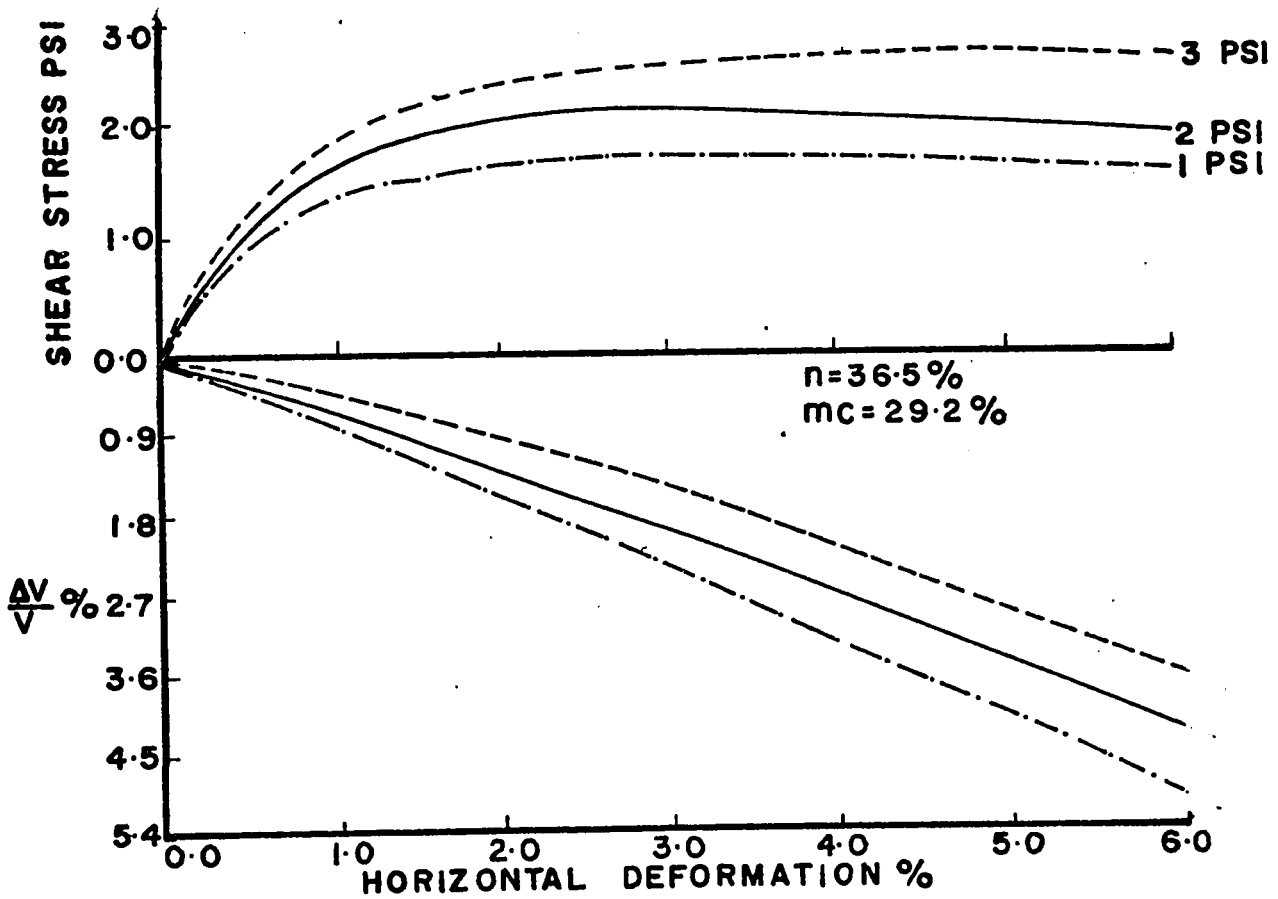
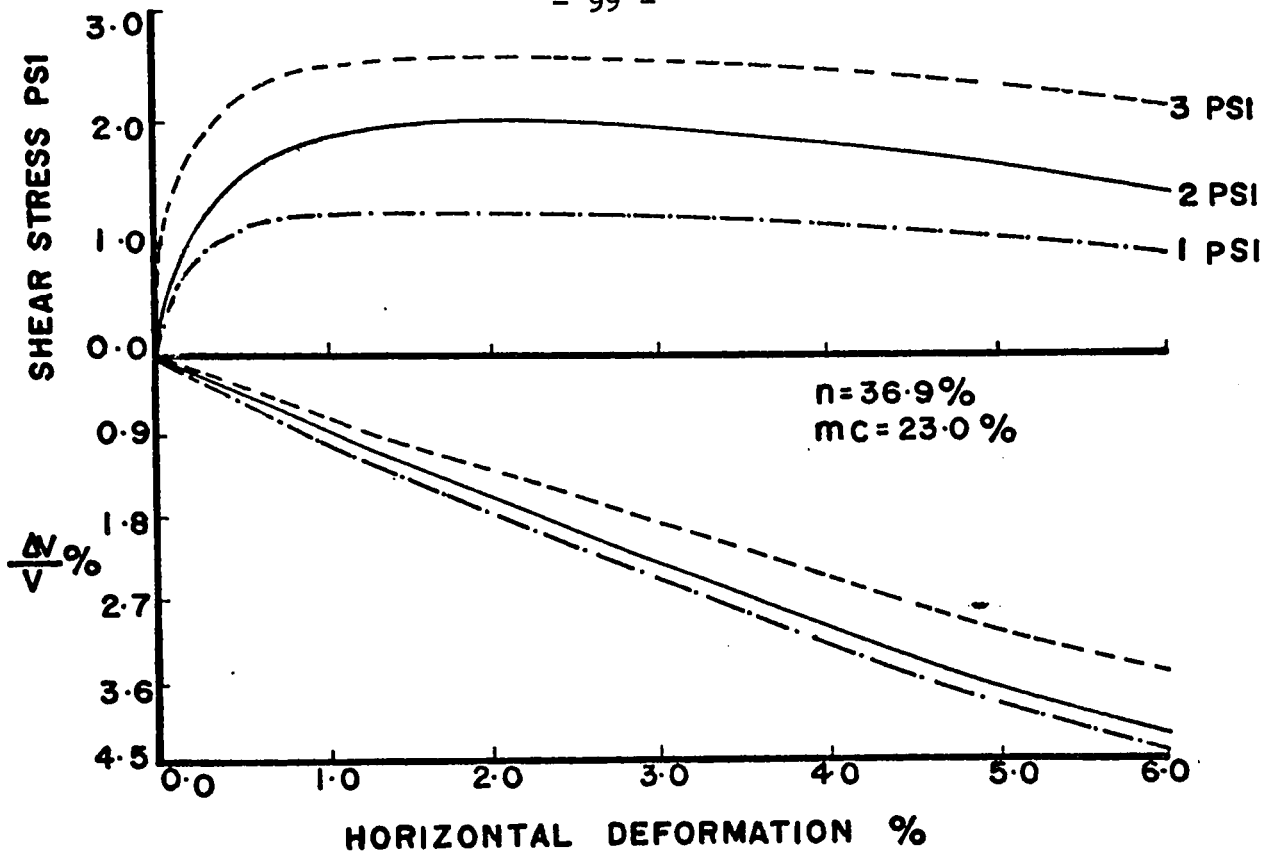


FIG.5-16 STRESS DEFORMATION CURVES FOR DIRECT SHEAR BOX

As can be seen from these stress-deformation curves, the stress increases with shearing strain for all confining pressures and reaches its peak at a deformation of about 1 to 3 per cent. It appears that as the moisture content of the sample increases, the horizontal deformation at failure increases slightly. The stress decreases slightly with further increase in horizontal deformation and reaches its ultimate value at a deformation of approximately 7 per cent.

The volume change characteristics (Fig. 5.16 and Figs. A.6 to A.10) show a reduction in the volume of the sample under all confining pressures and at each moisture content and porosity. The volume change curves generally decrease linearly with increase in horizontal deformation although there is a tendency in some tests for a reduction in the rate of volume change.

The volume change increases with increase in moisture content of the sample. It is observed that in the lower moisture content range the initial porosity has little effect on the volume change. The volume change at failure, in this moisture content range, is from +0.01 to - 1.5 per cent. In the higher moisture content range the volume change increases as the porosity of the sample decreases. The volume change at failure in the higher moisture content range is from +0.45 to -4.20 per cent.

For all confining pressures in the lower moisture content range (9.3 to 16.0 per cent) the volume change is generally similar. In the higher moisture content range the greater the confining pressure, the smaller is the volume change, and the smaller the confining pressure, the larger is the volume change.

In the lower moisture content range the shear strength parameters of wheat are small and do not change much with moisture content. This appears to be the reason why the confining pressure has very little effect on the magnitude of the volume change in this moisture content range. In the higher moisture content range the frictional resistance of the wheat grains goes up. When the grains are confined under higher pressure, the shearing resistance between the grains against sliding over each other is greater and the volume reduction in the sample is less. At smaller confining pressures, the shearing resistance against sliding between the grains is small which results in the volume reduction in the sample being more.

After the tests, the wheat grains at the lower moisture content range fell apart into individual grains when removed from the shear box, but at high moisture contents the wheat grains looked like a single bulk mass which had to be forced out of the shear box.

5.5.2.2 Failure Envelope Plots

The angle of internal friction and cohesion intercept were determined for each porosity and for each moisture content from the failure envelopes shown in Appendix A (Figs. A.11 to A.15). Typical failure envelopes are shown in Fig. 5.17. As can be seen from these figures, the points lie on a straight line. A clear picture of the cohesion intercept is obtained from the plots which could be drawn on a large scale because of the low confining pressures (1, 2 and 3 psi) used in the direct shear tests. These shear strength parameters are discussed later.

5.5.3 Triaxial Compression Tests

To determine the shear strength parameters in a triaxial compression test, it is necessary to test similar specimens at different confining pressures. In this research the technique of multi-stage testing was used with confining pressures of 10, 20 and 30 psi for each porosity and for each moisture content (Bauer 1969). The tests were made on samples at different porosities for each moisture content.

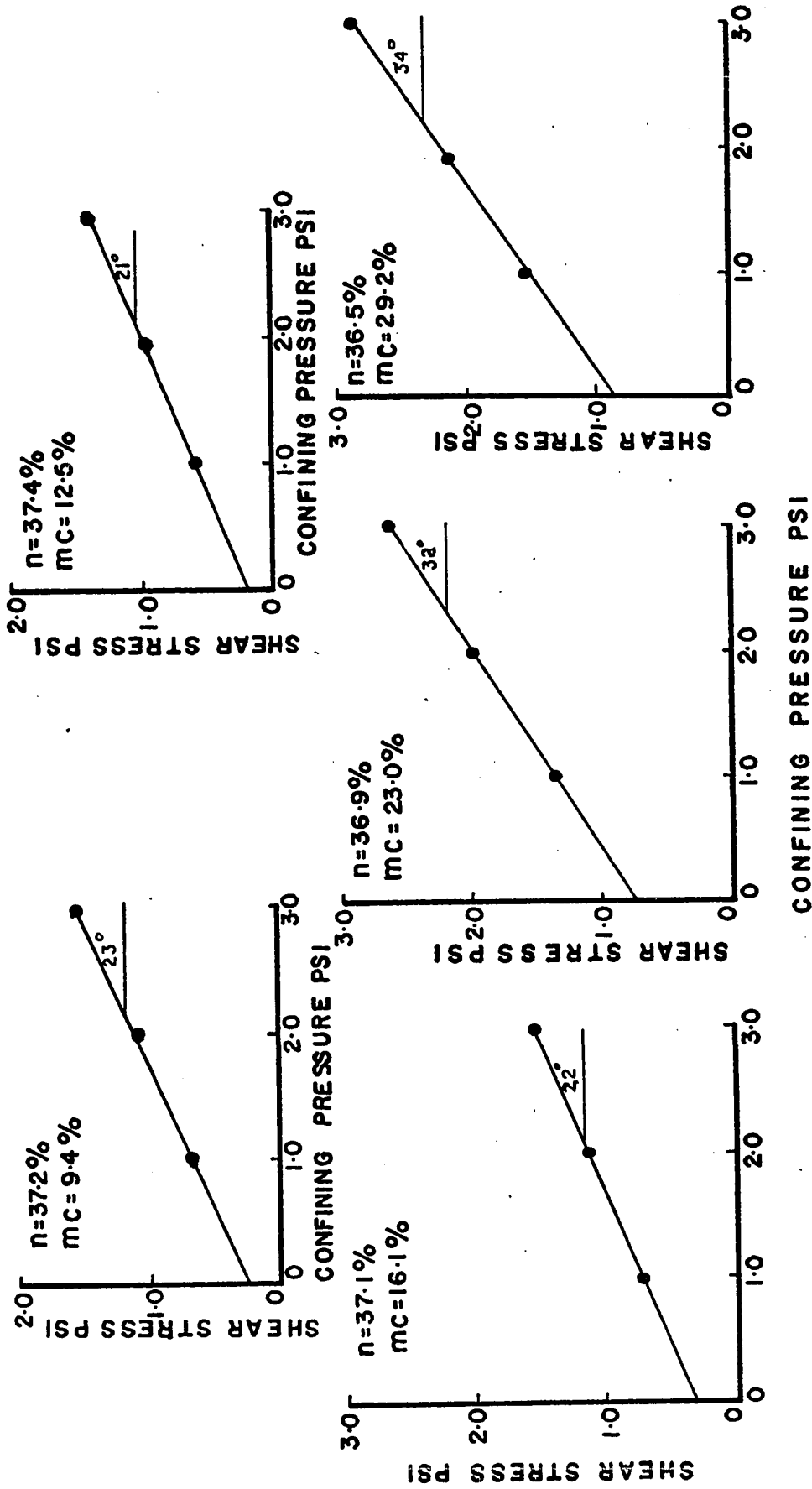


FIG.5.17 FAILURE ENVELOPE PLOTS FOR DIRECT SHEAR BOX TESTS

5.5.3.1 Stress-Strain Curves

The stress-strain curves for triaxial compression tests are presented in Appendix A (Figs. A.16 to A.19). Typical curves at one porosity are shown in Fig. 5.18. A test was started with a confining pressure of 10 psi and the deviator stress was applied until the peak stress was reached. The deviator stress and the confining pressure were then released and the rebound of the sample was measured. The test was then carried out at a confining pressure of 20 psi until the deviator stress again reached its peak value. The sequence was repeated for a confining pressure of 30 psi until or after sample failure had occurred.

Figure 5.18 shows that the deviator stress increases with strain and give a smooth curve for a confining pressure of 10 psi for the samples in the lower moisture content range (up to 16.4 per cent). But for confining pressure of 20 and 30 psi, the deviator stress increases rapidly at first and then approaches its peak value slowly.

For samples at 9.3 per cent moisture content the stress-strain curves follow in a stick slip pattern for confining pressures of 20 and 30 psi because of the reorientation of the grains along the failure plane. This phenomenon was, however,

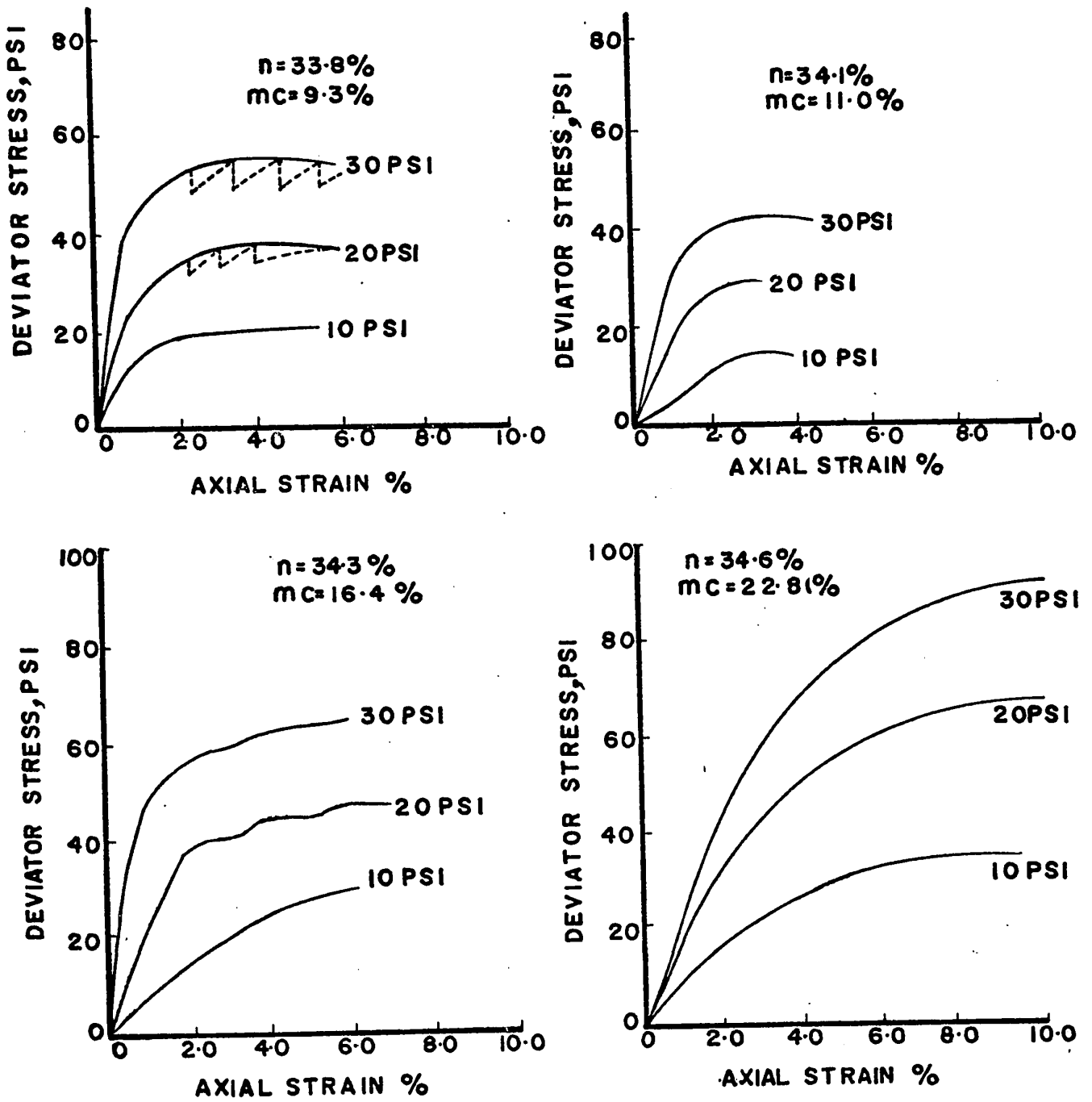


FIG. 5-18 STRESS STRAIN CURVES FOR TRIAXIAL TESTS

not obtained in the direct shear tests because in these tests a much larger sample was used and a greater number of grains were changing in position at the failure plane. This is the reason why the effect of the displacement of grains (stick slip action) in the direct shear tests was not noticed.

In the first stage the sample underwent a larger strain than in the second stage (at 20 psi confining pressure). In the third stage (30 psi confining pressure) the samples generally failed at 5 to 7 per cent strain in the lower moisture content range (9.3 to 16.4 per cent). For the 22.8 per cent moisture content samples at 30 psi confining pressure, the stress continued to increase with strain and did not reach a maximum at the maximum strain possible with this type of test. The tests were stopped after a maximum of 9 to 11 per cent strain at each stage.

The multi-stage tests on the 22.8 per cent moisture content samples probably suffer from some misinterpretation because the sample underwent a large deformation during each stage. The samples tested under the third stage had already been strained to approximately 20 per cent. It would be unrealistic to assume, therefore, that the sample had the same shearing characteristics during the last stage that it had during the first stage. The samples when taken out after the tests were a mass of deformed

and highly bonded grains. The grains were deformed and the voids in the sample appeared to be smaller than the initial voids. In all the tests, failure occurred because of bulging of the sample. A typical photograph of sample failure is shown in Fig. 5.18a.

5.5.3.2 Mohr Coulomb Failure Envelopes

The shear strength parameters of wheat at different porosities and moisture contents were obtained from the Mohr Coulomb failure envelopes shown in Appendix A (Figs. A.20 to A.23). Mohr Coulomb failure envelopes at different moisture contents for a typical porosity are shown in Fig. 5.19. The cohesion intercept of wheat is small in the lower moisture content range and could not be obtained from the Mohr Coulomb failure envelopes because of the small scale which had to be used for plotting these higher principal stresses.

5.5.4 Shear Strength Parameters

5.5.4.1 Coefficient of Friction

In Figs. 5.20 and 5.21 the coefficient of friction of wheat and the angle of internal friction obtained from direct

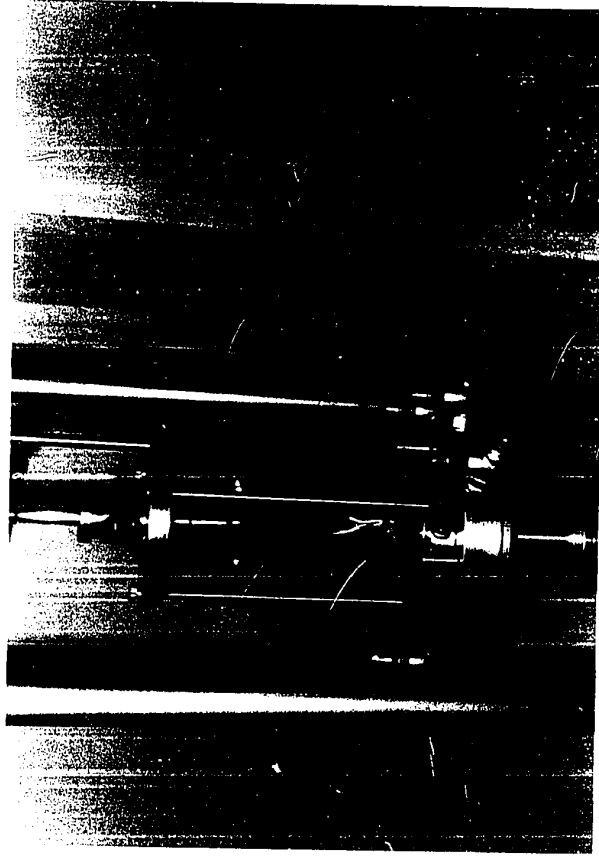


Fig. 5.18a Typical Photograph of Sample Failure

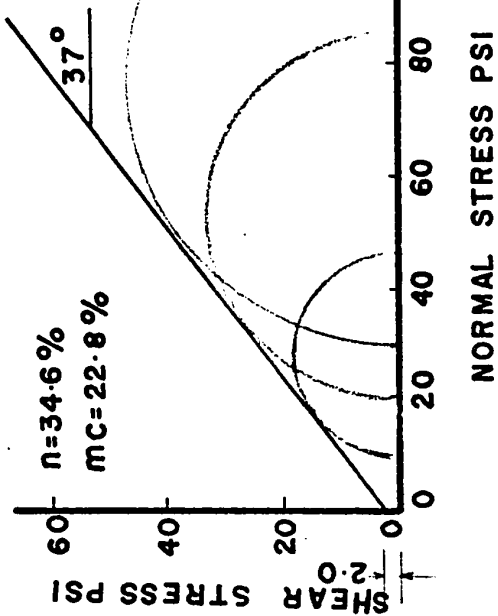
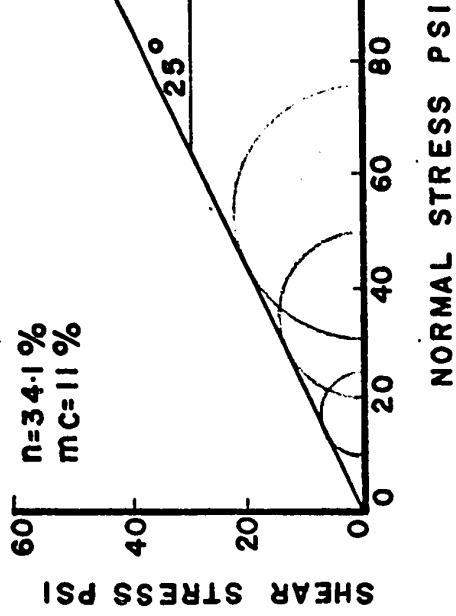
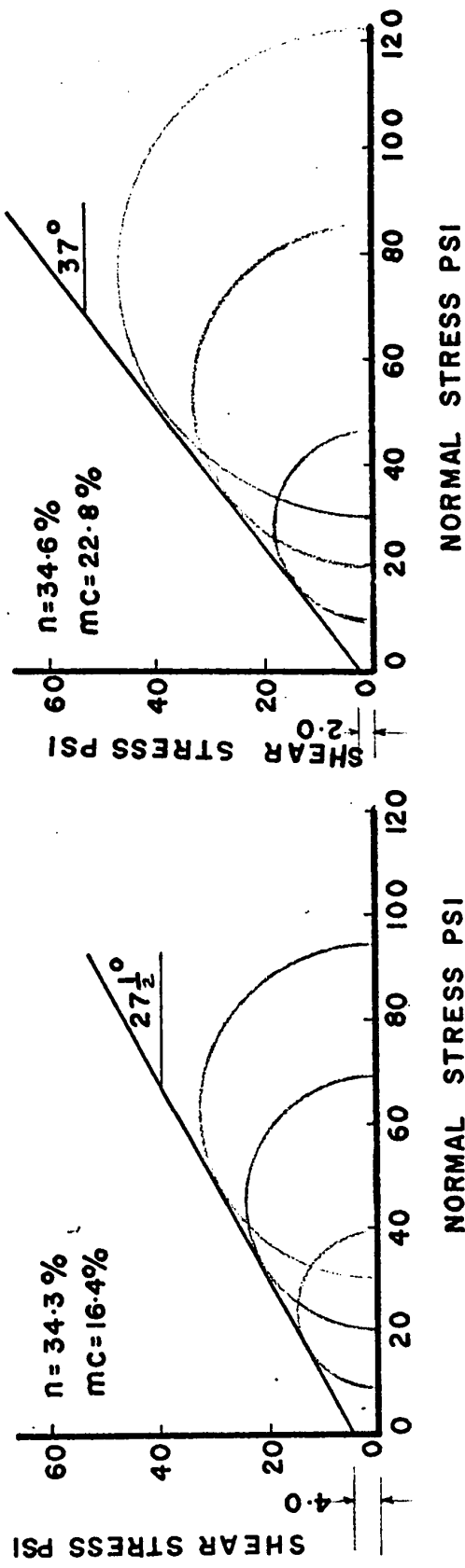
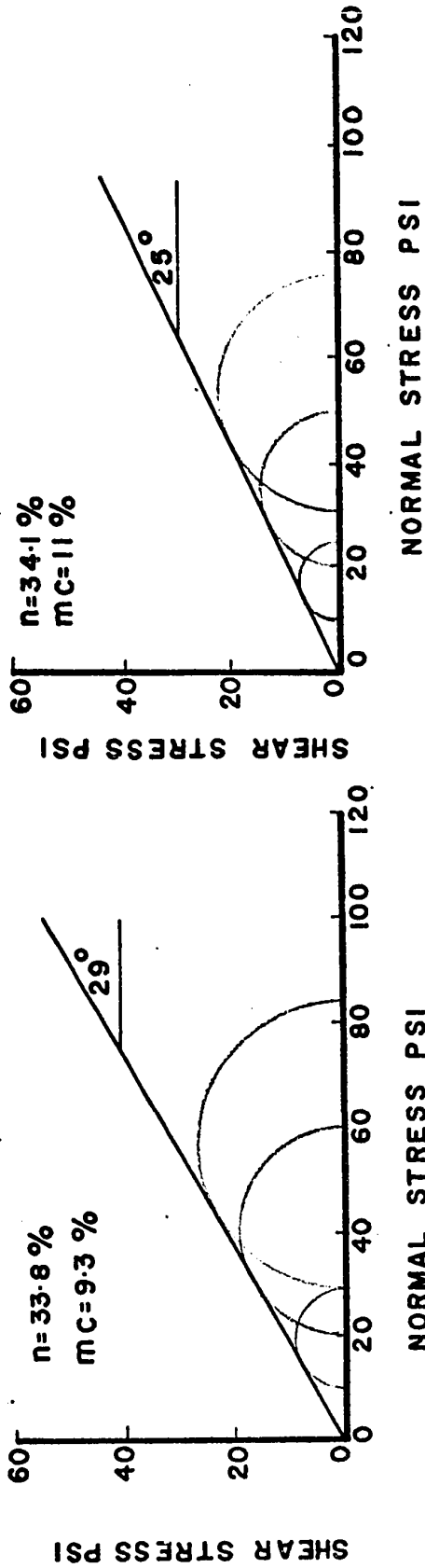


FIG. 5-19 MOHR COULOMB FAILURE ENVELOPES FOR TRIAXIAL COMPRESSION TESTS

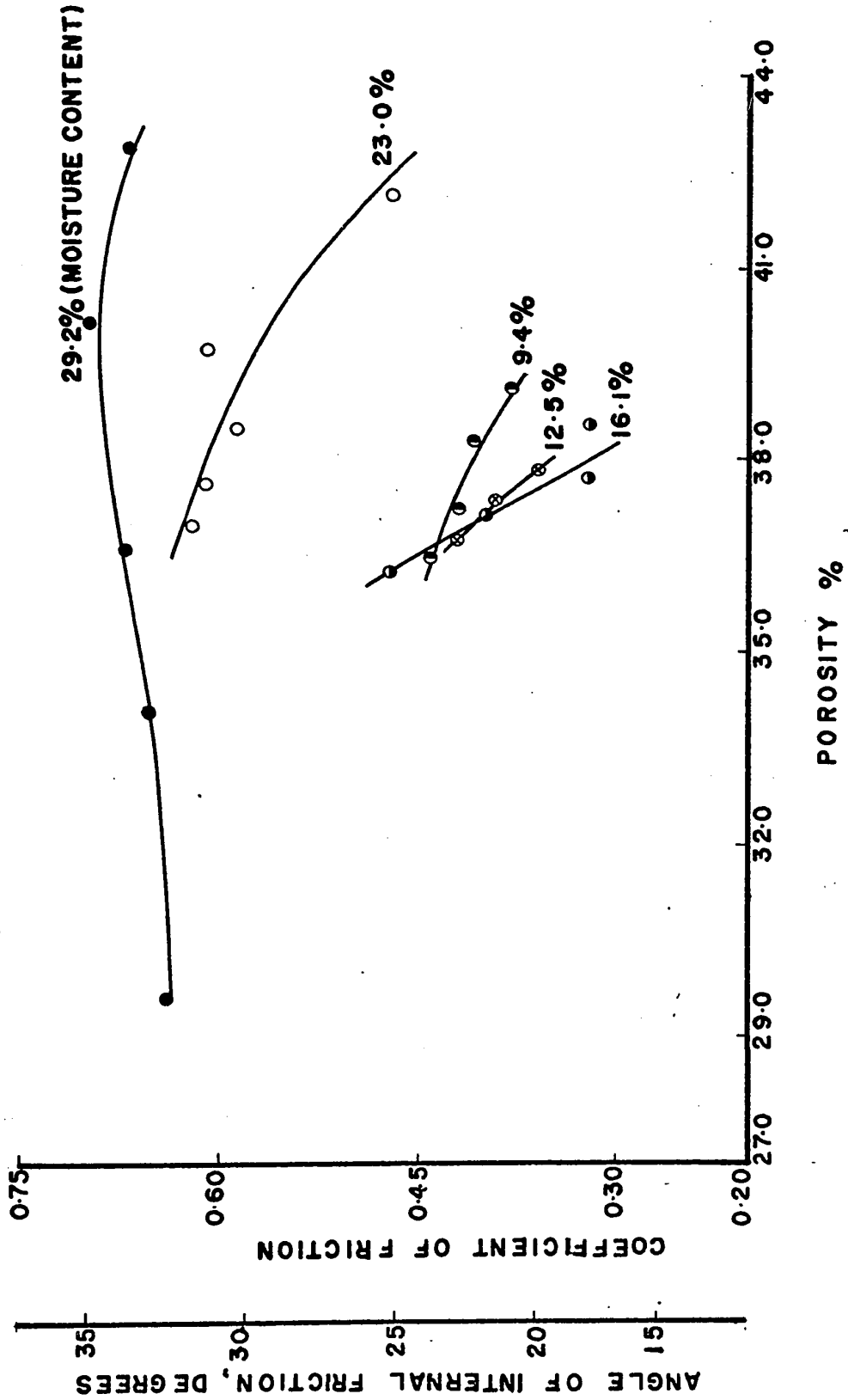


FIG.5.20 COEFFICIENT OF FRICTION FROM DIRECT SHEAR TESTS

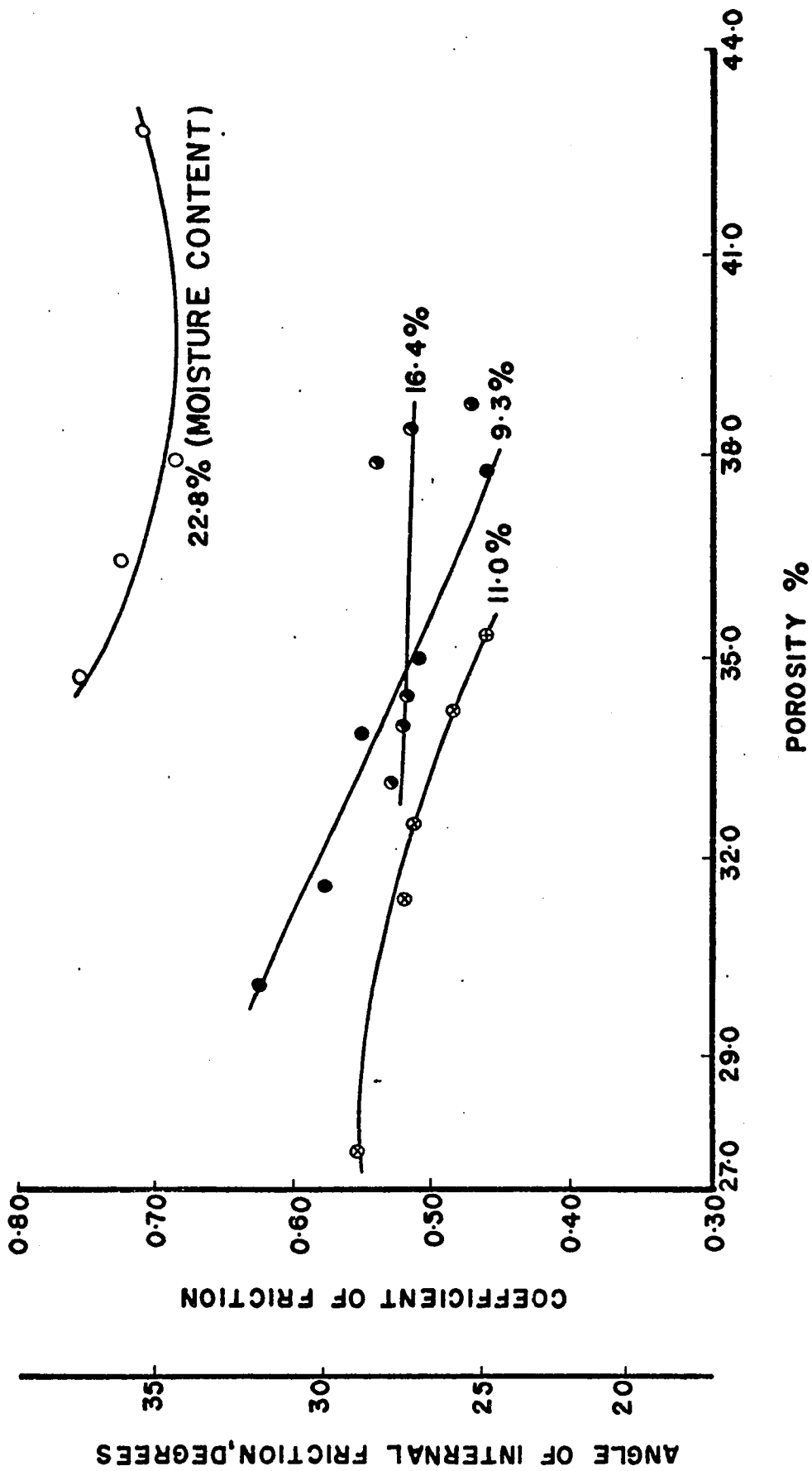


FIG. 5.21. COEFFICIENT OF FRICTION FROM TRIAXIAL TESTS

shear tests and triaxial compression tests respectively are plotted against porosity at different moisture contents. In both of the shear testing techniques it is observed that the coefficient of friction usually decreases as the porosity of the sample increases. At the higher moisture contents, however, the change in porosity has little effect on the value of the coefficient of friction.

The frictional component of shearing resistance mobilized in any shearing testing technique is governed by:

1. Sliding friction between the grains which is controlled by:
 - (a) the coefficient of surface friction of the individual grains or the surface roughness of the grains.
 - (b) the normal stress acting on the contact surface between the grains.
2. Density of the material and interlocking between the grains which depends upon the size, shape and structural packing of the wheat grains.

From Figs. 5.20 and 5.21, Fig. 5.22 is derived to isolate the effect of factor 1a. This figure shows the relationship between coefficient of friction and moisture content at varying porosities both for direct shear and triaxial compression tests.

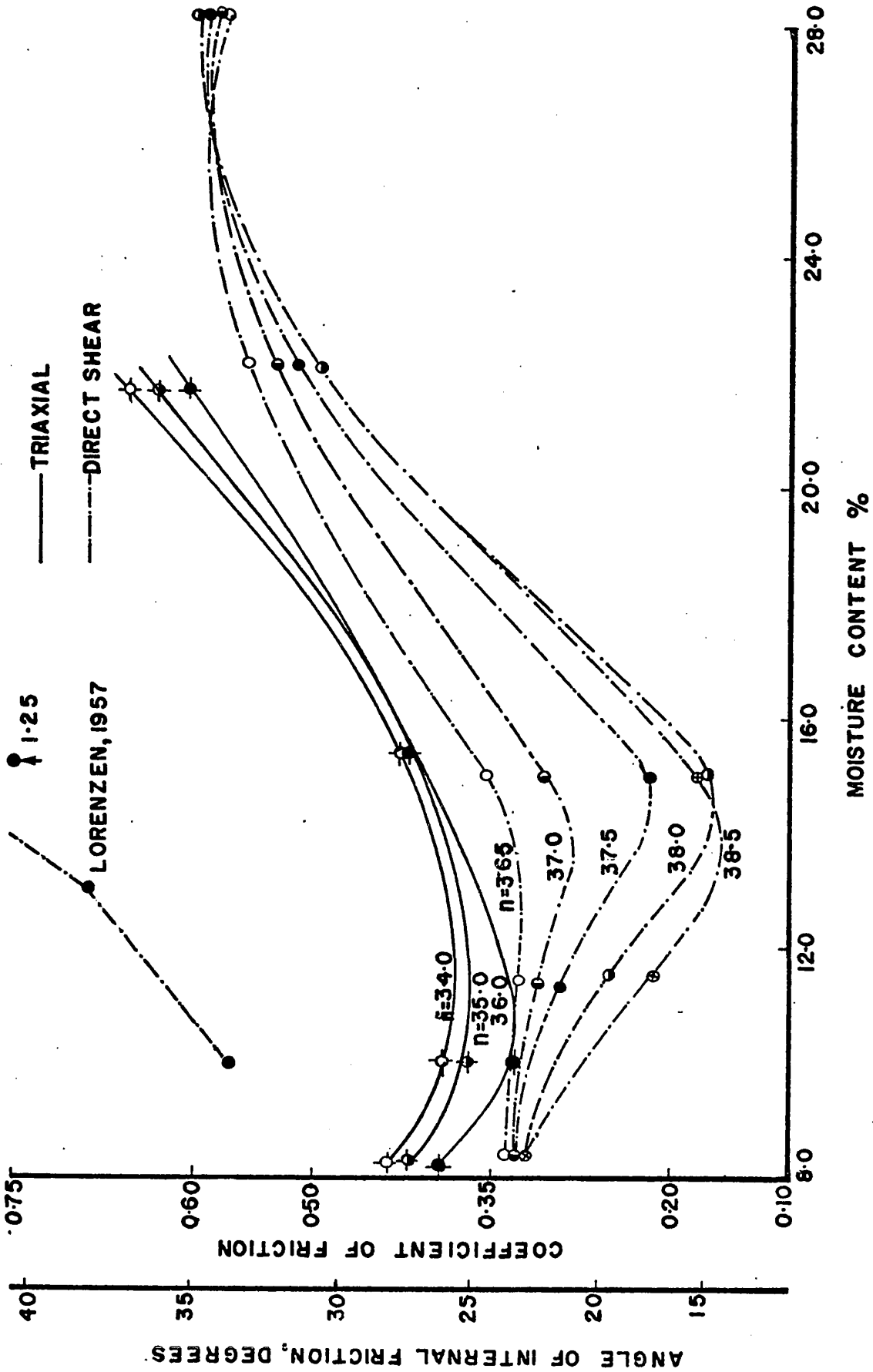


FIG. 5.22 COEFFICIENT OF FRICTION FROM DIRECT SHEAR AND TRIAXIAL TESTS

As can be seen from Fig. 5.22, the curves are plotted for 34.0, 35.0 and 36.0 per cent porosities for triaxial compression tests and for 37.0, 37.5, 38.0 and 38.5 per cent porosities for direct shear tests. The coefficients of friction could only be obtained for all moisture contents at these porosities. In the triaxial compression tests for any porosity the coefficient of friction decreased with increasing moisture content until it reached a minimum value of 12 ± 0.5 per cent moisture content; and it then rapidly increased with the increase in moisture content. The coefficient of friction varies from 0.47 to 0.75 in the moisture range from 9.3 to 22.8 per cent.

In the direct shear tests, the coefficient of friction decreases until 15 ± 0.5 per cent moisture content, after which there is a rather steep rise in the magnitude of the coefficient of friction with a further increase in the moisture content and then a levelling off at the highest moisture content. The coefficient of friction varies from 0.33 to 0.70 in the moisture content range of 9.4 to 29.2 per cent.

The effect of moisture content on the surface roughness of the grains can be seen by considering the curve for a single porosity where the influences of normal stress and structural packing are constant. The coefficient of friction is, therefore, only affected by the surface roughness of the grains.

At low moisture contents the grains are hard and fairly smooth. There is a small decrease in surface roughness as the moisture content is increased and then a large increase at the higher moisture contents. The change in surface roughness with moisture content must be related to the swelling and shrinking of the cells at the surface of the wheat kernel. As discussed in chapter 4 (4.2) the wheat kernels swell with an increase in moisture content, and it would appear that this swelling causes the small protuberances on the surface to swell and become more prominent.

As seen from Fig. 5.22, the coefficients of friction obtained from the direct shear tests and the triaxial compression tests are compatible at moisture contents of 9.0 to 13.0 per cent. Beyond 13.0 per cent moisture content, the coefficients of friction obtained from triaxial compression tests have higher values than those obtained from the direct shear tests. In the triaxial compression tests because of the deformation of the sample, the grains became more closely packed and thus reduced the void spaces in the sample during each stage. The decrease in void spaces resulted in the lowering of the porosity of the samples (the porosities shown in figures are all initial porosities and not porosities at failure where the coefficients of friction are measured). The lower porosities at failure of the

samples give higher coefficients of friction. In the direct shear tests, however, the samples tested at increasing confining pressures had the same initial porosity. The deformation and volume change at failure were also considerably smaller in the direct shear tests than in the triaxial compression tests. Therefore, the porosities would be high for direct shear tests, and the coefficient of friction at failure would be smaller even though the initial porosities were the same in both types of tests.

5.5.4.2 Cohesion

In Figs. 5.23 and 5.24, the cohesion of wheat obtained from direct shear and triaxial compression tests, respectively, is plotted against porosity at different moisture contents. From these data Fig. 5.25 is obtained which shows the relationship between cohesion and moisture content at varying porosities, both for direct shear and triaxial compression tests.

In the direct shear tests the cohesion intercept varies from 0.12 to 1.50 psi in the moisture content range from 9.4 to 29.2 per cent (Fig. 5.23). In the triaxial tests the cohesion intercept changes from 0 to 1.75 psi in the moisture content range from 9.3 to 22.8 per cent (Fig. 5.24).

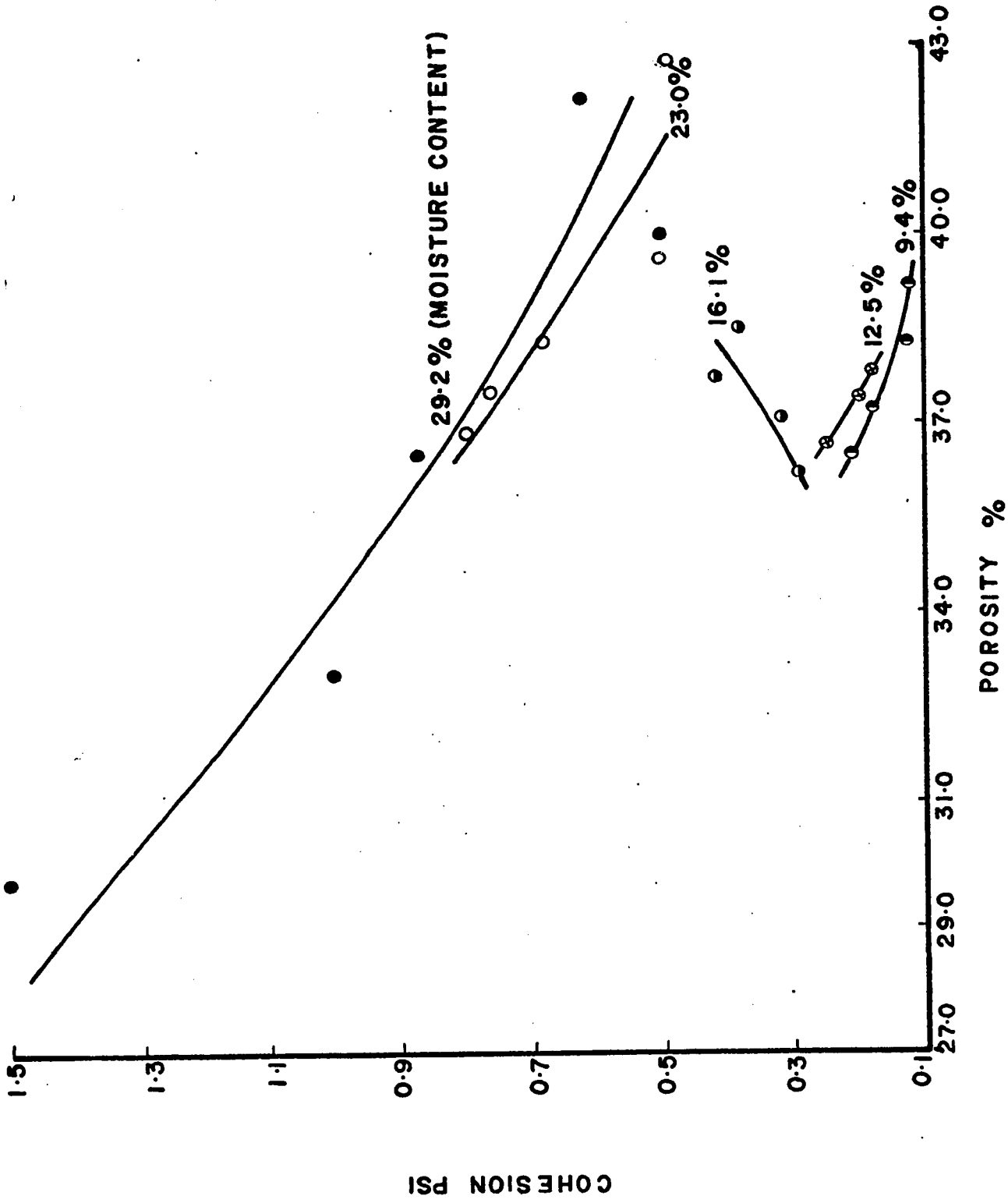


FIG.5.23 COHESION INTERCEPT FROM DIRECT SHEAR TESTS

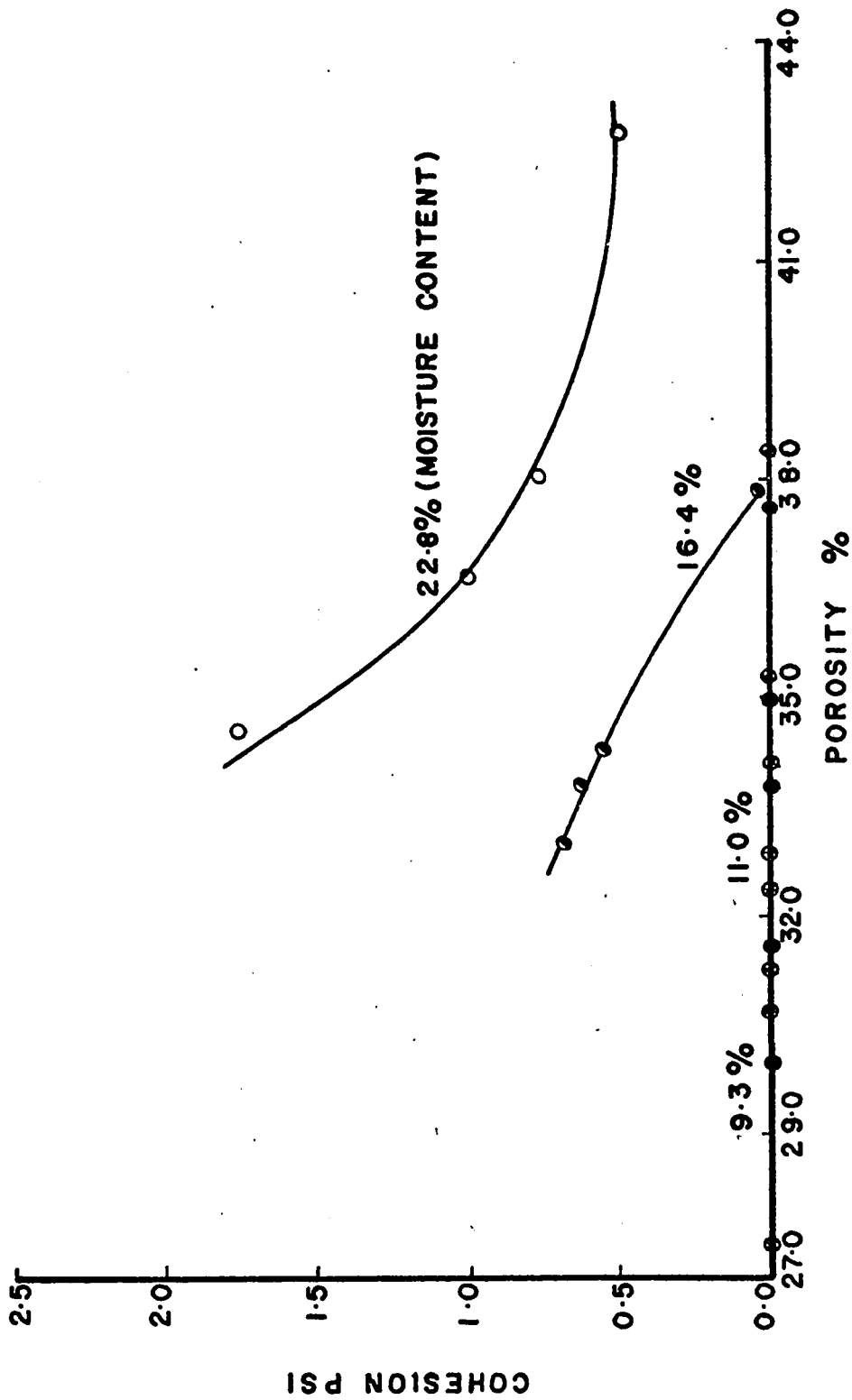


FIG.5.24 COHESION INTERCEPT FROM TRIAXIAL TESTS

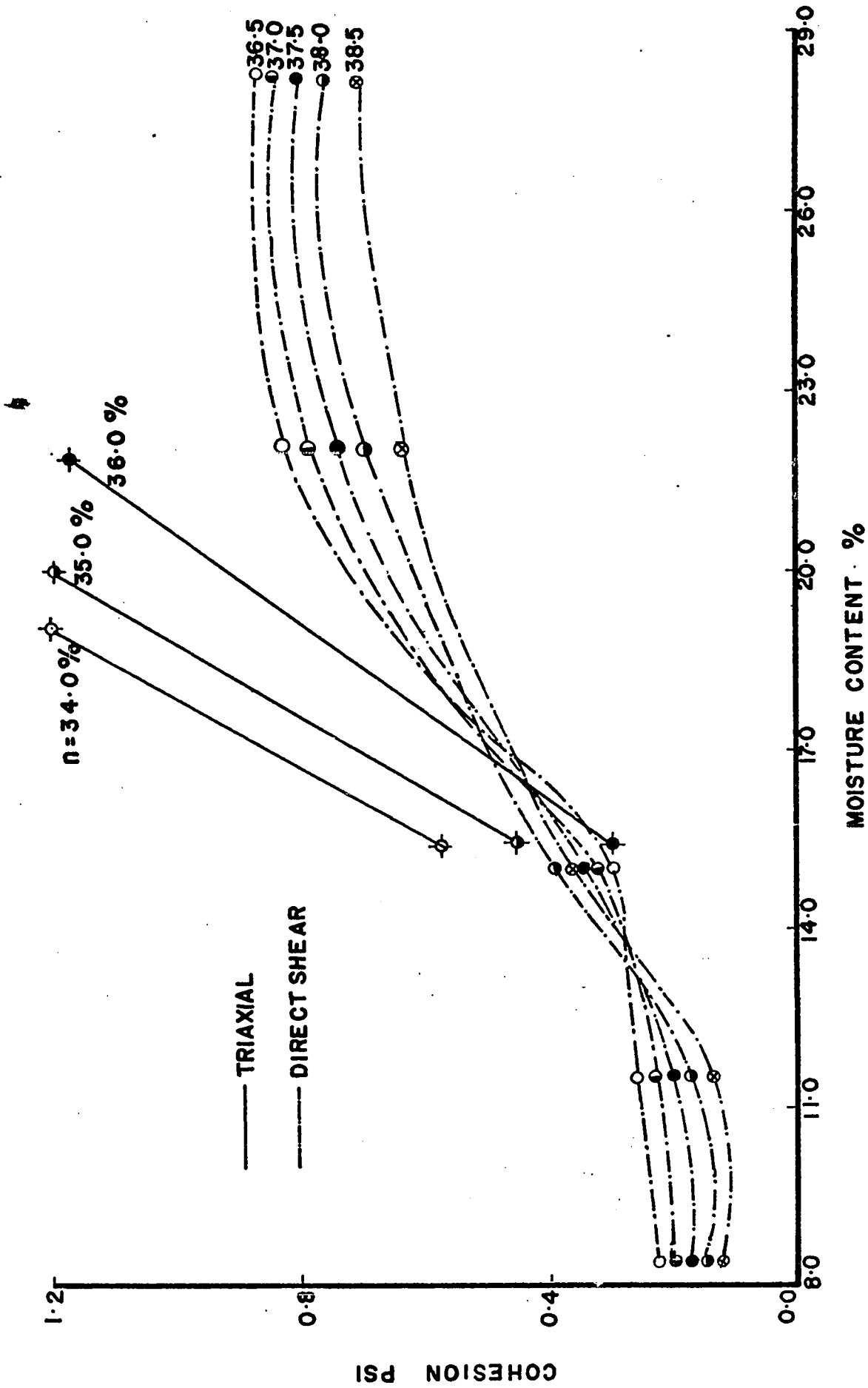


FIG. 5.25 COHESION INTERCEPT FROM DIRECT SHEAR AND TRIAXIAL TESTS

The cohesion between the wheat grains is affected by the two factors:

1. Grain to grain unit cohesiveness, and
2. Area of contact between the grains.

Figure 5.25 shows that the change in the value of the cohesion intercept is small in the lower moisture content range but increases rapidly as the moisture content is further increased and then levels off at the higher moisture content. The effect of moisture content on the cohesiveness between the grains can be seen by considering the curve for a single porosity where the area of contact between the grains is constant.

In the lower moisture content range, the grains are hard and brittle, and the cohesiveness between the wheat grains is small and does not change very much. As the moisture content of the wheat increases, the grains become deformable and soft and the cohesiveness increases between the wheat grains. This increase in cohesiveness with moisture content is probably connected with the influence of water on gluten and other substances in the wheat grains.

Figure 5.25 also shows that the cohesion intercept of wheat increases as the porosity of the sample is decreased. The cohesion of the wheat samples at a moisture content of 9.4 per cent increases from 0.12 to 0.21 psi in the porosity range from 38.5

to 36.5 per cent. At 29.2 per cent moisture content, the cohesion intercept varies from 0.71 to 0.88 psi in the porosity range of 38.5 to 36.5 per cent.

It is observed from this study that the triaxial compression tests give higher values for the cohesion intercept of wheat than do direct shear tests. It should be remembered that all porosities shown are initial porosities and not porosities at failure where the cohesion intercepts are measured.

In the triaxial compression tests due to the deformation of the sample, the grains were becoming closely packed, thus reducing the void spaces in the sample during each stage. The decrease in void spaces resulted in the lowering of the porosity of the samples. The lower porosities at failure of the samples give higher cohesion intercepts. In the direct shear tests, however, the samples tested at increasing confining pressures had the same initial porosity. The deformation and volume change at failure were also considerably smaller in these tests than in the triaxial tests. Therefore, the area of contact at failure between the grains would be smaller for the direct shear tests and the cohesion intercepts at failure would be smaller even though the initial porosities were the same in both types of tests.

5.5.5 Comparison with other Work

Lorenzen in 1957 measured the coefficient of friction of a wheat at different moisture contents using a shear box 8 x 8 inches. His results are given in Fig. 5.22. It can be seen from his results that an increase in the moisture content of the wheat kernels increases the coefficient of friction. This is in agreement with the results obtained in this research.

The coefficients of friction at different moisture contents found by Lorenzen are higher than those obtained here. Lorenzen performed tests on wheat samples at only one confining pressure and he determined the angle of internal friction assuming the cohesion of wheat as zero, which, appears to be incorrect. His results include both friction and cohesion and cannot be compared with the values obtained here.

The literature survey on the shearing strength properties of agricultural granular materials reveals that the cohesion in agricultural materials has not been investigated before. Lorenzen (1957) and Stewart (1968), in their work on agricultural granular materials, only mentioned that the cohesion between the materials increases as the moisture content of the materials increases, but they did not determine the magnitude of the cohesion in the materials.

In the previous research on wheat grain, the effect of porosity on the shear strength properties of wheat was not considered. Stewart (1968) studied the effects of bulk density on the coefficient of friction of a different material - sorghum grain. He found that an increase in bulk density increases the coefficient of friction of the sorghum grain.

In the research done here, the parameters, coefficient of friction and cohesion of wheat at different moisture contents were closely established for varying porosities. From the published literature it would appear that these relationships have not been studied or established before.

5.6 Sliding Resistance of Wheat on Structural Surfaces

As discussed in chapter 2, a knowledge of the sliding resistance of wheat on structural surface is required to determine the magnitude and distribution of lateral pressures on bin walls and to know how much frictional force between the stored materials and the walls of storage structures must be overcome before the materials can be moved out of storage. Direct shear tests were performed to determine the sliding resistance parameters of wheat on different structural surfaces. Structural surfaces used were: hard oak wood (the wheat movement being perpendicular

to the grain of the wood), hot rolled plate steel, and concrete (block made from 1:2:4 mix with a 2-inch slump).

5.6.1 Direct Shear Tests

The direct shear tests were carried out with wheat at different moisture contents of 9.3, 12.2, 16.8, 23.3 and 29.4 per cent against wood, steel and concrete. The tests were performed at the highest and lowest possible achieved porosities for each moisture content. The tests were generally carried out with confining pressures of 1, 2 and 3 psi for each moisture content and porosity. Several of the tests were made at confining pressures of 2, 4 and 6 psi.

5.6.1.1 Stress-Horizontal Deformation and Volume Change Curves

The stress-deformation plots and their corresponding volume change curves for wheat against different structural surfaces are shown in Appendix A (Fig. A.24 to A.26). Three typical curves, one for each structural surface, are shown in Fig. 5.26. The curves are discussed below separately for each structural surface.

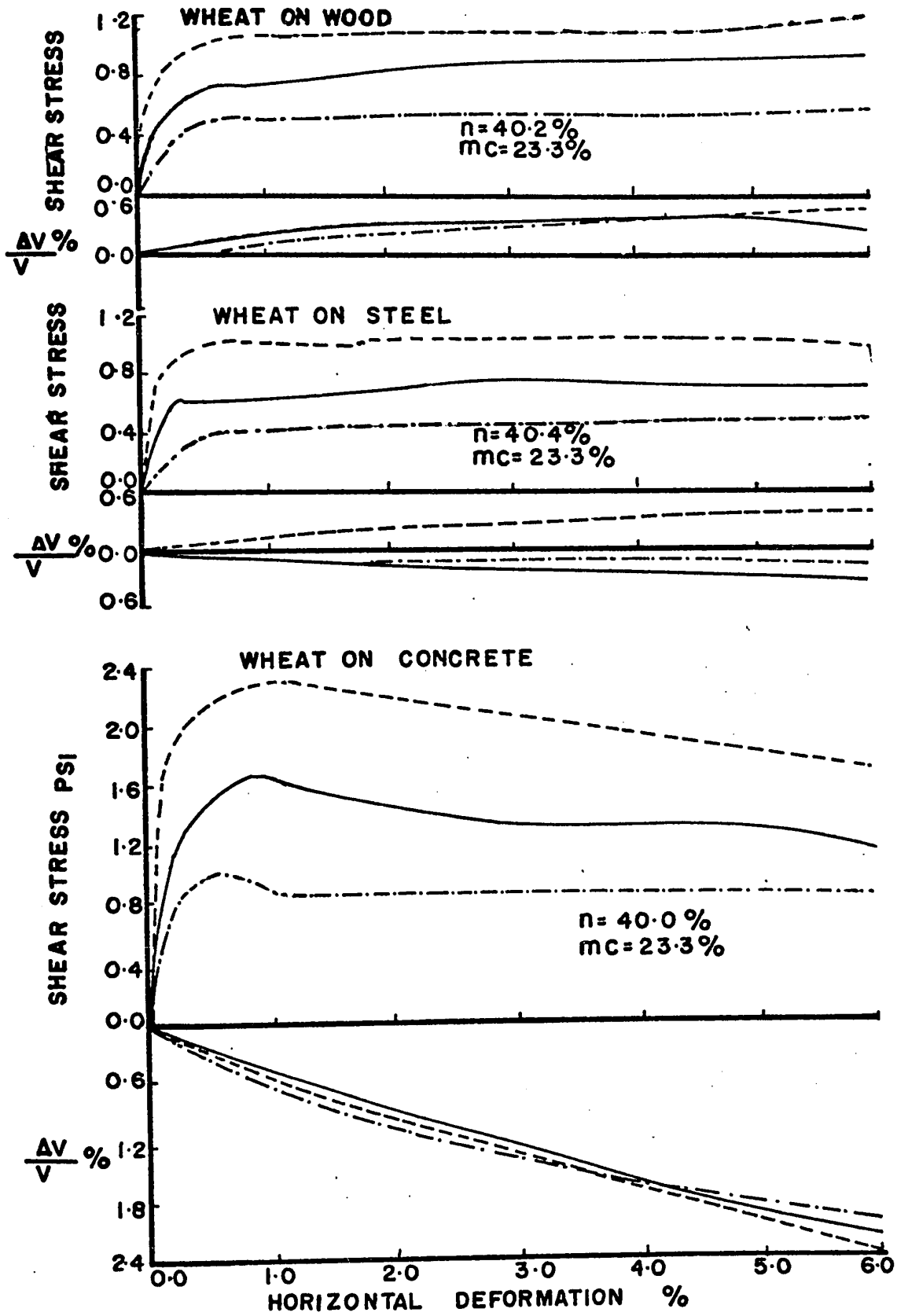


FIG.5.26 STRESS DEFORMATION OF WHEAT ON STRUCTURAL SURFACES

5.6.1.1.1 Wheat on Wood

As can be seen from the stress-deformation curves, in the lower moisture content range, the stress increased rapidly and reached its peak value at 0.5 to 1.0 per cent deformation. With further deformation, a stick-slip pattern, probably due to reorientation of the grains on the structural surface, occasionally developed. The stress usually reached its ultimate value at 4 to 6 per cent deformation. In the higher moisture range, the stress increased rapidly at first (up to 1 per cent deformation) and then increased more slowly with horizontal deformation, reaching its peak value at approximately 6 per cent deformation.

At low moisture contents, the peak stress is reached at a small deformation because the largest force is required to overcome the static shear resistance between the wheat mass and the structural surface. Once the static shear resistance is fully mobilized a smaller force is needed to keep the wheat mass moving over a surface. At higher moisture contents, the grains are soft and deformable. The grains deform with horizontal deformation and the contact area between the grains and the surface increases. The increase in contact area increases the adhesion component of the shear resistance. That is why the shear resistance for high moisture content samples is

not fully mobilized until larger deformations take place.

The volume change curves show that the high porosity samples generally expanded in volume but the lower porosity samples did not follow any definite pattern.

The volume change of the samples varied with the confining pressure applied, being small at high confining pressure and slightly larger at lower confining pressures.

The volume change at failure is -0.08 to $+0.34$ per cent in the lower moisture content range and -0.90 to $+0.44$ per cent in the higher moisture content range.

5.6.1.1.2 Wheat on Steel

The stress-deformation curves show that the stress increased rapidly (up to 0.5 per cent horizontal deformation) and then increased slowly in the stick-slip fashion with further horizontal deformation. The maximum stress was reached at 1 to 6 per cent horizontal deformation. As the moisture content of the sample increased, (in the range of 9.3 to 29.4 per cent) the horizontal deformation at failure decreased.

The volume change curves show that for a confining pressure of 3 psi, the volume of the sample usually expands during shear for all moisture contents and at all porosities. At 2 psi

confining pressure, the volume change-deformation curves did not follow a definite pattern. At 1 psi confining pressure, the sample always decreased in volume. This is true for all porosities and for all moisture contents. The volume change of the samples at failure varies from -0.50 to 0.39 per cent in the moisture content range of 9.3 to 29.4 per cent.

5.6.1.1.3 Wheat on Concrete

The stress increased rapidly with the horizontal deformation and reached its peak value at a low deformation, about 1 to 2 per cent, and then the curve followed a zig zag pattern as the horizontal deformation was increased. This characteristic of the curve is noticed at all confining pressures and for all moisture contents. The zig zag pattern of the stress-deformation curve was obtained because the grains become interlocked in the bumps on the concrete block which force the grains in the upper layer of the shear box to roll over the interlocked grains.

The volume change curves show, that, for all moisture contents, the volume of the samples first expanded and then contracted at a confining pressure of 3 psi as the horizontal deformation was increased. At 2 psi confining pressure, in the

lower moisture content range, the samples decreased in volume with deformation but in the higher moisture content range, the samples first expanded and then decreased in volume as the horizontal deformation was increased. At 1 psi confining pressure, the samples contracted in volume with horizontal deformation. This has been observed for all moisture contents.

At lower porosity, the samples decreased in volume at all confining pressures and for all moisture contents. The decrease was practically the same for all confining pressures in the moisture content range of 9.3 to 23.3 per cent. At 29.4 per cent moisture content, the contraction of the sample was a maximum at 1 psi confining pressure and decreased as the confining pressure was increased.

At higher porosity, in the moisture range of 9.3 to 23.3 per cent and at a confining pressure of 3 psi, the samples expanded in volume up to 1 per cent horizontal deformation and then decreased in volume with further increase in horizontal deformation. At 1 and 2 psi confining pressures, the samples decreased in volume as the horizontal deformation increased. At 29.4 per cent moisture content, for confining pressures of 2 and 3 psi, the samples expanded in volume and had their maximum expansion at 3-4 per cent deformation. The volume expansion then decreased with further increase in deformation. At 1 psi confining

pressure, the sample decreased in volume as the horizontal deformation increased.

The volume change of the samples at failure in the moisture content range of 9.3 to 29.4 per cent was from -1.50 to +0.75 per cent.

5.6.1.1.4 Discussion

As discussed in this chapter the volume changes of wheat samples tested on wood and steel are smaller than those for wheat on concrete. In the moisture content range of 9.3 to 29.4 per cent, the observed volume changes of wheat on wood, wheat on steel and wheat on concrete are +0.44 to -0.90, +0.39 to -0.50 and +0.75 to -1.50 per cent, respectively.

The surfaces of the wood and steel were smooth and the grains were moving as a mass adjacent to the structural surfaces. But the concrete block had small bumps on its surface, and the wheat grains on its surface were interlocked in these bumps. This interlocking (between the grains and the roughness of the concrete block surface) forced the grains of the upper layer, in the shear box, to roll over the interlocked grains and thus changed their relative positions. This is believed to be the reason for the greater volume change on the concrete than on

the wood and steel.

The volume changes recorded from the direct shear tests of wheat on wheat at failure varied from +0.45 to -4.20 per cent as compared to +0.75 to -1.50 per cent recorded from the direct shear tests for wheat on concrete. The volume changes from the tests of wheat on wheat are greater than wheat on structural surfaces because of the large volume of samples over which the volume changes were taking place and also because of the greater thickness of the failure plane for the wheat on wheat tests.

5.6.1.2 Failure Envelope Plots

The shear resistance properties of wheat at different moisture contents on structural surfaces at the minimum and maximum achieved porosities were obtained from failure envelope plots given in Appendix A (Figs. A.27 to A.29). Three typical plots, one for each structural surface, are shown in Fig. 5.27. As can be seen from these plots, the failure envelope lines generally pass through all the points. A clear picture of the adhesion intercept is obtained from plots drawn to a large scale at the low confining pressures.

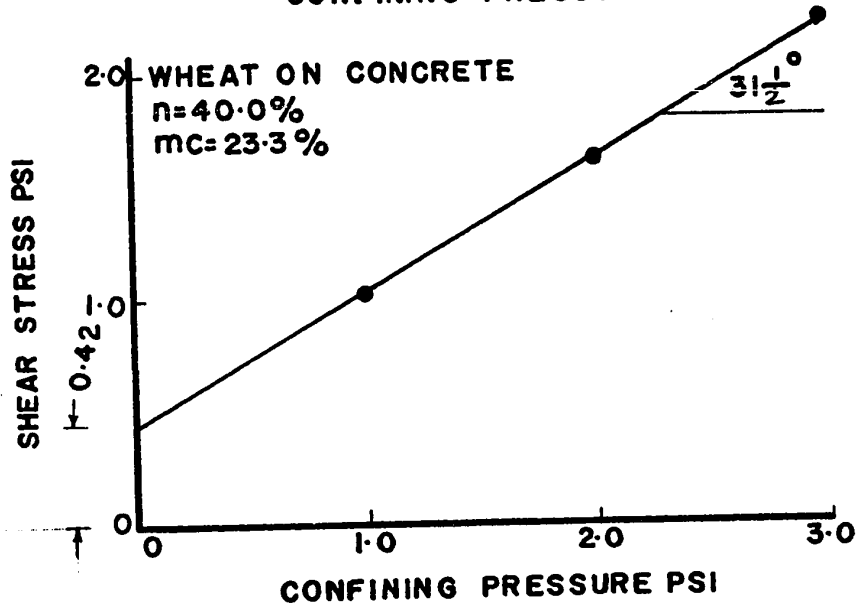
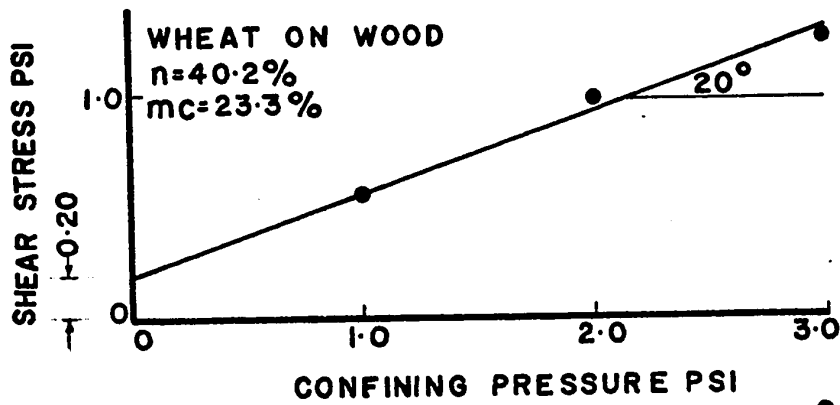
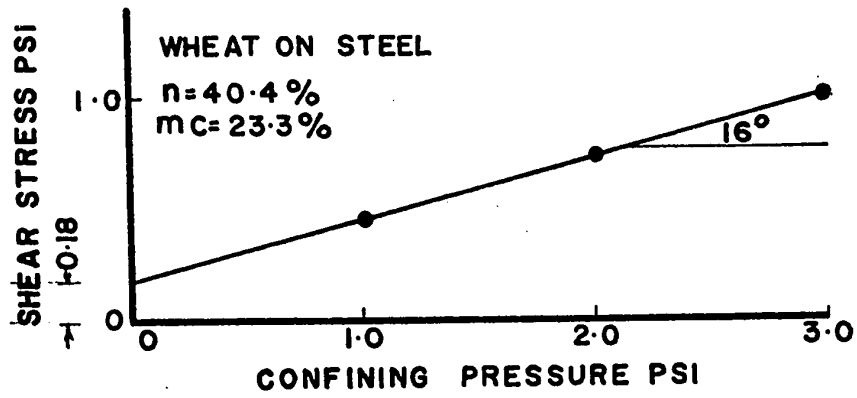


FIG.5-27 FAILURE ENVELOPE PLOTS OF WHEAT ON STRUCTURAL SURFACES

5.6.2 Sliding Resistance Parameters

The sliding resistance of wheat grain on structural surfaces depends upon two factors:

1. The coefficient of friction ($\tan \delta$) between wheat grains and material surfaces. The angle of friction (δ) depends upon the true friction angle between the grains and material surfaces (ϕ_w) and angle of interlocking (r) due to wall roughness.
2. Adhesion between the material surface and wheat.

As was discussed in section 5.5, the surface roughness and cohesion of the wheat grains increased as the moisture content of the wheat increased. When wheat samples of different moisture contents are tested on different structural surfaces, the magnitude of the coefficient of friction and the magnitude of the adhesion between the wheat and the material surface should, therefore, be small for the lower moisture content wheat samples and large for the higher moisture content samples.

The maximum and minimum values of the shear resistance parameters of the wheat on the structural surfaces are shown in Figs. 5.28 and 5.29. The plots are drawn this way because only the minimum and maximum porosities were known

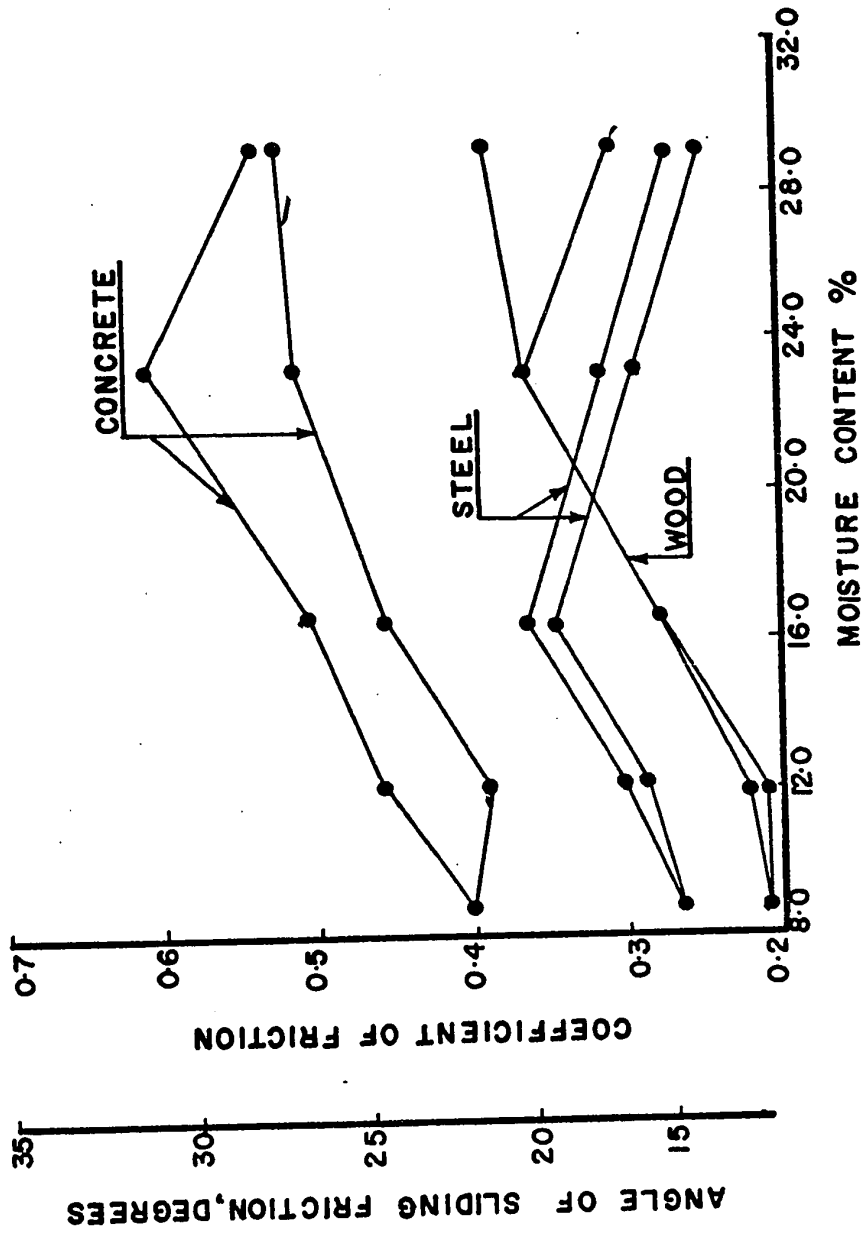


FIG. 5.28 COEFFICIENT OF FRICTION OF WHEAT ON STRUCTURAL SURFACES

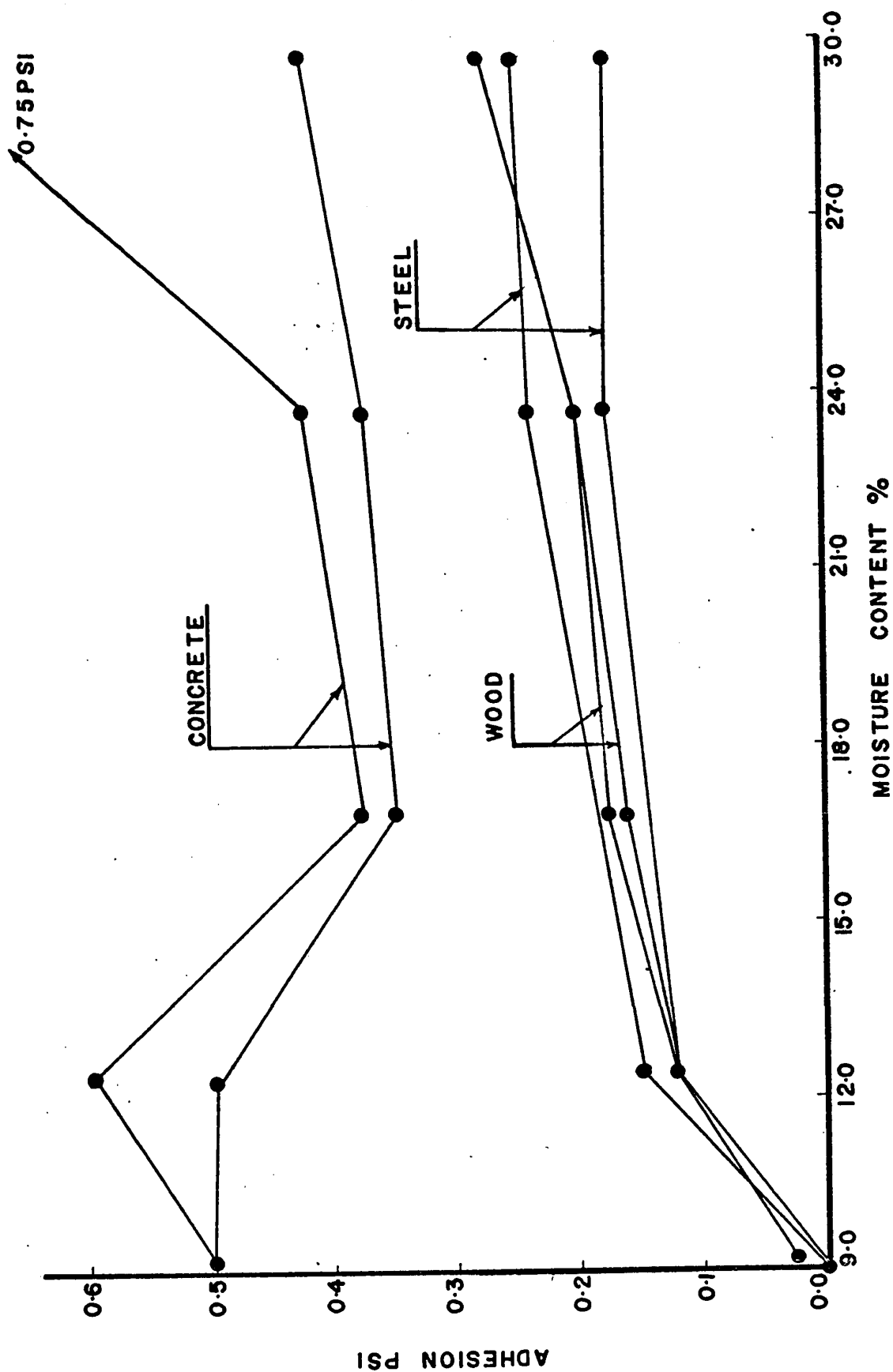


FIG. 5.29 ADHESION INTERCEPT OF WHEAT ON STRUCTURAL SURFACES

at each moisture content. The results are discussed separately for each structural surface.

5.6.2.1 Wheat on Wood

As can be seen from Fig. 5.28, the coefficient of friction ($\tan \delta$) increased as the moisture content of the wheat increased. The coefficient of friction varies from 0.20 to 0.38 in the moisture content range from 9.3 to 29.4 per cent.

The change in porosity of the wheat samples generally did not affect the coefficient of friction of wheat on wood, although at 29.4 per cent moisture content, the coefficient of friction changed from 0.31 to 0.38 when the porosity changed from 43.6 to 36.5 per cent.

The adhesion intercept of wheat on wood increased as the moisture content of the wheat increased (Fig. 5.29). Its values vary from 0.02 to 0.28 psi in the moisture content range from 9.3 to 29.4 per cent.

The change of the porosity of the sample had no effect on the magnitude of adhesion at all the moisture contents.

The sliding resistance parameters (the surface frictional component, δw , and adhesion component (A_w) between the wheat grain and the wood surface are always less than the

shear strength parameters of wheat at all moisture contents (Table 5.1). Thus the ratio $\frac{\delta w}{\phi}$ varies between 0.51 to 0.85 ($\delta w = 0.51 - 0.85 \phi$) and the ratio $\frac{A_w}{C}$ varies between 0.14 to 0.73 ($A_w = 0.14 - 0.73 C$). The average values of the ratios of $\frac{\delta w}{\phi}$ and $\frac{A_w}{C}$ are 0.63 and 0.40 respectively (Table 5.1).

5.6.2.2 Wheat on Steel

The coefficient of friction of wheat on steel increased from 0.26 to 0.37 as the moisture content of the wheat grains increased from 9.3 to 16.8 per cent. Beyond 16.8 per cent moisture content, the coefficient of friction decreased to 0.25 as the moisture content increased to 29.4 per cent.

For wheat samples in the higher moisture content range, moisture on the surface of the wheat grains may act as a lubricant between the grains and the steel. Within the grain mass redistribution of moisture takes place between grain and grain. But when grains slide over surfaces, moisture on the surface of the grain may affect the coefficient of friction depending upon the material of the surface. If the surface absorbs moisture from the grains (as wood and concrete do), the frictional resistance does not decrease. If the surface does not absorb the surface moisture of the grains, however, then the surface

Table 5.1 Relationship between shear strength parameters of wheat (ϕ and C) and sliding resistance parameters of wheat on wood (δw and A_w)

Moisture Content		9.4%	12.5%	16.1%	23.0%	29.2%
ϕ	min	21	20	17½	25	32½
	max	23½	23	25	32	35
δw	min	12	12	15	20½	17½
	max	12	13	15	20½	21½
$\frac{\delta w}{\phi}$	min	0.57	0.60	0.85	0.82	0.53
	max	0.51	0.57	0.60	0.65	0.61
C	min	0.12	0.18	0.29	0.50	0.50
	max	0.21	0.25	0.42	0.80	1.50
A_w	min	0.03	0.12	0.16	0.20	0.27
	max	0.03	0.12	0.17	0.20	0.27
$\frac{A_w}{C}$	min	0.30	0.73	0.55	0.40	0.54
	max	0.14	0.48	0.41	0.25	0.18

moisture may act as a lubricant and thus decrease the magnitude of frictional resistance.

The change in porosity had no appreciable effect on the coefficient of friction of wheat on steel. The difference between the minimum and maximum values of coefficient of friction is approximately 0.02.

The adhesion intercept of wheat on steel increased from 0 to 0.25 psi as the moisture content increased from 9.3 to 29.4 per cent (Fig. 5.29).

The adhesion intercept for wheat on steel was affected by the porosity, increasing as the porosity of the sample decreased. When the porosity is lower, the area of contact between the grains and per unit area of steel surface increases and therefore the adhesion of wheat on steel increases. The difference in the magnitude of the adhesion (Fig. 5.29) at the minimum and maximum porosities of the samples is a maximum of 0.07 psi.

The sliding resistance parameters (the surface frictional component, δ_s) between wheat grain and a steel surface are generally less than the shear strength parameters of wheat at all moisture contents (Table 5.2). The ratio $\frac{\delta_s}{\phi}$ varies between 0.64 to 1.07 in the lower moisture content range and between 0.43 to 0.65 in the higher moisture content range.

Table 5.2 Relationship between shear strength parameters of wheat (ϕ and C) and sliding resistance parameters of wheat on steel (δ_s and A_s)

Moisture Content		9.4%	12.5%	16.1%	23.0%	29.2%
ϕ	min	21	20	$17\frac{1}{2}$	25	$32\frac{1}{2}$
	max	$23\frac{1}{2}$	23	25	32	35
δ_s	min	15	$16\frac{1}{4}$	$18\frac{3}{4}$	$16\frac{1}{4}$	14
	max	15	$17\frac{1}{4}$	$20\frac{1}{4}$	17	15
$\frac{\delta_s}{\phi}$	min	0.72	0.81	1.07	0.65	0.43
	max	0.64	0.75	0.81	0.53	0.43
C	min	0.12	0.18	0.29	0.50	0.50
	max	0.21	0.25	0.42	0.80	1.50
A_s	min	0.02	0.12	0.14	0.17	0.18
	max	0.02	0.15	0.17	0.23	0.25
$\frac{A_s}{C}$	min	0.17	0.67	0.48	0.34	0.36
	max	0.10	0.60	0.40	0.29	0.17

(Experimental error probably account for values of $\frac{\delta s}{\phi}$ greater than 1.0). The ratio $\frac{As}{C}$ varies between 0.10 to 0.67 in the moisture content range of 9.4 to 29.2 per cent. The average values of the ratios of $\frac{\delta w}{\phi}$ and $\frac{As}{C}$ are 0.63 and 0.36, respectively

5.6.2.3 Wheat on Concrete

Figure 5.28 shows that the coefficient of friction of wheat on concrete increased as the moisture content of the wheat increased. The coefficient of friction varied from 0.40 to 0.61 in the moisture content range of 9.3 to 29.4 per cent.

The coefficient of friction was affected by porosity, increasing as the porosity of the wheat sample was decreased. It is obvious that as the porosity of a sample is decreased, the interlocking of the grains between the bumps on the concrete surface increases, thus increasing the net coefficient of friction of wheat on concrete.

The adhesion intercept of wheat on concrete varies over a range of 0.35 to 0.75 psi (Fig. 5.29) in the moisture range from 9.3 to 29.4 per cent.

The adhesion intercept of wheat on concrete increased as the porosity of the sample was lowered (Fig. 5.29

and Table A.8.3, Appendix A).

Table 5.3 shows that ratio $\frac{\delta c}{\phi}$ (ratio between coefficient of friction of wheat on concrete and coefficient of friction of wheat) is nearly unity. The ratio $\frac{A_c}{C}$ (ratio between adhesion of wheat on concrete and cohesion of wheat) varies between 0.50 to 4.20, in the moisture range of 9.4 to 29.2 per cent. The average value of ratio $\frac{A_c}{C}$ is 1.63 (Table 5.3).

5.6.3 Comparison with Other Work

Lorenzen (1957) and Brubaker and Pos (1965) determined the coefficients of friction of wheat on wood and steel. The coefficients of friction of wheat on wood found by Lorenzen are greater than his values for coefficients of friction of wheat on steel in the moisture content range of 8 to 17 per cent. This disagrees with the results obtained herein and by Brubaker and Pos. The coefficients of friction of wheat on wood and steel obtained herein and by Brubaker and Pos are lower than those obtained by Lorenzen. The values for coefficients of friction found by Brubaker and Pos are very close to the values obtained here (Fig. 5.30).

Table 5.3 Relationship between shear strength parameters of wheat (ϕ and C) and sliding resistance parameters of wheat on concrete (δ_c and A_c)

Moisture Content		9.4%	12.5%	16.1%	23.0%	29.2%
ϕ	min	21	20	$17\frac{1}{2}$	25	$32\frac{1}{2}$
	max	$23\frac{1}{2}$	23	25	32	35
δ_c	min	22	$21\frac{1}{2}$	$24\frac{1}{4}$	27	$27\frac{3}{4}$
	max	22	$24\frac{3}{4}$	$26\frac{1}{2}$	$31\frac{1}{2}$	-
$\frac{\delta_c}{\phi}$	min	1.05	1.07	1.38	1.08	0.85
	max	0.94	1.07	1.06	0.99	-
C	min	0.12	0.18	0.29	0.50	0.50
	max	0.21	0.25	0.42	0.80	1.50
A_c	min	0.50	0.49	0.37	0.37	0.42
	max	0.51	0.58	0.41	0.42	0.74
$\frac{A_c}{C}$	min	4.20	2.70	1.27	0.74	0.84
	max	2.20	2.32	0.98	0.53	0.50

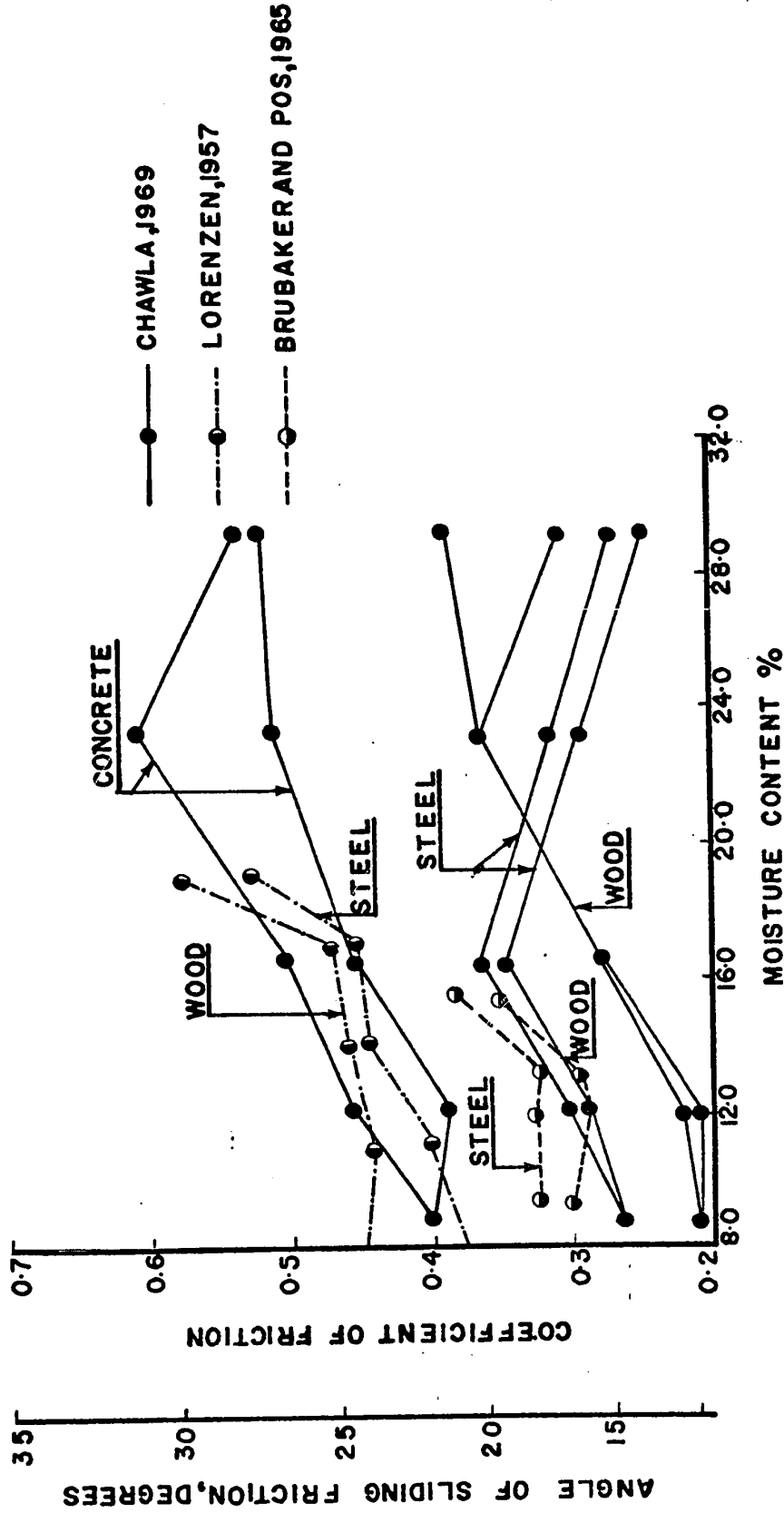


FIG. 5-30 COEFFICIENTS OF FRICTION OF WHEATS ON STRUCTURAL SURFACES

Lorenzen, and Brubaker and Pos performed tests on wheat against different structural surfaces at only one confining pressure. They determined the angle of friction from Coulomb failure plots, assuming that the adhesion intercept was zero. In the work done here, the tests were performed at three confining pressures for each porosity and for each moisture content. Both the angle of friction and adhesion intercept were obtained from Coulomb failure plots. So the results given by other investigators cannot be compared with the values obtained herein. Neither of the above investigators determined the coefficient of friction of wheat on concrete.

CHAPTER 6

CONCLUSIONS AND RECOMMENDATIONS

6.1 Conclusions

The following conclusions may be drawn from the previous chapter and from the interpretation of the test results.

1. The specific gravity of the wheat decreases as the moisture content of the wheat is increased. This is because of swelling of the wheat grains with increase in moisture content. The specific gravity varies from 1.43 to 1.36 in the moisture content range of 9.4 to 29.4 per cent.
2. The bulk density of the wheat decreases as the moisture content in the wheat kernels is increased. The minimum bulk density of the wheat found in this research was 50.5, 49.8 and 43.4 lbs. per cu. ft. at moisture contents of 8.9, 15.4, and 29.7 per cent, respectively. Twenty four per cent of this decrease in bulk density with increasing moisture content is due to the decrease in specific gravity of the wheat and the remaining 76 per cent decrease is due to an increase in shear resistance between the wheat grains.

3. Vibratory stresses are very effective in increasing the bulk density of the wheat grains at all moisture contents. There is an increase in the effect of vibratory stresses with an increase in moisture content, but this increase is rather small. When vibrated, the bulk density of the wheat samples used in this research increased by 5.7 and 7.6 lbs. per cu. ft. at moisture contents of 8.8 and 22.1 per cent respectively.

4. The magnitude of the static overburden pressure has practically no effect on the bulk density at low moisture contents. At high moisture contents, however, it has a significant effect. This influence of static pressure is possibly due to the deformation of wheat grains at high moisture contents. When subjected to static stresses by an overburden pressure of 21 psi, the bulk density of the wheat tested in this research increased by 0.8 and 4.8 lbs. per cu. ft. at moisture contents of 8.8 and 22.1 per cent respectively.

5. The coefficient of friction and cohesion intercept of the wheat tested, are greatly influenced by the moisture content in the wheat kernel and the porosity of the wheat mass.

At a particular porosity, the relationship between the coefficient of friction, and the moisture content shows that there is an optimum value of moisture content (15 per cent) at which the wheat has a minimum value of the coefficient of friction. The coefficient increases as the moisture content

of the wheat is either increased or decreased from this optimum value.

At a particular porosity, the cohesion intercept increases with increasing moisture content. For a particular moisture content, the greater the porosity, the smaller is the cohesion intercept. This is true for all moisture contents excepting the small range of ± 2.0 per cent of moisture content from the optimum value, where the porosity does not seem to have an appreciable effect on cohesion.

6. The coefficient of surface friction, and the adhesion between the wheat and the structural surfaces were dependent upon the moisture content of the wheat kernels.

The coefficient of surface friction of wheat on wood, and concrete increases as the moisture content of the wheat increases, but for wheat on steel surface, there is an optimum value of moisture content (17 per cent), where the coefficient of surface friction has a maximum value.

The change of the porosity of the wheat samples had no appreciable effect on the coefficient of friction of the wheat on wood and steel surfaces, but the coefficient of friction of the wheat on concrete increased as the porosity of the samples was decreased.

The adhesion of the wheat on wood and steel increases as the moisture content of the wheat is increased, but for wheat on concrete, the adhesion decreases in the lower moisture content range (9 to 16 per cent) and increases in the higher moisture content range (over 16 per cent) as the moisture content of the wheat kernels is increased.

The adhesion of wheat on steel and concrete was affected by the porosity, increasing as the porosity of the samples decreased. The change of porosity at all moisture contents had no effect on the magnitude of adhesion of wheat on wood.

7. The crushing load of individual wheat kernels is influenced by the size, moisture content, and position of the grain. At low moisture contents, the grains are brittle, resistant to deformation, and have higher crushing loads (varies from 15.4 to 19.8 lbs. in the tests carried out). At high moisture contents, the grains are easily strained, permanently deformed at low loads, and have small crushing loads (varies from 4.5 to 10.3 lbs.).

6.2 Recommendation for Future Research

The foregoing investigation suggests the following

several lines of future research.

1. The physical properties of wheat change considerably with change in the moisture content of the wheat grains. To understand the mechanistic picture of the behaviour of wheat grains, it is important to carry out research on the effect of moisture content on the physical and biological structure of wheat grains.
2. A more extensive testing program should be carried out to study the physical properties of wheat in the moisture content range of 15 to 23 per cent, where these properties have been observed to change rather drastically.
3. Vibratory compaction in the present research work was done at one frequency of vibration only. This gave maximum density at zero surcharge, which is difficult to explain. Further research needs to be carried out to study the effect of frequency and amplitude of vibration at different surcharge loads on the density of wheat.
4. This research should be repeated for other different types of wheats to see if tests on one type of wheat are a representation of wheat as a whole.
5. All experiments in this research were carried out at room temperature which varied between 70-80 F. The wheat being an organic material should obviously be apt to change its properties with change in its environmental conditions such as temperature and relative humidity. It is therefore suggested to carry out further research to study the effects of temperature and relative humidity on the engineering properties of the wheat.

BIBLIOGRAPHY

- Agricultural Engineers Year Book, 1965. American Society of Agricultural Engineers, St. Joseph, Michigan, U.S.A.
- Amundson, L.R., 1945. Determination of bond stresses and lateral pressures for cylindrical grain bins. Agricultural Engineering, August.
- Bauer, G.E.A., 1969. Stresses and deformation on braced cuts in sand. Ph.D. thesis, University of Ottawa, Ottawa, Canada.
- Bickart, W.G. and F.H. Buelow, 1965. Some coefficient of friction of grains sliding on surfaces. Quarterly Bulletin of Michigan Agricultural Experiment Station, Vol. 47 No. 5.
- Bishop, A.W. and D.J. Henkel, 1957. The measurement of soil properties in the triaxial test. Edward Arnold (Publishers) Limited, London
- Browne, D.A., 1962. Variation of bulk density of cereals with moisture content. Journal of Agricultural Engineering Research, Vol. 47 No. 4.
- Browne, D.A. and M.G.R. Warner, 1963. Investigation into oven methods of moisture content measurement for grain. Journal of Agricultural Engineering Research, Vol. 8 No. 4.
- Brubaker, J.E. and J. Pos, 1965. Determining static coefficient of friction of grains on structural surfaces. Transactions of American Society of Agricultural Engineers.

- Collins, R.V., 1962. Determination of pressure in cylindrical storage structures. Paper presented at annual meeting of A.S.A.E. No. 62:302.
- Dale, A.C. and R.N. Robinson, 1954. Pressure in deep grain structures. *Agricultural Engineering*, August 35:570-573.
- Deresiewicz, H., 1957. Mechanics of granular matter. Department of Civil Engineering and Engineering Mechanics, Columbia University in City of New York.
- Felt, Earl J., 1958. Laboratory methods of compaction of granular soils. American Society of Testing Materials, presented at the Sixty-First Annual Meeting, Boston, Mass.
- Forsblad, L., 1965. Investigation of soil compaction by vibration. *Acta Polytechnica, Scandinavica*, No. C134, Stockholm
- Hall, C.W. and E.A. Kazarian, 1965. Thermal properties of grains. *Transactions of the American Society of Agricultural Engineers*.
- Hlynka, I. and W. Bushuk, 1959. The weight per bushel. *Cereal Science Today*, Vol. 4 No. 8.
- International Critical Tables of Numerical Data, 1928. Physics, Chemistry and Technology, N.R.C. of U.S.A., Vol. III.
- Ketchum, Milo S., 1919. The design of walls, bins and grain elevators. McGraw-Hill Book Company, New York.

- Kramer, H.A., 1944. Factors influencing the design of bulk storage for rough rice. *Agricultural Engineering* 25: 463-466.
- Lambe, T.W., 1951. *Soil testing for engineers*. John Wiley & Sons, Inc., New York.
- Lenczner, D., 1963. An investigation into the behaviour of sand in a model silo. *The Structural Engineer* Vol. 41:389-398.
- Lorenzen, R.T., 1957. Effect of moisture content on mechanical properties of small grains. M.Sc. thesis, University of California, Davis, California.
- McCalmont, J.R. and Wallac Ashby, 1934. Pressure and loads of ear corn in cribs. *Agricultural Engineering* 15:123-125, 128.
- Pettibone, H.C. and J. Hardin, 1965. Research on vibratory maximum density test for cohesionless soils. A.S.T.M. Special Publication, 77. *Compaction of Soils*, 1965, pp. 3-30.
- Richey, C.B., 1961. *Agricultural Engineers Handbook*, McGraw-Hill Book Company, New York.
- Ross, I.J. and C.W. Issacs, 1961. Forces acting in stacks of granular materials. *Transactions of Americal Society of Agricultural Engineers* 4:92-96.
- Rowe, P.W., 1963. Stress-Dilatancy, earth pressures, and slopes. *Proceedings A.S.C.E. Journal of Soil Mechanics and Foundation Division* 89:No. SM3.

- Saul, Robert A., 1959. Effect of bin design factors on pressure of shelled corn. Paper presented at Winter Meeting of American Society of Agricultural Engineers, 59:820.
- Schmidi, J.L., 1955. Wheat storage research. Technical Bulletin No. 1113, U.S. Department of Agriculture.
- Shedd, K. Chaude, 1951. Some data on resistance of grains to air flow. Agricultural Engineering.
- Sowell, R. Seago, 1963. Effects of a change in moisture content of storage grain on bin pressure. M.Sc. thesis, Kansas State University
- Spangler, M.G., 1966. Soil Engineering. International Test Book in Civil Engineering.
- Stewart, B.R., 1968. Effect of moisture content and specific weight on internal properties of sorghum grain. Transactions of the American Society of Agricultural Engineers Vol. 11, No. 2.
- Taylor, D.W., 1948. Fundamental of soil mechanics. John Wiley & Sons, New York.
- Terzaghi, K. and R.B. Peck, 1967. Soil mechanics in engineering practice. John Wiley & Sons, New York.
- White, H.E. and S.F. Walton, 1936. Particle packing and particle shape. Paper presented at Annual Meeting American Ceramic Society, Columbus, Ohio.
- Zakrzewski, M.S., 1959. Design of silos for grain storage. Die Siviele Ingenier in Suidelike Afrika.

APPENDIX A

A.1 Strength Theory

Depending on the source of its strength, a material can be placed in one of two groups, namely, cohesive and cohesionless. This section is devoted to the study of the theoretical concepts of Direct Shear tests and triaxial compression tests on granular cohesionless materials.

A.1.1 Direct Shear Test on Granular Material

The resistance to shear of a granular material is derived from friction between the grains, the interlocking of the grains, and the strength of the individual grain. Friction between grains is similar to friction between surfaces, as, for example, between the two blocks as shown in Fig. A.1. When the top block

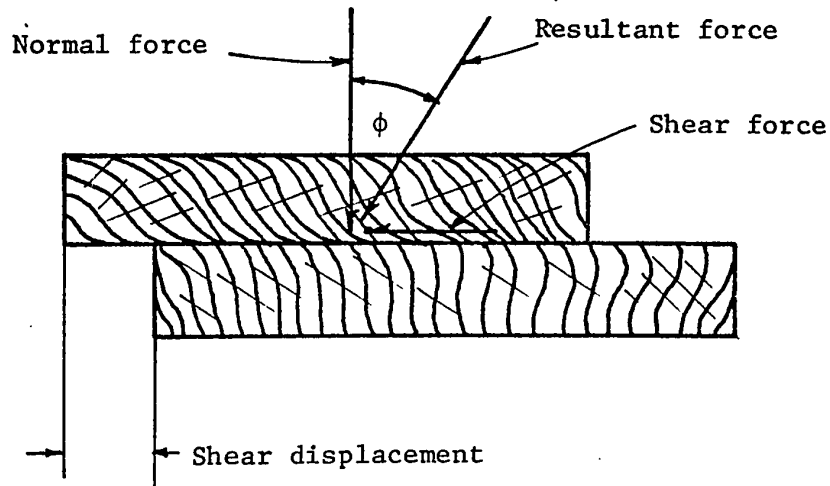


Fig. A.1 Friction between blocks

is sliding along the bottom block, a shear force is applied to the surface of the bottom block which is equal to the normal force acting between the blocks multiplied by a coefficient called the "Coefficient of friction". The friction may be either sliding friction (Fig. A.1) or rolling friction. For example if a large shear force were applied to grain A (Fig. A.2), it could be moved to position B by either sliding or rolling or a combination of the two. To move the grain from position B to position C against the applied normal force requires work equal to the distance d times the normal force. This work is the quantitative measure of the phenomenon termed interlocking. Because interlocking occurs to a greater extent when grains are touching close together,

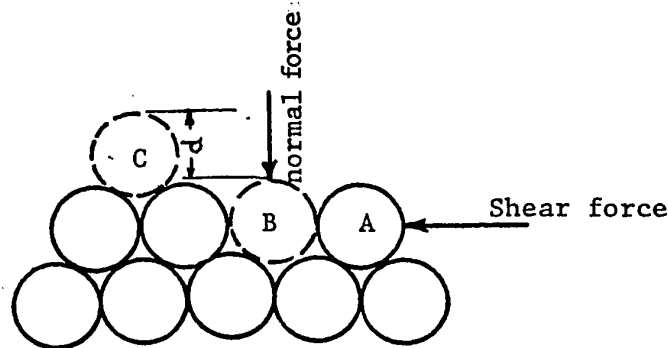


Fig. A.2 Friction in soil

dense materials show a higher shear strength at small displacements than loose materials.

In direct shear tests, an element of soil is subjected to a shear force (Fig. A.3) which is equal to normal force times $\tan \phi$. If the area of the potential shear surface is A ,

$$\text{Shear stress } \tau = \text{Shear force/Area (A)}$$

$$\text{Normal stress } \sigma = \text{Normal force/Area (A)}$$

$$\tau = \sigma \tan \alpha$$

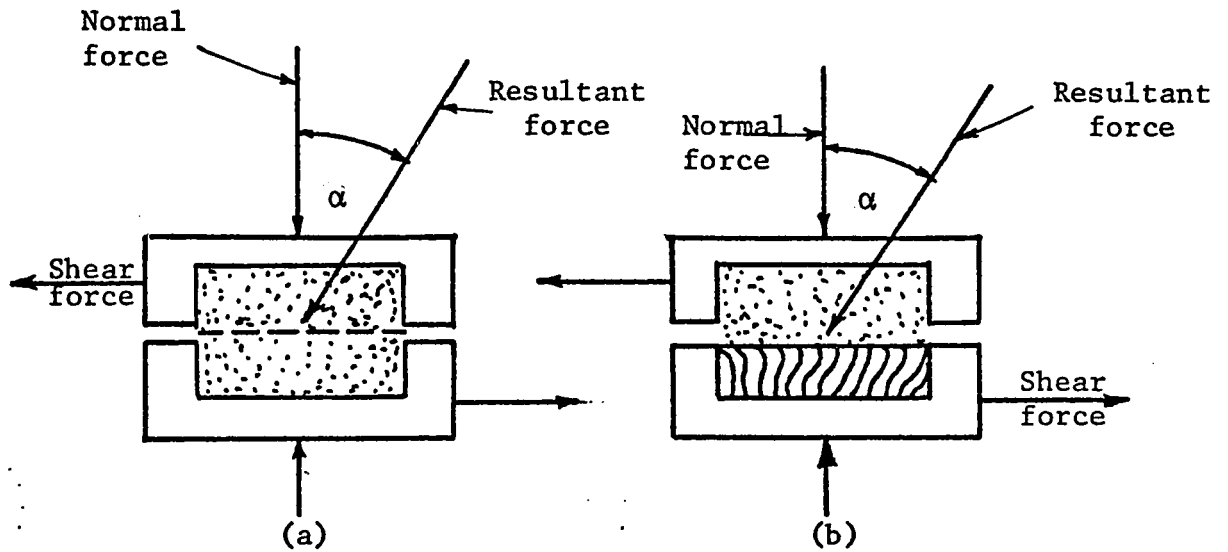


Fig. A.3 (a) Shear of soil in shear box, (b) shear of soil on block in shear box.

The shear strength S , is the shear stress which is necessary to cause slippage on a surface through the given material, or

$$S = \sigma \tan \phi$$

where ϕ is the angle at slippage. If cohesion is present in

the material, then the equation will be

$$S = C + \sigma \tan \phi$$

C = cohesion intercept.

This formula was first proposed by Coulomb in 1776.

A.1.2 Triaxial Compression Test on Granular Material

The cohesive properties (C) enter into the determination of the coefficient of friction (μ) of agricultural granular materials at high moisture content. Mohr's theory of failure through Mohr's diagram provides the best means of distinguishing between cohesion and friction, as discussed by Spangler (1966), Terzaghi and Peck (1967) and Taylor (1948). Spangler (1966) states that "The failure of a soil mass is more nearly in accordance with the principles of the Mohr Theory of failure, than with any other theory and the interpretation of the data of the triaxial compression tests depends to a large extent on this fact." Mohr's theory states that a material fails along the plane and at the time at which a certain optimum combination of normal stress and shearing stress occurs in a stressed body.

An analysis of the forces involved in the development of shear in a granular mass is given in Fig. A.4, parts a, b, c and d, with an explanation. Part a shows the forces acting on a

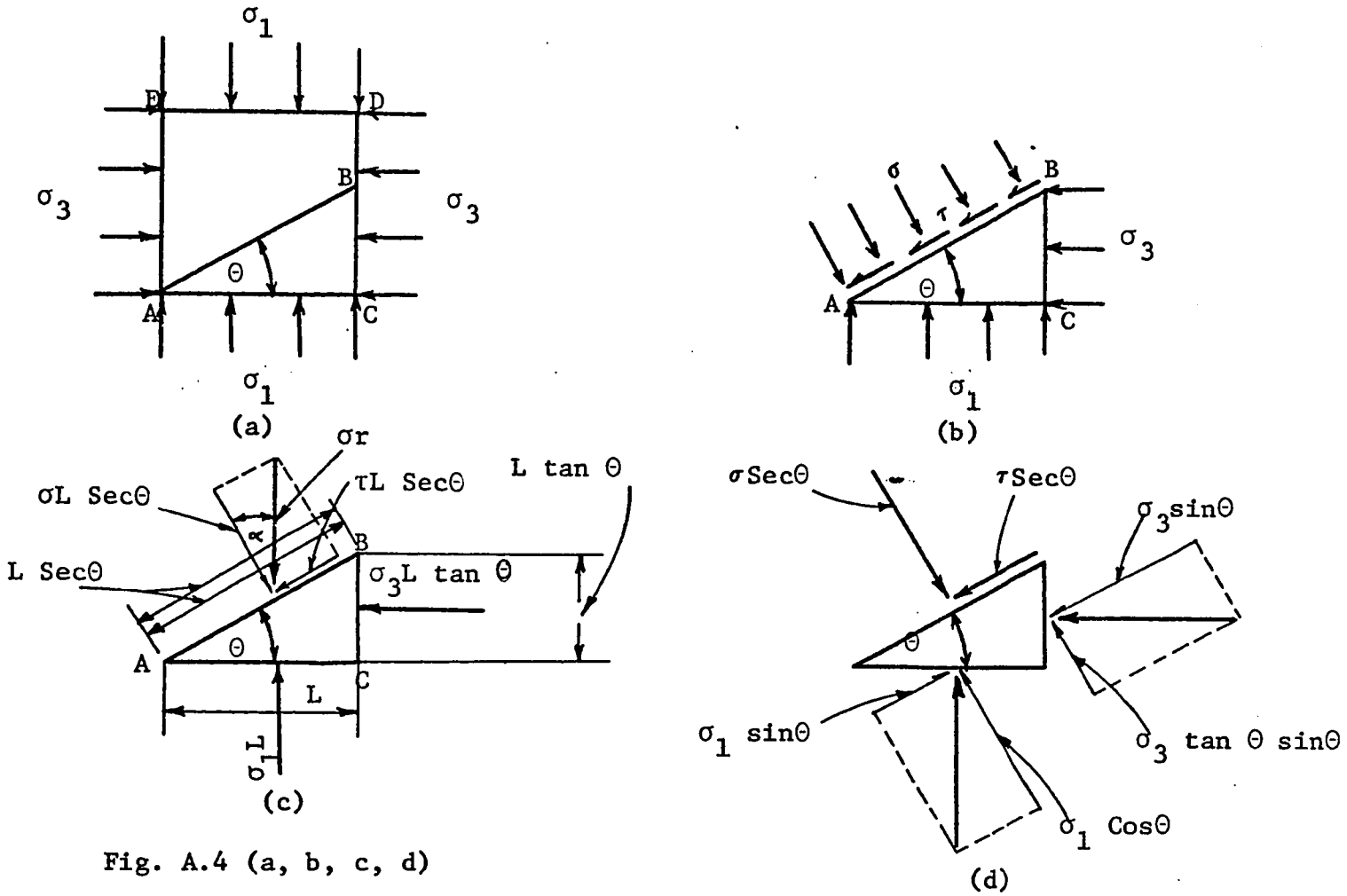


Fig. A.4 (a, b, c, d)

- (a) Stresses on a cubical unit oriented to principal planes.
- (b) Free body diagram of that portion of the cubical unit below plane A-B.
- (c) Evaluation of the forces on the portion of the cubical unit below plane A-B.
- (d) Forces normal and parallel to plane A-B, summation of which gives

$$\sigma = \sigma_1 \cos^2 \theta + \sigma_3 \sin^2 \theta$$

$$\tau = [\sigma_1 - \sigma_3] \sin \theta \cos \theta$$

small cubical unit in a granular mass oriented to mutually perpendicular planes. When a shear plane A-B is imposed in this cubical unit, the stresses (σ) which are normal, and the stresses (τ) which are parallel to this shear plane are resolved as shown in parts b, c and d. From part d these normal and parallel forces may be summed separately to give the following equations

$$\sigma = \sigma_1 \cos^2 \theta + \sigma_3 \sin^2 \theta$$

$$\tau = [\sigma_1 - \sigma_3] \sin \theta \cdot \cos \theta$$

in which

σ = stress normal to shear plane

τ = stress parallel to shear plane

σ_1 = major principal stress

σ_3 = minor principal stress

θ = angle of shear plane with major principal plane

These relationships expressed mathematically by these two equations can be expressed graphically by the Mohr's diagram as shown in Fig. A.4. In Mohr's diagram, the normal stresses are plotted along the abscissa and shear stresses are plotted along the ordinate. To construct Mohr's diagram, OA is plotted equal to σ_3 and OB is plotted equal to σ_1 . A semicircle with $\sigma_1 - \sigma_3$ as diameter, is drawn through point A and point B. Then a line is drawn through point A, making an angle θ with the abscissa and cutting the semicircle at C. σ and τ are then scaled off as indicated in Fig. A.4e.

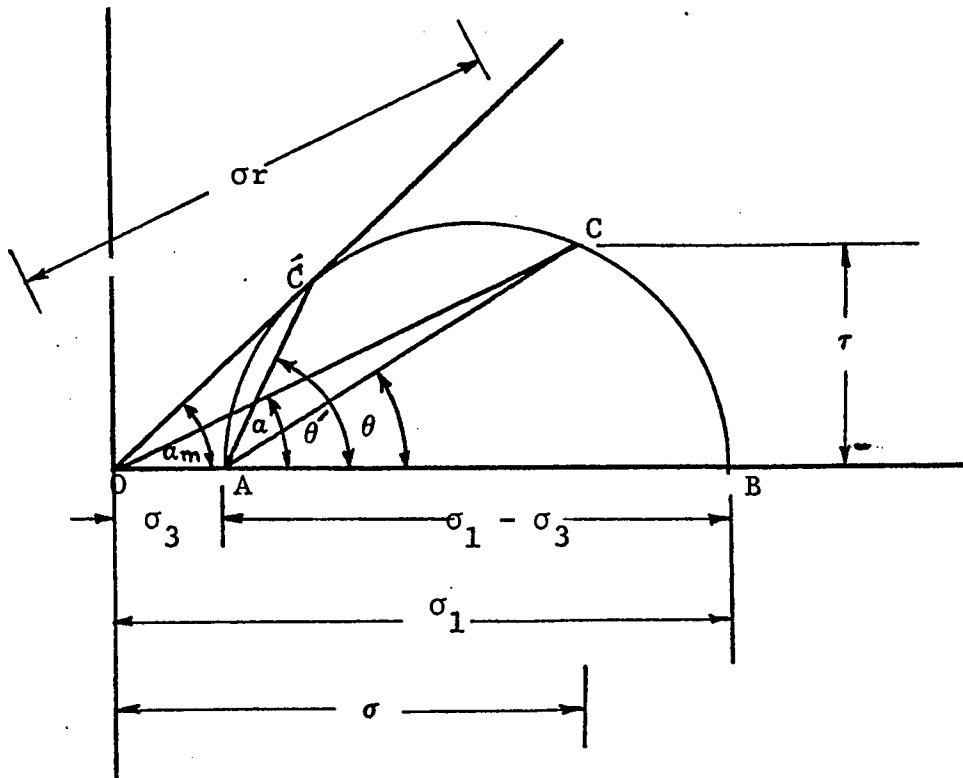


Fig. A.4 (e) The Mohr's diagram, which is a graphical representation of the relationships in the equations

$$\sigma = \sigma_1 \cos^2 \theta + \sigma_3 \sin^2 \theta$$

$$\tau = [\sigma_1 - \sigma_3] \sin \theta \cdot \cos \theta$$

According to Mohr's theory, a material fails along the plane and at the time at which the angle between the resultant of the normal and shearing stresses and the normal stress is a maximum; that is, when the combination of normal and shearing stresses produces the maximum obliquity angle α_m . $O\hat{C}$ represents the stress situation at failure, the maximum obliquity α_m is equal to the friction angle ϕ

Mohr's diagram, as it is applied to the analysis of triaxial compression tests is shown in Fig. A.5. The mathematical equation of Mohr's diagram used this manner

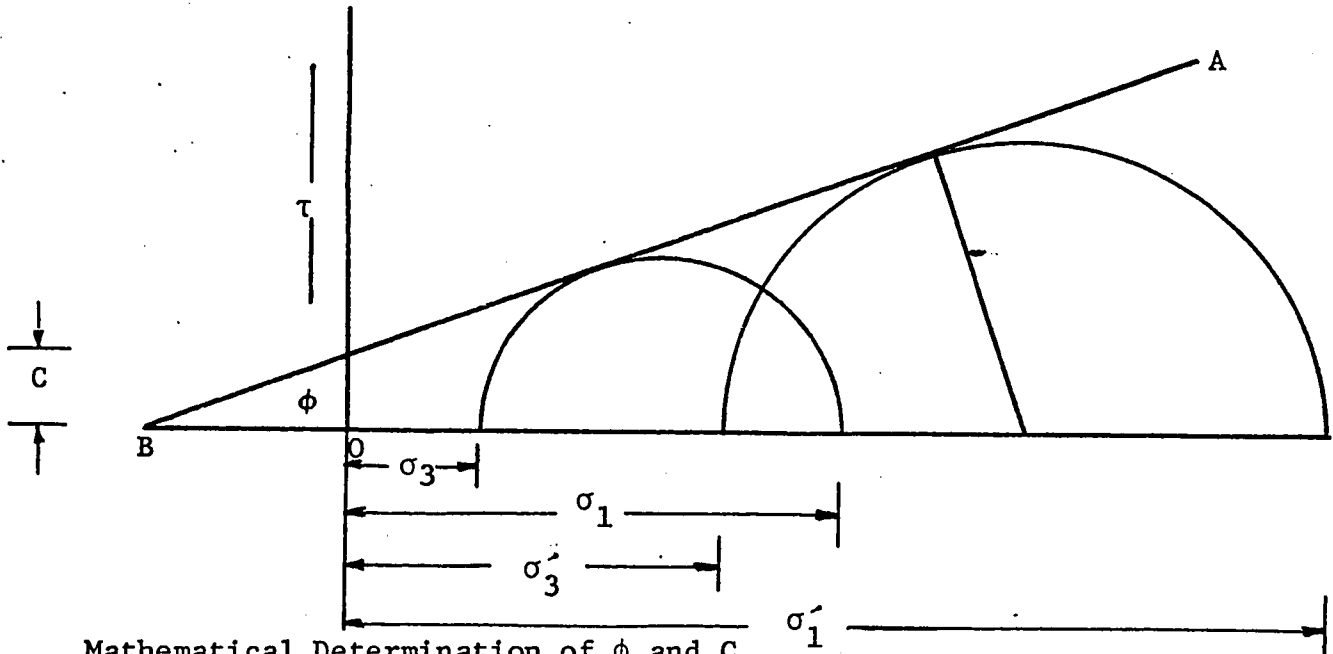
$$\sigma_3 \left(\frac{\sigma_1}{\sigma_3} - 1 \right) \operatorname{Cosec} \phi - \sigma_3 \left(\frac{\sigma_1}{\sigma_3} + 1 \right) - 2BO = 0$$

The development and description of the terms is shown in Fig. A.5.

When Mohr's diagram is used to reduce triaxial compression data, two or more sets of data are plotted as indicated in Fig. A.5. For each set of data, σ_1 and σ_3 are plotted and semi-circle drawn as described above. When two or more semicircles are plotted, a tangent can be drawn as shown in Fig. A.5, which cuts the abscissa at point B. The area between this tangent line and the base is an envelope of an infinite number of stress circles, and the angle which the tangent makes with the abscissa (ϕ) is the interior angle of friction of a granular mass. The tangent to the semicircles thus represents the optimum combination of normal stress and shear stress at which failure occurs, as stated by Mohr's theory. So the interior angle may be computed by use of the equations of Mohr's diagram given above. Two sets of data are needed as there are two unknowns ($\operatorname{Cosec} \phi$ and OB). Two equations can then be solved simultaneously to obtain values for ϕ and OB . Then

$$C = OB \tan \phi.$$

In the case of soil granular materials, C largely represents apparatus and procedure errors.



Mathematical Determination of ϕ and C

From the above figure, using one set of data, we find

that

$$\text{Cosec } \phi = \frac{OB + \sigma_3 + \frac{\sigma_1 - \sigma_3}{2}}{\frac{\sigma_1 - \sigma_3}{2}}$$

$$\text{Cosec } \phi = \frac{2 OB + \sigma_1 - \sigma_3}{\sigma_1 - \sigma_3}$$

$$\text{Cosec } \phi = \frac{2 OB + \sigma_3 \left(\frac{\sigma_1}{\sigma_3} - 1 \right)}{\sigma_3 \left(\frac{\sigma_1}{\sigma_3} - 1 \right)}$$

Rearranging

$$\sigma_3 \left(\frac{\sigma_1}{\sigma_3} - 1 \right) \text{Cosec } \phi - \sigma_3 \left(\frac{\sigma_1}{\sigma_3} + 1 \right) - 2 OB = 0$$

Fig. A.5 Mohr's graphical determination of ϕ and C.

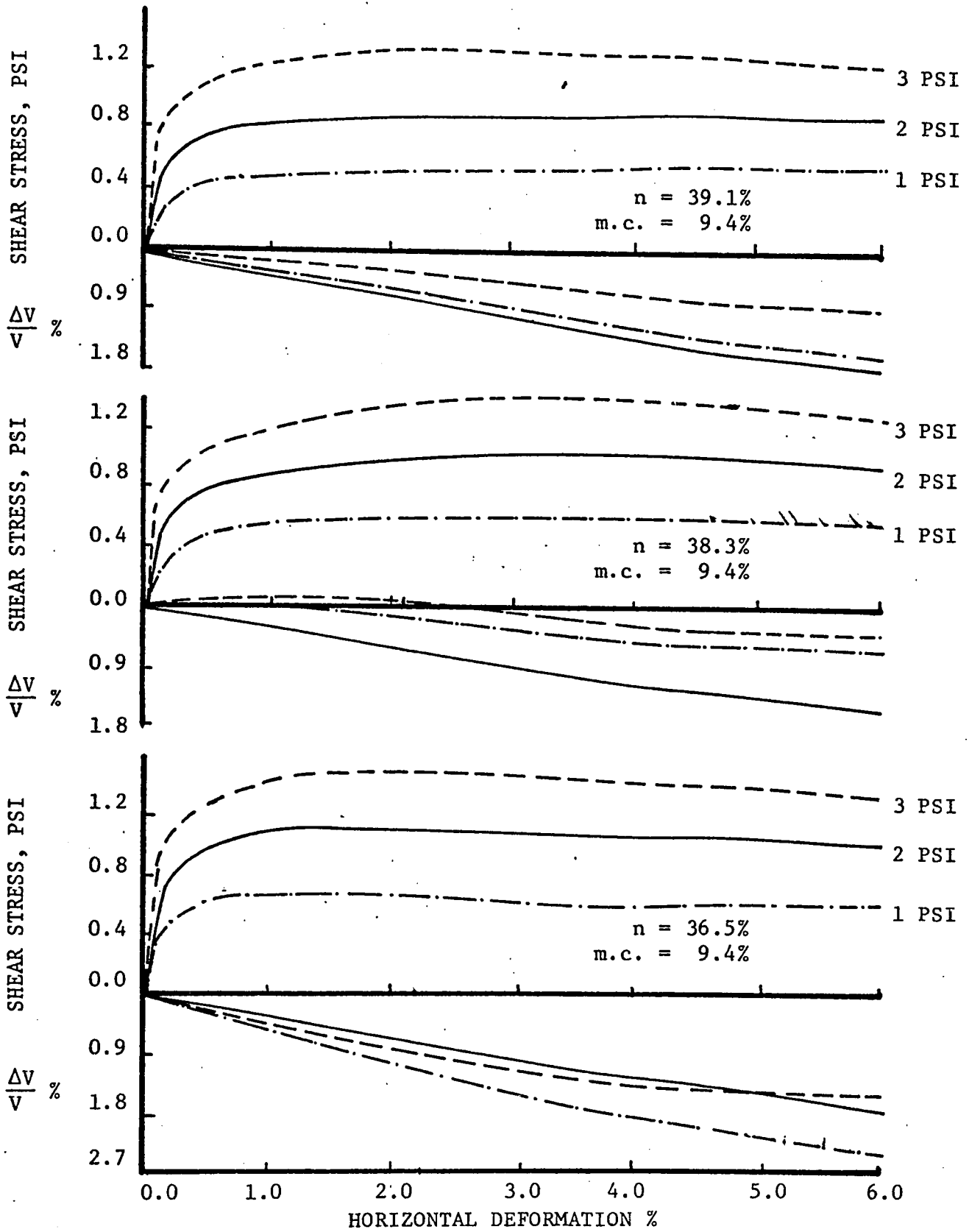


FIG. A.6 STRESS DEFORMATION CURVES FOR DIRECT SHEAR BOX

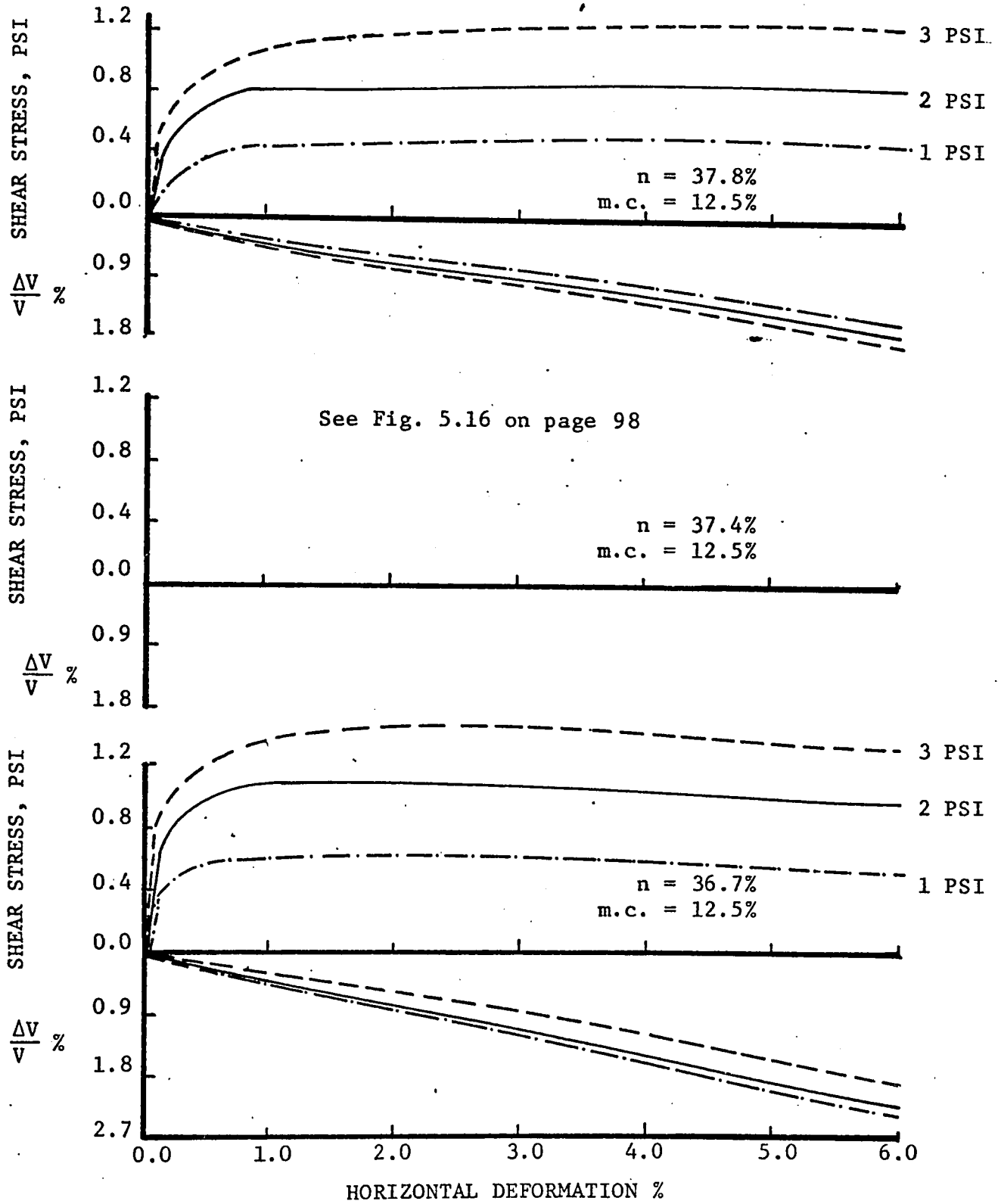


FIG. A.7 STRESS DEFORMATION CURVES FOR DIRECT SHEAR BOX

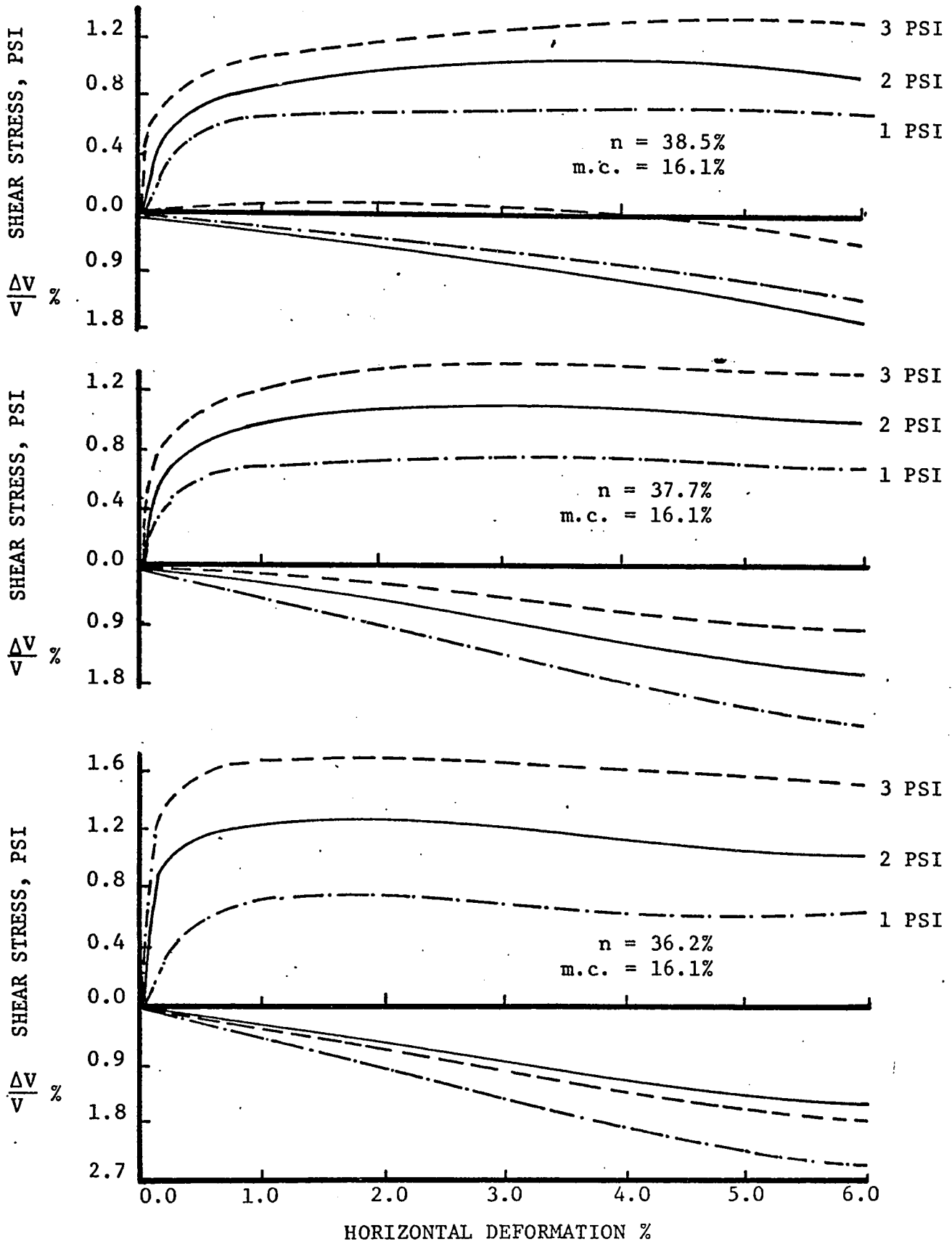


FIG. A.8 STRESS DEFORMATION CURVES FOR DIRECT SHEAR BOX

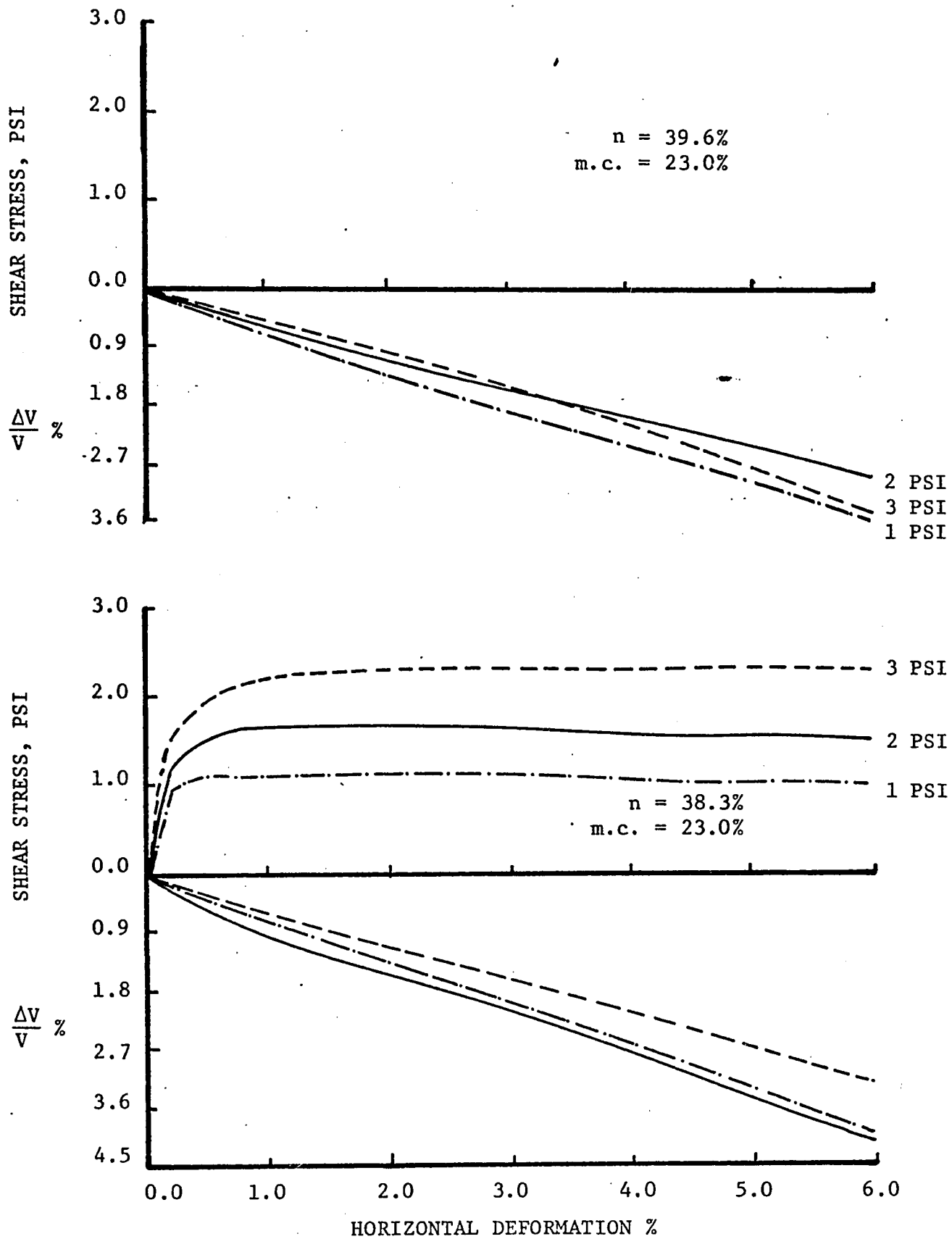


FIG. A.9 STRESS DEFORMATION CURVES FOR DIRECT SHEAR BOX

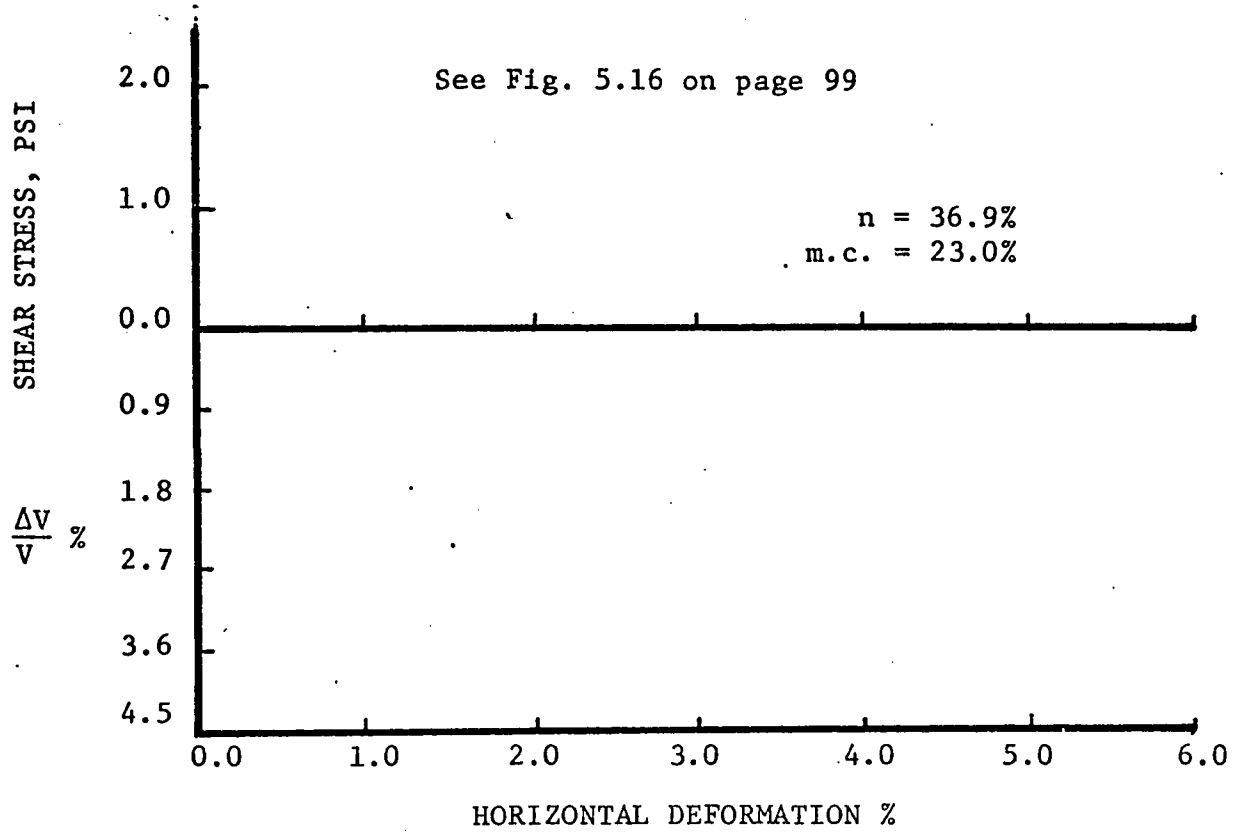
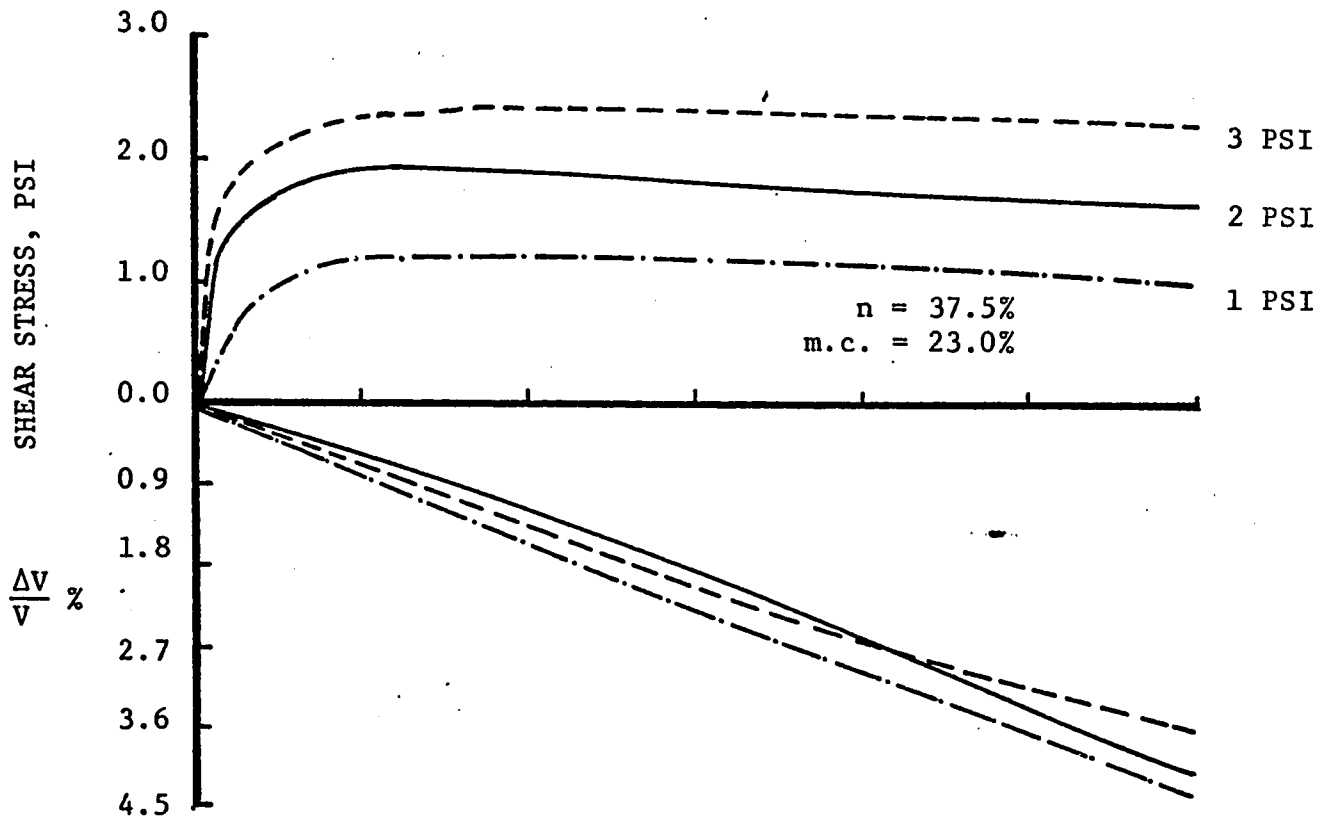


FIG. A.9 STRESS DEFORMATION CURVES FOR DIRECT SHEAR BOX

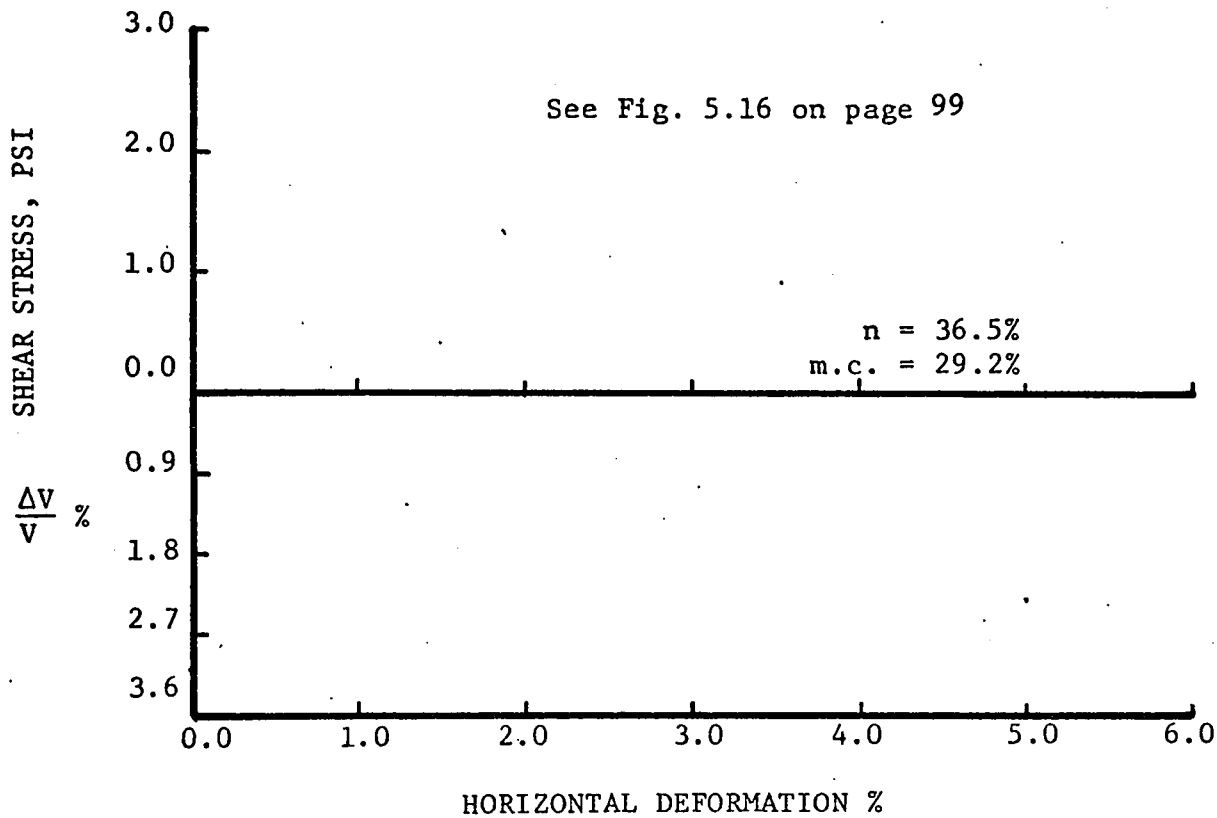
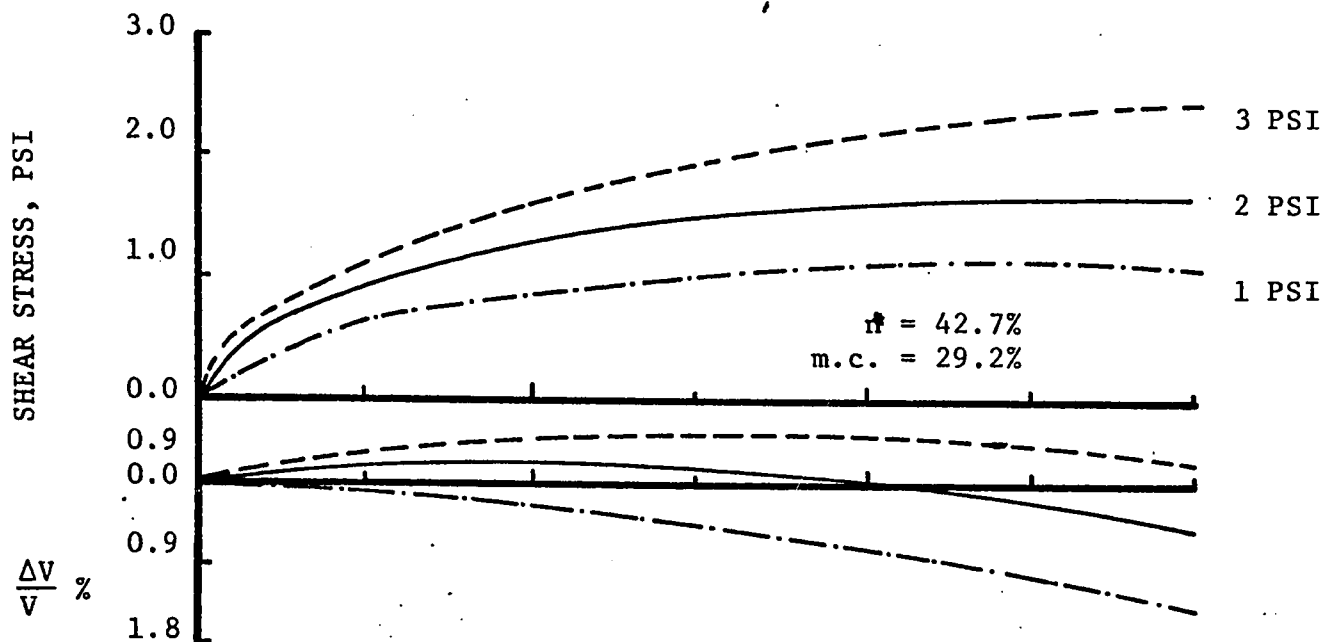


FIG. A.10 STRESS DEFORMATION CURVES FOR DIRECT SHEAR BOX

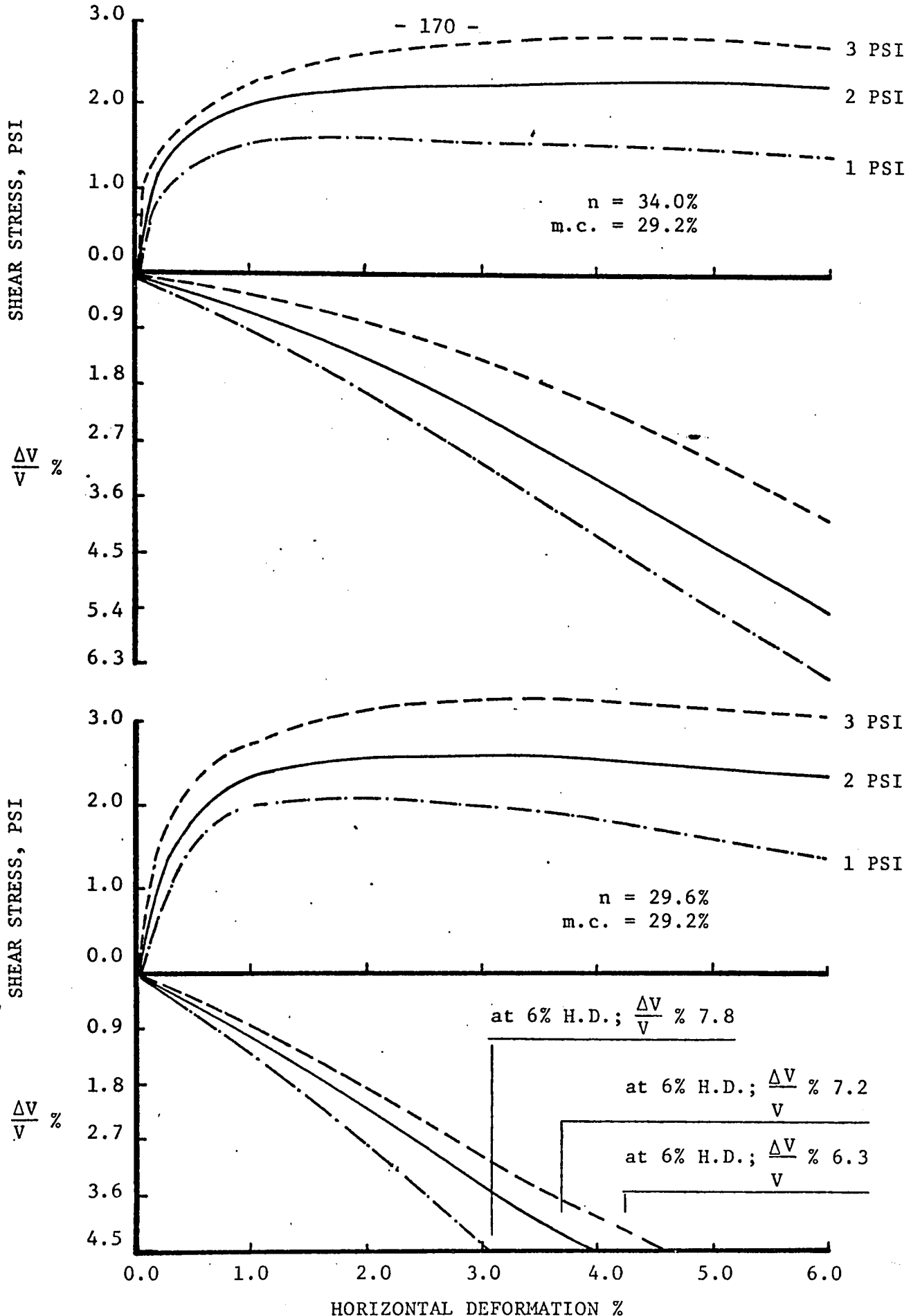


FIG. A.10 STRESS DEFORMATION CURVES FOR DIRECT SHEAR BOX

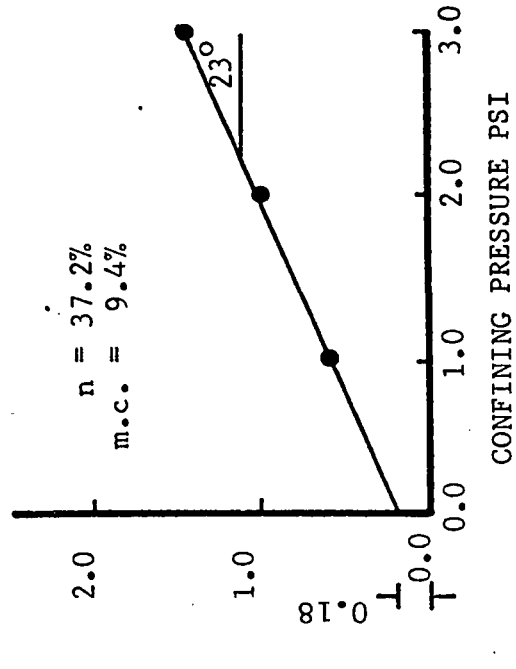
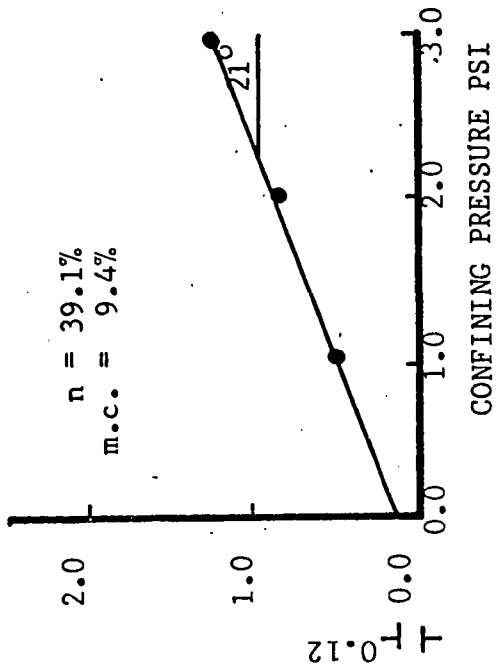
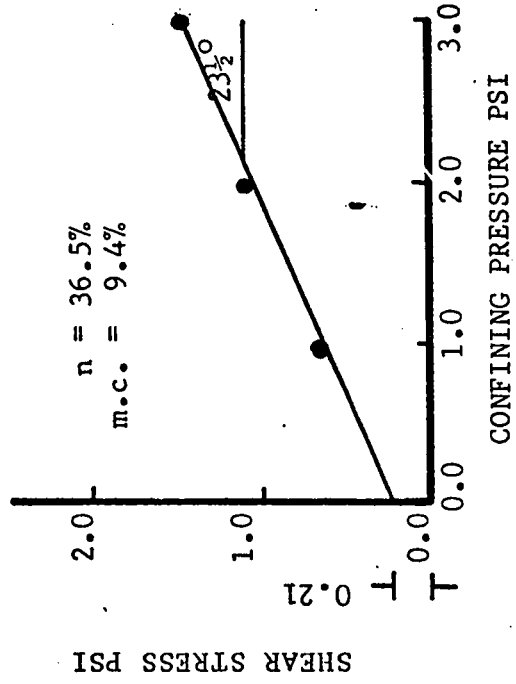
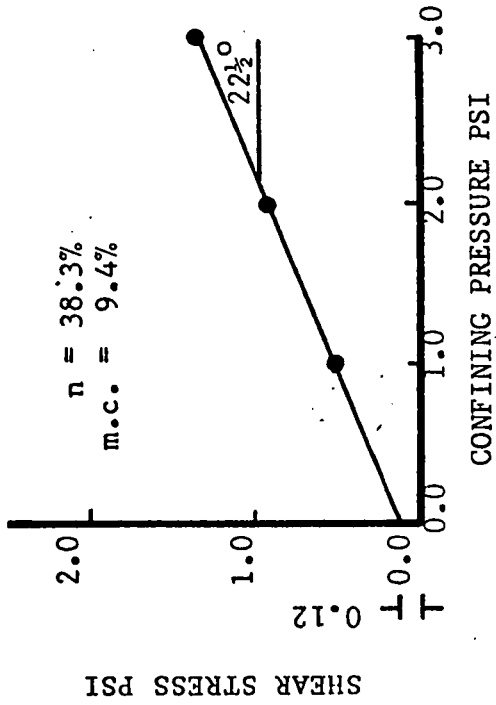


FIG. A.11 FAILURE ENVELOPE PLOTS FOR DIRECT SHEAR BOX

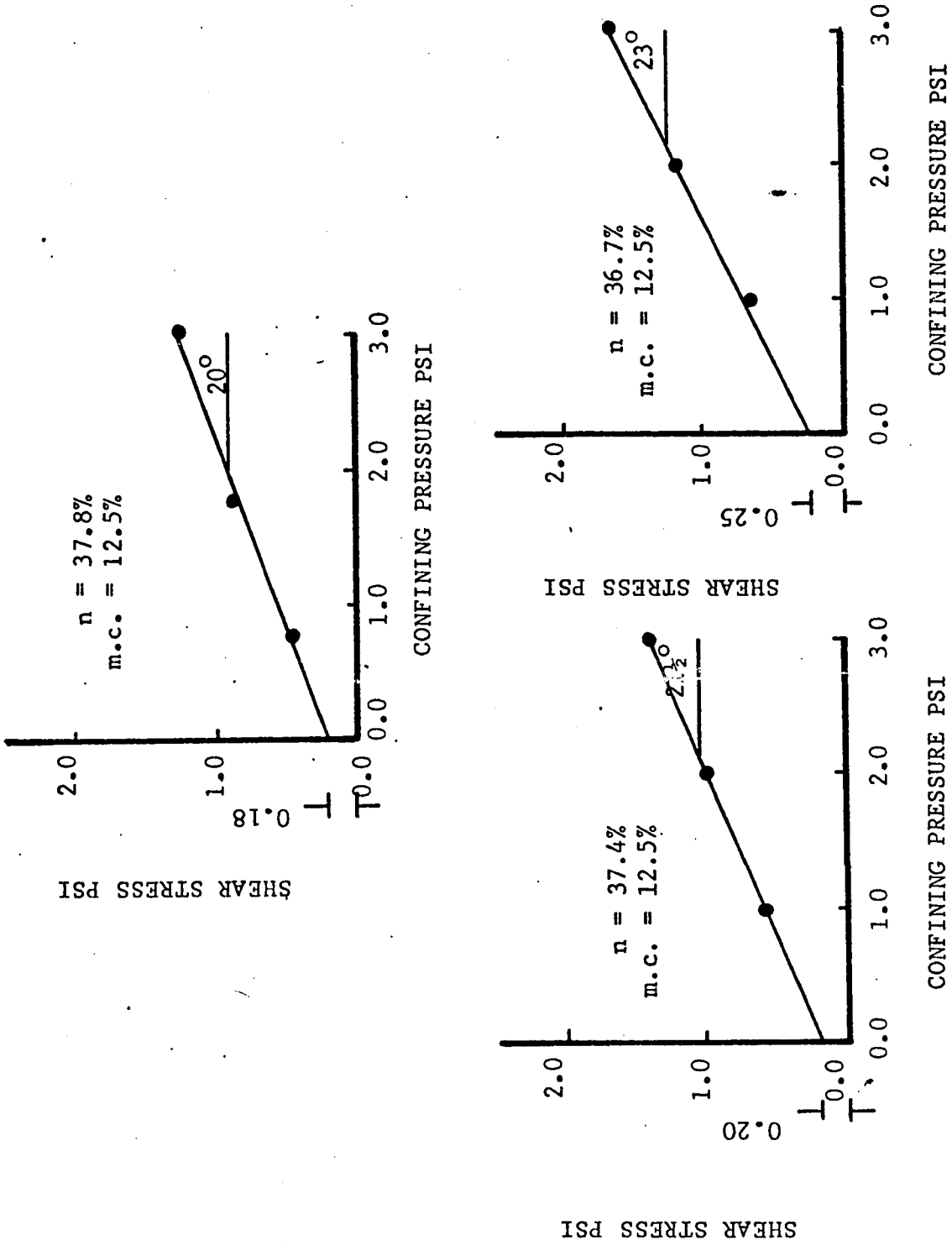


FIG. A.12 FAILURE ENVELOPE PLOTS FOR DIRECT SHEAR BOX

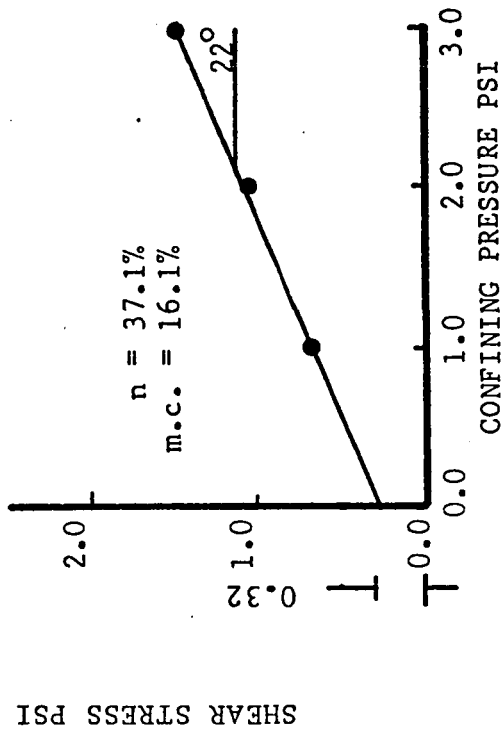
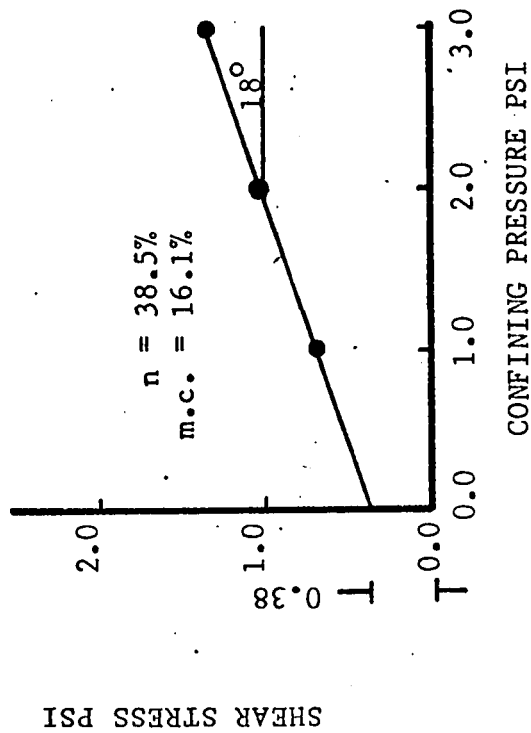
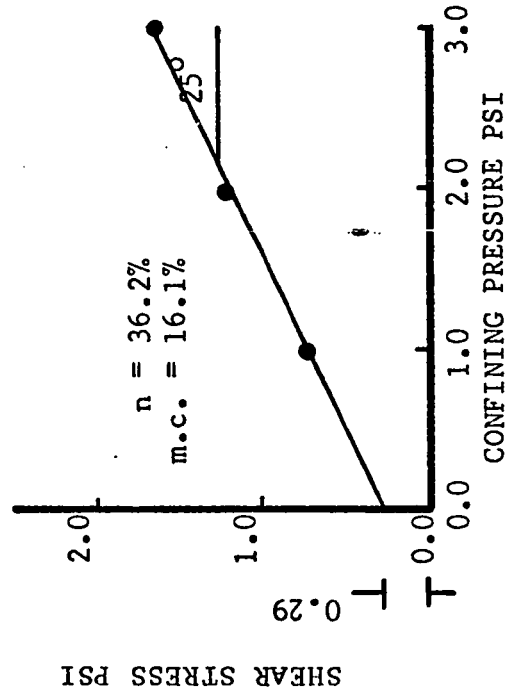
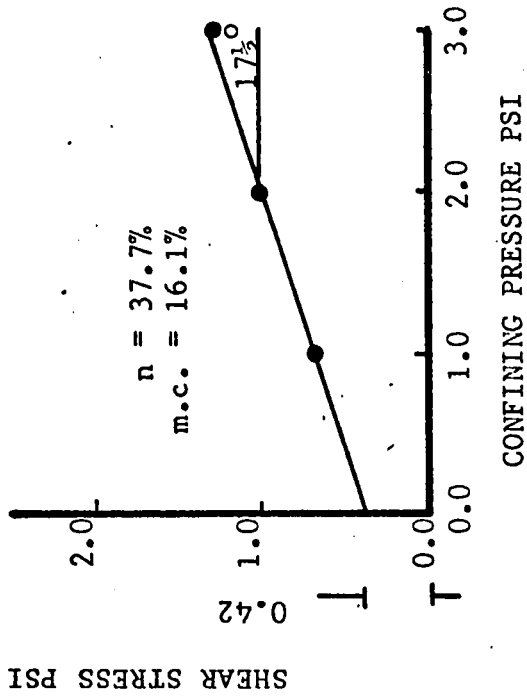


FIG. A.13 FAILURE ENVELOPE PLOTS FOR DIRECT SHEAR BOX

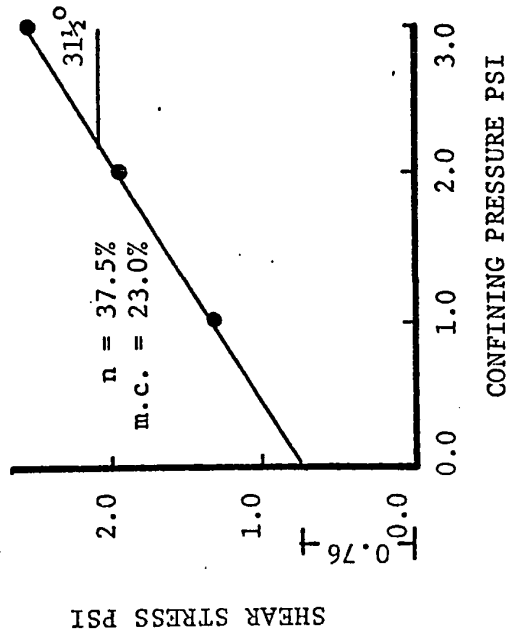
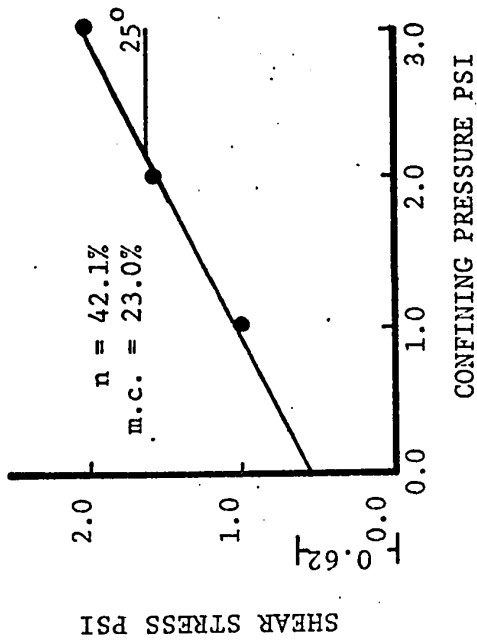
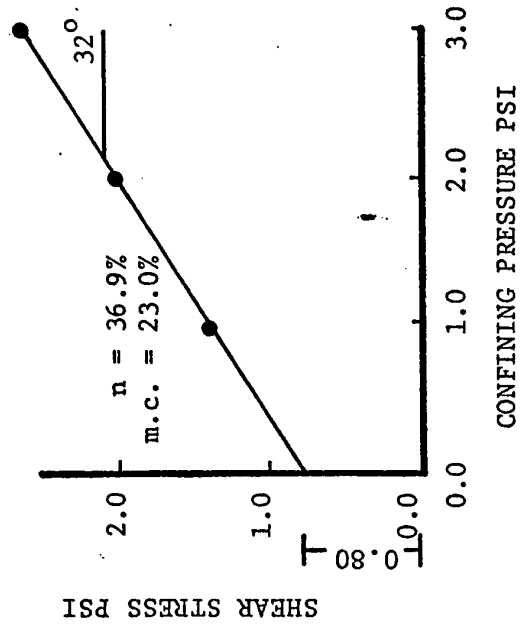
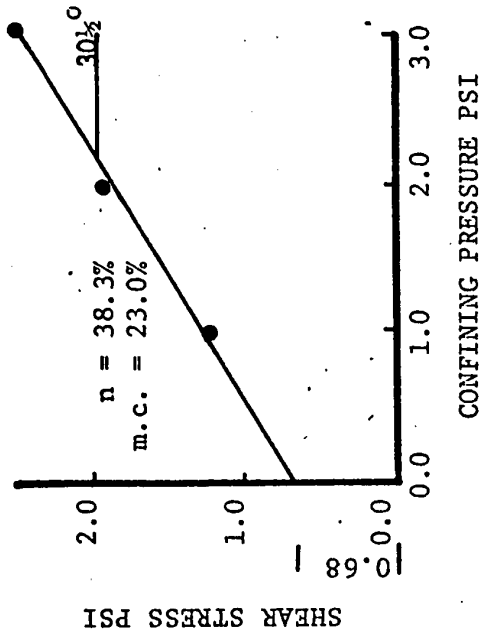


FIG. A.14 FAILURE ENVELOPE PLOTS FOR DIRECT SHEAR BOX

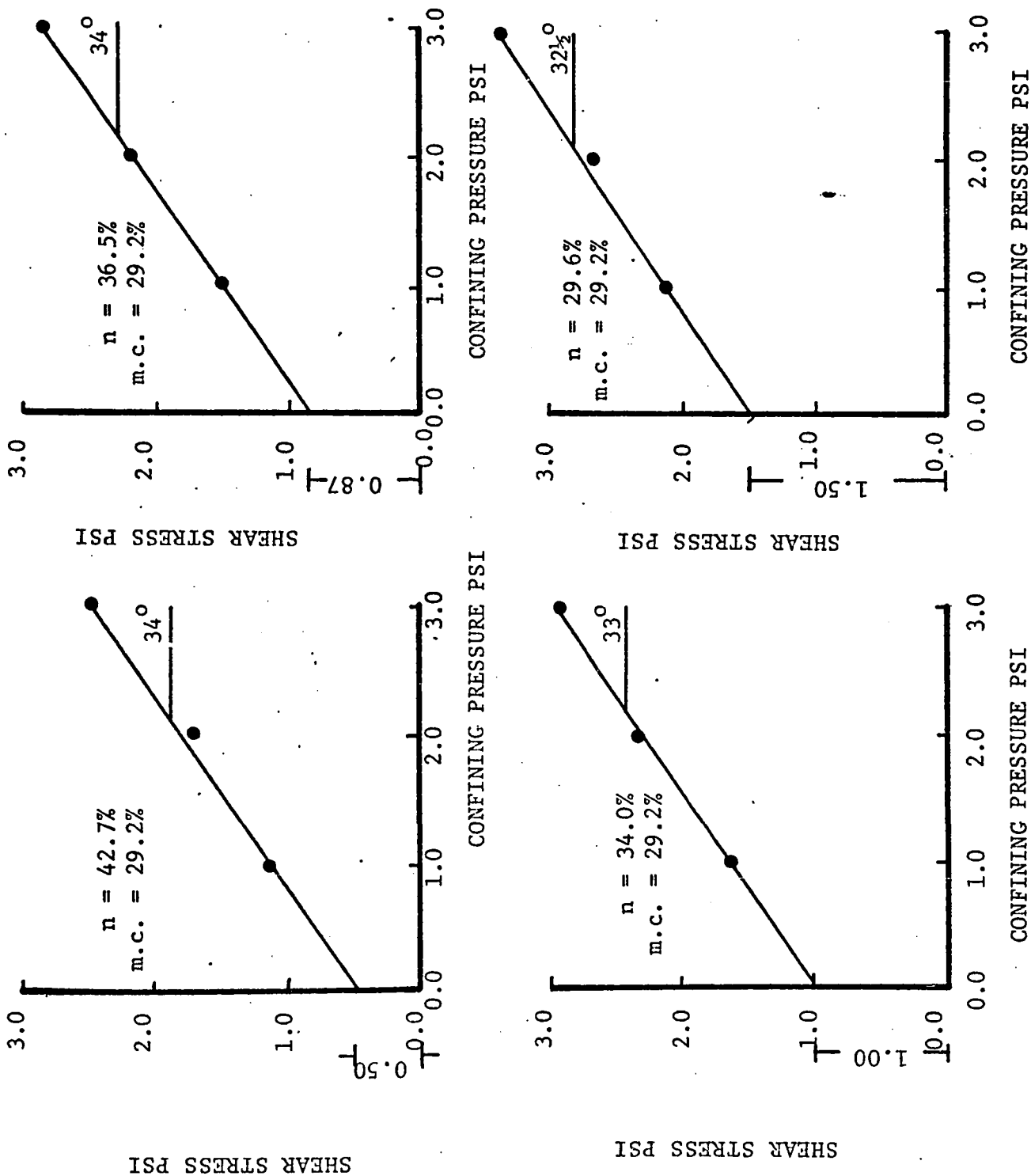


FIG. A.15 FAILURE ENVELOPE PLOTS FOR DIRECT SHEAR BOX

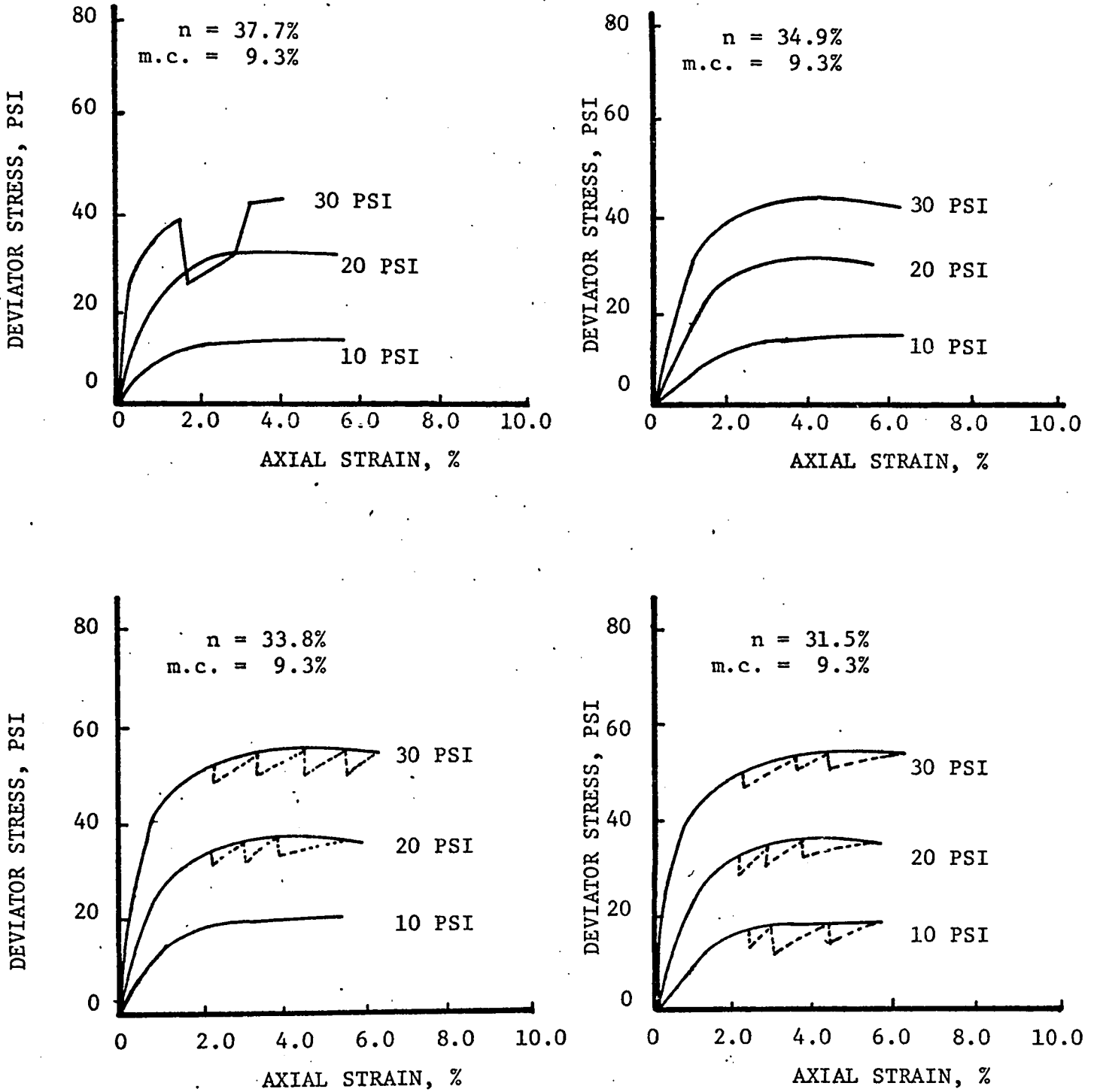


FIG. A.16 STRESS STRAIN CURVES FOR TRIAXIAL TESTS

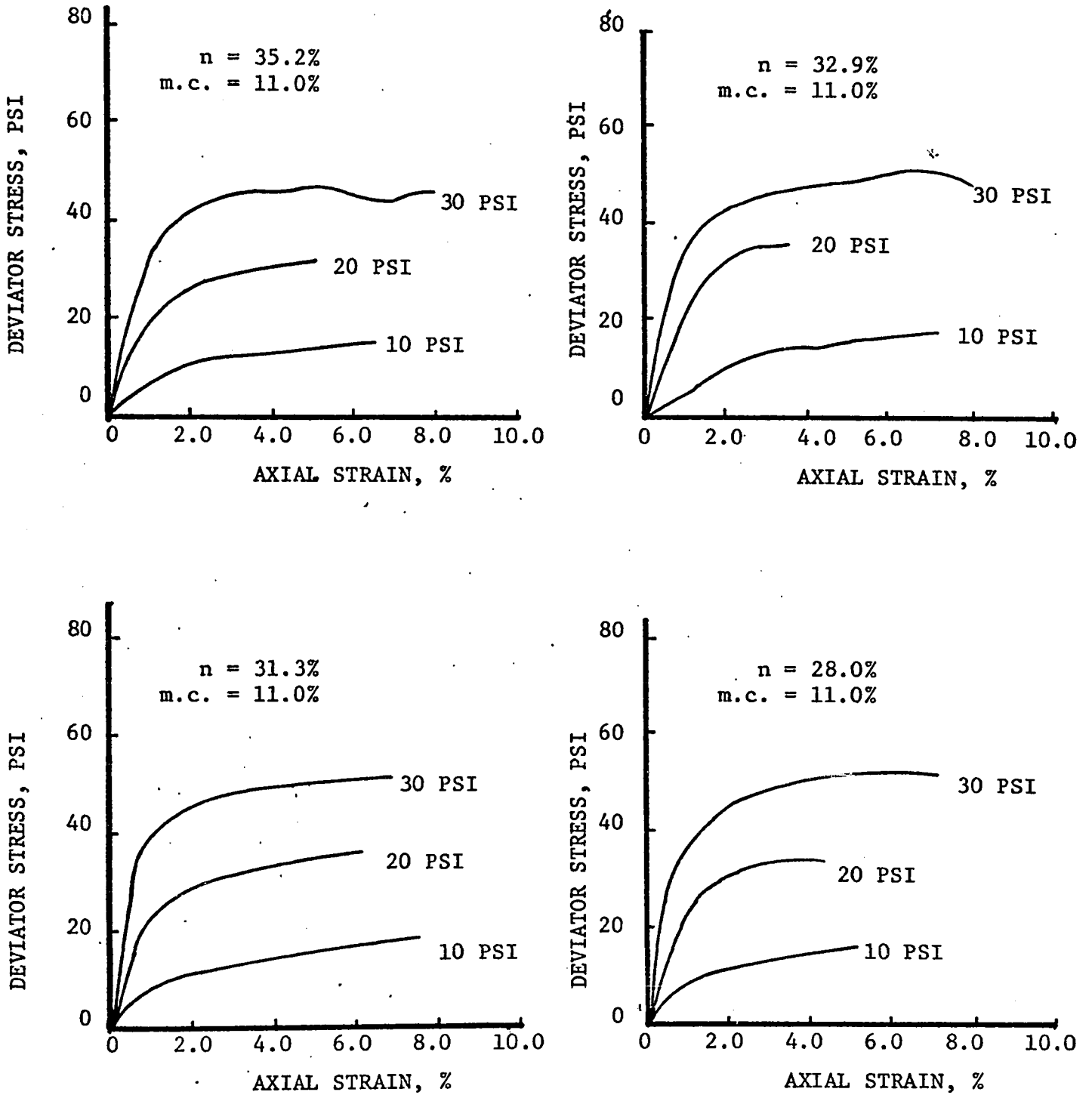


FIG. A.17 STRESS STRAIN CURVES FOR TRAXIAL TESTS

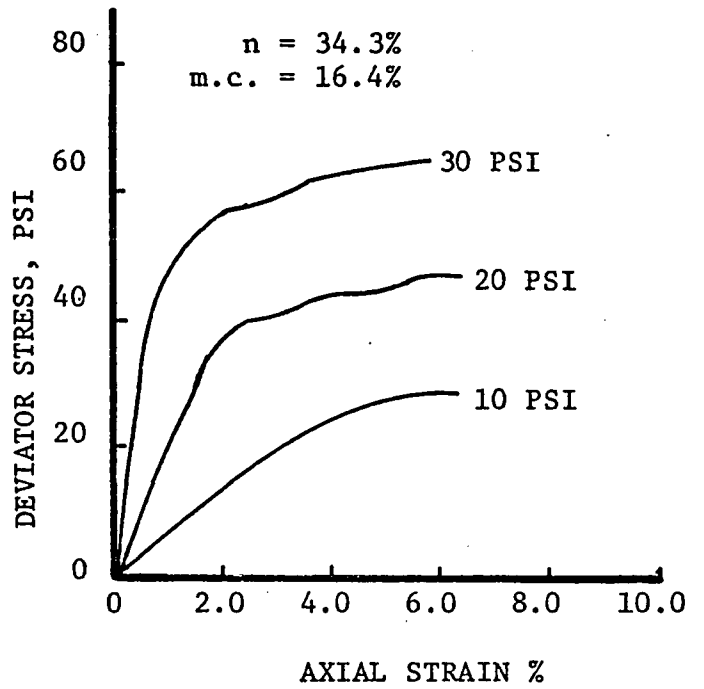
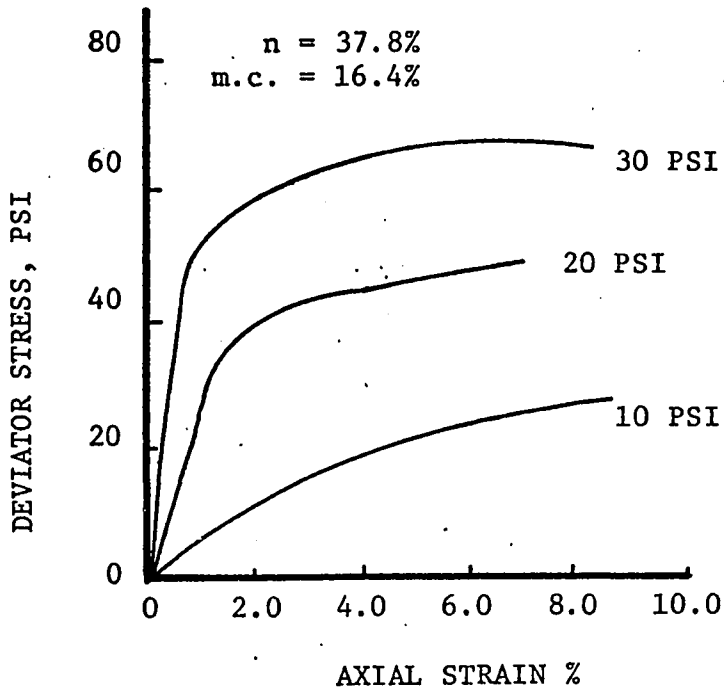
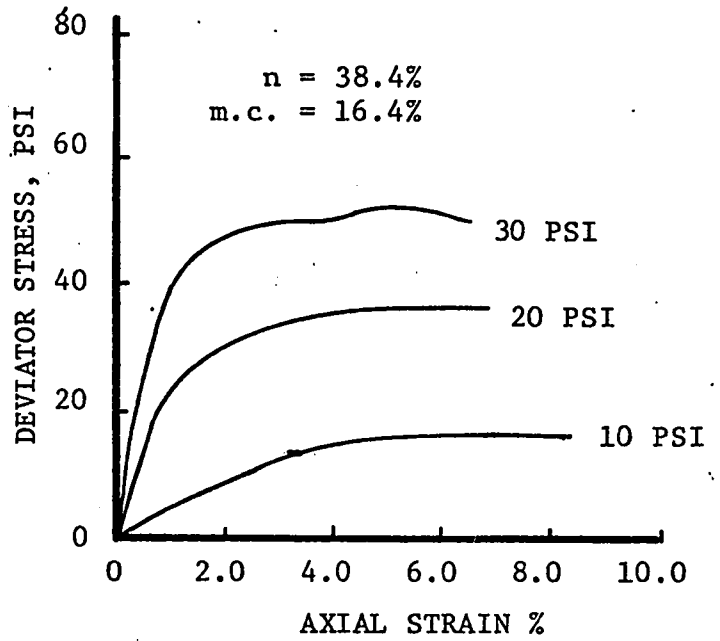
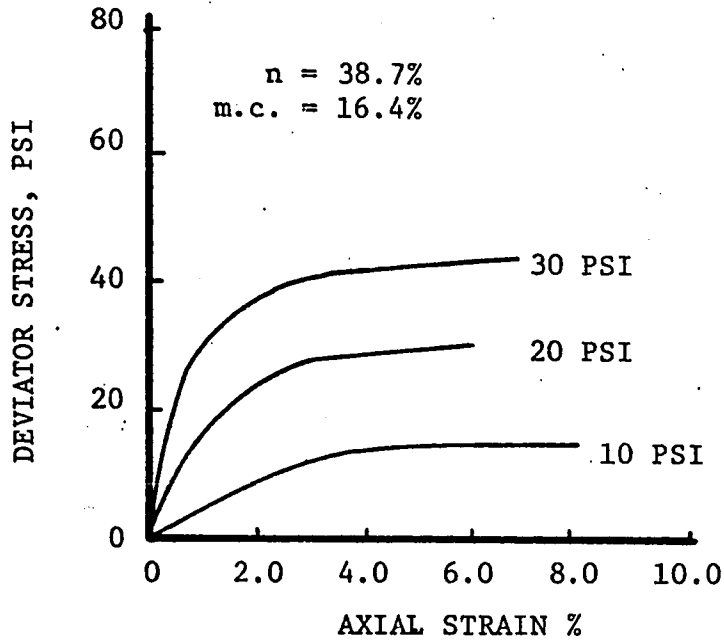


FIG. A.18 STRESS STRAIN CURVES FOR TRIAXIAL TESTS

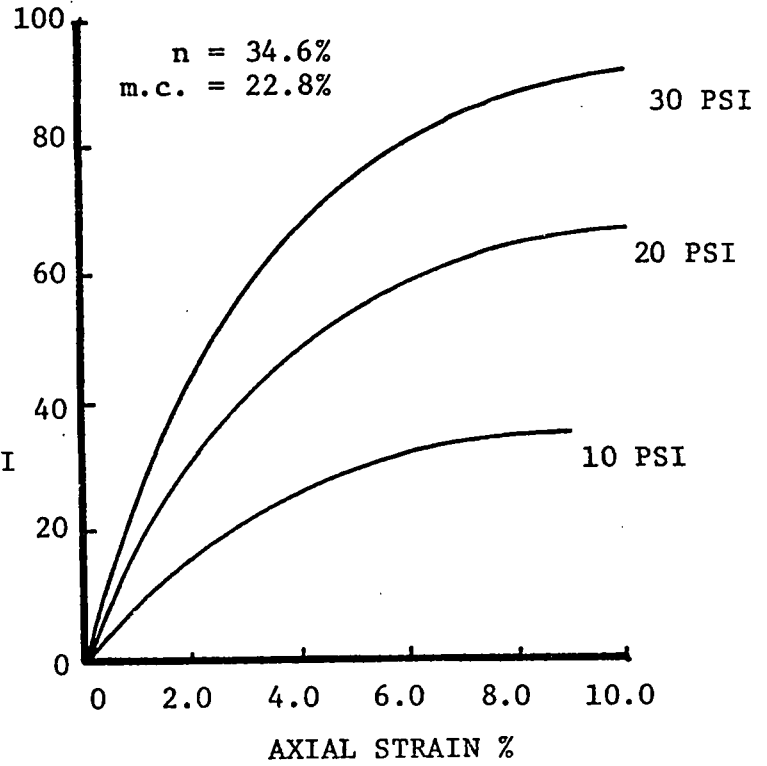
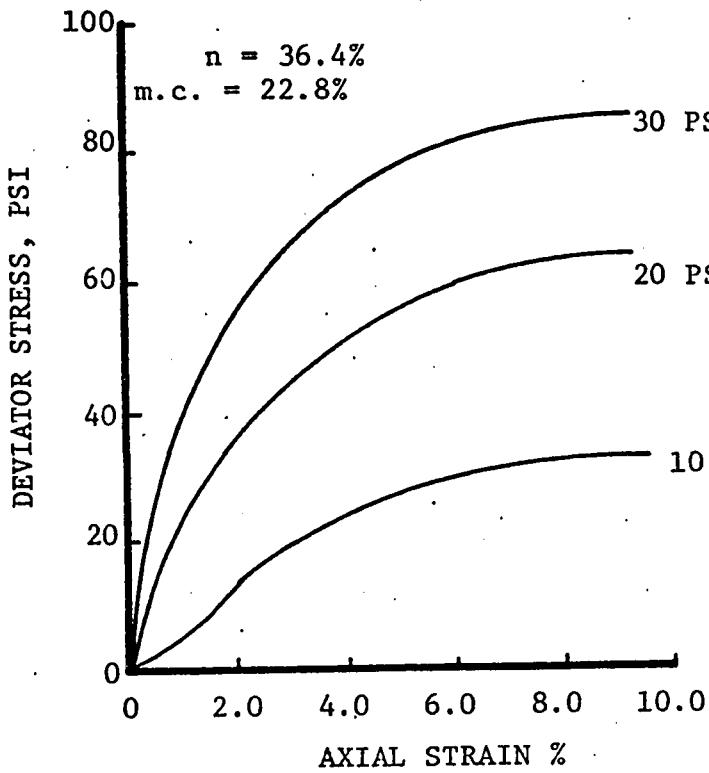
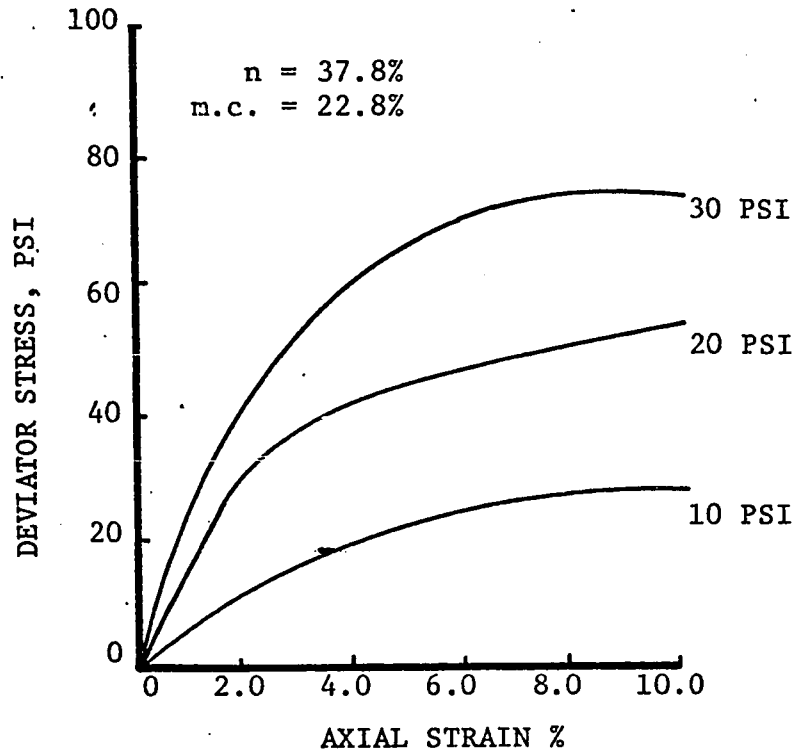
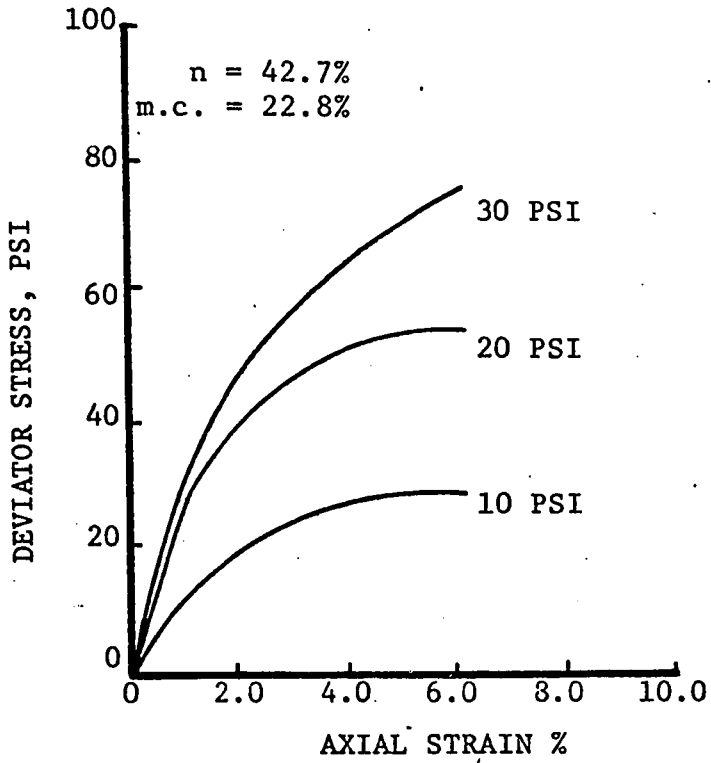


FIG. A.19 STRESS STRAIN CURVES FOR TRIAXIAL TESTS

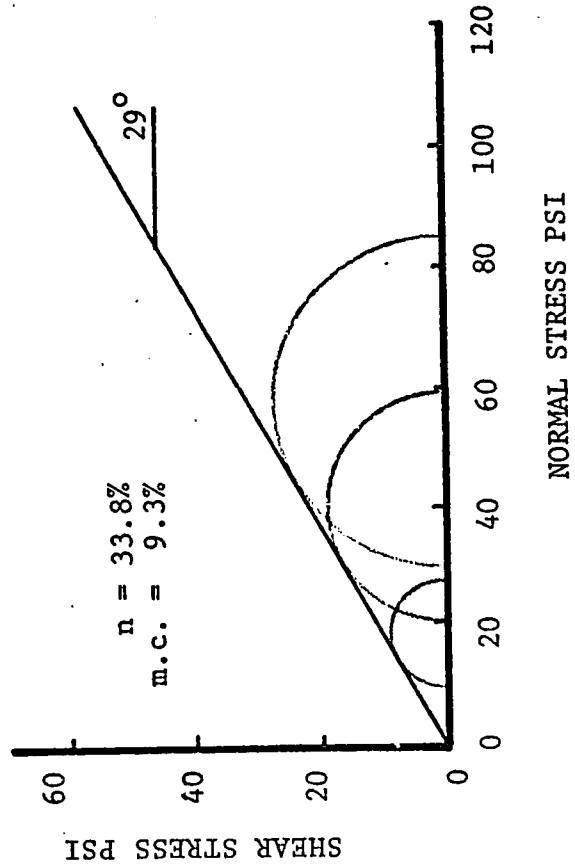
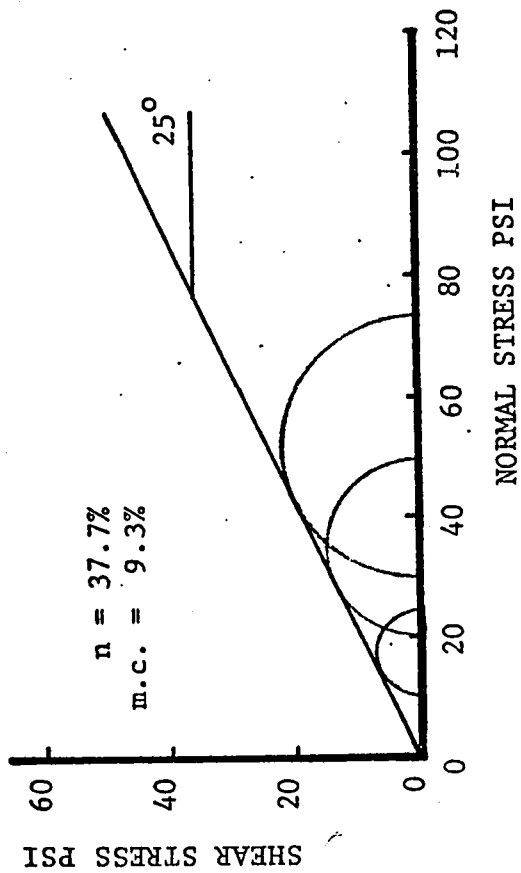
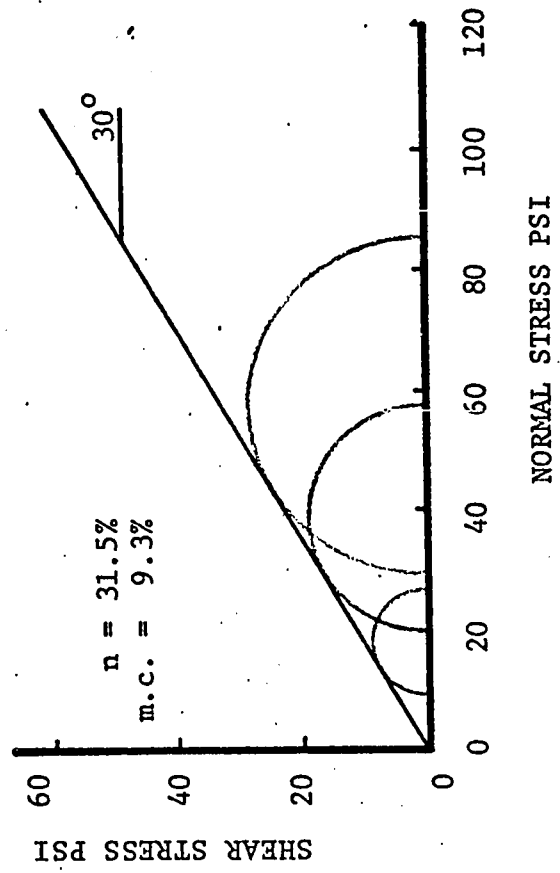
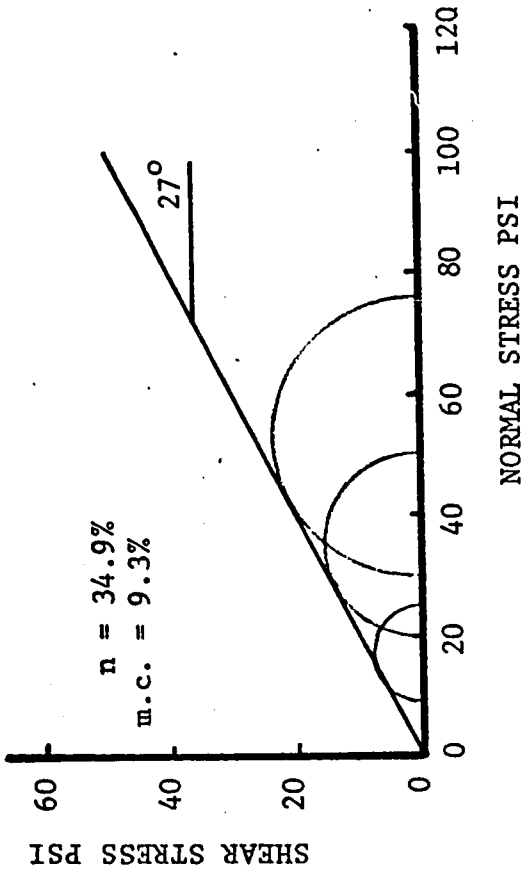


FIG. A.20 MOHR COULOMB FAILURE ENVELOPE FOR TRIAXIAL COMPRESSION TESTS

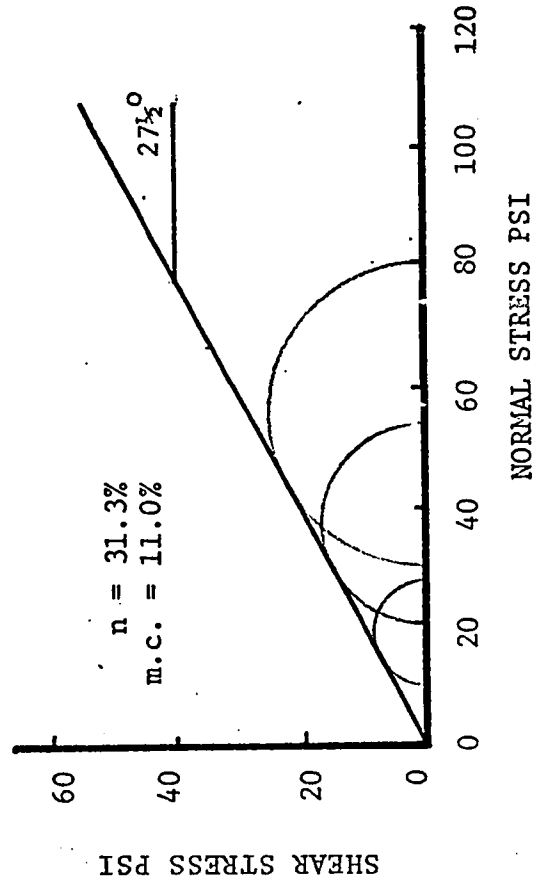
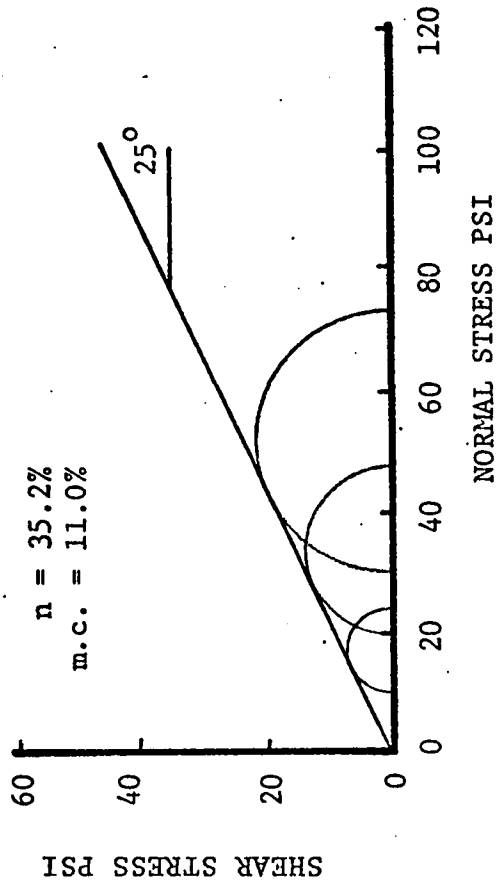
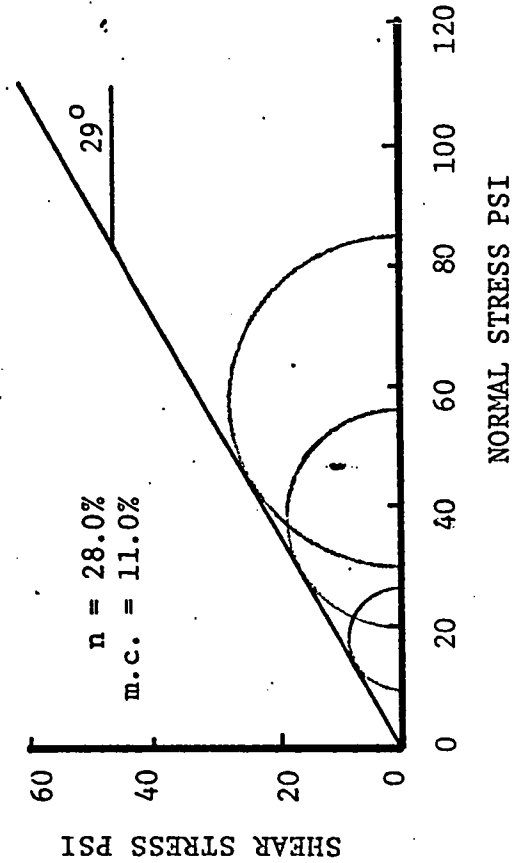
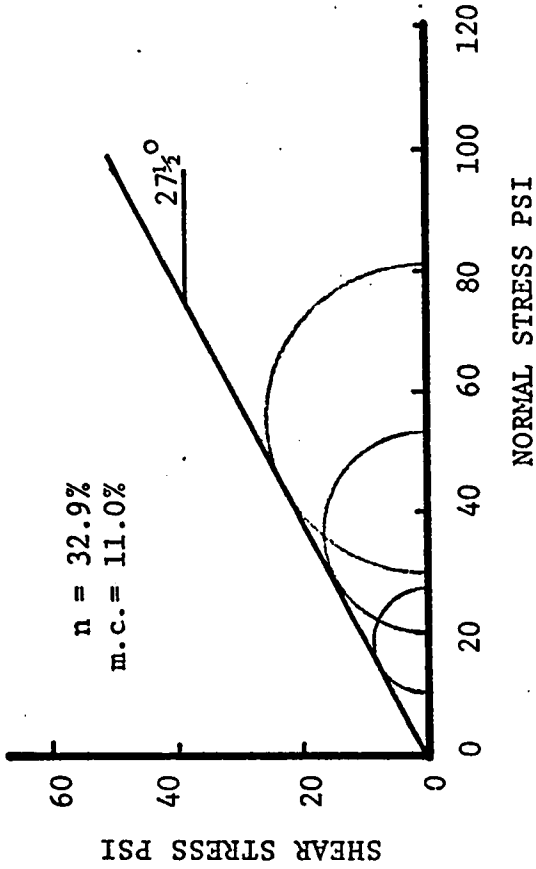


FIG. A.21 MOHR COULOMB FAILURE ENVELOPE FOR TRIAXIAL COMPRESSION TESTS

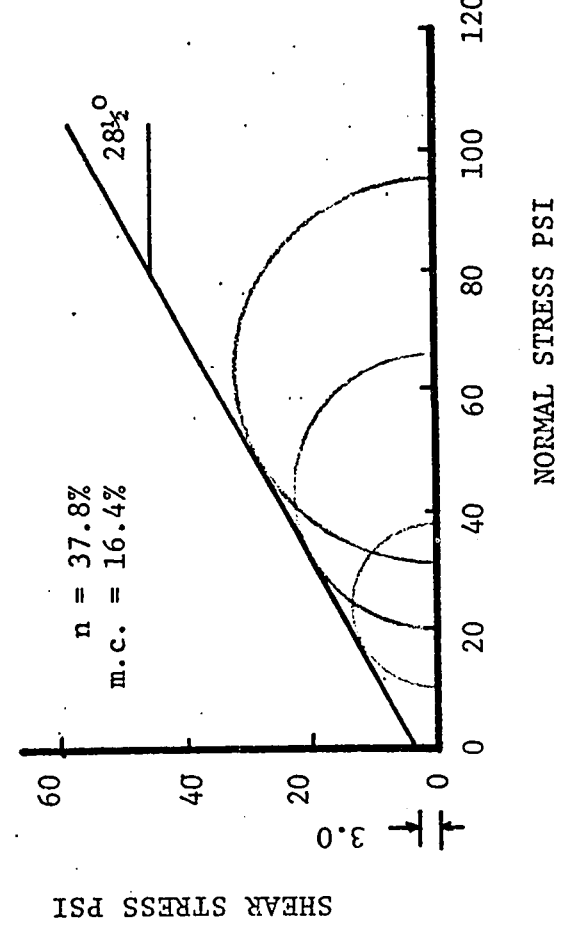
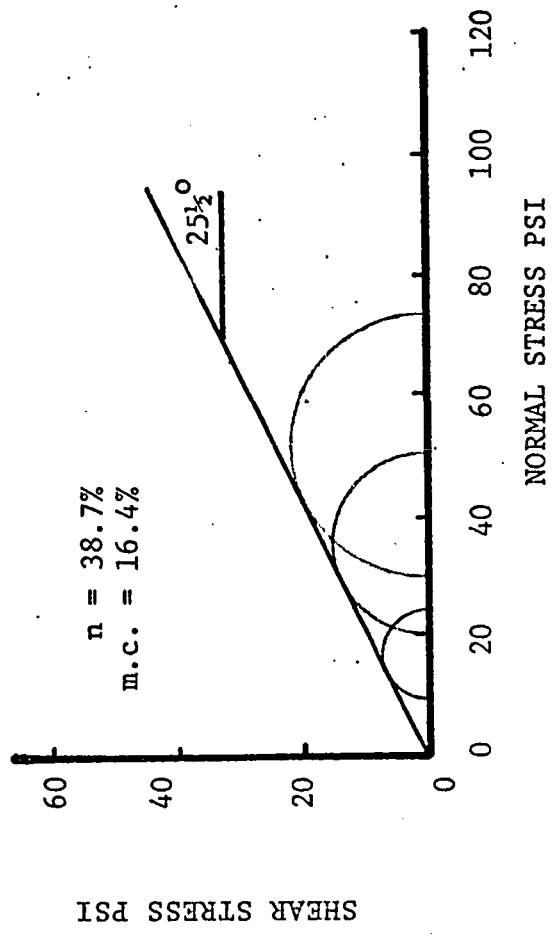
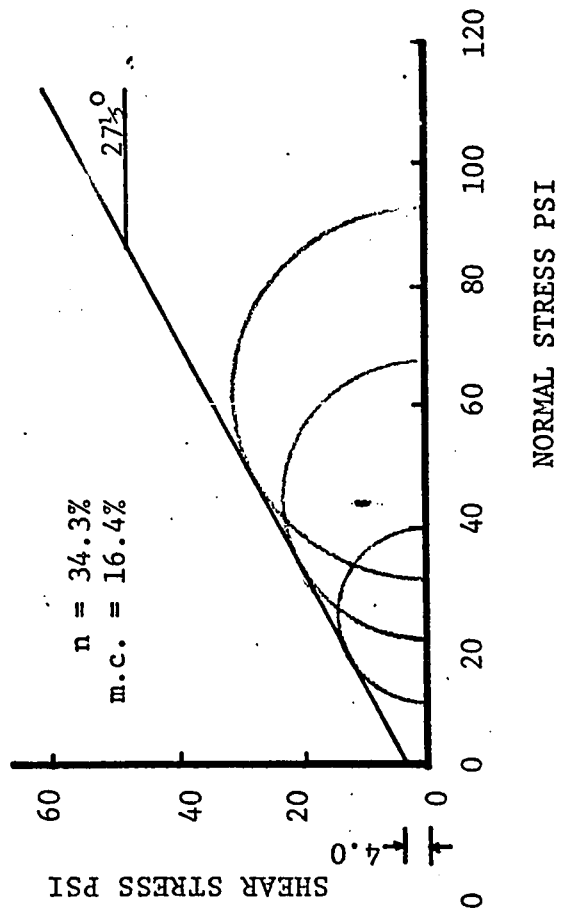
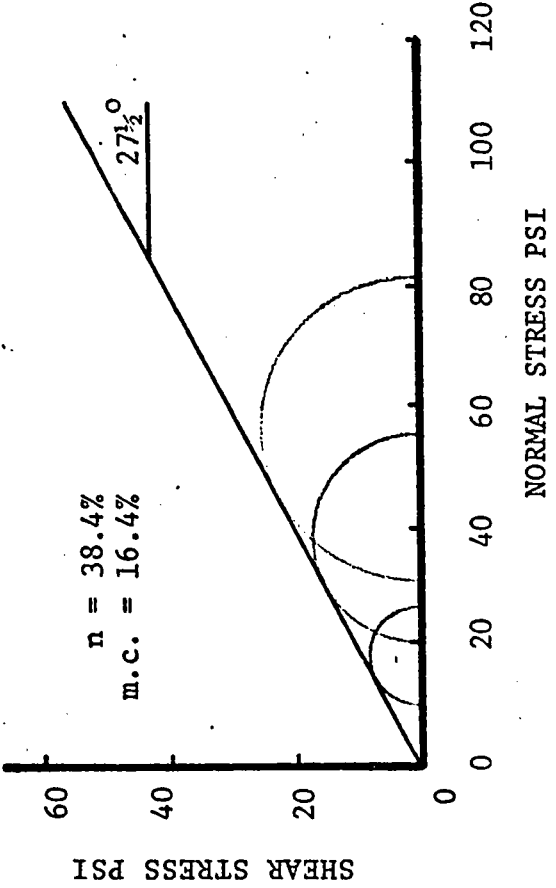


FIG. A.22 MOHR COULOMB FAILURE ENVELOPE FOR TRIAXIAL COMPRESSION TESTS

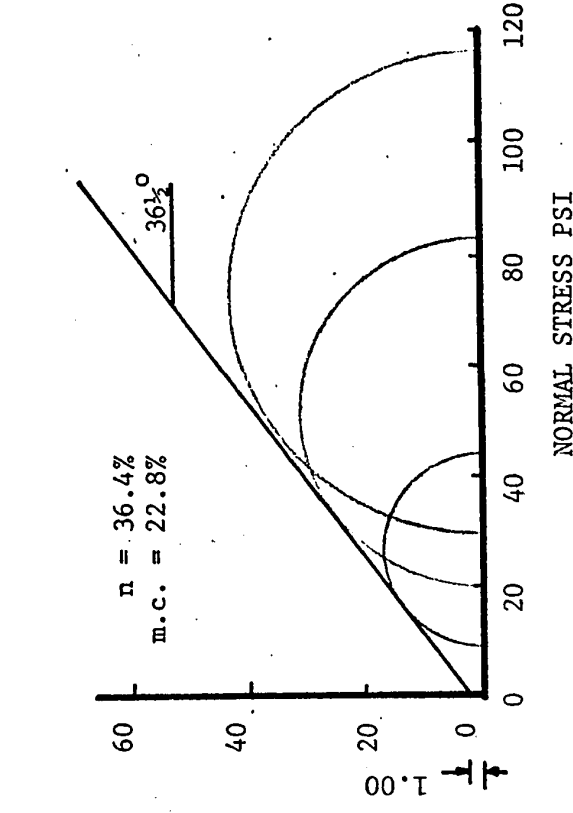
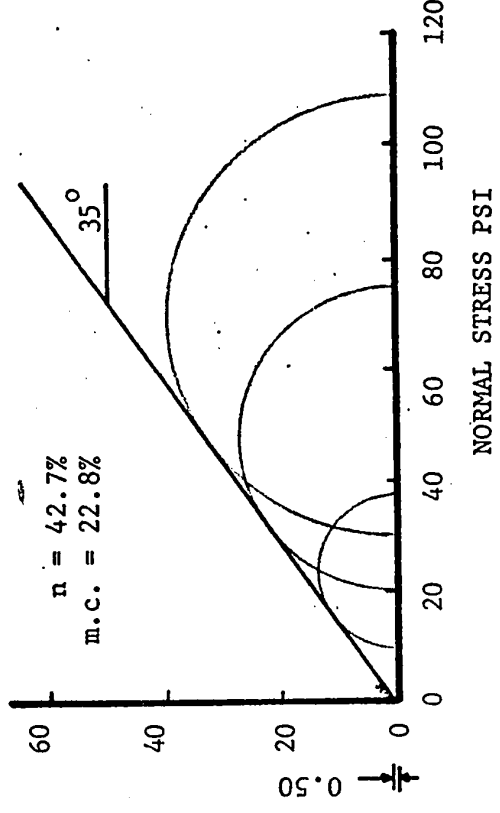
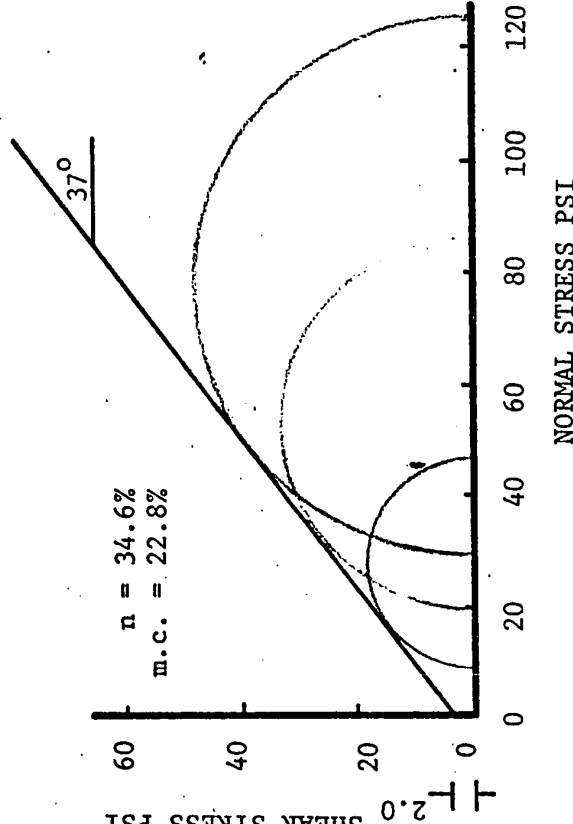
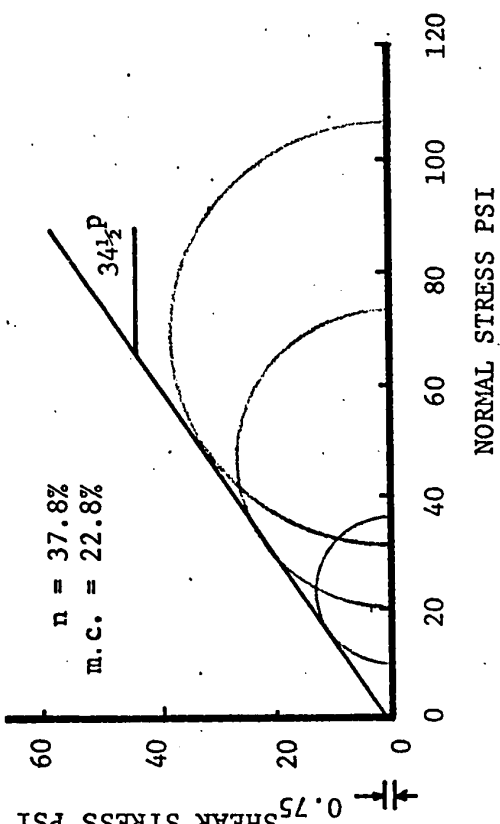


FIG. A.23 MOHR COULOMB FAILURE ENVELOPE FOR TRIAXIAL COMPRESSION TESTS

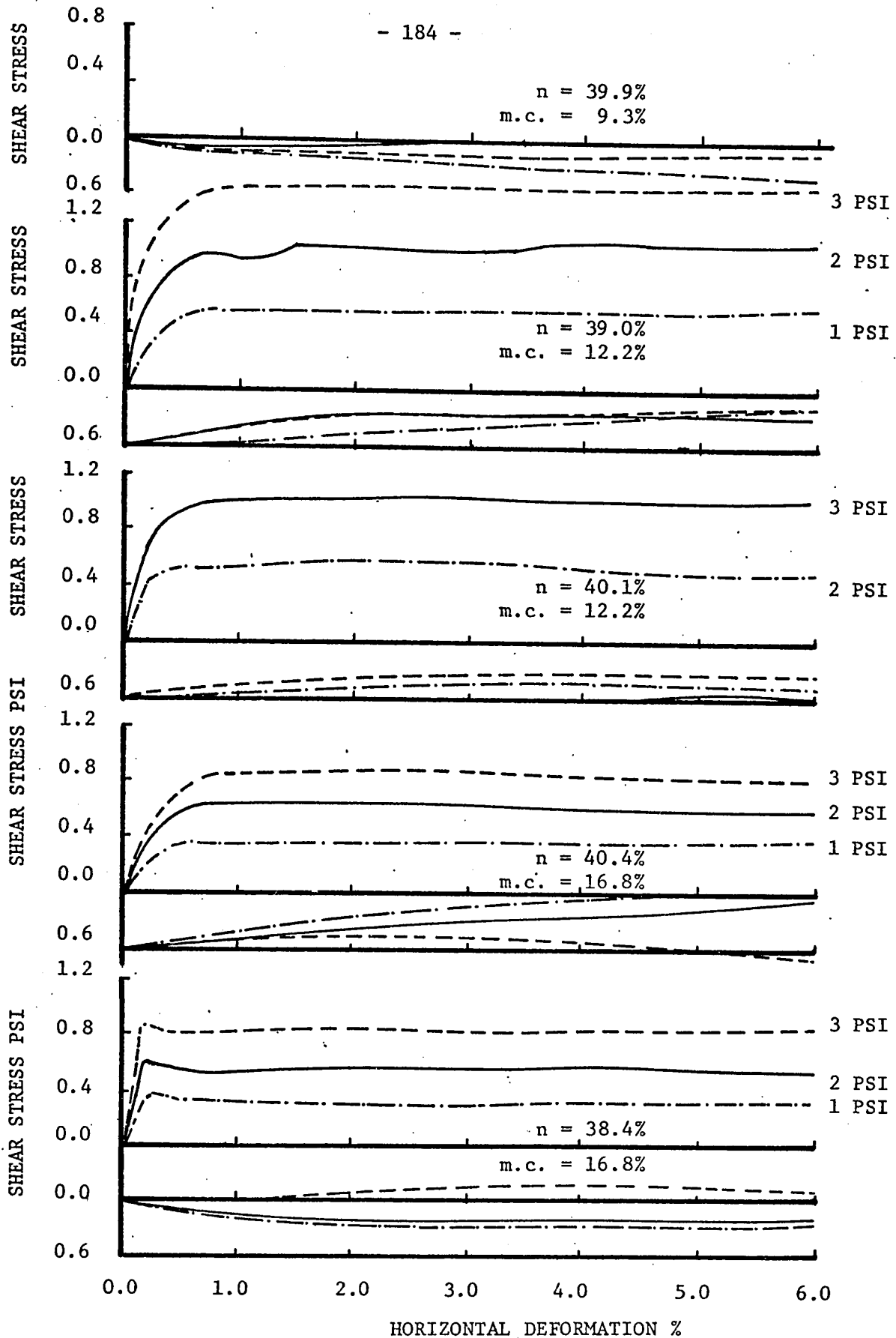


FIG. A.24 STRESS DEFORMATION OF WHEAT ON WOOD

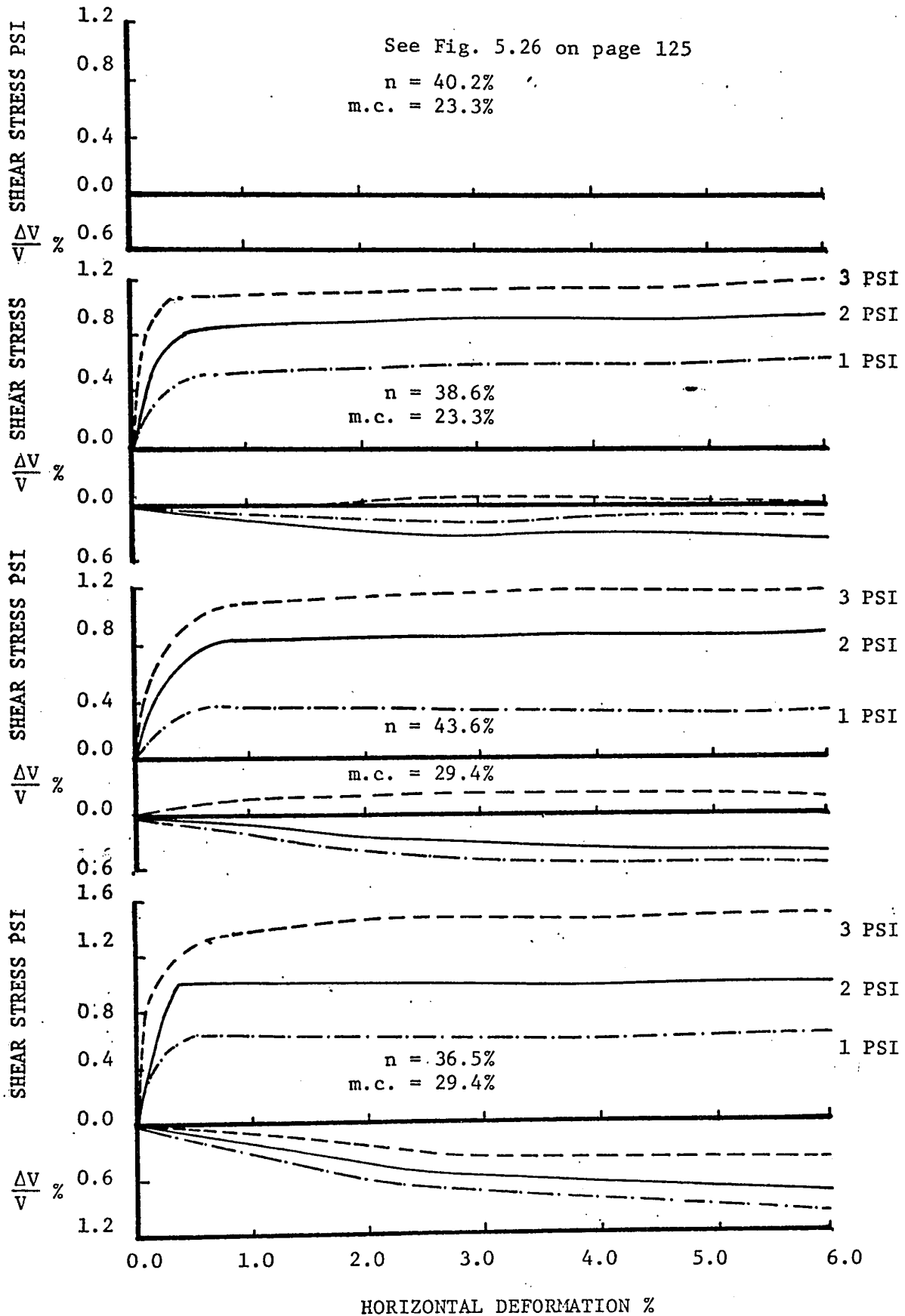


FIG. A.24 STRESS DEFORMATION OF WHEAT ON WOOD

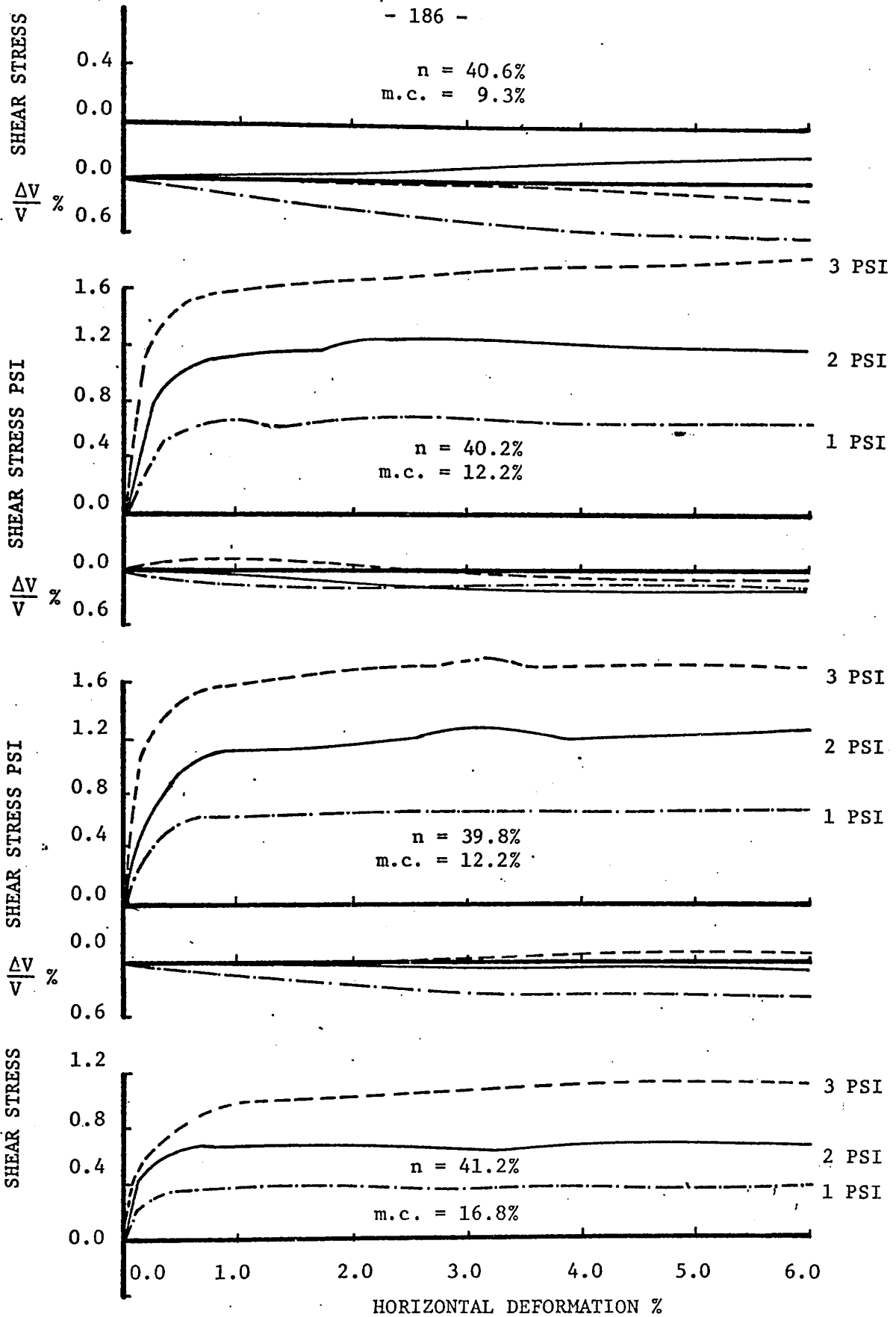


FIG. A.25 STRESS DEFORMATION CURVES OF WHEAT ON STEEL

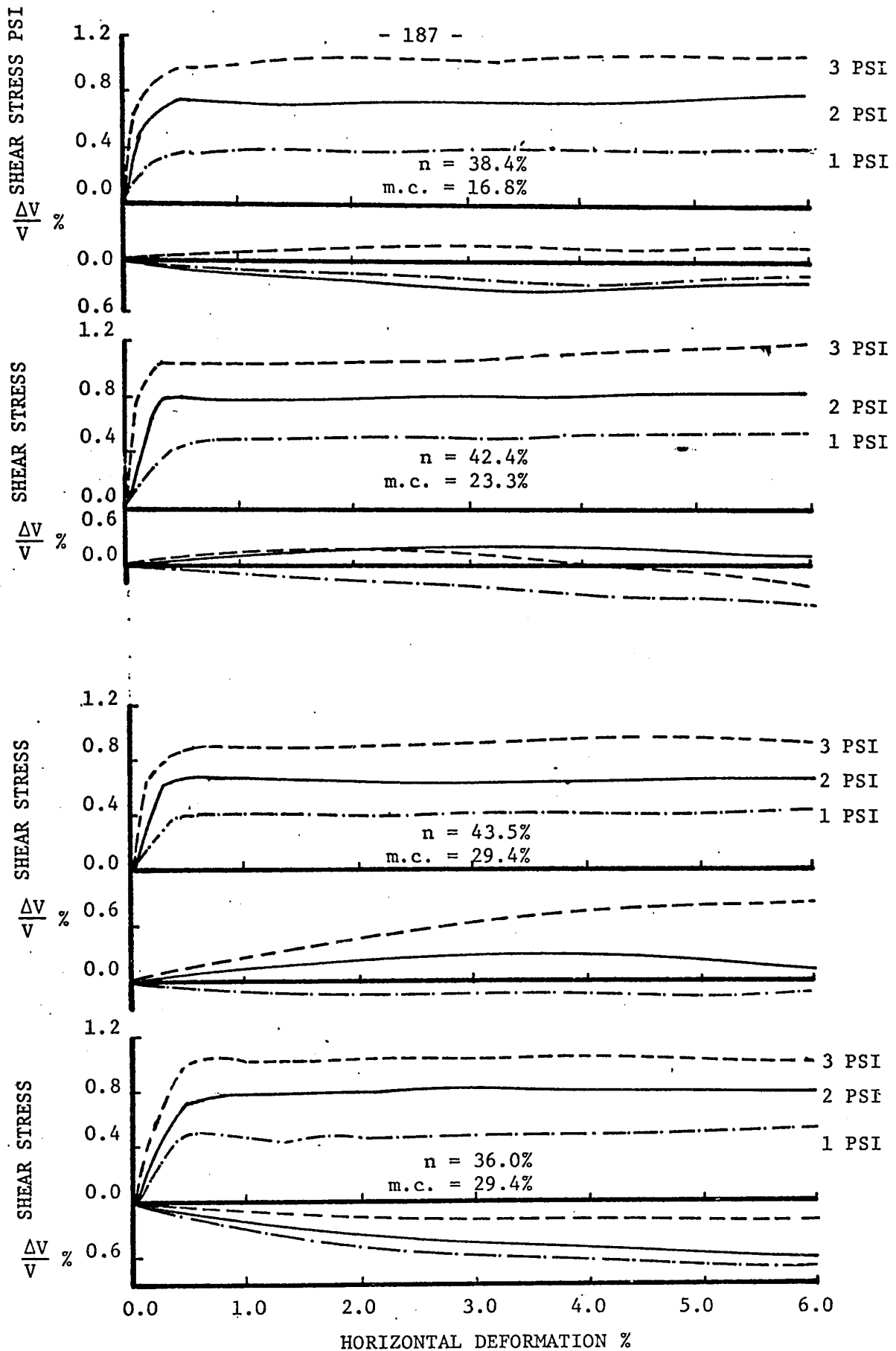


FIG. A.25 STRESS DEFORMATION CURVES OF WHEAT ON STEEL

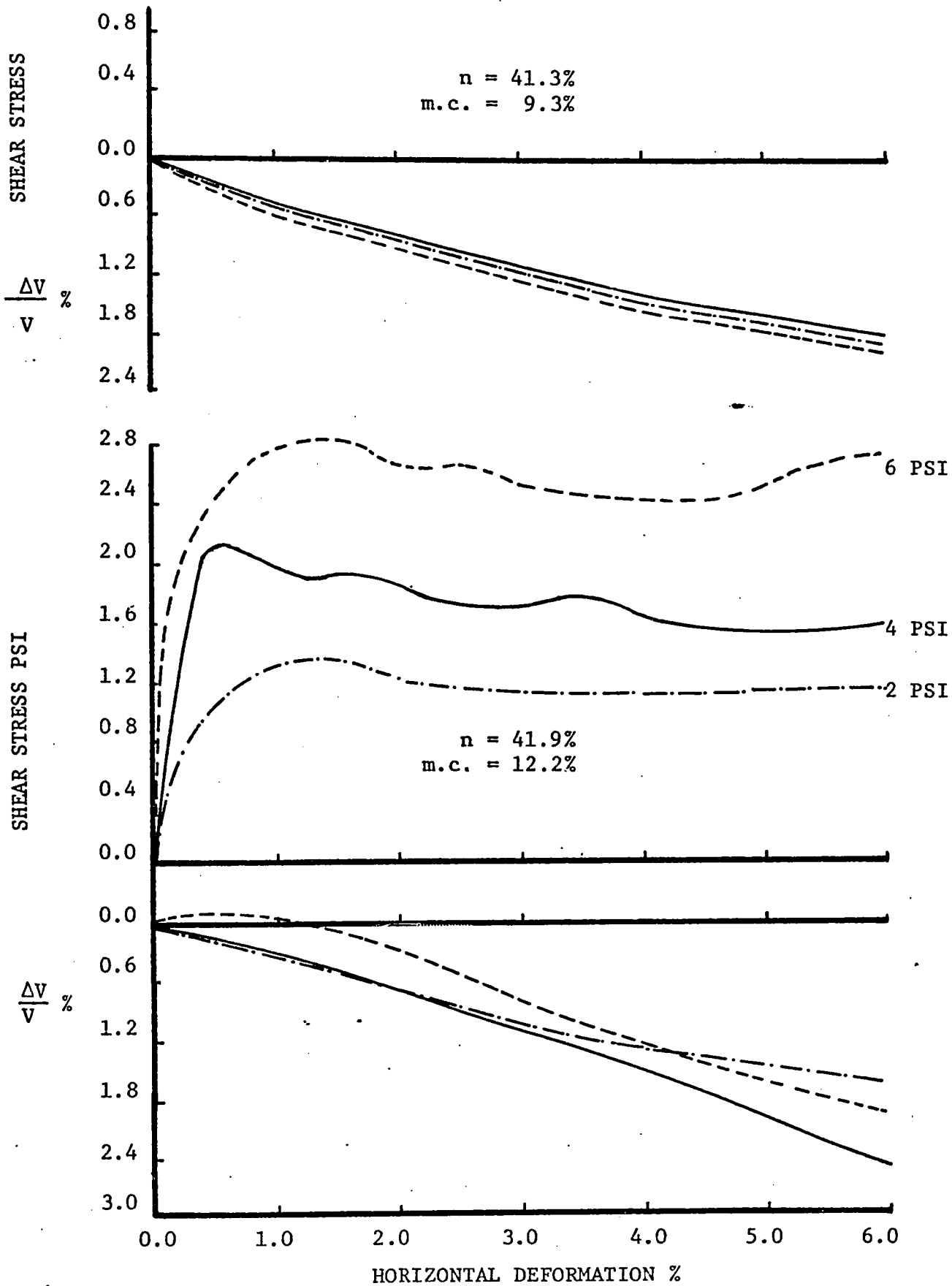


FIG. A.26 STRESS DEFORMATION CURVES OF WHEAT ON CONCRETE

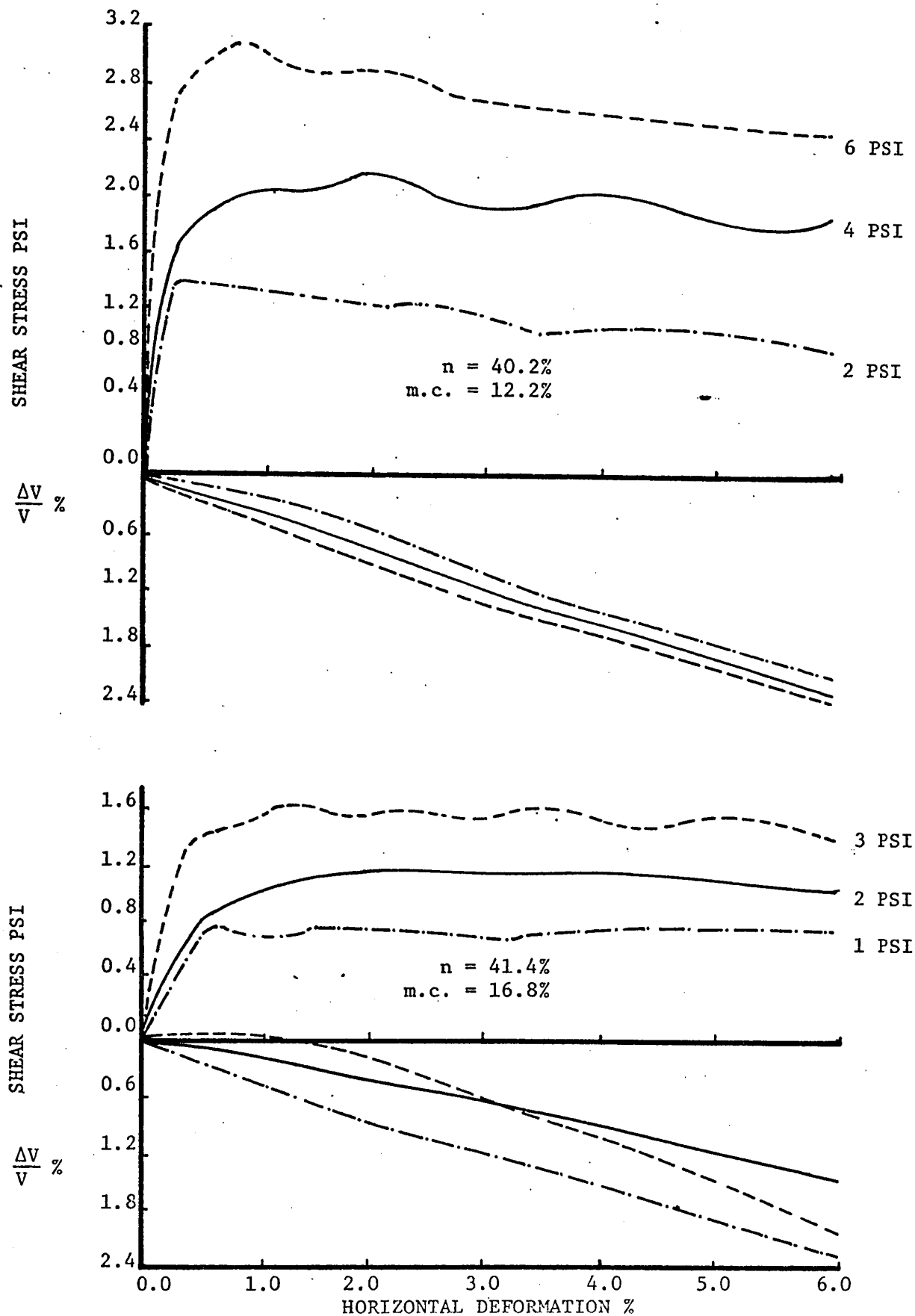


FIG. A.26 STRESS DEFORMATION CURVES OF WHEAT ON CONCRETE

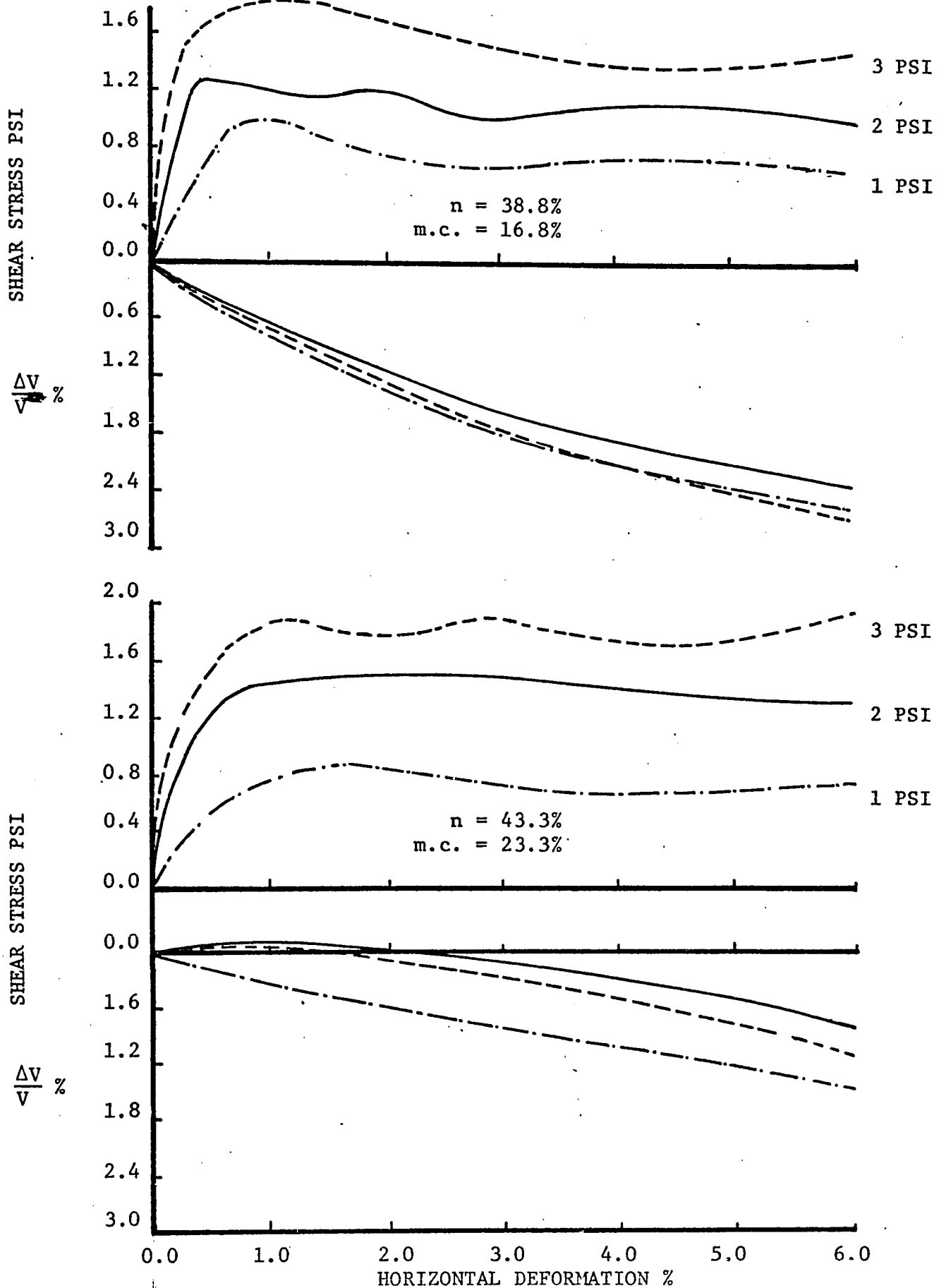


FIG. A.26 STRESS DEFORMATION CURVES OF WHEAT ON CONCRETE

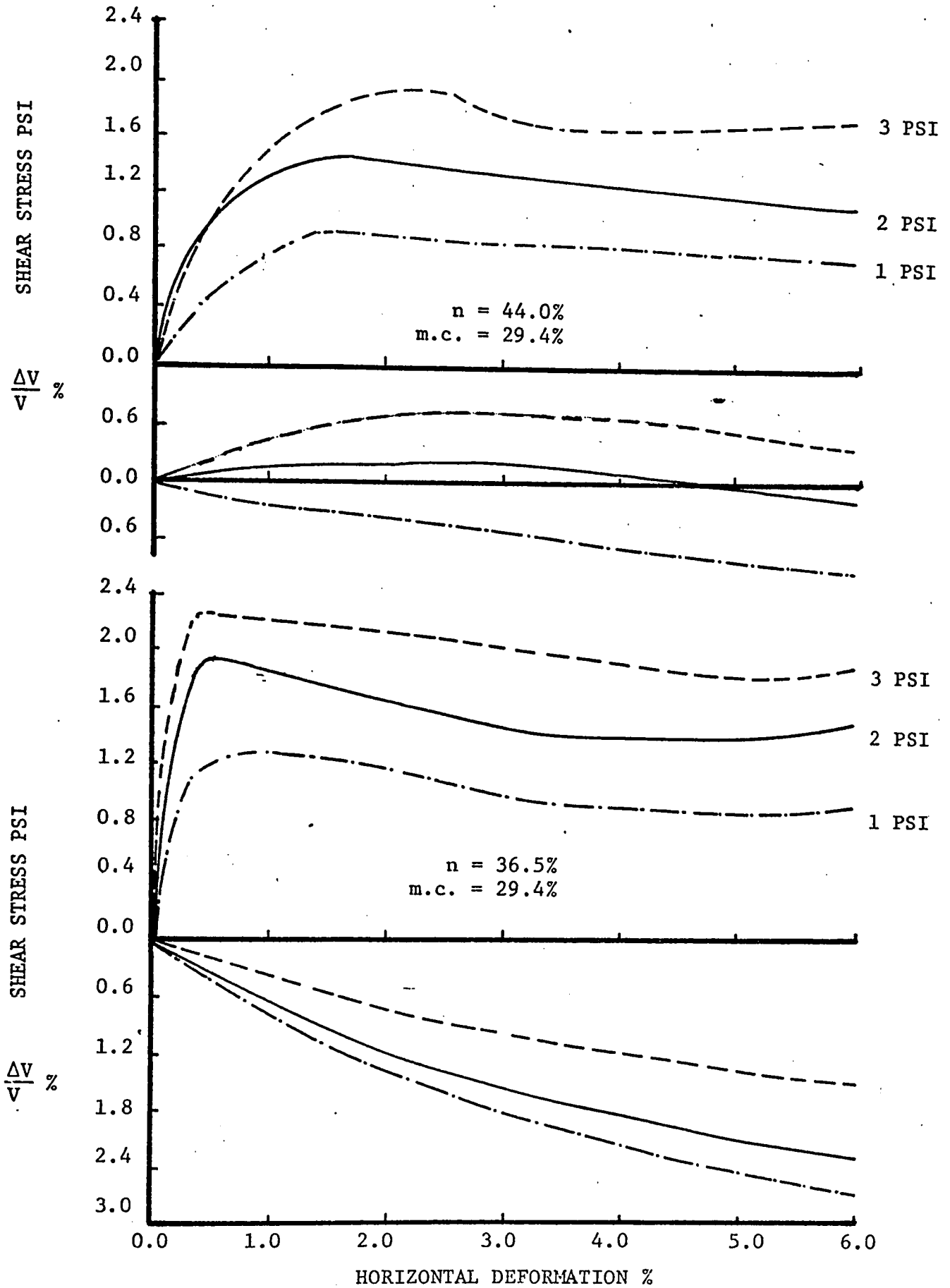


FIG. A.26 STRESS DEFORMATION CURVES OF WHEAT ON CONCRETE

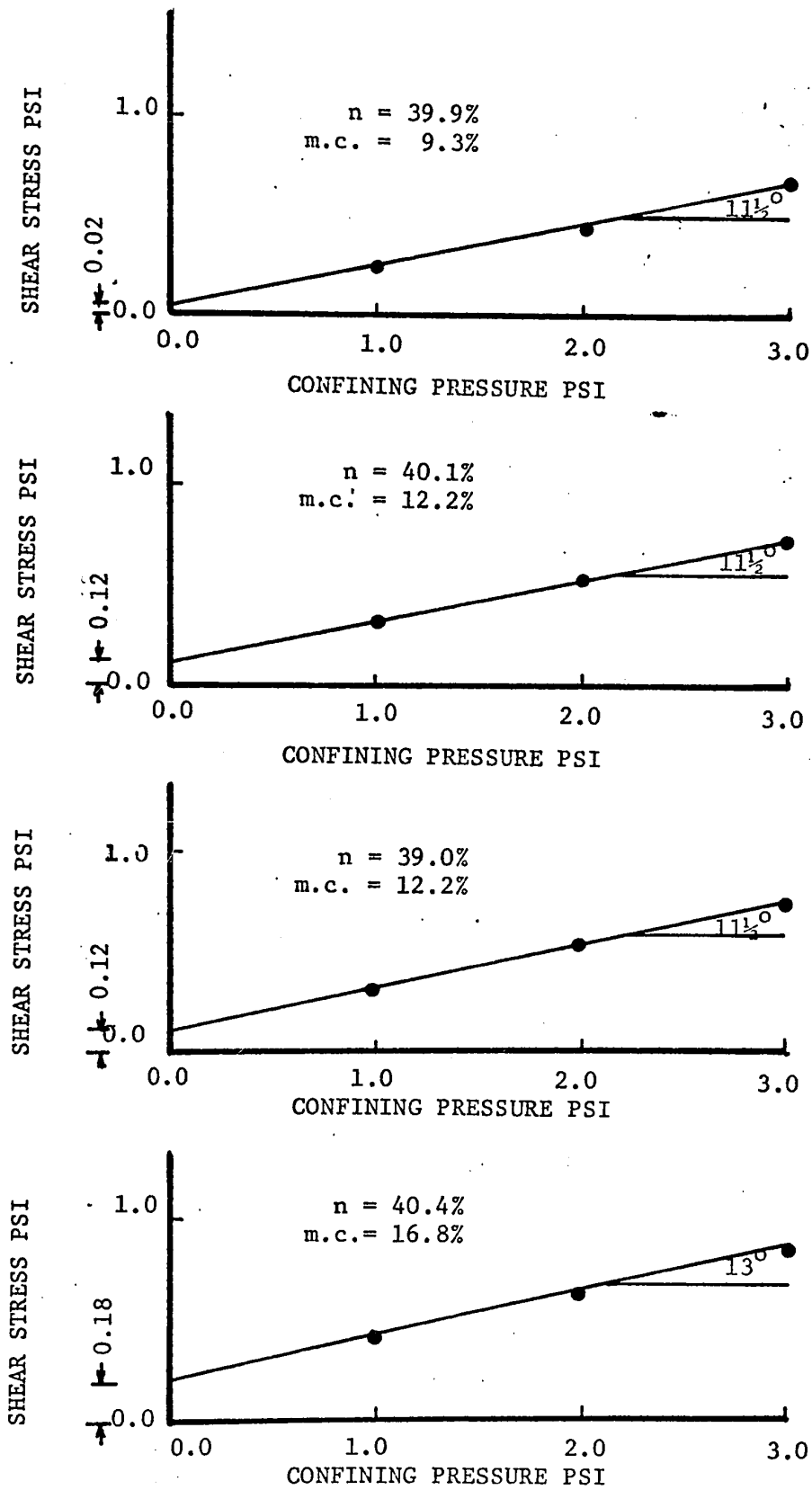
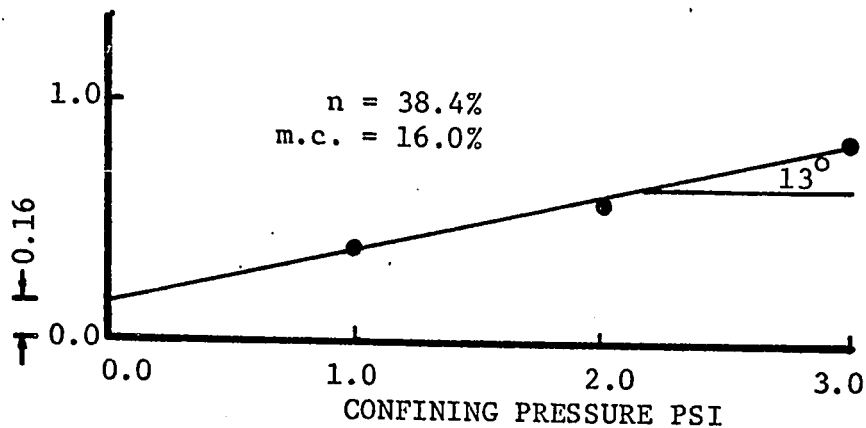
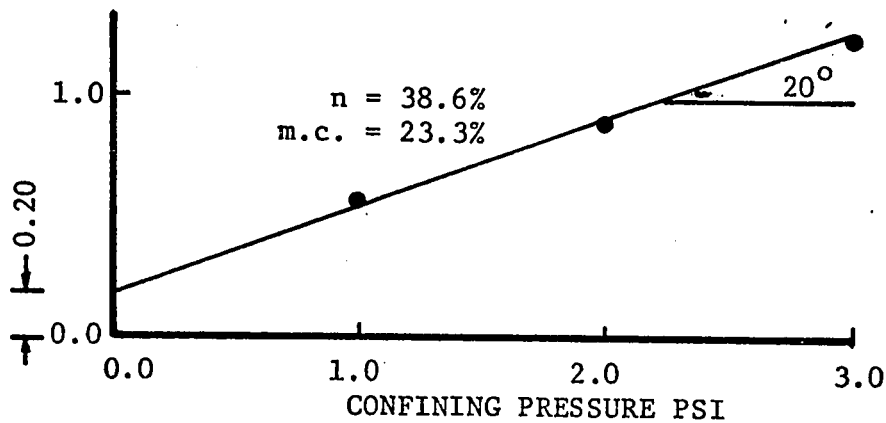


FIG. A.27 FAILURE ENVELOPE PLOTS OF WHEAT ON WOOD

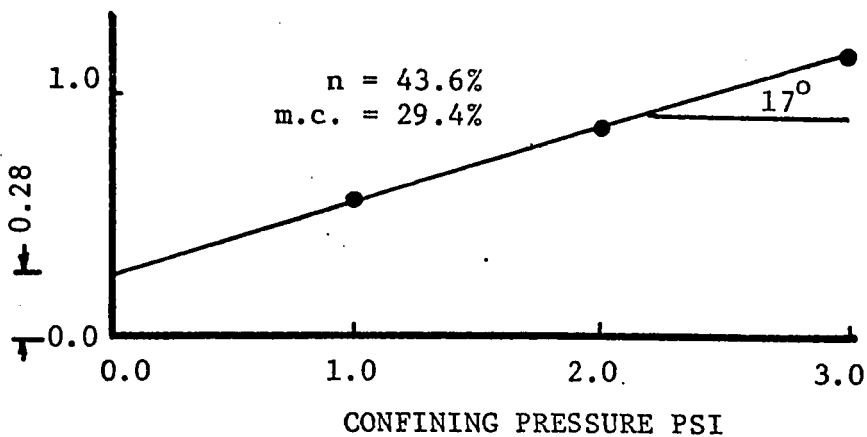
SHEAR STRESS PSI



SHEAR STRESS PSI



SHEAR STRESS PSI



SHEAR STRESS PSI

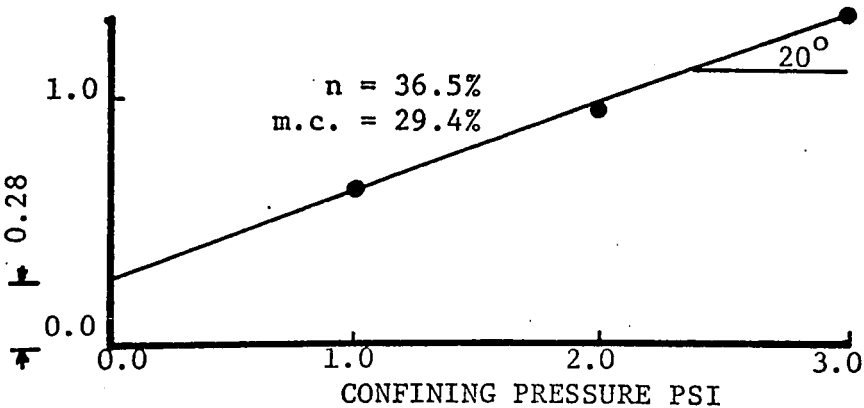


FIG. A.27 FAILURE ENVELOPE PLOTS OF WHEAT ON WOOD

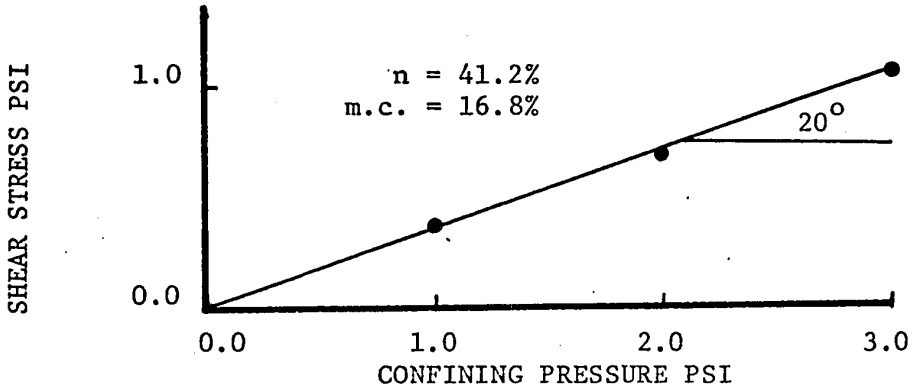
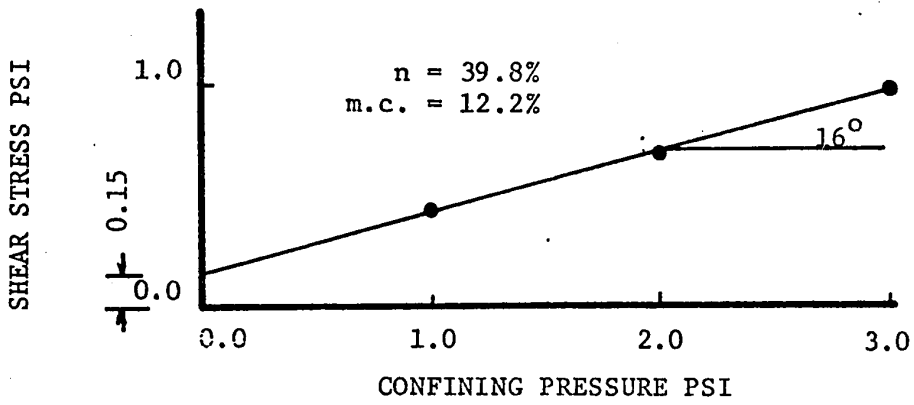
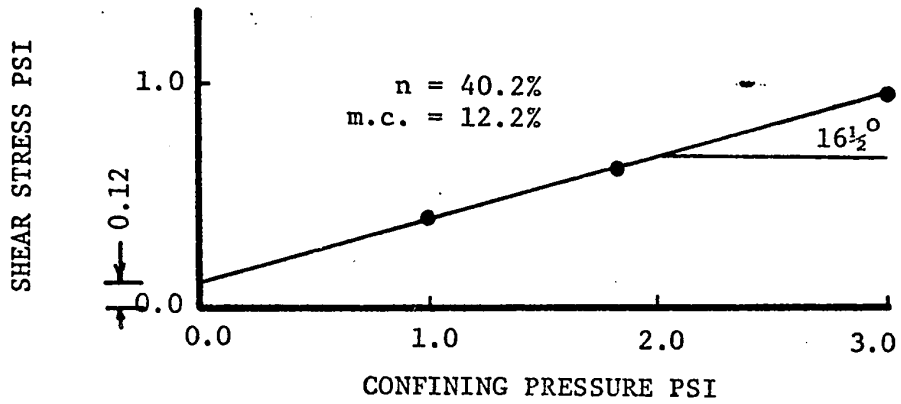
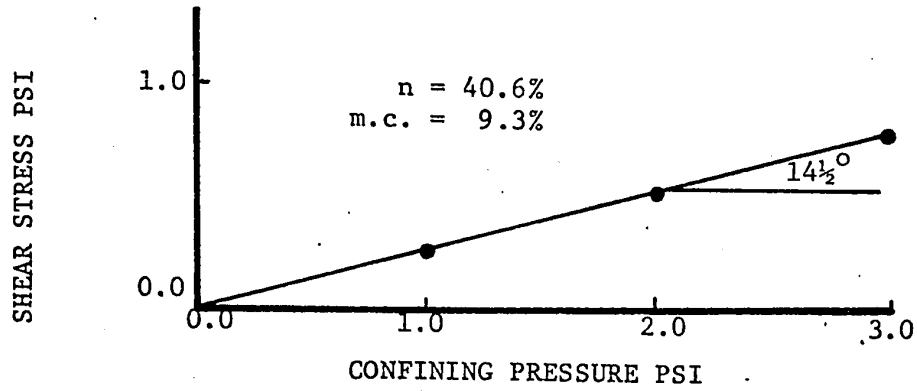


FIG. A.28 FAILURE ENVELOPE PLOTS OF WHEAT ON STEEL

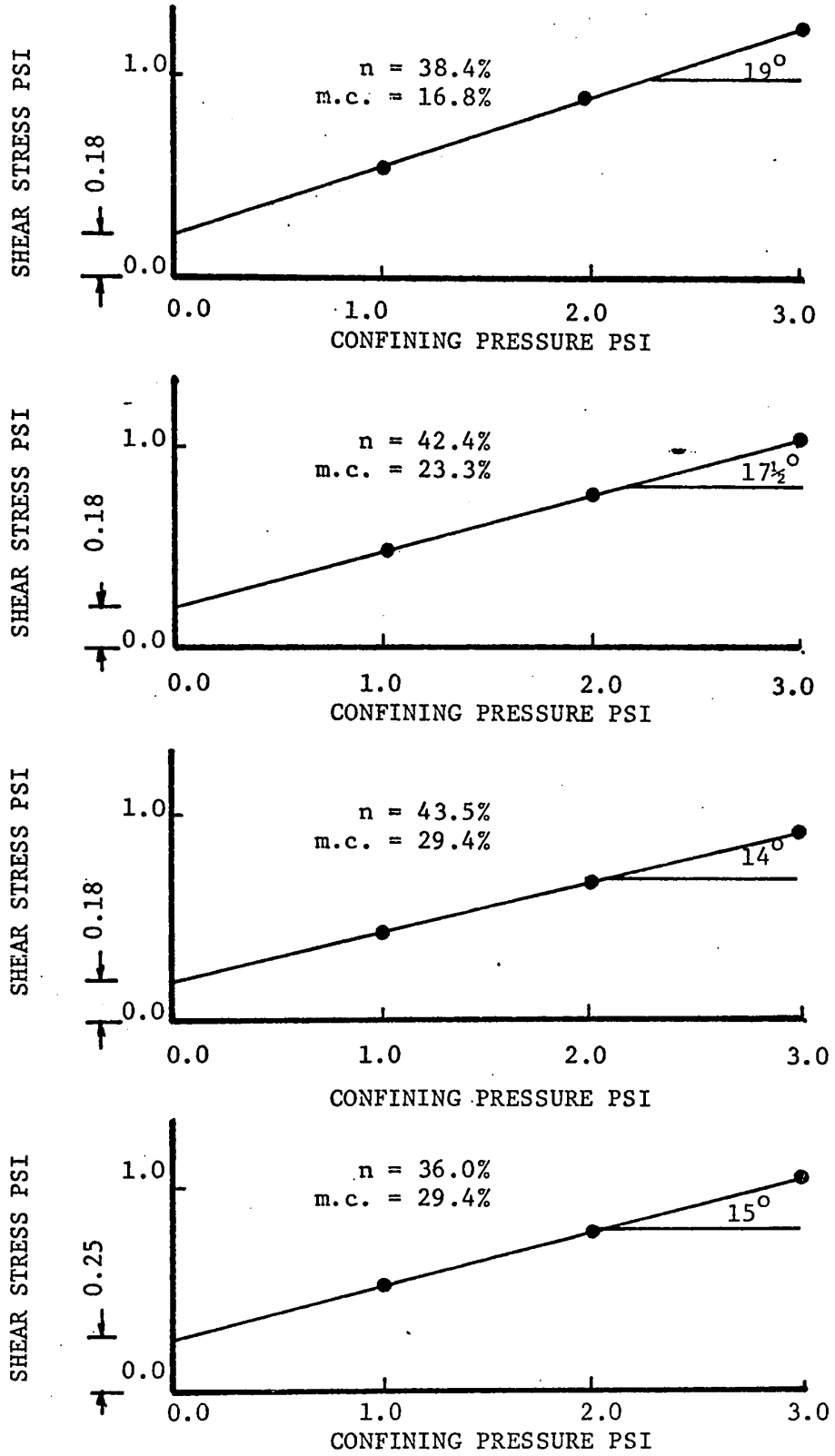
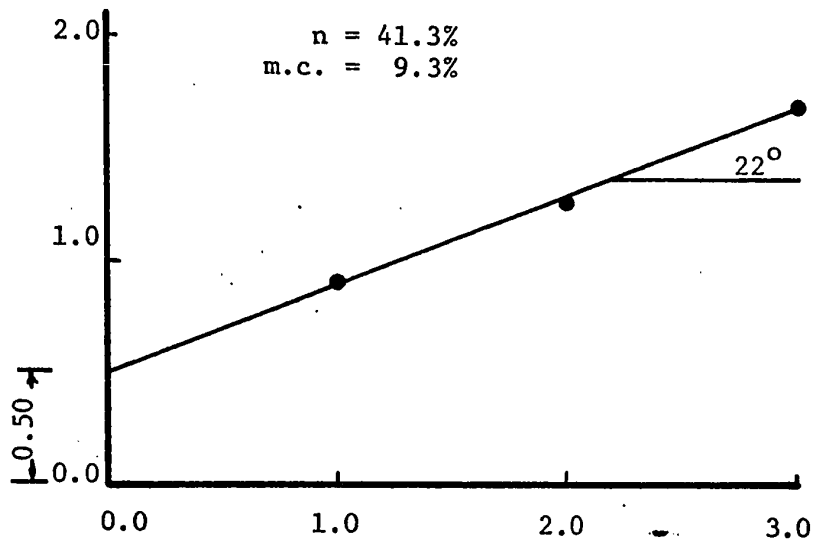
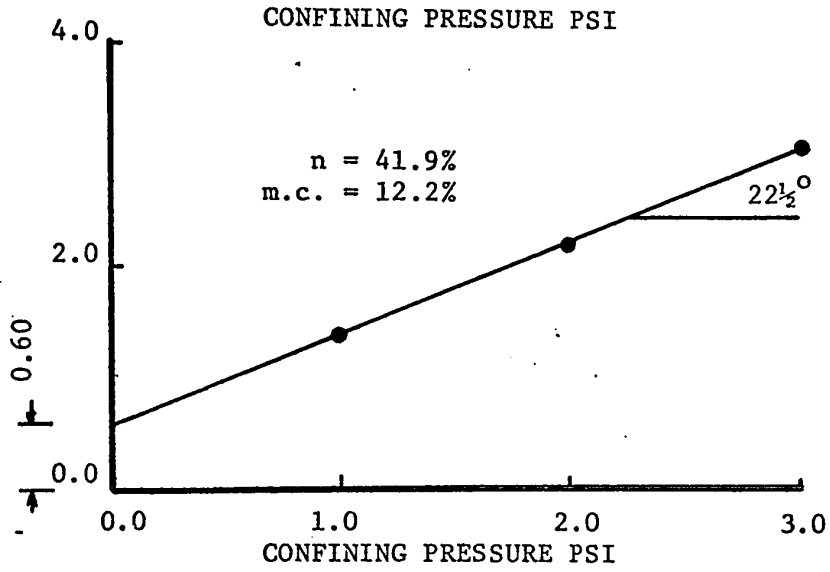


FIG. A.28 FAILURE ENVELOPE PLOTS OF WHEAT ON STEEL

SHEAR STRESS PSI



SHEAR STRESS PSI



SHEAR STRESS PSI

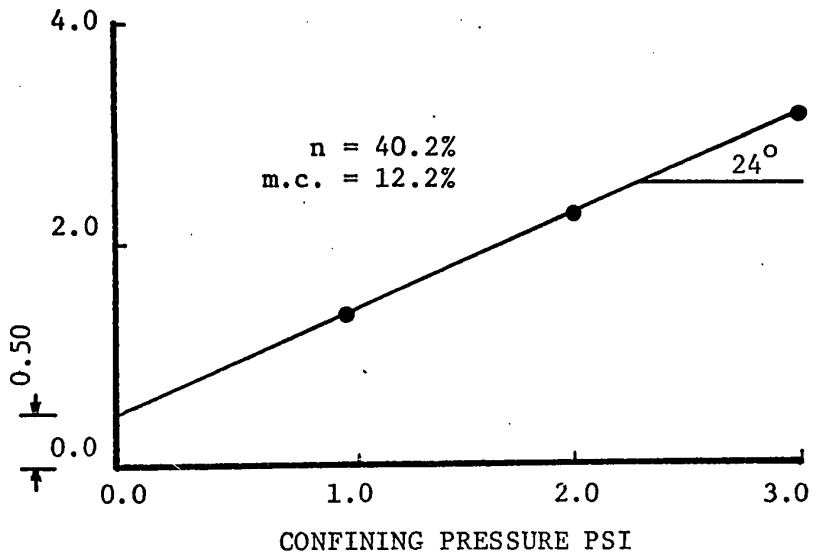
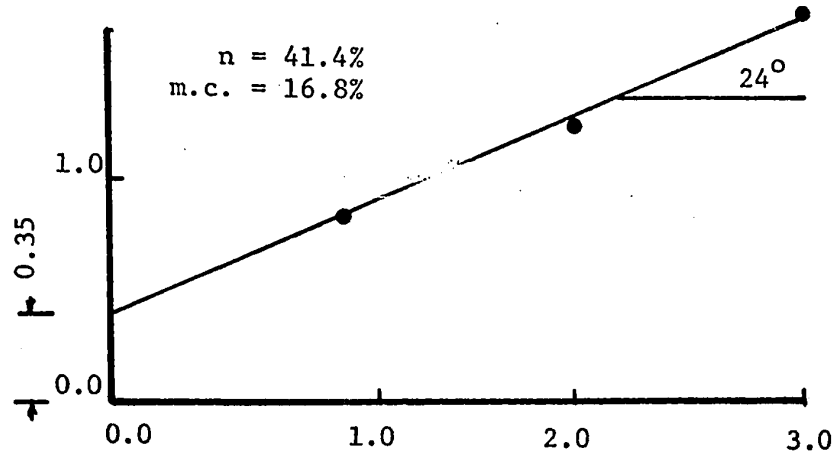
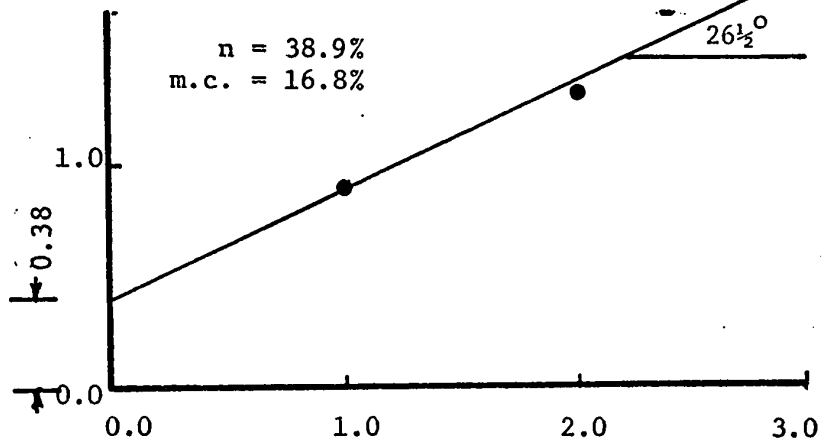


FIG. A.29 FAILURE ENVELOPE PLOTS OF WHEAT ON CONCRETE

SHEAR STRESS PSI

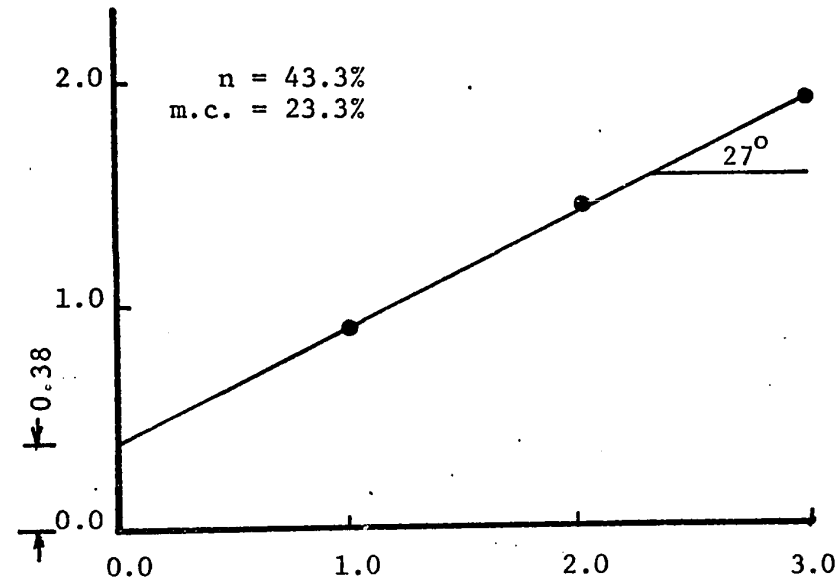


SHEAR STRESS PSI



CONFINING PRESSURE PSI

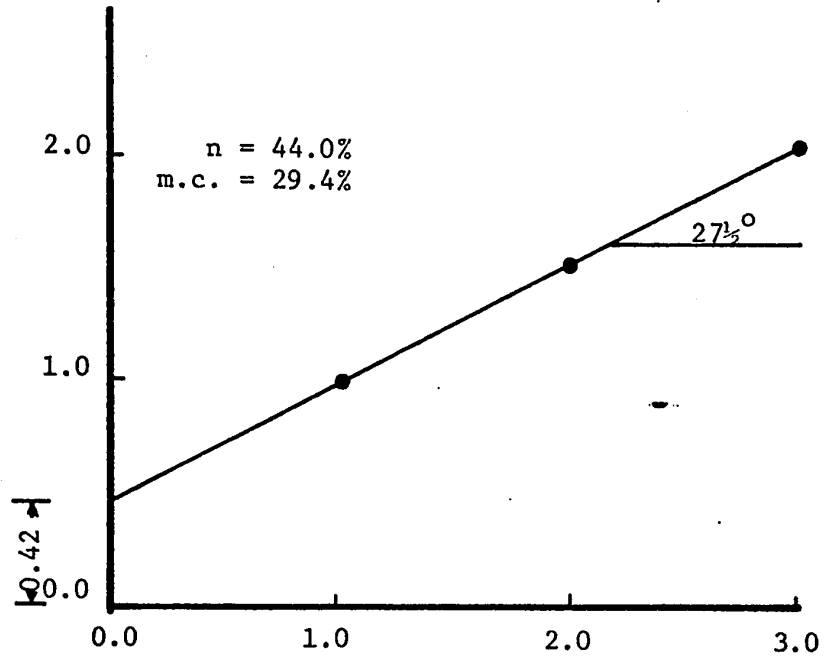
SHEAR STRESS PSI



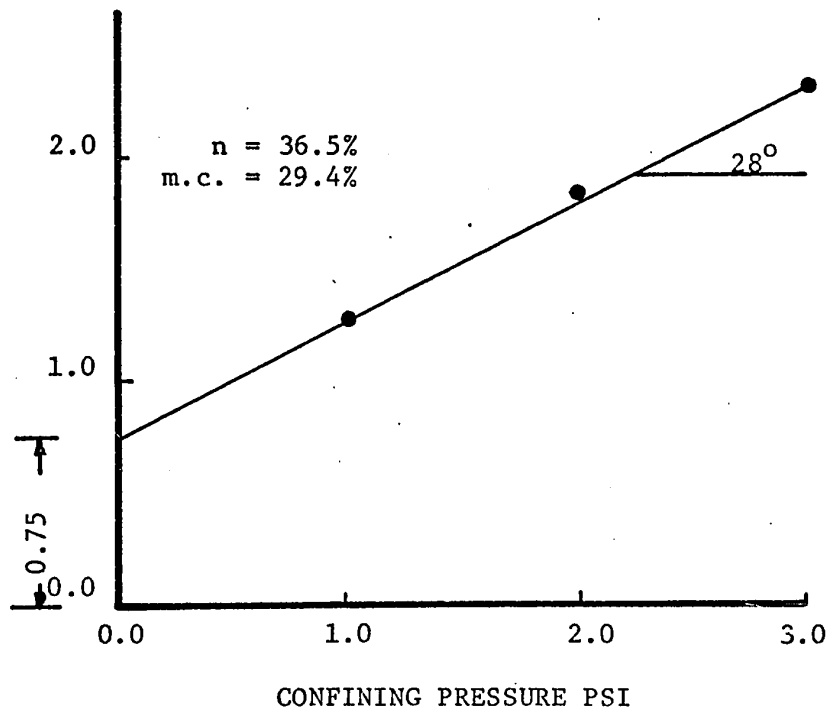
CONFINING PRESSURE PSI

FIG. A.29 FAILURE ENVELOPE PLOTS OF WHEAT ON CONCRETE

SHEAR STRESS PSI



SHEAR STRESS PSI



CONFINING PRESSURE PSI

FIG. A.29 FAILURE ENVELOPE PLOTS OF WHEAT ON CONCRETE

TABLE A.1 SPECIFIC GRAVITY OF WHEAT

Moisture Content %	Specific Gravity
9.4	1.43
12.2	1.42
16.8	1.40
23.3	1.39
29.4	1.36

TABLE A.2 CRUSHING LOAD OF INDIVIDUAL GRAIN

Moisture Content %	Crease Plane Vertical lbs.	Crease Plane Horizontal lbs.
9.0	19.2	13.7
	12.0	10.5
	16.1	13.7
	10.9	22.7
	21.5	14.6
	26.0	13.4
	16.6	15.1
	15.1	22.0
	18.1	16.1
	9.1	22.8
Average	16.5	16.3
12.3	12.6	16.5
	18.8	17.9
	22.2	22.7
	13.1	22.7
	24.1	28.8
	17.2	16.5
	19.8	13.0
	22.0	23.2
	16.5	21.3
	16.7	16.2
Average	19.4	19.8

Table A.2

- 200 -

Moisture Content %	Crease Plane Vertical lbs.	Crease Plane Horizontal lbs.
15.8	18.5	13.4
	18.3	15.0
	15.4	15.8
	13.0	19.0
	10.7	20.0
	Average	15.4
22.5	8.7	8.8
	9.6	10.4
	7.8	9.2
	10.0	13.0
	10.3	10.0
	Average	9.3
29.7	4.4	5.0
	4.5	6.0
	5.3	3.8
	4.9	4.4
	3.8	3.7
	Average	4.5

TABLE A.3 MINIMUM BULK DENSITY OF WHEAT

A.3.1 Pouring with a funnel 1 inch above the surface of wheat			
Moisture Content %	Density Pounds per cubic feet		Porosity %
8.9	50.6		43.2
12.8	50.0		43.3
15.4	50.8		42.2
22.5	46.1		46.7
29.7	44.2		48.0
A.3.2 Pouring with a scoop as close to surface as possible			
8.9	52.2		41.5
12.8	52.0		41.6
15.4	52.0		41.6
22.5	45.4		47.5
29.7	44.0		48.2
A.3.3 Pouring from 2 gallon pail (half filled) resting on lip of the mould			
8.9	51.2		42.9
12.8	51.1		42.4
15.4	50.5		42.9
22.5	45.3		47.7
29.7	43.4		49.1
A.3.4 Pouring with a half filled 2 gallon pail 6 inches above mould			
8.9	51.9		41.9
12.8	50.5		43.3
15.4	47.8		42.3
22.5	46.0		46.6
29.7	43.6		48.9

TABLE A.4 MAXIMUM BULK DENSITY OF WHEAT BY VIBRATORY METHOD

Moisture Content %	Amplitude Divisions	Surcharge psi	Density lb./cu. ft. and Porosity %	Time of vibration in minutes				
				1	2	4	8	16
8.8	25	0	Density	-	-	55.6	55.8	55.2
			Porosity	-	-	37.6	37.4	38.0
	0.28	Density	-	55.4	55.0	55.6	55.1	
		Porosity	-	37.8	38.3	37.6	38.2	
	0.45	Density	-	54.9	54.9	54.9	55.0	
		Porosity	-	38.4	38.4	38.4	38.3	
	0.64	Density	54.8	54.8	54.8	54.8	54.8	
		Porosity	38.5	38.5	38.5	38.5	38.5	
	0.81	Density	54.5	54.8	54.5	54.8	55.9	
		Porosity	38.8	38.5	38.8	38.5	38.4	
50	0	Density	-	-	-	-	-	
		Porosity	-	-	-	-	-	
	0.28	Density	55.0	55.2	55.2	55.6	55.5	
		Porosity	38.3	38.0	38.0	37.6	37.7	
	0.45	Density	54.9	54.8	54.8	54.9	54.9	
		Porosity	38.4	38.5	38.5	38.4	38.4	
	0.64	Density	-	54.9	54.8	54.9	54.8	
		Porosity	-	38.9	38.5	38.4	38.5	
	0.81	Density	54.8	54.8	54.9	55.0	-	
		Porosity	38.5	38.5	38.4	38.3	-	

100	0	Density	-	-	-	-	-
		Porosity	-	-	-	-	-
	0.28	Density	55.5	55.8	55.8	55.9	55.8
		Porosity	37.7	37.4	37.4	37.3	37.4
	0.45	Density	55.6	55.5	55.2	55.2	55.2
		Porosity	37.6	37.7	38.0	38.0	38.0
	0.64	Density	55.2	55.0	55.2	55.2	55.1
		Porosity	38.2	38.3	38.1	38.0	38.2
	0.81	Density	-	55.1	-	55.3	55.2
		Porosity	-	38.2	-	38.0	38.1
10.8	25	Density	-	-	55.9	56.0	56.0
		Porosity	-	-	37.0	36.9	36.9
	0.01	Density	-	55.8	55.8	56.0	55.8
		Porosity	-	37.2	37.2	36.9	37.2
	0.28	Density	55.6	55.6	55.8	55.8	-
		Porosity	37.3	37.3	37.2	37.2	-
	0.45	Density	55.6	-	55.7	55.7	55.7
		Porosity	37.4	-	37.3	37.3	37.3
	0.64	Density	55.5	-	55.6	55.6	55.5
		Porosity	37.5	-	37.4	37.4	37.5

50	0	Density	-	-	55.0	55.8	55.8
		Porosity	-	-	36.9	37.2	37.2
0.28	0.28	Density	55.7	55.6	55.8	56.1	55.9
		Porosity	37.3	37.4	37.2	36.8	37.0
0.45	0.45	Density	-	55.5	55.5	55.2	55.5
		Porosity	-	37.4	37.4	37.8	37.4
0.64	0.64	Density	-	55.2	55.3	55.2	55.2
		Porosity	-	37.8	37.7	37.8	37.8
0.81	0.81	Density	55.2	55.1	55.2	55.2	55.2
		Porosity	37.8	37.9	37.8	37.8	37.8
100	0	Density	-	56.0	56.3	56.0	56.3
		Porosity	-	36.9	36.6	36.9	36.6
0.28	0.28	Density	56.0	56.4	56.4	56.3	-
		Porosity	36.9	36.5	36.5	36.6	-
0.45	0.45	Density	54.8	-	55.8	56.0	55.5
		Porosity	38.3	-	37.2	36.9	37.5
0.64	0.64	Density	-	55.5	55.8	-	55.8
		Porosity	-	37.5	37.2	-	37.2
0.81	0.81	Density	-	-	55.8	55.9	55.9
		Porosity	-	-	37.2	37.1	37.1

13.8	25	0	Density	-	54.8	54.9	54.9	54.9	54.9
			Porosity	-	38.0	37.8	37.8	37.8	37.8
0.01	0.01		Density	-	54.9	54.5	54.8	54.8	54.8
			Porosity	-	37.8	38.3	37.9	37.9	37.9
0.28	0.28		Density	54.5	54.5	54.7	54.6	54.5	54.5
			Porosity	38.3	38.3	38.1	38.2	38.3	38.3
0.45	0.45		Density	54.3	-	54.3	54.3	54.4	54.4
			Porosity	38.5	-	38.5	38.5	38.2	38.2
0.64	0.64		Density	54.2	-	54.3	54.3	-	-
			Porosity	38.6	-	38.5	38.5	-	-
50	0		Density	-	54.9	54.8	54.9	54.9	54.9
			Porosity	-	37.8	37.9	37.8	37.8	37.8
0.01	0.01		Density	-	54.5	54.7	54.9	54.8	54.8
			Porosity	-	38.3	38.0	37.8	37.9	37.9
0.28	0.28		Density	54.7	54.6	54.7	54.8	54.7	54.7
			Porosity	38.0	38.2	38.0	37.9	38.0	38.0
0.45	0.45		Density	-	54.3	54.3	54.4	54.4	54.4
			Porosity	-	38.5	38.5	38.4	38.4	38.4
0.64	0.64		Density	-	-	54.2	54.2	-	-
			Porosity	-	-	38.6	38.6	-	-

100	0	Density	-	55.0	54.9	55.0	54.9	54.9
		Porosity	-	37.7	37.8	37.7	37.8	37.8
	0.01	Density	-	55.0	54.7	54.8	54.7	54.7
		Porosity	-	37.7	38.0	37.9	38.0	38.0
	0.28	Density	-	54.7	54.8	54.8	54.8	54.9
		Porosity	-	38.0	37.9	37.9	37.9	37.8
	0.45	Density	-	54.6	54.6	54.5	54.4	54.4
		Porosity	-	38.2	38.2	38.3	38.3	38.4
	0.64	Density	-	-	54.4	54.6	-	-
		Porosity	-	-	38.4	38.2	-	-
20.0	0	Density	-	51.0	51.3	51.8	51.6	51.6
		Porosity	-	41.4	41.0	40.6	40.7	40.7
	0.01	Density	-	49.3	50.2	50.4	51.0	51.0
		Porosity	-	43.4	42.4	42.2	41.4	41.4
	0.28	Density	-	49.3	49.7	50.2	50.2	50.2
		Porosity	-	43.4	43.0	42.4	42.4	42.4
	0.45	Density	48.6	49.2	49.3	49.3	-	-
		Porosity	44.1	43.4	43.4	43.4	-	-
	0.64	Density	-	-	49.7	-	-	-
		Porosity	-	-	42.9	-	-	-

50	0	Density	-	49.3	49.3	49.3	49.3
		Porosity	-	43.4	43.4	43.4	43.4
	0.28	Density	-	49.7	50.8	51.1	50.9
		Porosity	-	42.8	41.6	41.2	41.5
	0.45	Density	-	49.6	49.4	49.4	49.4
		Porosity	-	43.0	43.3	43.3	43.3
	0.64	Density	-	48.8	-	-	-
		Porosity	-	43.9	-	-	-
100	0	Density	-	52.3	52.4	53.2	53.2
		Porosity	-	40.0	39.8	38.9	38.9
	0.01	Density	-	51.1	51.5	50.6	51.5
		Porosity	-	41.2	40.8	41.8	40.8
	0.28	Density	-	50.3	50.4	50.6	50.6
		Porosity	-	42.2	42.1	41.8	41.8
	0.45	Density	-	-	50.2	50.2	50.4
		Porosity	-	-	42.3	42.3	42.1
22.1	25	Density	-	49.3	50.0	50.7	50.2
		Porosity	-	43.0	42.2	42.4	42.0
	0.01	Density	-	49.4	49.4	49.7	49.7
		Porosity	-	42.9	42.9	42.5	42.6
	0.28	Density	-	49.0	49.7	49.1	49.4
		Porosity	-	43.4	42.6	43.3	42.9
	0.45	Density	-	49.2	49.3	-	49.2
		Porosity	-	43.1	43.0	-	43.1

50	0	Density	-	50.4	51.1	51.5	50.1
		Porosity	-	41.8	40.9	40.5	41.9
0.01	0.01	Density	-	49.8	50.4	50.8	50.7
		Porosity	-	42.4	41.7	41.3	41.5
0.28	0.28	Density	-	50.2	50.7	50.7	50.7
		Porosity	-	41.8	41.5	41.5	41.5
0.45	0.45	Density	-	49.3	49.7	49.8	49.8
		Porosity	-	43.0	42.5	42.4	42.4
100	0	Density	-	52.3	-	52.8	51.3
		Porosity	-	39.6	-	39.0	40.7
0.01	0.01	Density	-	52.8	52.8	52.8	52.8
		Porosity	-	39.0	39.0	39.0	39.0
0.28	0.28	Density	-	52.3	51.9	52.9	52.8
		Porosity	-	39.6	40.0	38.9	39.0
0.45	0.45	Density	-	-	51.7	51.8	51.8
		Porosity	-	-	40.2	40.1	40.1

TABLE A.5 DEFORMATION UNDER STATIC LOADING

A.5.1 Container Size: 2.5 inches diameter and 1.1 inches height
 A.5.1.1 Vertical deflection dial readings of samples under compression

Moisture Content %	Loading or Unloading	Static Pressure psi							
		0	0.52	1.05	2.02	3.74	7.25	14.10	21.00
8.6	Loading	.0610	--	.0579	.0566	.0556	.0530	.0482	.0454
	Unloading	.0580	--	.0530	.0518	.0495	.0478	.0459	.0454
11.0	Loading	.1300	.1279	.1257	.1234	.1198	.1148	.1089	.1046
	Unloading	.1135	--	.1112	.1095	.1080	.1066	.1053	.1046
16.4	Loading	.0480	--	.0402	.0357	.0295	.0217	.0140	.0095
	Unloading	.0231	--	.0118	.0116	.0113	.0109	.0102	.0095
20.2	Loading	.1030	.0951	.0931	.0888	.0814	.0702	.0600	.0515
	Unloading	.0565	--	.0550	.0539	.0535	.0532	.0518	.0515
22.8	Loading	.0935	.0816	.0764	.0702	.0556	.0435	.0282	.0205
	Unloading	.0224	--	.0220	.0216	.0212	.0207	.0205	.0205

A.5.1.1.2 Values of vertical deformation ($\frac{\Delta L}{L}$) computed from A.5.1.1.1

Moisture Content %	Loading or Unloading	Static Pressure psi								
		0	0.52	1.05	2.02	3.74	7.25	14.10	21.00	
8.6	Loading	0	--	0.31	0.44	0.54	0.80	1.28	1.56	
	Unloading	0.30	--	0.80	0.92	1.15	1.32	1.51	1.56	
11.0	Loading	0	0.21	0.43	0.65	1.01	1.51	2.09	2.51	
	Unloading	1.65	--	1.88	2.05	2.17	2.31	2.44	2.51	
16.4	Loading	0	--	0.78	1.23	1.85	2.63	3.40	3.85	
	Unloading	2.49	--	3.62	3.64	3.67	3.71	3.78	3.85	
20.2	Loading	0	0.79	0.99	1.42	2.16	3.28	4.30	5.15	
	Unloading	4.65	--	4.80	4.91	4.95	4.98	5.12	5.15	
22.8	Loading	0	1.19	1.71	2.33	3.79	5.00	6.53	7.30	
	Unloading	7.11	--	7.15	7.19	7.23	7.28	7.30	7.30	

A.5.1.1.3 Variation of bulk density (lbs./cu. ft.) or porosity (%) under static pressure

Moisture Content %	Density or Porosity	Static Pressure psi							
		0	0.52	1.05	2.02	3.74	7.25	14.10	21.00
8.6	Density	54.6	--	54.8	54.8	54.9	55.0	55.3	55.4
	Porosity	34.8	--	34.6	34.6	34.4	34.3	34.0	33.8
11.0	Density	55.1	55.2	55.4	55.5	55.7	56.0	56.3	56.5
	Porosity	34.8	34.7	34.5	34.4	34.1	33.8	33.4	33.1
16.4	Density	--	--	--	--	--	--	--	--
	Porosity	--	--	--	--	--	--	--	--
20.2	Density	52.2	52.6	52.7	52.9	53.3	53.9	54.5	55.0
	Porosity	41.1	40.6	40.5	40.2	39.8	39.1	38.4	37.9
22.8	Density	51.4	52.0	52.3	52.6	53.4	54.1	54.9	55.9
	Porosity	41.1	40.4	40.0	39.7	38.8	38.0	36.9	35.7

A.5.2 Container Size: 6 inches diameter and 1½ inches height

A.5.2.1 Vertical deflection dial readings of samples under compression

Moisture Content %	Loading or Unloading	Static Pressure psi								
		0	0.46	0.92	1.65	3.08	5.95	8.80	14.50	
9.4	Unloading		.0850							
	Loading	.0085	.0045	.0825	.0804	.0776	.0733	.0707	.0662	
12.5	Unloading	.0773	--	.0722	.0712	.0698	.0684	.0675	.0662	
	Loading	.1021	.0980	.0960	.0935	.0899	.0852	.0822	.0765	
16.8	Unloading	.0852	--	.0821	.0813	.0800	.0787	.0778	.0765	
	Loading	.0775	.0705	.0676	.0640	.0592	.0519	.0483	.0406	
23.4	Unloading	.0488	--	.0459	.0452	.0444	.0429	.0421	.0406	
	Loading	.1310	--	.1255	.1215	.1154	.1060	.0991	.0886	
29.7	Unloading	.1017	--	.0983	.0970	.0951	.0925	.0919	.0886	
	Loading	.1163	.1131	.1056	.0972	.0834	.0619	.0451	.0145	
	Unloading	.0517	--	.0386	.0334	.0260	.0194	.0165	.0145	

A.5.2.2 Values of vertical deformation ($\frac{\Delta L\%}{L}$) computed from A.5.2.1

Moisture Content %	Loading or Unloading	Static Pressure psi							
		0	0.46	0.92	1.65	3.08	5.95	8.80	14.50
9.4	Loading	0.00	0.37	0.56	0.76	1.02	1.42	1.67	2.06
	Unloading	1.40	--	1.50	1.59	1.73	1.86	1.94	2.06
12.5	Loading	0.00	0.38	0.57	0.81	1.14	1.58	1.87	2.40
	Unloading	1.58	--	1.87	1.95	2.08	2.20	2.28	2.40
16.8	Loading	0.00	0.66	0.93	1.27	1.71	2.40	2.74	3.46
	Unloading	2.70	--	2.96	3.04	3.10	3.24	3.32	3.46
23.4	Loading	0.00	--	0.52	0.89	1.46	2.34	3.00	4.00
	Unloading	2.88	--	3.20	3.22	3.52	3.74	3.82	4.00
29.7	Loading	0.00	0.30	1.00	1.78	3.08	5.1	6.72	9.45
	Unloading	6.00	--	6.45	7.70	8.35	9.00	9.20	9.45

A.5.2.3 Variation of bulk density (lbs./cu. ft.) or porosity (%) under static pressure

Moisture Content %	Density or Porosity	Static Pressure psi							
		0	0.46	0.92	1.65	3.08	5.95	8.80	14.50
9.4	Density	54.2	54.4	54.5	54.6	54.7	55.0	55.1	55.3
	Porosity	39.2	38.9	38.8	38.7	38.5	38.3	38.1	37.9
12.5	Density	54.0	54.2	54.3	54.4	54.6	54.9	55.0	55.3
	Porosity	39.2	38.9	38.8	38.7	38.5	38.2	38.0	37.7
16.8	Density	53.3	53.6	53.8	54.0	54.2	54.6	54.8	55.2
	Porosity	39.2	38.8	38.6	38.4	38.1	37.7	37.4	37.0
23.4	Density	52.7	--	53.0	53.4	53.4	53.9	54.3	54.8
	Porosity	39.2	--	38.8	38.6	38.6	37.7	37.3	36.6
29.7	Density	51.7	51.9	52.2	52.7	53.4	54.5	55.4	57.1
	Porosity	39.2	39.0	38.5	38.0	37.2	35.9	34.9	32.9

TABLE A.6 DIRECT SHEAR TESTS ON WHEAT

Note: Three tests at confining pressures of 1, 2 and 3 psi respectively for each porosity and for each moisture content

Moisture Content %	Porosity %	Density lbs./cu. ft.	ϕ in degree	$\tan \phi$	C in psi
9.4	39.1	54.3	21	0.38	0.12
	38.3	55.0	22½	0.41	0.12
	37.2	56.0	23	0.42	0.18
	36.5	56.6	23½	0.44	0.21
12.5	37.8	55.0	20	0.36	0.18
	37.4	55.3	21½	0.39	0.20
	36.7	56.0	23	0.42	0.25
16.1	38.5	54.0	18	0.32	0.38
	37.7	54.7	17½	0.32	0.42
	37.1	55.2	22	0.40	0.32
	36.2	56.0	25	0.47	0.29
23.0	42.1	50.0	25	0.47	0.62
	39.6	52.2	31½	0.61	0.50
	38.3	53.3	30½	0.59	0.68
	37.5	54.0	31½	0.61	0.76
	36.9	54.5	32	0.62	0.80
29.2	42.7	48.8	34	0.67	0.50
	40.0	51.1	35	0.70	0.50
	36.5	54.1	34	0.67	0.87
	34.0	56.2	33	0.65	1.00
	29.6	60.0	32½	0.64	1.50

TABLE A.7 TRIAXIAL COMPRESSION TESTS ON WHEAT

Note: Stage triaxial tests with confining pressures of 10, 20 and 30 psi were made for each porosity and for each moisture content

Moisture Content %	Porosity %	Density lbs./cu. ft.	ϕ in degree	$\tan \phi$	C in psi
9.3	37.7	55.5	25	0.47	-
	34.9	58.0	27	0.51	-
	33.8	59.0	29	0.55	-
	31.5	61.0	30	0.58	-
	30.0	62.5	32	0.62	-
11.0	35.2	57.5	25	0.47	-
	34.1	58.5	26	0.49	-
	32.9	59.6	27½	0.50	-
	32.4	60.0	27¼	0.52	-
	31.3	61.0	27½	0.52	-
	30.7	61.5	28½	0.54	-
	28.0	64.0	29	0.55	-
16.4	38.7	53.8	25½	0.48	-
	38.4	54.0	27½	0.52	-
	37.8	54.5	28½	0.54	3.00
	34.3	57.6	27½	0.52	4.00
	33.8	58.0	27½	0.52	0.75
	33.0	58.8	28	0.53	6.00
22.8	42.7	49.5	35	0.70	0.50
	37.8	53.8	34½	0.69	0.75
	36.4	55.0	36½	0.74	1.00
	34.6	56.5	37	0.75	1.75

TABLE A.8 DIRECT SHEAR TESTS OF WHEAT ON THREE STRUCTURAL SURFACES

Note: Three tests at confining pressures of 1, 2 and 3 psi (some at 2, 4 and 6 psi) respectively for each porosity and for each moisture content

A.8.1 Wheat on Wood

Moisture Content %	Porosity %	Density lbs./cu. ft.	δ in degree	tan δ A in psi	
9.3	39.9	53.5	11½	0.20	0.02
12.2	40.1	53.3	11½	0.20	0.12
	40.0	53.4	12	0.21	0.12
	39.0	53.6	11½	0.20	0.12
16.8	40.4	52.2	13	0.23	0.18
	38.4	54.0	13	0.23	0.16
23.3	40.2	51.8	20	0.36	0.20
	38.6	53.1	20	0.36	0.20
29.4	43.6	48.0	17	0.31	0.28
	36.5	54.0	20	0.38	0.28

A.8.2 Wheat on Steel

9.3	40.6	53.0	14½	0.26	-
12.2	40.2	53.2	16½	0.30	0.12
	39.8	53.5	16	0.29	0.15
16.8	41.2	52.5	20	0.36	-
	38.4	54.0	19	0.34	0.18
23.3	42.4	49.6	17½	0.32	0.18
	40.4	51.5	16	0.29	0.18
29.4	43.5	48.1	14	0.25	0.18
	36.0	54.5	15	0.27	0.25

A.8.3 Wheat on Concrete

9.3	41.3	52.3	22	0.40	0.50
12.2	41.9	51.5	22½	0.41	0.60
	40.2	53.2	24	0.46	0.50
16.8	41.4	51.3	24	0.46	0.35
	38.9	53.6	26½	0.50	0.38
23.3	43.3	49.0	27	0.51	0.38
	40.0	51.0	31½	0.61	0.42
29.4	44.0	47.3	27½	0.52	0.42
	36.5	54.0	28	0.53	0.75